Eugene Barsky

Fluid Mechanics and Its Applications

Critical Regimes of Two-Phase Flows with a Polydisperse Solid Phase

Springer

Critical Regimes of Two-Phase Flows with a Polydisperse Solid Phase

FLUID MECHANICS AND ITS APPLICATIONS
Volume 93

Series Editor: R. MOREAU
MADYLAM
Ecole Nationale Supérieure d'Hydraulique de Grenoble
Boîte Postale 95
38402 Saint Martin d'Hères Cedex, France

Aims and Scope of the Series

The purpose of this series is to focus on subjects in which fluid mechanics plays a fundamental role.

As well as the more traditional applications of aeronautics, hydraulics, heat and mass transfer etc., books will be published dealing with topics which are currently in a state of rapid development, such as turbulence, suspensions and multiphase fluids, super and hypersonic flows and numerical modeling techniques.

It is a widely held view that it is the interdisciplinary subjects that will receive intense scientific attention, bringing them to the forefront of technological advancement. Fluids have the ability to transport matter and its properties as well as to transmit force, therefore fluid mechanics is a subject that is particularly open to cross fertilization with other sciences and disciplines of engineering. The subject of fluid mechanics will be highly relevant in domains such as chemical, metallurgical, biological and ecological engineering. This series is particularly open to such new multidisciplinary domains.

The median level of presentation is the first year graduate student. Some texts are monographs defining the current state of a field; others are accessible to final year undergraduates; but essentially the emphasis is on readability and clarity.

For further volumes:
http://www.springer.com/series/5980

Eugene Barsky

Critical Regimes of Two-Phase Flows with a Polydisperse Solid Phase

Springer

Eugene Barsky
Jerusalem College of Engineering
91035 Jerusalem
Ramat Beit Ha-Kerem
Israel
eugene@jce.ac.il

ISSN 0926-5112
ISBN 978-90-481-8837-6 e-ISBN 978-90-481-8838-3
DOI 10.1007/978-90-481-8838-3
Springer Dordrecht Heidelberg London New York

Library of Congress Control Number: 2010925500

Cover design: eStudioCalamar Figures, Berlin

Printed on acid-free paper

Springer is part of Springer Science+Business Media (www.springer.com)

Annotation

This book brings to light peculiarities of the formation of critical regimes of two-phase flows with a polydisperse solid phase. A definition of entropy is formulated on the basis of statistical analysis of these peculiarities. The physical meaning of entropy and its correlation with other parameters determining two-phase flows are clearly defined. The interrelations and main differences between this entropy and the thermodynamic one are revealed. The main regularities of two-phase flows both in critical and in other regimes are established using the notion of entropy. This parameter serves as a basis for a deeper insight into the physics of the process and for the development of exhaustive techniques of mass exchange estimation in such flows.

The book is meant for university students of engineering specialties studying two-phase flows. It can also be of use to those working for a doctor's degree, and to scientists and engineers engaged in specific problems of such fields as chemical technology, mineral dressing, modern ceramics, microelectronics, pharmacology, power engineering, thermal engineering, etc. using flows with solid particles in their respective production methods.

Introduction

Two-phase flows are widely used in applications of systems analysis to problems encountered in all segments of modern industry. A special category of systems is the one that contains discrete formations distributed in a continuum. These discrete formations consist of either solid particles of constant shape and size, or liquid drops or gas bubbles that can change their size in the course of a process, whereas the continuum in which they exist is either liquid or gaseous. Modern technology's concern with two-phase flows is caused by a large contact surface of dispersed and continuous phases ensuring high velocities of mass transfer and other processes. The simplest among them are dispersed systems containing a solid phase – in a certain sense, they can be used as simplified models of systems containing drops and gas bubbles.

As shown in Fig. 1, two-phase flows can be of various kinds depending on the correlations between the velocities of the continuum and the solid phase particles contained therein.

A so-called transport regime is realized at flow rates ensuring the ascent of the entire solid phase. Its velocity is limited from below by the value at which even the coarsest particles do not settle against the flow. The minimal value of this velocity is called the critical pneumatic or hydraulic transport velocity depending on the continuum used – air or water.

An opposite regime of two-phase flows with the formation of a so-called descending layer is also used in some technologies. In this regime, all solid particles settle against the flow. In this case, the flow velocity is limited from above. The maximal velocity at which even the finest particles of solid phase are not transported by the flow is called critical for the descending layer. A particular case of a descending layer is a so-called motionless layer; in this case, solid material lies motionless on a grating and is blown through from below.

The ratio of these critical velocities is of certain theoretical and practical interest from the point of view of mass exchange processes within their range. For instance, the velocity of a boiling bed process, which is widely used in present-day technology, lies within this range, which points to the importance of studying such flow regimes. Critical regimes of two-phase flows are most widely used in industry for

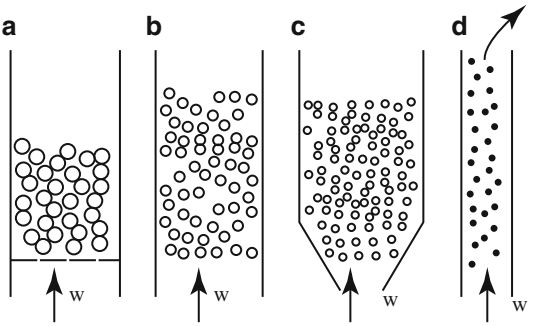

Fig. 1 Various regimes of two-phase critical flows: (**a**) motionless layer, (**b**) incident layer, (**c**) boiling layer, (**d**) pneumatic transport and separation regime

fractionating bulk materials according to particle sizes or densities. Only such regimes allow transportation of fine lightweight particles with the flow and a simultaneous motion of coarse heavy particles against the flow. Until now, these processes have not been sufficiently studied and formalized.

Critical regimes of two-phase flows can be realized not only in vertical flows, but also in a centrifugal field, fields of magnetic and electrostatic forces and in other situations with the solid phase motion directed differently with respect to the flow.

Separation of bulk materials in critical regimes of two-phase flows is an extremely complicated physical process. Its complicated character is caused by oppositely directed motions and mutual influence of an enormous quantity of particles of various sizes in the carrier medium flows, whose structure is extremely inhomogeneous. Such motions give rise to a broad range of various random factors. The most important among them are hydrodynamic and contact interactions of particles in the flow and with the walls confining the flow; unpredictable non-uniformity of the flow velocity and pressure fields; solid phase distribution within the flow; nature of the interactions between the phases; as well as the discrete component effect on the continuum motions. Among these factors are also principal parameters of real bulk materials, such as particle size, shape, weight, density, size grade distribution, all of which are random values.

All these complexities make any attempt to formulate a rigorous analytical description of the process completely hopeless. As well known, there is no acceptable analytical theory as yet even for a single-phase turbulent flow. The more so, there are no analytical solutions for two-phase flows. Thus researchers have usually studied the main regularities of such processes and then formalized the experimental data obtained from them at a semi-empirical theoretical level. This follows the usual pattern in science of dealing with the evolution from simpler to more complicated notions.

Initially, the study of the process under consideration in this book started from the analysis of the behavior of isolated particles. The first works on the topic were published in the second half of the nineteenth century. Rittinger established the regularities of simple deposition of isolated particles of spherical shape in an unbounded motionless liquid. In many subsequent works related to deposition,

the influence of various factors was revealed, such as medium and material density, final velocities of particles deposition, their resistance coefficients, etc.

At the same time, the transition to working with real materials consisting of particles of irregular shape proved to have additional complications. Articles are still being published nowadays reflecting a variety of approaches to these problems. We have ample evidence that even the phenomena occurring during a simple deposition of particles of real materials in a motionless medium are very complicated.

Attempts to apply the main regularities obtained in the studies of isolated particles in a flow to actual processes have not provided generalized results. In fact, proceeding from this standpoint, one has to admit that an ascending flow can carry out of the separation zone only those particles whose deposition velocity is below the flow velocity. On the contrary, all the particles with deposition velocity exceeding the flow velocity are deposited against the flow.

However, experience shows that in bulk materials fractionating, this is not the case. Thus, we have to admit that although the problem of, e.g., powders separation in flows has been studied for more than a century, it has not reached the theoretical level suitable for solving practical problems. Therefore, commercial needs often continue to be satisfied by extensive empirical studies. Usually, the principal characteristics of a separation process under industrial conditions will be obtained on a laboratory model or a pilot plant. The obtained parameters are then extended to a working industrial unit. Because of imperfect modeling, it is not always successful.

An enormous number of experimental studies performed in recent years have made it possible to develop many empirical methods of estimating principal parameters for specific units. Beyond any doubt, these studies are important. However, researchers do not always realize that empirical methods influence only slightly the development of the theory of the process.

Empirical dependencies differ from theoretical ones; they do not naturally follow from the regularities of the phenomena under study, but only quantitatively reflect them. Even a carefully conducted experiment does not allow taking into account various permanent and random factors, both quantitative and qualitative ones. One can manage to specify, to some extent, the average effect of quantitative factors only by increasing the number of experiments. As for qualitative factors, their effect is mainly beyond all estimations.

Even the best and the most grounded empirical formula can be applied with a satisfactory result only within a limited range determined by the conditions of its derivation. Rather often, extrapolation beyond the limits of the experimental range is carried out on the basis of such dependencies, but it can result in gross errors. Application of empirical dependencies is also limited in time, since they cannot take into account the forthcoming development of science and technology. Some attempts have been made to refine calculated relationships from previous research and adjust them to present-day knowledge by introducing various correction factors. However, application of a large number of more or less arbitrarily chosen factors leads to the accumulation of errors, as well known in the effects of multiple round-off in even simple calculations.

Recent decades have produced certain achievements in the development of various aspects of two-phase flow theory. However, for the solid phase distribution in critical regimes of two-phase flows, the situation is different. Beyond any doubt, it is one of the most complicated and intricate theoretical issues, and it is, as a rule, either left out or examined on the basis of empirical relationships only. This practice can be easily observed in recent review monographs and handbooks.

In the present book, we attempt to solve this problem from a somewhat different standpoint. Usually, two-phase flows are considered, in the first place taking into account peculiar properties of a continuum motion altered by solid particles placed into this continuum. We are making an attempt to use the laws of solid phase mass motion as a basis of critical regimes of motion.

It is practically impossible to describe simultaneous mass motion of solid particles in a non-uniform continuum flow from the standpoint of classical mechanics. It is well known that classical mechanics developed by Newton, Lagrange and Hamilton can predict the behavior of either an ordered system of bodies or a system with a moderate number of elements. On this basis, one can obtain an exact solution of a celestial mechanics problem easily enough, but the three-body problem has not yet been solved in a general form.

Meanwhile, there exists a statistical approach to the study of mass continuum phenomena that has been developing for more than 100 years. The works of Boltzmann and Gibbs, which have already become classical, laid the basis of this approach. Its principal ideas were widely used and developed in quantum mechanics and its applications to optics, theory of magnetism, solid state theory and other fields of science. They have become corner stones in the foundations of the state-of-the-art knowledge in these fields. The principal distinctive feature of this approach is that it is based on a definition of the state of the entire system, no matter whether one examines a large or a small system comprising an infinite number of particles or a single particle.

Here the methods of analyzing mass processes (involving a large number of particles) are considered as essentially statistical ones. Data obtained as a result of such analysis should be considered as averaged over an ensemble, but not as absolutely rigorous in each case. This inevitably follows from the nature of a statistical approach, which is applicable either in the absence of the necessary initial data or when practical solutions are very complicated. To justify statistical methods, it should be emphasized that they should finally lead to conclusions consistent with experimental data.

Here the basic point is how to determine average values. Instead of time averaging within a single system, it is possible to examine a set of a large number of respectively organized systems. An ensemble of systems represents a mental structure reflecting the properties of a real system. It consists of a large number of similarly organized systems, each system of the ensemble being equivalent to a real system.

The theory of L. Boltzmann was based on the notion that a molecule of gas consists of ideal balls of the same diameter placed into a closed volume, and their velocity is determined by the temperature of the medium. Such a simplified model

allowed Boltzmann to develop a well-composed statistical theory of gases, which in many respects agrees with experimental data.

In recent decades, interest in this theory has been growing in two aspects. On the one hand, a large number of researches expanding Boltzmann's theory have appeared. On the other hand, principal ideas and methods of this theory have been successfully applied to other non-gaseous systems, such as solid-state theory, nuclear matter, magnetism, polymerization, etc.

These efforts have given additional support to the well-known principle that the physically grounded method of analogies is extremely fruitful for the development of science. We make an attempt in this book to apply certain ideas of this theory to the problem under study. Critical regimes of solid phase flow form the basis of this problem. Therefore we start with the analysis of solid particle characteristics and dynamics, as well as with the analysis of all achievements in the empirical study of two-phase critical flows.

We make one additional remark. Physics, hydraulics, mineralogy, etc. provide a conceptual tool and phenomenological approach to the analysis of the phenomena under study. Mathematics is not only a tool for the analysis of these processes. It determines, in many respects, ways and methods of this analysis, constituting the main line of scientific thought. Therefore, mathematical transformations are presented in the book in detail, so that the problem setting, derivation and analysis of the obtained results are clear. It is not always reasonable to give a final result without its derivation, because in the course of solving a particular problem, one often comes across instructive techniques and even intermediate results.

The book is intended for a broad circle of research specialists including students of respective specialties. Therefore, the mathematical apparatus is intentionally used in its simplest version, corresponding to the level of students of the first degree in engineering sciences.

The author is grateful to Ms. N. Goldbaum for the manuscript translation into English.

Contents

Chapter 1
General Ideas of Mass Transfer Processes in Critical Regimes

Abstract Experimental studies have shown that despite a visual chaos in critical regimes of two-phase flows, there is a definite, almost deterministic order in the polyfractional solid phase distribution along the flow and counter the flow. The affinity of separation curves as a function of principal parameters of the flow in a turbulent regime is substantiated. Criteria of the affinization of separation curves are empirically established and experimentally substantiated.

Keywords Regularity · Granulometric composition · Size · Density · Concentration · Velocity · Process stability · Fractional extraction · Affinity · Separation curve · Productivity · Separation

1.1 Granulometric Characteristics of Bulk Material

First of all, we examine characteristics of a solid phase constituting a two-phase flow, because in critical regimes the process of particles separation according to their size grade or density can be organized most easily.

Processing of ground materials is among the most widespread processes in today's industry. Many millions of tons of various materials are ground daily in mining, in various branches of chemical industry, in metallurgy, at the production of cement, ceramics, glass and other building materials, as well as in most novel branches of industry. Various natural and artificial materials become pourable when ground, and in this state they pass all the stages of technological processes, namely, extraction of useful components, production of powders with a specified particle size, compounding of necessary mixtures and compositions, treatment of particle surface and addition of various elements, drying, baking, etc. In this state it is convenient to granulate materials from particles of any composition or press products of any shape. As a rule, a solid phase is introduced into moving flows in this state only.

E. Barsky, *Critical Regimes of Two-Phase Flows with a Polydisperse Solid Phase*,
Fluid Mechanics and Its Applications 93,
DOI 10.1007/978-90-481-8838-3_1,

At present, more and more low-quality raw materials are being processed because of growing production volumes. At the same time, the requirements for the quality of the final products constantly grow. To meet these requirements, separation processes are becoming more and more important.

Most often, the separation is performed by particle size or density, and more rarely – by shape, color or other parameters. While formerly, with a rather rough technology, it was sufficient to use various sieves for the separation by size, present-day operations with fine powders require separation carried out using moving media – air or water. As for separation by other parameters (density, particle shape), it can be realized only in moving media.

Before determining separation parameters, we examine principal characteristics of a bulk material. Such a material can be characterized by its specific density of particles, bulk density, humidity, porosity, etc. Usually a ground material contains, depending on its size grade, many millions of particles. These particles can differ in size, shape, surface state, etc. However, the material's principal characteristic is connected with dispersity. One can assert with a high degree of probability that among all particles it is impossible to find two identical ones. There is nothing paradoxical in this assertion. It is analogous to the fact that among more than six billion people living today on the Earth there are no two identical fingerprints. A way out of this difficulty consists in passing from individual features of each particle to certain averaged characteristics determined for a whole class of particles. On the basis of such averaging, so called grain-size composition is obtained, that is, averaged function of particle size distribution. There are several methods of determining this function, for example, sieve methods, sedimentation and microscopic analysis. Sieve analysis is the simplest and the most visual one. To carry out this analysis, several sieves are chosen with strictly definite mesh sizes. These sieves are assembled into a set as shown in Fig. 1.1. Below is a bottom without holes, a sieve with the finest mesh size is installed on it, then a sieve with coarser meshes, etc. This way, a set of sieves is formed with mesh size monotonically growing from bottom to top. Depending on the material to be analyzed, a sieve with minimal meshes through which all analyzed material passes, is placed on the top.

A size grade axis for the holes of the set of sieves is arranged vertically. Whenever necessary, for instance when plotting grain-size distribution, it can be arranged horizontally as well.

A representative sample of bulk material is taken for the analysis, poured into the set of sieves from above and subjected to vibration during the time period sufficient for complete sieving. As a result, particles that have not passed remain on each sieve. These residues are weighed and recorded in tables either in grams or in percents of the total sample.

By way of example, Table 1.1 (columns 3 and 4) shows the results of the analysis of ground quartzite sample and products of its separation on a cascade classifier at a certain fixed flow velocity. A schematic diagram of a gravitational classifier is presented in Fig. 1.2. Bulk material of a certain composition is fed into the middle part of a vertical pipe. An air or water flow with the velocity w is realized in this

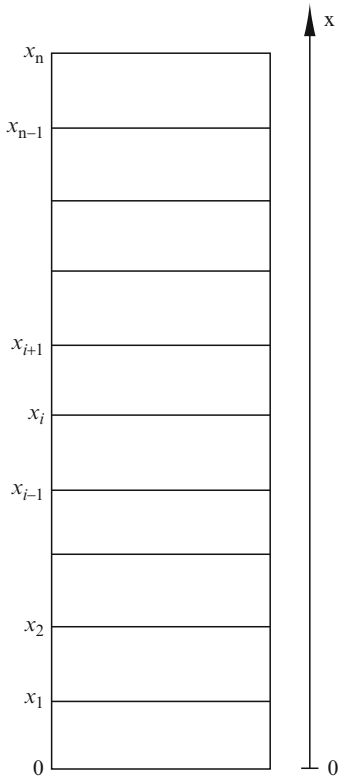

Fig. 1.1 A set of sieves for granulometric analysis

pipe from bottom to top, against the gravity force. The velocity is chosen within such range that fine particles are carried out upwards, and coarse particles are settled in the counter-flow direction.

In column 1, sieve holes sizes are given in meshes, and in column 2 – in microns. Column 3 shows residues on each sieve in %. To explain how total residues and passes are determined, we consider, by way of example, an 80 mesh (or 180 μm) sieve. Everything that is coarser than this sieve (in Fig. 1.1 – everything located above it) is the total residue; it amounts to 59.8%. Everything that passes through this sieve (is below it) is the total pass amounting to 40.2%.

Thus, bulk material composition by particle sizes can be described by distribution functions $R(x)$ or by the $D(x)$ function connected with the latter. The function $R(x)$ is determined as an overall characteristic reflecting the ratio of the weight of all particles with the diameter exceeding x to the total weight of the material expressed in percents. Figure 1.3 shows curves plotted on the basis of Table 1.1.

Since in any point $D(x) + R(x) = 1$, the curves $D(x)$ and $R(x)$ are mirror symmetrical and intersect in the point $D(x) = R(x) = 50\%$.

We assume that the functions R(x) and $D(x)$ are continuous and monotonic, differentiable everywhere and having continuous derivatives.

Table 1.1 Principal parameters of ground quartzite and its separation products at a fixed air flow velocity

Sieve mesh size		Sieve residue in initial material	Total residue	Total passes	Sieve residue in fine product	Sieve residue in coarse product	Fraction extraction into fine product	Fraction extraction into coarse product	Average narrow class size
Mesh	μm	r_s%	R_s%	D_s%	r_f%	r_c%	$F_f(x)$%	$F_c(x)$%	x (μm)
1	2	3	4	5	6	7	8	9	10
16	1,000	0	0	100	0	0	–	–	–
20	850	4.5	4.5	95.5	0	4.5	0	100	925
30	600	9.2	13.7	86.3	0.3	8.9	3.26	96.74	725
45	355	13.6	27.3	72.7	2.1	11.5	15.44	85.56	478
60	250	15.2	42.5	57.5	6.4	8.8	42.1	57.9	300
80	180	17.3	59.8	40.2	9.1	8.2	52.6	47.4	215
120	125	18.3	78.1	21.9	12.7	5.6	69.4	30.6	152
200	75	13.3	91.74	8.6	9.0	4.3	67.7	32.3	100
270	53	4.0	95.4	4.6	2.9	1.1	72.5	27.5	64
400	38	3.1	98.5	1.5	2.7	0.4	87.1	129	45
Bottom	0	1.5	100	0	1.5	0	100	0	20

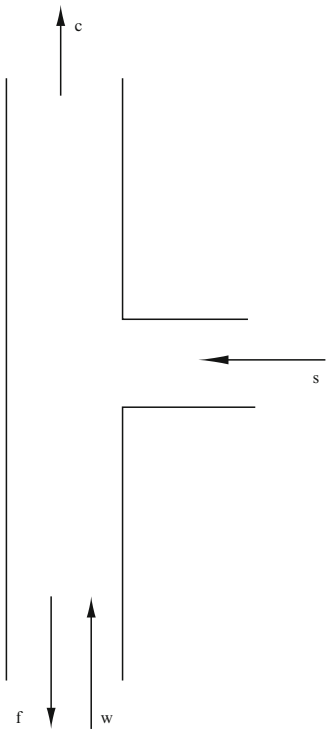

Fig. 1.2 Schematic diagram of separation regime realization. s – initial product feeding; c – coarse product output; f – fine product output; w – flow velocity

It means that there exists a certain function $r(x)$ that can be obtained by differentiating the function R(x) and is continuous within the range from $x_{\min}$ to $x_{\max}$

$$\int_{x_{\min}}^{x_{\max}} r(x)dx = R(x_{\max}) - R(x_{\min}). \tag{1.1}$$

The function $r(x)$ is normalized to a unity by the density of the material weight distribution by the particle diameters:

$$r(x) = \frac{dR(x)}{dx} \tag{1.2}$$

This function is called partial residues distribution.

1.2 Distribution of Different Fractions in the Process of Separation

Bulk materials separation by particle size or density can be carried out in different ways – in gravity, centrifugal, electric fields and, probably, in fields of other nature. Anyway, the separation principle remains unchanged. It consists in counter-motion

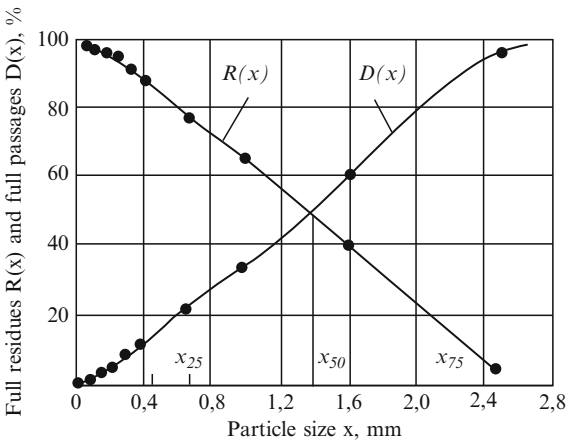

Fig. 1.3 Granulometric characteristic of ground material in full residues R(x) and full passages D(x)

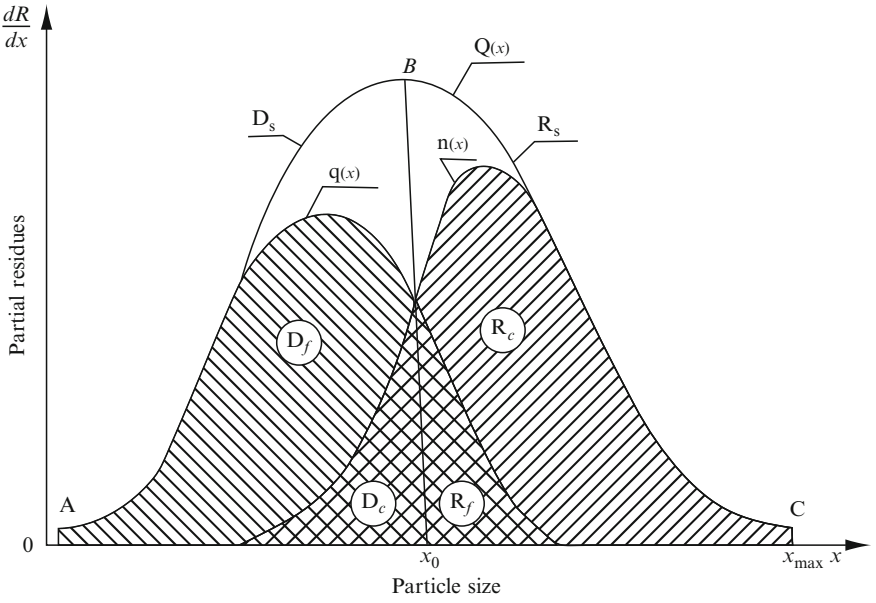

Fig. 1.4 Redistribution of fractions during separation

of particles of different size grades, that is, fine particles move predominantly in one direction and coarse particles in another.

The most visual way of presenting material distribution is graphical. The curve ABC in Fig. 1.4 shows grain-size composition of a bulk material in partial residues. We assume that this material has to be separated by size of x_0. Note that according to Eq. (1.1), the area limited by the curve ABC and axis x corresponds, in a certain scale, to the total quantity of the initial material. In an ideal case, the separation

should proceed along the line Bx_0. This line divides the initial material into two parts with respect to the size x_0 – fine initial product D_s and coarse initial product R_s.

In real processes, even if the flow velocity w is optimal, the separation process is not ideal, that is, practically always a part of a fine product gets into a coarse one and vice versa.

We assume that the composition of fine product is shown by the curve ADE. Then the coarse product is described by the curve KDC, that is, there is a balance dependence between the initial fine and coarse products.

Thus, in a general case, the plot area is divided by the lines of ideal and real processes into four parts:

D_c – quantity of fine particles extracted into fine product;

R_f – quantity of coarse particles extracted into fine product;

R_c – quantity of coarse particles extracted into coarse product;

D_f – quantity of fine particles extracted into coarse product.

The following equalities are derived from Fig. 1.4:

$$\begin{aligned} D_s+R_s &= 1 \quad D_f+R_f = \gamma_f \\ D_f+D_c &= D_s \quad D_c+R_c = \gamma_c \\ R_c+R_f &= R_c \quad \gamma_f+\gamma_c = 1 \end{aligned} \tag{1.3}$$

where $\gamma_f; \gamma_c$ – are, respectively, fine and coarse products outputs.

On the basis of relationships (1.3), we can find various parameters describing separation processes, for instance:

$\varepsilon_f = \frac{D_f}{D_s}$ – fine particles extraction;

$\varepsilon_c = \frac{R_c}{R_s}$ – coarse particles extraction;

$k_f = \frac{R_f}{R_s}$ – fine particles contamination;

$k_c = \frac{D_c}{D_s}$ – coarse particles contamination.

All these parameters depend on the initial material composition, material concentration in the flow and the value of boundary separation size, which does not allow finding any general approach to the analysis of separation processes. The latter becomes possible using so-called fractional separation curves.

1.3 Fractional Separation Curves and Their Properties

It is generally accepted that Nagel was the first to introduce fractional separation curves into practice in 1936. However, they are most frequently associated with the name of a Dutch engineer Tromp, who published his work in 1937. The idea of fractional separation curves is rather simple. It is based on the determination of fractional extraction of different narrow size classes during classification. Fractional separation curves are plotted proceeding from the relationship between the obtained separation products and the initial composition without any complicated calculations. To plot these curves, we use columns 6 and 7 in Table 1.1.

Fractional extraction for each narrow size class expressed in percents is described by the following dependencies:

$$\left.\begin{aligned} F_f(x) &= \tfrac{r_f}{r_s} \cdot 100 \\ F_c(x) &= \tfrac{r_c}{r_s} \cdot 100 \end{aligned}\right\} \tag{1.4}$$

Extractions of different fractions into separation products obtained using these formulas are shown in Table 1.1 (columns 8 and 9), and the curves based on these data are presented in Fig. 1.5. In this graph, fractional separation value correlates with the average size of a narrow size class determined as an arithmetic mean of adjacent sieves (Table 1.1, column 10).

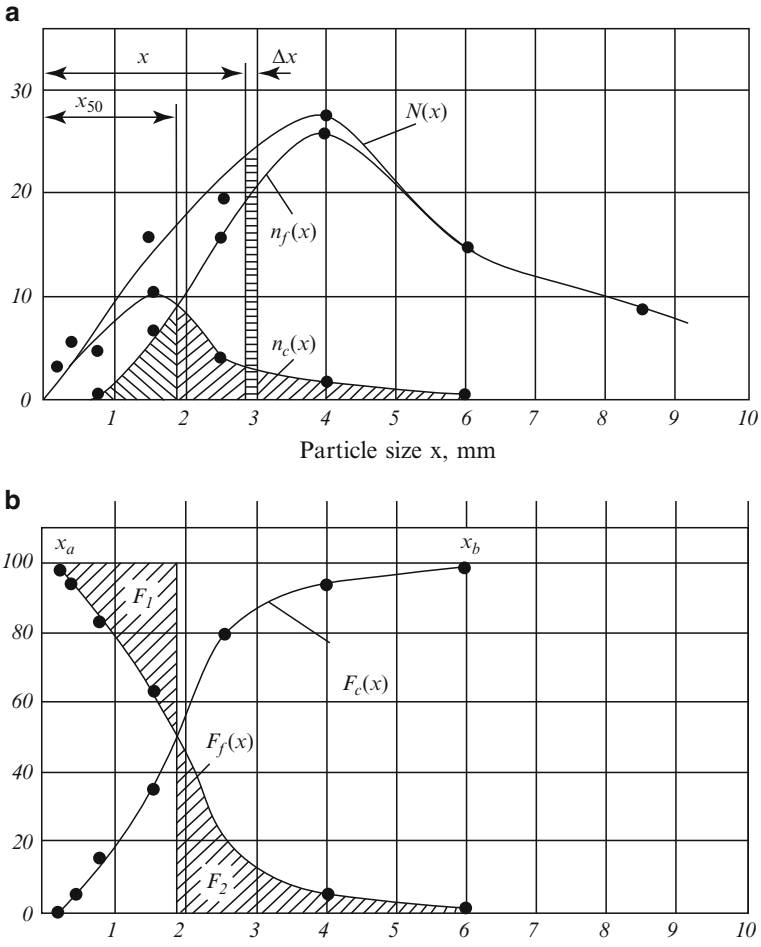

Fig. 1.5 Plotting separation curves (**b**) on the basis of the plot of redistribution during separation (**a**)

These curves cover the area between the points x_a and x_b, such that

$$\left.\begin{array}{ll} F_f(x_a) = 100 & F_f(x_b) = 0 \\ F_c(x_a) = 0 & F_c(x_b) = 100 \end{array}\right\} \tag{1.5}$$

The expression (1.5) and relations

$$F_f(x_i) + F_c(x_i) = 100 \tag{1.6}$$

lead to a complete mirror symmetry of these curves with respect to a horizontal axis passing though the ordinate point corresponding to 50%.

It is noteworthy that fractional separation curves contain complete information about the changes in grain-size composition of final products in comparison with the initial material. The narrower the area between x_a and x_b, the more complete is the separation. Clearly, at an ideal separation, $x_a = x_b$. In case of simple partition without changes in fractional composition, the functions $F(x)$ degenerate into straight lines parallel to the abscissa axis. We can prove that the abscissa of the intersection point of the curves x_{50} is the size corresponding to optimal separation. Fractional separation dependence on the air flow velocity is shown in Fig. 1.6. These curves have some important qualities allowing us to find general laws of this process. These qualities are examined below.

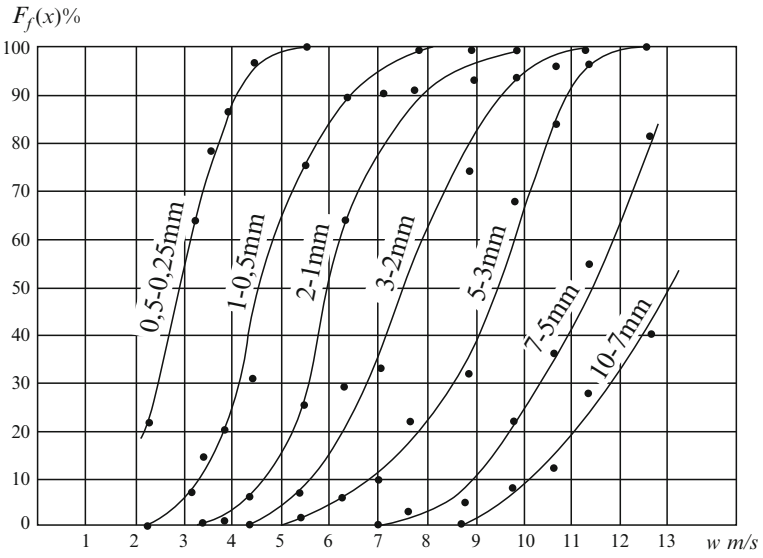

Fig. 1.6 Dependence of fractional extraction of various size classes on the air flow rate in a cascade classifier at $z = 4$; $i^* = 1$

1.3.1 Initial Composition

Investigations of the influence of the initial composition on the separation results at the air flow velocities of 3.15, 4.35 and 5.45 m/s were carried out on a shelf cascade classifier (Fig. 1.7). In the first set of experiments, the initial product distribution was continuous, and each size class was charged according to the following scheme: 3.3%; 6.7%; 10%; 12.5%; 30%; 50%; 76.7%; 100%. It was assumed that the contents of other classes in each experiment was uniformly distributed. Each of seven narrow classes acquired these values, and then the classification was performed at each mentioned velocity. The results of one set of experiments are presented in Fig. 1.8.

Experimental dependencies show that each narrow size class behaves independently during separation, as if other classes were non-existent.

At first sight, these results seem somewhat unexpected, because it has been experimentally proved that under such conditions particles of different size classes intensely interact. This interaction is markedly random. This process is also characterized by other random factors, but nevertheless, this parameter is invariant with

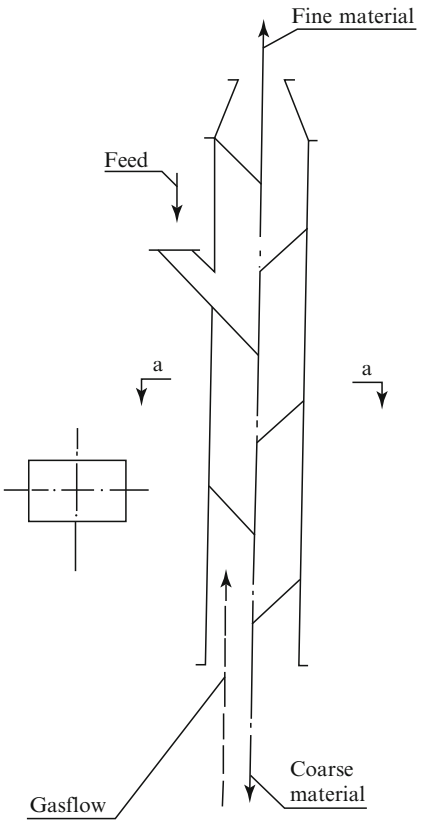

Fig. 1.7 Basic circuit of a cascade classifier with inclined shelves

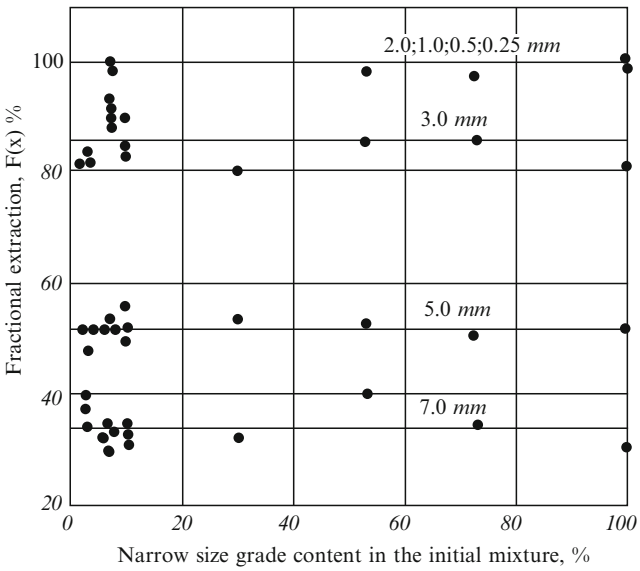

Fig. 1.8 Dependence of fractional extraction of various size classes into the fine product on their content in the initial material

respect to the initial composition. It seems physically analogous to the law of partial pressures of a gas mixture.

According to this law, the pressure of a gas mixture in a certain volume equals the sum of pressures of each component of the mixture as if it occupied the entire volume. It is generally accepted that pressure is a result of impact interaction of chaotically moving gas molecules with vessel walls. Although impact interactions of molecules of different components of a mixture inside the vessel are beyond any doubt, the resulting pressure value suggests that each component of the mixture behaves independently.

Fractional separation invariance with respect to the initial material composition is of basic importance for the general theory of the process. This property of separation curves was described without any explanation as early as in the mentioned paper of Tromp. Other properties of this curve were established later.

1.3.2 Solid Phase Concentration in the Flow

Optimal output of classifiers is closely connected with the apparatus dimensions and solid phase concentration in the flow. The influence of concentration on the results of separation has been studied by many authors. However, this factor could not have been taken into account thoroughly enough due to the absence of

well-grounded and clear ideas of process mechanism. Experimental material was reduced, at best, to purely empirical dependencies having no clear physical meaning. This relationship can be explained only after an in-depth study of basic physics of the process.

The effect of solid particles on two-phase flow character is twofold. First, with growing concentration, particle motion becomes more constrained. Secondly, the probability of their contact interaction increases. The attempt of revealing the influence of material concentration in a flow on fractional separation curves led to unexpected results.

Experimental studies were carried out in a hollow pipe and in cascade apparatuses with special nozzles. In all the cases, qualitatively similar results were obtained. They can be illustrated by the dependence obtained for a hollow pipe (Fig. 1.9). A characteristic feature of experimental dependencies is a section practically parallel to the concentration axis. For a hollow apparatus, this section is limited by the concentration $\mu \approx 2\,\mathrm{kg/m^3}$, while for an apparatus with nozzles, the validity area of this rule is extended up to $\mu \approx 6\,\mathrm{kg/m^3}$.

Within this section, fractional separation is practically independent of the material concentration in a flow. However, the mechanisms of the formation of this section remain unclear.

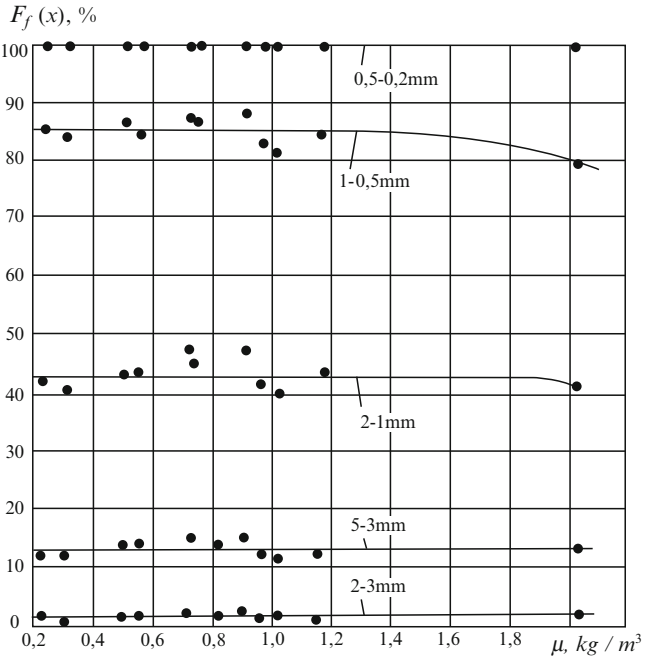

Fig. 1.9 Dependence of fractional extraction of various narrow size classes on the material concentration (material – ground quartzite, $\rho = 2{,}650\ \mathrm{kg/m^3}$)

1.3.3 Process Stability

Repeated laboratory experiments at a thoroughly adjusted air flow velocity give the same separation curve even in case of variations of grain-size composition in the initial feeding and changes in feeding by a feeder. It was confirmed by an 11-fold repeated experiment. In industrial conditions, the separation curve was determined on a classifier with the productivity of 35–40 t/h in a week after its setting into operation. For some reasons, reanalysis of the apparatus operation was performed only after 11 months, and the obtained separation curve was exactly the same. However, the spread of experimental points with respect to the curve somewhat increased, the maximal deviation reaching 7.3%. It is surprising, since a huge number of particles take part in the process. At the concentration $\mu = 2$ kg/m^3, each cubic meter of air contains up to 10^{10} particles with the size of 30 μm, whose content in the initial feed is 10% only. Air flow through the separator amounts to 20,000 m^3/h. Visually, the process is purely chaotic, and its result proves to be strictly deterministic. Such stability can be explained only from the standpoint of statistical analysis of parameters and results of the process under study.

1.3.4 Flow Velocity and Particle Size

Using separation curves, we have experimentally revealed general rules of the separation process for apparatuses of any configuration and height separating different natural and ground powdered materials. These rules are based on the affinity of fractional separation curves.

By way of example, Fig. 1.6 shows an experimental dependence of separation of different narrow size classes of ground quartzite on the air flow velocity in a cascade classifier. All these curves merge into a single line (Fig. 1.10) when a dimensionless parameter

$$Fr = \frac{gx}{w^2},$$

where x is the average size of narrow size class particles, m; g is gravity acceleration, m/s^2, and w is air flow velocity, m/s, as shown along the abscissa axis.

Affinization of separation curves takes place in turbulent flows of a continuum, which was experimentally confirmed for more than 150 designs of gravitational classifiers. The mentioned criterion Fr can be applied only to the analysis of separation of materials with the same density.

However, this rule also holds at the separation of materials of different densities in the same separator. In the course of special investigations, each of the materials was separated both individually and in a mixture with other materials. The obtained results lead to a unified affinized curve. Figure 1.11 shows such a curve obtained at the classification of materials having different grain size compositions and densities

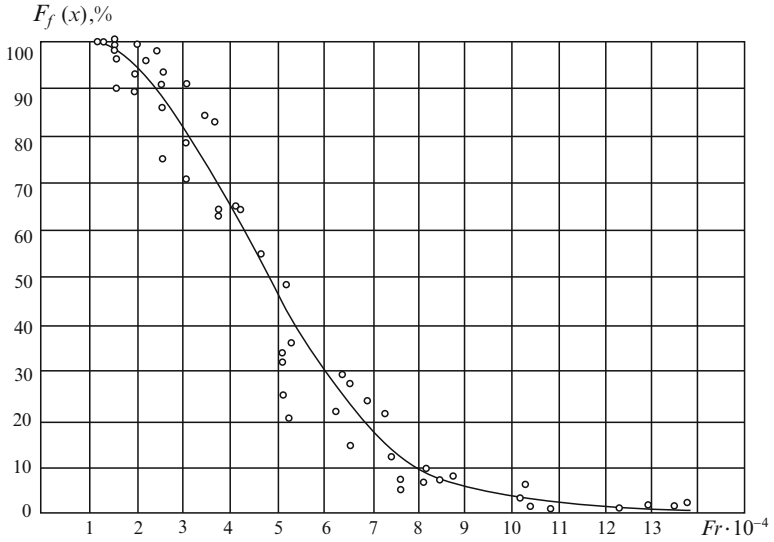

Fig. 1.10 Affinization of separation curves using the Froude criterion $F_f(x) = f(Fr)$

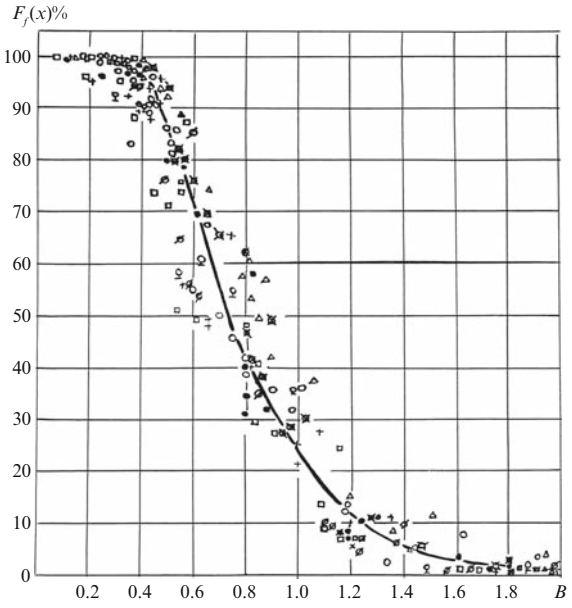

Fig. 1.11 Universal curve $F_f(x) = f(B)$ at the separation of materials of different densities and their mixtures

of 1,070, 1,980, 2,270, 2,675, 3,170, 4,350, 6,210, 7,810 and 8,650 kg/m^3. In this case, a generalized dimensionless affinization parameter

$$B = \frac{gx(\rho - \rho_0)}{w^2 \rho_0}$$

is shown along the abscissa axis, where ρ is the material density, kg/m^3; ρ_0 is the density of the medium, kg/m^3.

It is noteworthy that the same result was obtained in the experimental study of different gravitational air classifiers operating on industrial powders representing polyfractional mixtures with a broad size range from 50 μm to 10 mm. In this size range, separation occurs in a developed turbulence regime.

The affinity of separation curves obtained for materials of different compositions and densities on the same apparatus points to the existence of a strict regularity inherent to the entire class of gravitational separation processes.

The main point of this regularity is that any powdered material is equivalently separated in a specific apparatus according to its master curve. The character of such separation is not affected at all by any regime parameters, granulometric characteristics, solid phase concentration or boundary particle size, because at any changes in all these parameters, the separation proceeds according to the same curve.

A unified curve contains complete information about all possible two-phase flow regimes in a specific apparatus. If we turn to Fig. 1.11, the pneumatic transport regime takes place at $B < a$, the descending bed regime – at $B > b$, and a regime close to the boiling bed – at B_{50}.

Separation as such takes place within the interval of the parameter B variation from a to b. Respectively, fractional extraction varies from 100% to 0%.

It clearly follows from this dependence that no fractional separation values are obtained at random. It seems rather strange, because the process is characterized by an immense quantity of random factors changing both in space and in time. Hence, the influence of all these factors is leveled under actual separation conditions. How can it happen and why is this curve formed?

Until now, hovering conditions for particles of limiting size, or optimal separation conditions (i.e. those at which $B_{50} = \text{const}$) have been the main object of the theory and practice of gravitational separation.

It is evident from the obtained dependence that both this and any other separation has its own permanent condition in case of 10%, 20%, 35%, 70%, etc. extraction of a narrow class. Therefore, we can put a question of the conditions of equal extractability of different size classes. It is reached at a constant determining parameter of the process $B = \text{const}$, that is,

$$\frac{gx(\rho - \rho_0)}{w^2 \rho_0} = \text{const}$$

All this creates reliable prerequisites for the prediction of separation results and controlling of the process.

The position of the obtained universal dependence, which is unified and invariant with respect to all factors of the process listed above, in the coordinate system

$$F(x) = f(B)$$

reflects only the design of the classifier realizing the process. To obtain a different curve, one has either to introduce changes into the design, or to change boundary conditions, or else to replace the entire apparatus.

In fact, it is very surprising that in such a complicated process, which resists any accurate analysis, a rather clear determinate regularity has been revealed at a purely empirical level. From the standpoint of today's ideas of gravitational separation, it is impossible to explain or to understand how such regularity is formed.

Therefore, we approach this problem using the obtained regularities, from the standpoint of mass process taking into account solid phase interaction with the flow. Here a notional and physical analogy between the process under study and statistical mechanics arises.

As a matter of fact, two-phase flows are most close to the kinetic theory of gases. However, when drawing an analogy between these processes, many difficulties arose. Recently, some of these difficulties were overcome, and the first steps towards the development of a statistical approach to the theory of two-phase flows in critical regimes were made. This work is not completed yet, but it seems expedient for further development of the theory to sum up and discuss the obtained results in this book.

A basic feature of the statistical approach is that it is based on the determination of the state of a whole system, no matter whether it is large or small, comprising an infinite number of particles or one particle only. To make one more observation, we revert to Fig. 1.5.

Separation curves are characterized by two parameters – fractional extraction into a fine product $F_f(x)$ and fractional extraction into a coarse product $F_c(x)$. It is known that their sum in any point of the abscissa axis is

$$F_f(x) + F_f(x) = 100\%$$

Obviously, these two parameters can be replaced with one, which unambiguously characterizes the narrow class redistribution between two products. We call this parameter a separation factor, denote it as z and define it as fractional separation at the transfer of the point of origin in Fig. 1.5 from the 0 point to the 50% point in such a way that

$$\left.\begin{aligned} F_f(x) &= 50 + z_f \\ F_c(c) &= 50 - z_c \end{aligned}\right\} \tag{1.7}$$

Owing to the symmetry, the moduli $|z_f| = |z_c|$, and the range of variation of this parameter is $-50 \leqslant z \leqslant +50$. In the optimal regime, z = 0. We conventionally accept the direction upwards, that is into a fine product, as positive, and the direction downwards, that is into a coarse product, as negative. The difference between the extraction values is

$$F_f(x) - F_c(x) = 2z \tag{1.8}$$

and their sum is, naturally, 100%.

The value $2z$ shows the narrow class extraction imbalance between two product yields, or, in other words, total deviation of its extraction from equiprobable conditions, which are optimal.

The separation factor unambiguously characterizes the process results irrespective of the way of expressing fractional extraction (in percents, parts of a unity or even number of particles). This simple substitution will be very useful later on.

Before modeling a system consisting of particles in a flow, we should clarify the general approach to the state-of-the-art relationship between a model and a full-scale object.

Chapter 2
Principles of Modeling Processes in Moving Media

Abstract It is extremely difficult to model two-phase flows. A scientific model that should adequately reflect the process regularities is, to a considerable extent, "synthetic". It widely uses mathematical apparatus and knowledge from various areas of physics, hydraulics, mineralogy, etc. The scientific analysis is based on quantitative relations between various factors of the process. Mathematical models reflecting even idealized enough relations between the flow parameters allow the generation of principal similarity criteria based on their solution.

Keywords Nature · Model · Process parameters · Linearization of regularities · Simplification · Mathematical models · Model solution · Similarity criteria · Combinations of similarity criteria

2.1 Correlation Between a Full-Scale Process and Its Model

Critical regimes of two-phase flows are characterized by many peculiarities and interrelations. Most often it is impossible to take into account all of them thoroughly and accurately. Therefore, when performing a scientific analysis, the most general ones are singled out. As a result, a simplified idealized approximate enough model of the process is obtained.

Despite this, a serious scientific model is, to a large extent, synthetic. It widely uses mathematical tools and knowledge from various fields of physics, hydraulics, mineralogy, etc. Basing on these, a model is developed which should describe the process exactly enough and adequately reflect its regularities. When developing a mathematical model, we have to put aside a large number of process features. As a result, a model correlates with an object or a process as a caricature – with the reality. Anyway, any caricature should be recognizable, because it contains some features of a real object.

E. Barsky, *Critical Regimes of Two-Phase Flows with a Polydisperse Solid Phase*, Fluid Mechanics and Its Applications 93,
DOI 10.1007/978-90-481-8838-3_2,

Therefore, the results of mathematical investigation of a problem and constructive solutions based on these should not be considered as the only possible ones. Today, when physics of objects consisting of many elements is not sufficiently developed yet, different ways and results of solving the problem should not be ruled out, and it is rather difficult to choose the optimal variant of the solution. Therefore, the choice is made by comparing advantages and drawbacks of the obtained variants.

A scientific analysis is based on the establishment of quantitative relationships between different factors of a process. A strict analysis based on physical laws and mathematical analytical methods gives the most reliable results. Ideally, such an analysis does not need any experimental data. However, since cause-and-effect relations are complicated and diverse, such analysis can be realized very rarely, only in the simplest cases. Meanwhile, in the absence of strict theoretical solutions, practical engineering seeks additional opportunities.

Experimental data obtained on industrial equipment and laboratory experimental equipment are generalized. Based on these generalizations, empirical relations are derived, which are, as a rule, of a particular character. Their application beyond the range of parameters in which they were obtained leads to gross errors, and it is not always possible to extend the range of parameters in the experiments. For example, it is impossible to study a full-scale apparatus under laboratory conditions. Therefore, a transition from a laboratory model to a pilot plant is, most frequently, rather complicated and fraught with numerous mistakes and corrections.

Among the ways of simplification of regularities under study, the linearization of relationships between the phenomena under study and the results of the process is of special importance. The diversity and complexity of these relationships predetermine their nonlinear character, which makes difficult the analysis and mathematical description of the process. A transition to linear relationships significantly simplifies the analysis, but its accuracy is reduced. Therefore, it is important to allow the accuracy decrease only within the limits that do not distort the final result of the analysis to a considerable extent.

The diversity of relationships between the object properties and process parameters aggravated by insufficient understanding of physics of the processes leads to insuperable difficulties in finding quantitative regularities and to cumbersome and confusing calculations. This fact is usually passed over in silence. However, we should clearly point to a gap in the level of turbulent two-phase flow problems, their critical flows and potentialities of analytically derived equations. The arising difficulties call for simplifications both in the derivation of equations and in unambiguity conditions, which leads to accuracy loss. In such cases, numerical methods are frequently used.

Numerical methods of solving differential equations are associated with specific parameters of the process and limited by the accepted range of their variation. The obtained results are not of general character and can be used in a particular case.

Attempts to solve theoretical equations by numerical methods have been made in a sufficiently wide range of variables. Then empirical relationships have been matched to suit the obtained results. Because of a large number of factors, the

realization of this method is highly labor-consuming. Besides, it does not guarantee the accuracy of the obtained results.

A transition to generalized variables composed of elementary factors of the process according to certain rules facilitates, to some extent, the overcoming of this situation. These new variables are dimensionless and have a certain physical meaning. They allow establishing connection between generalizing complexes that combine the process factors, and not between the process factors, which are numerous.

The correlations obtained in generalizing complexes possess the following features:

– They are more compact than relationships with dimensional factors.
– They admit analytical solutions in a more laconic form.
– They are useful for the formalization of experimental data.
– They allow calculations in any system of units because they are dimensionless.

It should be emphasized that such combination of factors is not formal. In real processes the influence of individual factors is revealed jointly, and not separately. Therefore, if these factors are combined into a complex, the latter reflects the overall status of the process.

The use of generalized variables involving several factors each, leads to a more general description of a process, since one value of a complex can be realized, strictly speaking, at an infinite number of combinations of numerical values of the factors involved. Hence, these complexes can describe not only single phenomena or processes, but also a group of similar phenomena and processes, for which these complexes have the same numerical value. This is the basis of the notion of physical similarity. Therefore, such complexes are called similarity criteria. They are used in laboratory simulation of complicated processes and apparatuses, in the processing of experimental data and in analytical solving of technological problems. Beyond any doubt, the introduction of similarity criteria is an important stage in the development of science.

It has turned out that cumbersome differential equations derived by analytical methods are valuable *per se*. When initial conditions and unambiguity conditions are used, it is practically impossible to obtain their exact solution. However, on the basis of these equations, similarity criteria can be correctly formulated without solving them. These criteria allow a competent setting of an experiment and processing of the obtained results.

2.2 Mathematical Models Construction

Principal analytical equations of moving flows were obtained proceeding from elementary simple models. Thus, principal equations of hydraulics are based on balance correlations without taking into account such important flow characteristics as the flow structure, turbulence with its developed spectrum of fluctuations or conditions on channel walls, but only the respective balances.

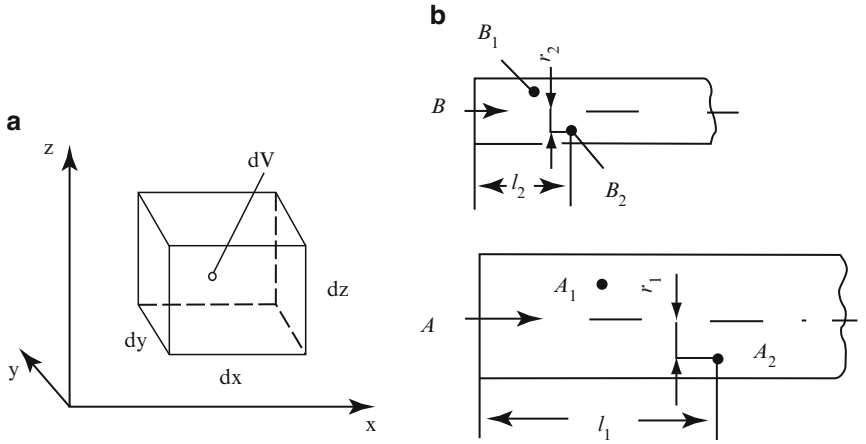

Fig. 2.1 On the modeling of processes in moving media: (**a**) motionless elementary volume; (**b**) on the notion of similarity in flows

However, even such an analytical model allows determining principal regularities and similarity criteria.

Let us examine this procedure, because later on, we will develop a model of critical regimes of two-phase flows using similar methods.

First consider the kinetic aspect of the problem. We place a motionless infinitesimal elementary cuboid with the edges d_x, d_y, d_z into a flow (Fig. 2.1a) and consider the flows through pairs of its parallel faces $dxdy$, $dxdz$ and $dydz$ in an infinitesimal time interval dt, as well as changes inside a certain elementary volume $dV = dxdydz$.

During the time interval dt, an elementary amount of moving medium equal to

$$dG_x^+ = \rho w_x dydzdt$$

enters a motionless contour along the x-axis through the face $dydz$ at the velocity w_x, and the amount

$$dG_x^- = \left[\rho w_x + \frac{\partial(\rho w_x)}{\partial x}\right] dydzdt$$

goes out through a parallel face. Here ρ is the density of the medium in some point of the contour; w_x is the velocity along the x-axis at some point of the contour. After the removal of brackets and cancellations, the difference between dG_x^+ and dG_x^- for the x-axis amounts to

$$-\frac{\partial(\rho w_x)}{\partial x} dxdydzdt = -\frac{\partial(\rho w_x)}{\partial x} dVdt.$$

Similar differences for y- and z-axes can be written as

$$-\frac{\partial(\rho w_y)}{\partial_y} dVdt \quad \text{and} \quad -\frac{\partial(\rho w_z)}{\partial_z} dVdt.$$

The amount of mass in the volume dV at the moment t equals ρdV. Since ρ can vary along the coordinates (x, y, z) and with time (t), the change in mass inside this volume by the moment of time $t + dt$ can be written using partial derivatives:

$$\frac{\partial(\rho dV)}{\partial t} dt = \frac{\partial \rho}{\partial t} dVdt.$$

Now we bring together the obtained elements of balance and, after reducing by dV and dt, we obtain

$$-\frac{\partial \rho}{\partial t} = \frac{\partial(\rho w_x)}{\partial x} + \frac{\partial(\rho w_y)}{\partial y} + \frac{\partial(\rho w_z)}{\partial z}.$$

We can rewrite it in a different form:

$$\frac{\partial \rho}{\partial t} + \frac{\partial(\rho w_x)}{\partial x} + \frac{\partial(\rho w_y)}{\partial y} + \frac{\partial(\rho w_z)}{\partial z} = 0.$$

This is an equation of the flow continuity. Integration of this equation using specific unambiguity conditions leads to the mass conservation law in an integral form.

Now consider the dynamic aspect of the problem. A crucial problem in the analysis of the momentum or impulse transfer is to determine pressure (p) and velocity (w) in a certain point of the flow at an arbitrary moment of time t:

$$p = p(x; y; z; t); \quad w = w(x; y; z; t).$$

We consider an elementary cuboid again.

First we carry out the analysis as applied to one coordinate axis (x). The obtained results can be extended to other axes (y, z). We examine, one after another, forces of various nature.

1. Normal forces (pressure) acting along the x-axis on the left face $dydz$ are equal to $pdydz$. On the right, a force $\left(\rho + \frac{\partial \rho}{\partial x} dx\right) dydz$ acts on the parallel face. The difference between these normal forces is

$$pdydz - \left(p + \frac{\partial p}{\partial x} dx\right) dydz = -\frac{\partial p}{\partial x} dxdydz = -\frac{\partial p}{\partial x} dV.$$

2. Tangential forces (of internal friction, shear, viscosity – τ)

The force $\tau_1 dxdy$ acts along the lower face, and for the upper face we can write $\tau_2 dxdy$. We denote the velocity on the lower face by w_x; at the transition to the upper face along the z-axis, the velocity acquires a certain value $w_x + \frac{\partial w_x}{\partial z} dz$.

According to the Newton law, the relation between the tangential force and velocity gradient in a liquid or gas is linear, that is,

$$\tau = -\mu \frac{dw}{dz},$$

where μ is the dynamic viscosity coefficient of the medium. Taking this into account, we can write the following for the upper and lower faces:

$$\tau_1 dxdy = -\mu \frac{\partial w_x}{\partial z} dxdy;$$

$$\tau_2 dxdy = -\mu \frac{\partial}{\partial z} \left(w_x + \frac{\partial w_x}{\partial z} dz \right) dxdy.$$

After the removal of brackets and cancellations, the difference between these forces amounts to

$$(\tau_1 - \tau_2) dxdy = \mu \frac{\partial^2 w_x}{\partial z^2} dxdydz = \mu \frac{\partial^2 w_x}{\partial z^2} dV.$$

Similar tangential forces along the x-axis act on other pairs of faces, and by analogy with the above expressions, we can write

$$\mu \frac{\partial^2 w_x}{\partial_y^2} dV \text{ and } \mu \frac{\partial w_x^2}{\partial_x} dV.$$

Total balance of all tangential forces along the x-axis is expressed by the sum

$$\mu \left(\frac{\partial^2 w_x}{\partial x_2} + \frac{\partial^2 w_x}{\partial y^2} + \frac{\partial w_x}{\partial z^2} \right) dV = \mu \nabla^2 w_x dV$$

where $\nabla^2 -$ is the Laplace operator (Laplacian).

3. External mass forces

External mass forces also act on a mass of liquid or gas with the density ρ in the volume dV. We denote a projection of a resultant unit mass force along the x-axis by P_x. Then the total force acting on the volume under study is $P_x \rho dV$.

4. According to the Newton law, inertia force equal to a product of the volume mass and its acceleration along the x-axis acts on this volume:

$$\rho dV \frac{dw_x}{dt}.$$

Making a total balance of these four components, after reducing by dV with respect to the x-axis, we can write

$$-\frac{\partial p}{\partial x} + \mu \nabla^2 w_x + P_x \rho = \rho \frac{dw_x}{dt}.$$

Dividing each component by ρ and substituting $\frac{\mu}{\rho} = V$ (kinematic viscosity coefficient), we can finally write:

$$\frac{1}{\rho}\frac{\partial p}{\partial x} = P_x - \frac{\partial w_x}{d\tau} + v\nabla^2 w_x.$$

If we write, by analogy, similar expressions for y and z axes, the obtained system of equations is called a Navier–Stokes equation or the principal equation of hydrodynamics.

Note that when deriving equations in this chapter, we neglected the signs of differences in all intermediate relationships.

According to mathematical rules, it was assumed that all these increments are positive, and the sign should appear when we determine integration limits or unambiguity conditions (for example, boundary conditions) or specify conditions of the process (for example, gravity force is always directed opposite to an ascending flow).

It is accepted that the system of Navier–Stokes equations together with the continuity equation completely describe the motion of a moving medium. To obtain an unambiguous solution of the system even in the simplest case of a hollow pipe, it is necessary to specify initial velocity field values in space and time and to take into account the fact that the velocity should be zero on the channel walls and on the surface of all solids submerged into the flow. The solution of this system of equations was discussed in many papers.

As early as in 1920s, L. Keller and A. Friedman showed that in order to determine statistical moments of any order for hydrodynamic fields of single-phase turbulent flows, it is necessary to solve an infinite system of equations, that is this system is not closed. It is possible to solve this system using various assumptions idealizing the moving medium. Idealized flows of Newton, Euler, Couette, Poiseille, Haden, etc. are well known. These solutions are of a certain theoretical interest, but of no practical importance in the general case.

Thus, it is impossible to find an exact solution of the obtained system of equations. However, it contains information on the flow motion that can be obtained in the form of dimensionless complex parameters. It becomes possible to determine these parameters using the methods of similarity theory.

2.3 Similarity Criteria Determination

Groups of processes, phenomena or objects that can be mathematically described using similarity criteria are assumed to be similar. The notion of geometrical similarity is studied as early as in secondary school. Physical similarity has a different meaning. One can assume that two physical phenomena are similar, if the respective characteristics of this phenomenon at analogous points of geometrically similar systems differ only by a coefficient that is constant for all the points. Mathematical description of such systems is identical. If we deal with two geometrically similar facilities (Fig. 2.1b), the larger one is usually called an apparatus (A), whereas the smaller one – a model (B). Let moving media with different properties (density, viscosity, velocity, heat capacity, etc.) flow through these facilities.

We choose two pairs of similarly located points A_1 and A_2, B_1 and B_2 in these systems. Geometrical parameters of each pair are characterized by a certain relationship of the following type:

$$\frac{x_1}{D_1} = \frac{x_2}{D_2} = \cdots$$

The ratio

$$\frac{x_1}{x_2} = \frac{D_1}{D_2} = \cdots = m_1.$$

By definition of physical similarity, for any pair of analogous points A_1 and B_1, A_2 and B_2 and any other pairs, the following equalities should be satisfied:

$$\frac{\rho_1}{\rho_2} = m_\rho; \quad \frac{\mu_1}{\mu_2} = m_\mu; \quad \frac{w_1}{w_2} = m_w; \quad \frac{c_1}{c_2} = m_c, \text{ etc.}$$

In these expressions, m_i are similarity factors. Naturally, they are different for different parameters ($m_\infty \neq m_w \neq m_c \neq \cdots$), but have a constant value of the same parameter in any pair of analogously located points. Each similarity factor plays the role of a kind of scale of the respective physical magnitude.

The notion of similarity factors is the basis for deriving similarity criteria. By way of example, we derive one of such criteria from the flow continuity equation. For two geometrically similar flows, we can write

$$\frac{\partial \rho_1}{\partial t_1} = \frac{\partial (\rho_1 w_1)}{\partial x_1} + \cdots = 0,$$

$$\frac{\partial \rho_2}{\partial t_2} = \frac{\partial (\rho_2 w_2)}{\partial x_2} + \cdots = 0.$$

Other summands are omitted here, because they structurally coincide with the second summands. We apply scaling transformations to these two equations:

$$\rho_1 = m_\rho \rho_2; \quad t_1 = m_t t_2; \quad w_1 = m_w w_2; \quad x_1 = m_l x_2.$$

Geometrical similarity factor m_i is constant for all coordinates (x, y, z), as well as for linear dimensions l_1 and l_2.

Let us substitute the values of all process parameters of the apparatus into the first equation, expressing them through the corresponding similarity factors and process parameters of the model. Then, after the removal of constant multipliers from the derivatives, we obtain a new expression for the apparatus through the parameters of the model:

$$\frac{m_\rho}{m_t}\frac{\partial \rho_2}{\partial t_2} + \frac{m_\rho m_w}{m_l}\frac{\partial(\rho_2 w_2)}{\partial x_2} + \cdots = 0.$$

Compare the obtained expression with the above continuity equation for the model. Their adequacy is possible only if the complexes comprising similarity factors can be factorized and reduced, because the right-hand part is zero. It means that these complexes are equal:

$$\frac{m_\rho}{m_t} = \frac{m_\rho m_w}{m_l}.$$

Here we can reduce by the factor m_ρ and finally obtain:

$$\frac{1}{m_t} = \frac{m_w}{m_l}.$$

However, it is well known that

$$m_t = \frac{t_1}{t_2}; \quad m_w = \frac{w_1}{w_2}; \quad m_l = \frac{l_1}{l_2}.$$

Substitute these values into the final expression:

$$\frac{t_2}{t_1} = \frac{w_1}{w_2} \cdot \frac{l_2}{l_1}$$

and collect magnitudes with the same indices in different parts of the equality. We obtain:

$$\frac{w_1 t_1}{l_1} = \frac{w_2 t_2}{l_2} = \frac{wt}{l} = idem.$$

It means that the obtained result is valid for all similar flows. This complex is dimensionless. The coincidence of the numerical value of a dimensionless complex or group of complexes is a necessary and sufficient similarity condition for several systems, objects, flows, processes, etc. The obtained complex is called a homochronism criterion and denoted by

$$Ho = \frac{wt}{l}.$$

Most often, physical criteria are called after great scientists and denoted by the first two letters of their names.

The physical meaning of the homochronism criterion is clear from the prerequisites of the analysis – two opposite effects are compared, namely, forced medium transfer and accumulation.

Growing *Ho* value shows that the influence of the factor in the numerator grows, that is mass transfer grows. With decreasing *Ho*, the role of the factor in the denominator grows, that is mass accumulation is predominant.

In case of stationary processes, where mass accumulation in the working volume does not take place, *Ho* criterion degenerates, and its numerical values tend to infinity.

Note another important aspect. In many cases, total geometrical similarity is not necessary, an approximate one being sufficient. Geometrical dimensions can affect the course of a process in different ways. For example, it is clear that the shelf thickness in a cascade classifier does not affect the character of the separation process. Therefore, it does not require the fulfillment of geometrical similarity of the type

$$\frac{\delta_1}{l_1} = \frac{\delta_2}{l_2}.$$

A less obvious example concerns the velocity profile of a flow entering the classifier. Its formation is completed at the channel inlet, and then the value of the velocities does not considerably change. Beyond the channel inlet, the influence of the longitudinal coordinate degenerates, and in this sense, geometrical similarity becomes non-obligatory.

Using the same pattern of reasoning, we make an attempt to derive a similarity criterion from the system of Navier–Stokes differential equations. For the process under study, it is most convenient to analyze similar flows with respect to the z-axis. We can write the following for an apparatus and a model at their analogous points:

$$\frac{1}{\rho_1}\frac{\partial p_1}{\partial z_1} = P_1 - \left(w_1\frac{\partial w_1}{\partial z_1} + \cdots\right) + v_1\left(\frac{\partial^2 w_1}{\partial z_1^2} + \cdots\right),$$

$$\frac{1}{\rho_2}\frac{\partial p_2}{\partial z_2} = P_2 - \left(w_2\frac{\partial w_2}{\partial z_2} + \cdots\right) + v_2\left(\frac{\partial^2 w_2}{\partial z_2^2} + \cdots\right).$$

We express all apparatus characteristics through similarity factors and model characteristics:

$$\rho_1 = m_\rho \rho_2; \quad p_1 = m_\rho p_2; \quad P_1 = m_m P_2; \quad z_1 = m_l z_2; \quad w_1 = m_w w_2; \quad v_1 = m_v v_2.$$

Note that m_m is the same for all mass forces. Now we substitute all these ratios into the first equation:

$$\frac{m_p}{m_\rho m_l}\frac{1}{\rho_2}\frac{\partial \rho_2}{\partial z_2} = m_m P_2 - \frac{m_w^2}{m_l}\left(w_2\frac{\partial w_2}{\partial z_2} + \cdots\right) + \frac{m_v m_w}{m_l^2} v_2\left(\frac{\partial w_2}{\partial z_2^2} + \cdots\right).$$

According to the meaning of this mathematical operation, the second derivative is a quotient of the value to be differentiated, divided twice by the argument. Therefore m_l in the last expression is squared. Hence, following the same reasoning as in the previous case,

$$\frac{m_p}{m_\rho m_l} = m_m = \frac{m_w^2}{m_l} = \frac{m_v m_w}{m_l^2}.$$

The physical meaning of these parts of the equality is as follows: $\frac{m_p}{m_\rho m_l}$ – pressure forces; m_m – mass forces; $\frac{m_w^2}{m_l}$ – inertia forces; $\frac{m_v m_w}{m_l}$ – viscosity forces. Usually these parts of the equality are examined pairwise.

1. Comparison of pressure and inertia forces:

$$\frac{m_p}{m_\rho m_l} = \frac{m_w^2}{m_l}.$$

After reducing by m_l and substituting multipliers

$$m_\rho = \frac{\rho_1}{\rho_2}, \quad m_p = \frac{p_1}{p_2}, \quad m_w = \frac{w_1}{w_2},$$

we obtain

$$\frac{p_1\rho_2}{p_2\rho_1} = \frac{w_1^2}{w_2^2},$$

and hence

$$\frac{p_1}{\rho_1 w_1^2} = \frac{p_2}{\rho_2 w_2^2} = \frac{p}{\rho w^2} = Eu = idem.$$

Here Eu is Euler's criterion. It is used to determine the relationship of inertia and pressure forces. In practical problems, most often the pressure drop in a certain

interval is of interest, and not the absolute value of pressure. Therefore, a somewhat different expression is used:

$$Eu = \frac{\Delta p}{\rho w^2}.$$

2. Comparison of mass and inertia forces

In this case,

$$m_m = \frac{m_w^2}{m_l}.$$

Along the vertical z-axis, a value numerically equal to acceleration g corresponds to a unit mass gravity force. Taking this into account, substitution of $m_{w_1} m_l$ and $m_m = \frac{g_1}{g_2}$ values leads to

$$\frac{g_1}{g_2} = \frac{w_1^2 l_2}{w_2^2 l_1}.$$

Hence

$$\frac{g_1 l_1}{w_1^2} = \frac{g_2 l_2}{w_2^2} = \frac{gl}{w^2} = Fr = idem$$

where Fr is Froude's criterion, which is a measure of the ratio of mass forces and inertia forces. The comparison of these forces predetermines the character of critical flow processes under study, and therefore, this criterion plays a crucial role, which is confirmed experimentally.

3. Comparison of inertia and viscous forces

$$\frac{m_w^2}{m_l} = \frac{m_v m_w}{m_l^2}.$$

After reducing by m_w/m_l and substituting all similarity factors, we can obtain

$$\frac{w_1}{w_2} = \frac{v_1 l_2}{v_2 l_1}.$$

Hence

$$\frac{w_1 l_1}{v_1} = \frac{w_2 l_2}{v_1} = \frac{wl}{v} = Re = idem.$$

Thus, we obtain the Reynolds criterion, which is widely used for describing liquid and gas flows, as well as particles displacements with respect to moving media.

Usually the linear dimension in the Reynolds criterion is either channel diameter or particle diameter:

$$Re = \frac{wd}{v}.$$

4. To derive other similarity complexes, these three principal ones can be used, for example, a relationship between the gravity force and viscosity force. In this case, we can write $Fr \cdot Re$. Other combinations of similarity criteria having a clear physical meaning can be also obtained.

Usually it is impossible to establish quantitative relationships between similarity criteria purely theoretically. In each specific case they are established by means of a specially set experiment. These relationships are called criterial equations of $Eu = f(Re)$ type. Such relationships are valid only within experimentally checked ranges of similarity criteria variation.

Similarity criteria should not be considered as parameters determining the ratio between respective forces, because the value of this ratio is different at different points of the flow. They should be considered as a measure characterizing correctly the relationship between respective forces. For example, the higher the Reynolds number, the larger are inertia forces with respect to friction forces in a specific flow.

Chapter 3
System of Particles of the Same Size Class in a Critical Flow

Abstract Two-phase flow is a mass system. Kinetic approach to such systems makes it necessary to take into account interactions of particles of various sizes in a flow and their interactions with the channel walls. Having overcome mathematical complications, a model of particles interactions with the channel walls was developed. The solution of this model leads to relations obtained earlier by various authors in a purely empirical way. A definition of a statistical system of particles in a flow it given and substantiated. Mathematical equations describing a statistical system of particles are derived. The solution of these equations made it possible to substantiate main parameters characterizing flow regimes under study.

Keywords Statistical system · Probability · Reliability · Stability · Self-similarity · Averaging over an ensemble · Separation factor · Potential separation · Lifting factor

3.1 Dynamics of Mass Motion of Particles in a Flow

We mentally single out particles of a certain *i*-th size class in a two-phase ascending flow moving in a critical regime and examine the behavior of a continuum of such particles.

Particle collisions are unlikely, since their velocity values are within a narrow range, and even if such collisions take place, their intensity is low. Particles of this fixed size class collide with particles of other classes, whose mean velocities are essentially different.

Particle collisions, their irregular shapes, non-uniformity and fluctuations of velocity and concentration fields, Magnus' effect and other random factors result in the appearance of a radial component in the motion of particles.

As follows from experimental studies, the motion of particles in a two-phase flow is practically always non-parallel to the channel axis. This leads to mass collisions of particles with the walls confining the flow. To confirm this fact, it is sufficient to mention a well-known effect of the wear of pneumatic transport

E. Barsky, *Critical Regimes of Two-Phase Flows with a Polydisperse Solid Phase*,
Fluid Mechanics and Its Applications 93,
DOI 10.1007/978-90-481-8838-3_3,

pipelines and gravitational separation apparatus walls. Numerous researches show that turbulent fluctuations of the medium considerably affect the trajectories of fine particles only. For coarser particles, their collisions are the main cause of deviations from rectilinear trajectories. The influence of this mechanism on the intensity of transverse displacements grows, in comparison with other stochastic factors, with increasing particle size.

Therefore, the instantaneous velocity of particles of any size can be represented as consisting of two components – axial and radial. The ratios between their mean values are determined by particular conditions. The radial component is the cause of random impact interactions of particles with channel walls.

At each collision, a part of kinetic energy is lost. The magnitude of this loss depends on elastic properties of the disperse material and solid wall, as well as on the state of their surface in the contact point. After the collision, a particle loses a part of its velocity. This loss is further compensated at the expense of the carrier flow energy, since the particle accelerates in it gaining the initial velocity values.

If the apparatus is large enough, after a certain time interval the same particle can collide again with the wall, since the causes generating radial components remain. Hence, particle interaction with a wall in a two-phase flow is of a jump-wise, fluctuating character. Evidently, such interaction leads to an increase in the total flow resistance, that is an additional force acts against the motion of each narrow size class.

It is perfectly clear that all the components of the interaction under study are of markedly random nature.

It is necessary to convert the solution of such stochastic model into a deterministic one using calculations of mathematical expectations of random values. This makes it possible to consider the system as a deterministic one and to reveal a general character of the regularities.

To perform basic calculations, we single out an element with the height of Δl (Fig. 3.1) in a hollow apparatus and denote by F the cross-section area of the apparatus and by D – its equivalent diameter.

We assume that in a stationary process, the total amount of material passing through this section in both directions per unit time at a certain flow velocity w amounts to:

$$\Delta G = \sum_{k} \Delta G_i,$$

where ΔG_i is the weight flow rate of the i-th fraction passing through the section under study, kg/s; k is the quantity of distinguishable size classes in a mixture.

The weight of the i-th narrow size class located in the section Δl can be determined as

$$\Delta G_i = g m_i n_i,$$

where m_i is an average mass of a particle of i-th narrow size class; n_i is the number of particles of i-size in the section Δl.

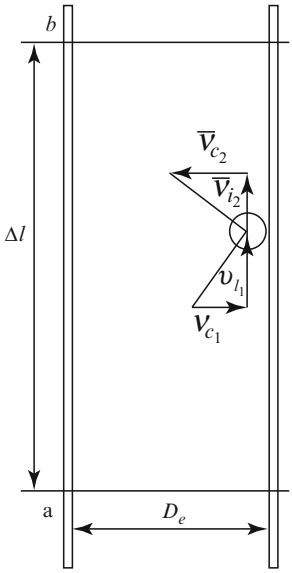

Fig. 3.1 Transformation of particle velocity at its interaction with a wall

On the other hand, we can write:

$$\Delta G_i = F v_i \gamma_i,$$

where v_i is the mean velocity of narrow-class particles, m/s; γ_i is the weight flow rate content of particles in a unit volume, kg/m^3.

Hence,

$$\gamma_i = \frac{\Delta G_i}{F \cdot v_i}.$$

The weight of solid particles of this class in a flow section with the height of Δl is equal to $\gamma_i \cdot F \cdot \Delta l$. It is practically impossible to determine the force experienced by the wall at the collision of each separate particle with it. It is sufficient to determine an average force arising at the collision of many particles of the same average size with the wall, if their velocities are known and the collisions are perfectly elastic. In this case, the force acting on the wall can be determined on the basis of the second Newton law. It is equal and opposite in sign to the change in the momentum of particles colliding with the wall per unit time.

Irrespective of particle velocity direction in space, it can be always decomposed into components, one of them being perpendicular to the apparatus wall and another – parallel to the flow axis (Fig. 3.1). For particles of the *i*-th size class:

v_i is an axial component of particles velocity before the collision;

v_r is a radial velocity component before the collision;

$\overline{v_i}$ is an axial velocity component after a reflection from the wall;

$\overline{v_r}$ is a radial velocity component after the reflection.

If a particle with the mass m_i has a radial velocity component v_r, the respective momentum equals $m_i v_r$. After a collision, the particle acquires a radial velocity component $\overline{v_r}$, whose value is determined by the angle of attack and the elasticity of the particle and the wall in their contact point. Denoting by k a generalized average transformation coefficient, we can write:

$$\overline{v_r} = -kv_r$$

The change in the momentum for one particle amounts to:

$$\Delta p = m_i v_r - m_i \overline{v}_r = m_i v_r (1 + k).$$

Mass of the particles of the narrow size class under study reaching the apparatus walls per unit time is proportional to the material contents in each volume unit of the apparatus, to the radial velocity component and to the wall area, that is

$$\Delta G_i = \psi \cdot \theta \cdot \Delta l v_r \cdot \frac{\gamma_i}{g},$$

where θ is the apparatus perimeter; ψ is a generalized proportionality coefficient.

If we denote by n_0 the number of particles of a given class reaching the wall per unit time, the total change in their momentum per unit time is:

$$\Delta P = \sum_n \Delta p = \sum_n m_i v_r (1 + k) = n_0 m_i v_r (1 + k).$$

Only the particles that are located at a distance not exceeding v_r from the wall, that is those contained in the volume of a ring with the lateral side area $\theta \cdot \Delta l$ and thickness of v_r, can reach the wall in a unit time. We denote the average quantity of particles in a unit of space by

$$n = \frac{\gamma_i}{m_i} = \frac{\Delta G_i}{F \cdot \Delta l m_i g}.$$

The quantity of these particles in an annular space is

$$N_0 = n v_r \theta \cdot \Delta l = \frac{\Delta G_i v_r \cdot \theta}{F m_i g}.$$

Due to the absence of direct experimental data, we can suppose that owing to stochasticity, approximately half of particles in this space moves towards the wall, and another half from the wall. We can write:

$$n_0 = \phi N_0,$$

where $\phi < 1$ (according to statistical meaning, $\phi = 0.5$). The average pressure experienced by the surface in a unit time equals

$$P_i = \phi \frac{\Delta G_i v_r \cdot \theta}{F m_i g} m_i v_r (1 + k).$$

The pressure acting on a unit surface is

$$\rho_i = \frac{P_i}{Q \cdot \Delta l} = \phi \frac{\Delta G_i v_r^2 (1 + k)}{gF \cdot \Delta l} = c \frac{\Delta M_i}{V} v_r^2,$$

where $V = F \cdot \Delta l$ is the volume of the section under study, m^3; $\Delta M = \frac{\Delta G_i}{g}$ is the mass of i-th class material in this section, kg/m^3; $c = (1 + k)\phi$ is a common aspect ratio.

Note that

$$\frac{\rho_i V}{v_r^2} = c \Delta M_i. \tag{3.1}$$

Evidently,

$$q_{\sum} = \sum_i q_i = \frac{\sum\limits_i \Delta M_i v_r^2}{V}.$$

It means that the specific pressure experienced by the wall on the part of disperse flow particles is proportional to the product of the mass of these particles per unit volume by the squared radial velocity component for each size class. This force acting normally on the apparatus wall produces a friction force with a specific value

$$\tau_i = f g_i,$$

where f is the friction coefficient between the wall and the material.

It follows from numerous publications that at the material concentration up to $\mu = 3\,\mathrm{kg/m^3}$, the magnitude of radial velocity component of moving particles is proportional to the particles velocity v_i, that is we can write

$$v_r^2 = \phi_1 v_i^2,$$

hence

$$\tau_i = cf\phi_1 \frac{\Delta M_i}{V} v_i^2 = \lambda \frac{\Delta G v_i^2}{2g \Delta l F},$$

where $\lambda = \frac{1}{2cf\phi_1}$.

The total force of resistance to the motion of particles of i-th size at the flow section under study amounts to

$$T_i = \lambda \frac{\Delta G_i}{2g} \frac{v_i^2 \theta \cdot \Delta l}{F \cdot \Delta l} = \lambda \frac{\Delta G_i \cdot v_i^2}{2gD_e},$$

where D_e is an equivalent diameter of the channel.

This formula was derived purely empirically and is widely used in calculations of pneumatic transport. Friction coefficients in the form of

$$\lambda_z = \lambda \frac{v_i}{w}$$

were experimentally and theoretically determined by Gasterschtadt, Zegler, Uspensky and others for the conditions of pneumatic transport. Two conclusions can be made from the analysis above:

1. The magnitude of λ_z coefficient cannot be determined by the total pressure drop in a transmission pipeline. This method considerably overestimates the coefficient magnitude, because it involves not only friction losses, but also other losses.
2. The model under study describing a narrow class interaction with the wall has been developed correctly, since it leads to already known empirical results.

3.2 Definition of a Statistical System

The behavior of a set of solid particles constituting, together with a continuous medium, a two-phase flow can be described, strictly speaking, from the standpoint of classical mechanics. In principle, the behavior of the whole continuum can be specified by the behavior of each separate particle, writing

$$\frac{dv_i}{dt} = P_i; \qquad \frac{dx_i}{dt} = v_i$$

for it, or

$$\frac{d^2x}{dt^2} = P_i,$$

where P_i is the force acting on the i-th particle related to a unit mass; x_i is the radius-vector of the i-th particle; v_i is the velocity vector of the i-th particle.

In general, P_i is composed of gravitational forces, flow forces and interaction of the i-th particle with other particles and walls confining the flow. To determine in full the behavior of the system using such approach, we have to solve $6N$ (N being

the number of particles in a flow) differential equations of the first order with $6N$ unknown quantities. It is also necessary to specify $6N$ initial values of the parameters. It is perfectly clear that this problem cannot be solved even by high-speed computers not only because of a large number of particles, but also because all these equations are interconnected, since the force exerted by a specific particle at any moment of time is a function of the positions of all other particles of the system, that is

$$P_i = f(x_j) \qquad (j = 1; 2; 3; \ldots N).$$

Supposing that, anyway, we manage to solve this problem having spent lots of time and means, the obtained information would be absolutely useless, because one can hardly make any concrete conclusions on the basis of enormous amount of data determining the force value and direction of each particle at various moments of time. Note that the quantity of particles in the apparatus under the conditions of fractionating powders is on the order of $N \approx 10^{10}$.

Clearly, such method of solution leads to a deadlock. However, there is another way, too. Referring to the history of scientific analysis, one can see its two sources. The first one comprises dynamic Newton's laws (classical mechanics). They describe well the behavior of solitary objects, even complicated ones such as the planetary system, where the past and the future play the same part. This is due to the fact that the notion of time appears in the second Newton law in the second power only, which makes it invariant with respect to time reversal ($t \rightarrow -t$).

The second source is based on thermodynamics that started developing in the beginning of the nineteenth century. It deals with enormous numbers of particles (molecules) and irreversible processes. Here the number of particles is comparable to the Avogadro constant (on the order of 10^{23}). Irreversibility in thermodynamics is connected with the notion of entropy, which was called a time arrow by A. Eddington. This notion appeared in connection with technical problems to be solved, but very soon acquired a cosmological status.

That was a revolution in science, because the existence of irreversible processes contradicted time-reversible notions of dynamics. Note that in the beginning of the twentieth century classical mechanics gave way to quantum theory and relativity theory. However, the contradictions remained, since in these theories principal dynamic laws are time-reversible.

The process under study is markedly irreversible. Since 1872, when L. Boltzmann introduced a statistical definition of entropy, it has been considered as a measure of disorder of a system. As a rule, natural processes occur with increasing disorder.

The main difference between reversible and irreversible processes is that the latter give rise to entropy. However, the relationship between dynamics and entropy is not so simple, and not all dynamic processes call for the use of the notion of entropy. For example, the Earth's travel around the Sun can serve as an example of a case that may be described by equations symmetric in time neglecting the irreversibility (high and low tides).

However, most of natural systems reveal a chaotic irreversible behavior, and the notion of entropy has a physical meaning of the time arrow for them.

All this predetermines, to a certain extent, the analogy between critical regimes of two-phase flows and thermodynamics, especially in the area of gas laws.

Hence, it is clear that such problems should be solved by statistical mechanics methods. Obviously, not only initial positions of particles, but also details of their interaction should be averaged. Practical result of such averaging is reduced to the necessity of operating with probabilities instead of reliabilities. Within such an approach, we cannot determine a position and velocity of a given particle, but only a probability of the realization of its various positions and velocities.

We make an attempt to consider this problem from the standpoint of a statistical approach. From this standpoint, it is necessary to connect the general behavior of the whole system with the behavior of its numerous parts. The study of such connections constitutes the subject of statistical mechanics. Since the system contains a great number of particles, we have to define a way of describing their averaged behavior and then connect it with final results of the separation process.

Here we can make use of some ideas of statistical mechanics – naturally, applying them to specific conditions of the problem under study. However, the specific character of two-phase flows calls for a fundamental reinterpretation of these ideas. We can mention three principal aspects of the main difficulties arising at the study of such flows from the standpoint of a statistical approach in comparison with gas systems.

First, gas systems are examined in statistical mechanics within a limited volume, and all possible directions of molecules motions are considered as equiprobable. In two-phase flows, a closed volume is out of question, and besides, the resulting flow motion has a preferred direction.

Secondly, a basic parameter in the statistical approach to gaseous systems is the potential energy of the continuum of particles determined by the temperature. As known, temperature change does not affect principal parameters of such flows.

The last but not least for the problem under study is that we are forced, for the first time in theory, to abandon generally accepted parameters of a system (temperature, energy, heat capacity, work, etc.) and introduce new parameters defining the extent of fractional separation, regimes of the medium motion, probability of the direction of particles motion, etc.

Nevertheless, we should unambiguously emphasize that the main ideas and methods of the statistical approach developed for gaseous systems are used in the study of the present problem. In this respect, it would be wrong to present the situation as utterly novel. The process under study is examined from the standpoint of statistical mechanics using main principles of thermodynamics and theory of gases, because, as we show below, there is a reliable conceptual and physical analogy between these processes.

Since we start considering this physical phenomenon from the standpoint of statistical mechanics, it is necessary to develop new terminology.

The general behavior of a two-phase system should be somehow connected with the behavior of the multitude of its components. The study of such kind of connections constitutes the subject of statistical mechanics.

When it is impossible to describe physical phenomena in terms of individual particles trajectories, one can resort to their description in terms of statistical ensembles.

It was determined experimentally that from the point of view of separation results, each narrow size class behaves in the process of separation autonomously, independently of the presence of other classes in the flow. Therefore, we examine one narrow size class consisting of similar particles. Since the system under consideration contains a large number of particles, it is necessary to define a way of describing averaged behavior of a particle and then connect it with the process results.

Boltzmann's theory of gases demonstrates that to develop a successful model of a process, one should not aim at its comprehensive description. It is sufficient to make up a simple scheme of the process, but it should reflect, to a certain extent, its essence.

In this respect, a characteristic example is the model of gas or other bodies temperature. As known, gas temperature is proportional to the kinetic energy of the motion of its molecules. Molecules move at random, interact with each other and with the walls of gas-containing vessel. No one would think of determining gas temperature taking into account all the elements of this complicated process. Usually, temperature is determined according to our natural perception of heat and cold as of something one-dimensional, allowing the arrangement of objects from the hottest one to the coldest. It is reflected in the structure of a thermometer with zero located in the middle of the scale, which makes its readings more visual. It is more convenient in comparison with a thermometer with zero at the bottom of the scale.

To develop a model, we examine a certain quantity of similar solid particles moving in any direction together with an ascending flow through a limited spatial volume. This volume can be considered as a natural space of the entire classifier or its part confined by two horizontal planes placed at a distance l apart. In such a flow, only the initial powder redistribution is of interest, to put it more precisely – fractional extraction of different size classes into upper and lower products. Therefore, we disregard the magnitude of particles velocity and examine only the direction of this velocity, that is its projection onto the vertical axis (Fig. 3.2). It corresponds to the implication of the process under study, and therefore we take the difference in the velocity directions of particles as the basis of our model.

Naturally, it is a very simplified model of the process under study. However, it is not simpler than the model of a mobile medium examined in the previous chapter, which forms the basis of all principal regularities and similarity criteria for hydraulic systems.

The direction of velocity projection of each particle can be of two kinds only – upwards or downwards. Note that the probability of this orientation for each particle is independent of the orientations of others. Moreover, we are not interested in any other parameters of the process, such as actual velocity directions, their magnitudes, interactions of particles with each other and walls confining the flow,

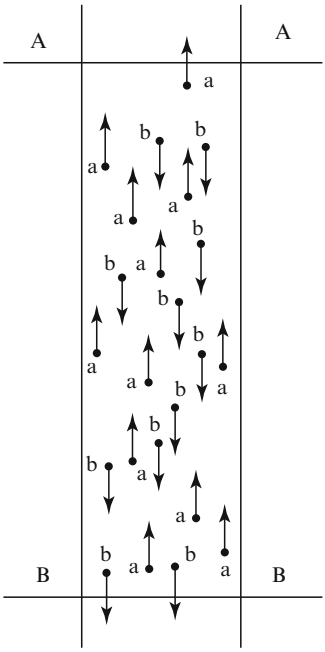

Fig. 3.2 On the model of a statistical two-phase flow

local concentration inhomogeneities or any other features of the flow – but only in the instantaneous particle velocity projection onto the vertical axis. Thus, the suggested model of the process reflects the main idea of separation – oppositely directed motion of particles in a flow.

Taking into account only velocity directions, we introduce notations of probabilities according to Fig. 3.2: a – upward direction, b – downward direction.

It is noteworthy that the probability of zero velocity projection onto the vertical axis is vanishingly small, because at this moment a particle should either stand still with respect to the walls, or move strictly normally to them. The probability of such state is approximately equal to the probability for a coin to stand on its edge when cast. From the point of view of the process under consideration, this probability is so low that it is not of any interest.

In principle, for other kinds of two-phase flows, the principal axis can be arranged otherwise, for example horizontally for horizontal and centrifugal flows and obliquely – for inclined flows.

Vertical direction of the principal axis is the most natural for gravitational separation. A system implies a totality of all particles passing in both directions through a height-confined flow space. In Fig. 3.2 the system is confined by lines A and B.

We examine a system with a stationary process, and not any kind of a system. Since there is no constant accumulation of the material in the assigned space

because the total output of both separation products in a stationary process always equals the initial input, we can assume that the number of particles in the assigned volume is approximately constant.

It is noteworthy that the total number of particles located in the apparatus volume at a certain fixed moment of time can be rather significant. Under actual conditions, the number of particles with $d = 0.1$ mm amounts to $N \approx 5 \cdot 10^{10}$ even if the quantity of product in a multi-ton apparatus is only 100 kg. The number of smaller particles is much higher.

In our further study, a statistical system implies a totality of such particles passing through a limited space.

Thus, a statistical system is determined by constant volume, number of particles and dynamic conditions (velocity of the ascending flow of the medium).

Here we need only one notion of statistical mechanics, namely, the notion of a stationary state of a system. The stationary state of a physical system has the following property: the probability of finding a particle in any element of volume is time independent. This state can be defined more rigorously as a state of a system where all observable physical properties do not explicitly depend on time.

Such state of a system with the velocity of the ascending flow of the medium remaining constant in time is characterized by the following property. Fractional separation degree of different size classes does not explicitly depend on time, that is its fluctuations are slight and markedly random. Such state comes, as a rule, after the expiry of a certain time after the beginning of the process or external disturbances (relaxation time). Nevertheless, we assume that here certain fluctuations are possible.

The most important point is that such stationary states of the system under study can be counted, although their number can be infinitely large.

From a mathematical point of view, disorder in a system is determined by a number of different ways of distributing a certain set of objects. The more objects we have, the higher the probability of their random distribution rather than an ordered state. Further on, these notions take on crucial significance, and therefore we clarify them using an illustrative example – a pack of 36 cards constituting a system under study.

Under ordinary conditions, this pack is in the state of random arrangement of cards. The probability of cards grouping in a certain order is extremely low, if, surely, it was not done on purpose. The number of various ways of ordering cards in a pack, obviously, equals 36!, since there are 36 possibilities of choosing the first card, 35 possibilities of choosing the second card, 34 possibilities of choosing the third, etc. Another important point is that if we assume that all 36 cards are identical, there is only one way of their arrangement, and we always see them perfectly ordered.

Let us try to estimate the number of various ways of distributing particles in a two-phase flow so that to satisfy certain limitations imposed on the system. For this purpose, we should first clarify which parameters distinguish particles from each other.

3.3 Estimation of the State of a Statistical System

It is accepted above that in a stationary state the system under study consists of N identical particles placed into a flow providing for their separation into two outputs.

A system consisting of one particle has two different stationary states with the velocities directed upwards (a) and downwards (b). A system of two particles has four states (aa; ab; ba; bb), a system of three particles – eight states (aaa; aab; aba; baa; abb; bab; bba; bbb), etc.

Hence, the total number of all possible states of a system consisting of N particles can be written as

$$\phi = 2^N.$$

We should emphasize again that each particle can be oriented in two ways irrespective of the orientation of the remaining particles.

The basis of our consideration of a system is the probability of potential extraction of particles in each of its states. Potential extraction implies the quantity of all the particles with upward-oriented velocity in a stationary system. If the number of particles in the system is N, the potential extraction can vary for different stationary states of the system within the limits

$$0 \leqslant \varepsilon \leqslant N.$$

Thus, here we are dealing with a directional mass transfer in two directions. It can be characterized by two numbers, for example 70% upwards and 30% downwards. Such two-valuedness is inconvenient for the analysis of the system, and in this case it was possible to find a unified estimation.

By analogy with dependence (1.7), we can write an expression for potential extraction as follows:

$$\varepsilon_f = \frac{N}{2} + z, \qquad \varepsilon_c = \frac{N}{2} - z. \tag{3.2a}$$

We call the parameter z unambiguously characterizing potential separation in both directions a potential separation factor or just separation factor. Clearly, it varies within the range

$$-\frac{N}{2} \leqslant z \leqslant +\frac{N}{2}.$$

It is also clear that at an equiprobable distribution

$$z = 0.$$

Physically, this parameter determines the quantity of particles constituting the deviation of fractional extraction from the equilibrium one.

The number of particles with the velocity directed upwards $n(\uparrow)$ equals $\frac{1}{2}N + z$; the number of particles with the velocity directed downwards $n(\downarrow)$ equals $\frac{1}{2}N - z$. The total number of particles is:

$$n(\uparrow) + n(\downarrow) = \left(\frac{1}{2}N + z\right) + \left(\frac{1}{2}N - z\right) = N.$$

If N is even, z is an integer, and if N is odd, z is a half-integer. Since N is very large, we can practically always assume without any error that N is an even number. Then the integer z can acquire all the values between $-\frac{N}{2}$ and $\frac{N}{2}$. A classical description of the state of an object consisting of a large number of particles is given in a well-known article by Niels Bohr published in 1913. This article was dealing with the behavior of atoms and molecules. Although particles in the process under study are incommensurably bigger, the application of the same methods seems rather promising, because here we can observe a direct analogy consisting in the fact that critical regimes of two-phase flows are also characterized by simultaneous participation of a large number of particles.

A system can consist of both one particle and an enormous number of particles. In our further study we deal with the state of a system of many particles. Each stationary state has a certain separation factor, but it may happen that several states have the same or nearly the same separation factor.

It is shown that the number of states of a system equals 2^N. It is noteworthy that in this case the quantity of possible values of potential extraction amounts to $(N + 1)$. In our example, three values of separation factor can be obtained for two particles:

1. *aa* – both particles are oriented upwards $(z = +2)$;
2. *bb* – both particles are oriented downwards $(z = -2)$;
3. *ab* and *ba* – particles have different orientation $(z = 0)$.

Note that the latter values of the system are self-similar.

Thus, the number of states exceeds the number of possible values of potential extraction. For instance, at $N = 10$, there are $2^{10} = 1,024$ states corresponding to only 11 different values of potential extraction. We can easily find an analytical expression for the number of states with $\left(\frac{N}{2} + z\right)$ particles with the velocity oriented upwards and $\left(\frac{N}{2} - z\right)$ particles with the velocity oriented downwards. Their difference is

$$\left(\frac{N}{2} + z\right) - \left(\frac{N}{2} - z\right) = 2z.$$

Surely, at any specified moment of time, each particle can acquire only one value of contribution to the total separation factor. We observe a system of N particles at

successive moments of time $t_1; t_2; t_3 \ldots t_m,$ the number of such observations being large and equal to m. Let the system be in one of its states at each observation. We denote by $n(i)$ the number of cases with the system in the state i (i.e. in the self-similar state i). Then the probability of such a state is

$$P(i) = \frac{n(i)}{m}.$$

With increasing number of observations m, the magnitude $P(i)$ tends to a certain limit, which constitutes the probability of the system stay in the state $n(i)$. Note that it follows from the definition of probability that

$$\lim_{n\to\infty} \sum_i P(i) = 1.$$

In other words, the probability of the system being in any of its states equals a unity.

Statistical approach determines mean parameters of magnitudes under study operating with probabilities instead of reliabilities. It is possible to determine more precisely the probability of any experimental result obtained in a certain system by repeating this experiment on a large number of similar systems. Although it is impossible to predict a reliable result of a specific experiment, the statistical approach makes it possible to determine the probability of each possible result of this experiment.

Naturally, it is impossible to predict the behavior of each particle in a system consisting of a large number of particles N. The use of statistical method implies the study of an ensemble of ϕ similar systems instead of one system. Since the essence of statistical approach consists in the ways of determining mean values, we examine them in detail.

Assume that a variable u characterizes a certain parameter of the system and acquires α possible discrete values $u_1; u_2; u_3 \ldots u_\alpha,$ with respective probabilities $P_1; P_2; P_3 \ldots P_\alpha$.

It means that in an ensemble of ϕ analogous systems, the variable u has a self-similar value z for the following number of systems:

$$\phi_z = \phi \cdot P_z.$$

The average value of the quantity under study or averaging over an ensemble denoted by $<u>$ equals

$$<u> = \frac{\sum_{z=1}^{\alpha} \phi_z \cdot u_z}{\phi},$$

but $\frac{\phi_z}{\phi} = P_z$, hence, $<u> = \sum_{z=1}^{\alpha} P_z u_z$. Similarly, if $f(u)$ is a certain function of u, its average value $<f(u)>$ is determined by the expression:

$$<f(u)> = \sum_{z=1}^{\alpha} P_z \cdot f(u). \tag{3.2b}$$

Some simple but useful features of averages can be determined from this relationship.

1. If $f(u)$ and $q(u)$ are two arbitrary functions of u, then

$$\begin{aligned} <f+q> &= \sum_{z=1}^{\alpha} P_z[f(u_z)+q(u_z)] = \sum_{z+1}^{\alpha} P_z f(u_z) + \sum_{z=1}^{\alpha} P_z q(u_z) \\ &= <f> + <q>. \end{aligned} \tag{3.3}$$

It means that the average value of a sum of functions equals a sum of average values of each function.

2. If c is a certain constant, then

$$<cf> = \sum_{z=1}^{\alpha} P_z[cf(u_z)] = c\sum_{z=1}^{\alpha} P_z f(u_z) = c<f>.$$

3. If $f(u_z) = const$, the obtained dependence shows that the average value of a constant equals the constant itself
4. We assume two discrete-variable quantities u and v acquiring the values:

$$u_1; u_2; \ldots; u_\alpha,$$

$$v_1; v_2; \ldots; v_\beta.$$

Denote by P_z the probability for the variable u to acquire the value u_z, and by P_s the probability for the variable v to acquire the value v_s.

If these variables are independent, the joint probability of these events equals

$$P_{zs} = P_z \times P_s.$$

If there exist two functions of these variables $f(u)$ and $q(u)$, it follows from (3.3) that

$$<f(u)q(u)> = \sum_{z=1}^{\alpha}\sum_{s=1}^{\beta} P_{zs}\cdot f(u_z)\cdot q(u_s) = \sum_{z=1}^{\alpha}\sum_{s=1}^{\beta}[P_z f(u_z)][P_s q(u_s)]$$
$$= <f(u)>\cdot <q(u)>.$$

5. Sometimes it is necessary to measure the deviation of a variable from its average value, that is

$$\Delta u = u - <u>.$$

The average value of this quantity is zero, since

$$<\Delta u> = <u - <u>> = <u> - <u> = 0.$$

However, the square of this value is not zero:

$$<\Delta u>^2 = \sum_{z=1}^{\alpha} P_z(u_z - <u_z>)^2.$$

This value is always positive, that is,

$$<\Delta u>^2 \geqslant 0$$

and it is called dispersion. A linear measure of the scatter in parameter values is an expression:

$$\Delta u = \sqrt{<\Delta u>^2}.$$

This quantity is called standard deviation.

6. The totality of all probabilities P_z for various values of u_z provides a total statistical information on the distribution of the parameter u values in the ensemble

Let us revert to the process under study. N particles in the system have two realizations in the orientation of their velocities – upwards or downwards, that is either $+\mu$ or $-\mu$ is possible.

Potential extraction is composed of an algebraic sum for all particles of the system:

$$I = \sum_{i=1}^{N} \mu_i. \tag{3.4}$$

To obtain an average value I, it is sufficient to average both parts of equality (3.4):

$$<I> = <\sum_{i=1}^{N} \mu_i> = \sum_{i=1}^{N} <\mu_i> = N<\mu_i>.$$

This result is obvious. It means that the average value of potential extraction I for a system of N particles is N-fold greater than the value of this parameter for one particle. In this case, the deviation is determined as follows:

$$I - <I> = \sum_{i=1}^{N} (\mu_i - <\mu_i>).$$

This expression can be simplified:

$$\Delta I = \sum_{i=1}^{N} \Delta\mu_i,$$

hence, $<\Delta I>^2 = \sum_{i=1}^{N} <\Delta\mu_i>^2 = N \cdot \Delta\mu_i^2$, $\Delta I = \sqrt{N} \cdot \Delta\mu_i$, and $\frac{\Delta I}{I} = \frac{1}{\sqrt{N}} \cdot \frac{\Delta\mu_i}{<\mu_i>}$.

If we denote the probability of upward orientation for a certain region of space by ρ, and of downward orientation – by g(it is clear that $\rho + g = 1$), then

$$<\mu> = \rho\mu_i + g(-\mu_i) = \mu_i(\rho - g) = \mu_i(2\rho - 1).$$

Consequently,

$$<I> = N(\rho - g)\mu_i,$$

$$<\Delta I>^2 = 4N\rho g\mu_i^2,$$

and the standard deviation amounts to

$$<\Delta I> = 2\sqrt{N\rho g} \cdot \mu_i.$$

Stationary states of a system or its part possessing the same separation factor or separation factor value within a narrow interval are self-similar. We call self-similar such states of a system that ensure the same separation factor, and their number should be taken into account when establishing the total number of states ϕ. If the separation factor z_i can be realized in y_i different ways $(z_i y_i)$, we assume that

the state z_i is y_i-fold self-similar. We emphasize two basic points in the definition of self-similarity.

First, this definition is applicable to the magnitude of separation factor, and not to the states of a system that are all different.

Secondly, practical establishment of self-similarity in a real process is determined in many respects by the perfection of experimental method. Using a more sophisticated method, difference in the extraction can be found, although it seems to be absent if particles are divided into narrower classes.

When the number of particles is limited, it is easy to reveal self-similar states. We have demonstrated that if the total number of states for N particles is 2^N, then the number of separation factor values amounts to $(N + 1)$ only.

If a specific configuration of a system is chosen at random, the probability of finding it equals $\frac{1}{2^N}$. If this configuration has C self-similar states, its probability amounts to $\frac{C}{2^N}$.

Before starting calculations, two more remarks should be made.

First, we assume, without going into details, that any of the states of a system self-similar with respect to separation factor are equiprobable.

Secondly, there are states of a system whose statistical properties are of no interest from the point of view of the process under study, since their probability is vanishingly small.

To represent some state of a system, one can use either a visual image as in Fig. 3.2 or a symbolic notation:

$$a_1 b_2 a_3 a_4 b_5 a_6 b_7 \ldots a_i b_j \ldots b_N. \tag{3.5}$$

We start with simple calculation. In a system of two particles, we obtain four possible states

$$(a_1 + b_1)(a_2 + b_2) = a_1 a_2 + a_1 b_2 + b_1 a_2 + b_1 b_2 \tag{3.6}$$

by multiplying $(a_1 + b_1)(a_2 + b_2)$. We can equally well multiply expressions $(\uparrow_1 + \downarrow_1) \cdot \ \cdot (\uparrow_2 + \downarrow_2)$. We can assume that the left side of expression (3.6) is a function determining the state of the system. A determining function for three particles is

$$\begin{aligned}(a_1 + b_1)(a_2 + b_2)(a_3 + b_3) = {} & a_1 a_2 a_3 + a_1 a_2 b_3 + a_1 b_2 b_3 + a_1 b_2 a_3 \\ & + b_1 a_2 b_3 + b_1 b_2 b_3 + b_1 a_2 a_3 + b_1 b_2 a_3.\end{aligned}$$

We obtain eight states of the system, which corresponds to

$$2^3 = 8.$$

The product of N multipliers in (3.5) can be written without the account for the order numeration, which is not of fundamental importance for the process.

Since in our case the projection of particle velocity has only two orientations, the total number of states of a system of N particles is:

$$\phi = (a+b)^N. \tag{3.7}$$

In a general case, this dependence can be expanded using the binomial theorem:

$$(a+b)^N = a^N + Na^{N-1}b + \frac{1}{2}N(N-1))a^{N-2}b^2 + \cdots + b^N.$$

We can write this expression in a more compact way:

$$(a+b)^N = \sum_{k=0}^{N} \frac{N!}{(N-k)!k!} a^{N-k}b^k.$$

In the present case, it is more convenient to perform the enumeration of states within other limits, with separation factor varying from $-\frac{N}{2}$ to $+\frac{N}{2}$, that is by analogy with expression (1.7). In this case,

$$(a+b)^N = \sum_{-\frac{N}{2}}^{+\frac{N}{2}} \frac{N!}{\left(\frac{1}{2}N+z\right)!\left(\frac{1}{2}N-z\right)!} a^{\frac{N}{2}+z}b^{\frac{N}{2}-z}.$$

Expression $a^{\frac{N}{2}+z}b^{\frac{N}{2}-z}$ enumerates all possible separation factors within the range of $-\frac{N}{2} \leqslant z \leqslant +\frac{N}{2}$, while binomial coefficients show the number of self-similar states of the system with a fixed number of particles oriented upwards or downwards.

We perform calculations under the condition that $N>>1$ and $z \leqslant \left|\frac{N}{2}\right|$. We determine binomial coefficients:

$$\phi(N;z) = \frac{N!}{\left(\frac{1}{2}N+z\right)!\left(\frac{1}{2}N-z\right)!}. \tag{3.8}$$

The parameter $\phi(N;z)$ determines the number of states of a system of N particles with a common separation factor $2z$. Hence, in a general case we can write

$$(a+b)^N = \sum_{z=-\frac{N}{2}}^{z=+\frac{N}{2}} \phi(N;z) a^{\frac{N}{2}+z}b^{\frac{N}{2}-z}.$$

In this expression z is any integer between $-\frac{N}{2}$ and $\frac{N}{2}$. We call the value $\phi(N;z)$ a self-similarity degree. Finding the logarithm of the left and right part, we obtain the following situation in (3.8):

$$\ln\phi = \ln(N!) - \ln\left[\left(\frac{N}{2}+z\right)!\right] - \ln\left[\left(\frac{N}{2}-z\right)!\right]. \tag{3.9}$$

We examine separate parts of this expression:

$$\begin{aligned}\ln\left[\left(\tfrac{N}{2}+z\right)!\right] &= \ln\left(\tfrac{N}{2}!\right) + \sum_{k=1}^{z}\ln\left(\tfrac{N}{2}+k\right)\\ \ln\left[\left(\tfrac{N}{2}-z\right)!\right] &= \ln\left(\tfrac{N}{2}!\right) - \sum_{k=1}^{z}\ln\left(\tfrac{N}{2}-k+1\right)\end{aligned} \tag{3.10}$$

and add up these two expressions:

$$\ln\left[\left(\frac{N}{2}+z\right)!\right] + \ln\left[\left(\frac{N}{2}-7\right)!\right] = 2\ln\left(\frac{N}{2}!\right) + \sum_{k=1}^{z}\ln\frac{1+\frac{2k}{N}}{1-\frac{2k}{N}}. \tag{3.11}$$

Proceeding from the assumption that $\frac{N}{2}-k+1$ approximately equals $\frac{N}{2}-k$, the second summand in (3.10) amounts to

$$\sum_{k=1}^{z}\ln\frac{\frac{N}{2}+k}{\frac{N}{2}-k} = \sum_{k=1}^{z}\ln\frac{1+\frac{2k}{N}}{1-\frac{2k}{N}} = \sum_{k=1}^{z}\ln\frac{1+x}{1-x} \tag{3.12}$$

where $x = \frac{2k}{N}$. It is clear from the definition that $x \ll 1$ always.

To disclose the contents of (3.12), we perform additional calculations. We recall that

$$e^x = 1 + x + x^2 + \cdots$$

For $x<1$, we can restrict ourselves with the first two terms. Then,

$$e^x \approx 1+x; \qquad \text{i.e.} \qquad x \approx \ln(1+x),$$

$$e^{-x} \approx 1-x; \qquad \text{i.e.} \qquad -x \approx \ln(1-x).$$

This means that

$$\ln\frac{1+x}{1-x} \approx 2x; \quad \ln\frac{1+\frac{2k}{N}}{1-\frac{2k}{N}} \approx \frac{4k}{N},$$

and the dependence (3.12) acquires the form:

$$\sum_{k=1}^{z}\ln\frac{1+x}{1-x} = \frac{4}{N}\sum_{k=1}^{z}k = \frac{4(z+1)(z)}{2N} \approx \frac{2z^2}{N}. \tag{3.13}$$

Thus, dependence (3.8) is transformed into the form

$$\phi(N;z) \approx \frac{N!}{\left(\frac{N}{2}\right)!\left(\frac{N}{2}\right)!} e^{\frac{-2z^2}{N}} \tag{3.14}$$

The obtained result can be written as

$$\phi(N;z) = \phi(N;0) e^{\frac{-2z^2}{N}}. \tag{3.15}$$

That is this expression should be understood as follows: the number of states of a system under study equals the number of equilibrium states ($z = 0$) multiplied by an exponent at any value of separation factor.

The value of exponential coefficient can be obtained using Stirling's formula:

$$n! \approx (2\pi n)^{\frac{1}{2}} n^n e^{\left(-n+\frac{1}{12n}+\cdots\right)}.$$

Taking this into account,

$$\frac{N!}{\left(\frac{N}{2}\right)!\left(\frac{N}{2}\right)!} = \frac{\sqrt{2\pi N} N^N e^{-N}}{\pi N \frac{N^N}{2^N} e^{-N}} = 2^N \sqrt{\frac{2}{\pi N}}.$$

Hence, relationship (3.15) amounts to

$$\phi = 2^N \sqrt{\frac{2}{\pi N}} e^{\frac{-2z^2}{N}}. \tag{3.16}$$

Let us analyze dependence (3.16) at various ratios of probabilities of the class output into fine and coarse products. First examine the simplest case of equilibrium class distribution.

3.4 Principal Statistical Characteristics of the Separation Factor

We analyze the derived dependence (3.16). Its validity can be checked by summing over all z values from $-\frac{N}{2}$ to $+\frac{N}{2}$:

$$\sum_{z=-\frac{N}{2}}^{z=+\frac{N}{2}} 2^N \sqrt{\frac{2}{\pi N}} e^{\frac{-2z^2}{N}}.$$

Summing over all the values of z gives an integral

$$\int_{-\infty}^{+\infty} 2^N \sqrt{\frac{2}{\pi N}} e^{\frac{-2z^2}{N}} dz = 2^N \sqrt{\frac{2}{\pi N}} \int_{-\infty}^{+\infty} e^{\frac{-2z^2}{N}} dz$$

We introduce a new variable

$$\frac{2z^2}{N} = y^2,$$

then

$$\sqrt{\frac{2}{N}} dz = dy; \text{ and } dz = \sqrt{\frac{N}{2}} dy.$$

Taking this into account, the dependence under study is transformed into

$$2^N \sqrt{\frac{2}{\pi N}} \int_{-\infty}^{+\infty} e^{-y^2} \sqrt{\frac{N}{2}} dy = \frac{2^N}{\sqrt{\pi}} \int_{-\infty}^{+\infty} e^{-y^2} dy.$$

Since, according to reference data,

$$\int_{-\infty}^{+\infty} e^{-y^2} dy = \frac{\sqrt{\pi}}{2},$$

we obtain

$$\int_{-\infty}^{+\infty} 2^N \sqrt{\frac{2}{\pi N}} e^{\frac{-2z^2}{N}} \cdot dz = 2^N,$$

which exactly corresponds to the total number of states of the system.

The distribution defined by the right side of dependence (3.16) is Gauss distribution with a maximum centered at $z = 0$. For such curves, mean square deviation is a measure of the relative distribution width. As already shown, its value is

$$\sigma = \sqrt{N}.$$

The ratio of mean square deviation to the maximal value is

$$\frac{\sqrt{N}}{N} = \frac{1}{\sqrt{N}}.$$

If the total number of particles in a system, as defined for separation conditions, equals $N \approx 10^{10}$, the relative distribution width is on the order of 10^{-5}. It means

that in this case we obtain a sharp maximum at the mean value of $z = 0$. The physical meaning of this expression is that the separation factor reached in a given apparatus is not, basically, the only possible, but the most probable one.

Thus, we have demonstrated that the probability of this separation exceeds so greatly any other conceivable distribution that it can be considered the only possible, that is determinate under given conditions.

This explains reliably enough the constancy of separation curve for a process involving simultaneously myriads of particles. Such constancy is confirmed by all available experimental material.

Let us introduce one more notion for the system under study – parameter $2z$, which determines the disbalance in the distribution of particles of a narrow size class.

Among principal parameters of a narrow size class distribution is the ascending flow velocity. Obviously, the separation factor value ($2z$) is functionally of correlationally connected with the flow velocity. However, flow velocity reflects only one aspect of the process – its kinetic component. We introduce another parameter reflecting the potential component of the process, which should be proportional to the separation factor, and denote it by I. We call this parameter "lifting factor".

$$I = 2zc,$$

where c is proportionality coefficient.

By analogy with the kinetic theory of gases, this coefficient should involve the gravitational parameter equal, as known, to gd. Besides, in order to reflect the potential component, it should include the mass of particles of the narrow size class. Finally,

$$I = -2zgdm.$$

The dimension of this parameter is [kgm].

Lifting factor expresses the potential energy of particles disbalance. The minus sign appears because the gravity force is directed downwards. On the whole, this parameter determines the potential extraction magnitude and direction.

The importance and universality of this parameter is assessed later. It has a generalizing meaning for fields of different origins – centrifugal, magnetic, electrical, etc. For these fields, its form differs from that of gravitational field, although the method of its derivation remains the same.

Lifting factor differential is written as

$$dI = -2gdmdz.$$

By a differential of I and z or N we mean a number of particles several orders smaller than these values, and not an infinitesimal number. Such approach is successfully applied in the kinetic theory of gases, where gas molecules are regarded as hard balls.

The kinetic energy needed to provide the potential energy I on the part of the flow is measured by the minimal effort per unit area of the flow cross-section, which can be denoted by f. The dimension of this parameter is $[\mathrm{kg/m^2}]$.

The potential extraction determines the deviation of particles orientation from the equilibrium one at $z = 0$. At the same time, it should be taken into account that the potential energy of a particle in a flow is gdm. Therefore, such extraction characterizes only the potential energy of disbalance in different orientations of particles. In this dependence,

$$m = V(\rho - \rho_0),$$

where m is the particle mass; $V$is the particle volume; ρ, ρ_0 are the densities of the material and the medium. For air flows, $\frac{\rho}{\rho_0} > 1{,}000,$ therefore, in this case we can assume

$$m = V\rho.$$

By definition, the average value of the potential extraction can be written as

$$\langle I \rangle = \sum_{S=1}^{N} \langle \varepsilon_S \rangle,$$

where ε_S is the potential extraction of one particle.

If the orientations of particles are chosen at random, each of 2^N states can appear with the same probability, that is it can amount to $+gdm$ or $-gmd$. Therefore, the average value in each point

$$\langle \varepsilon_S \rangle = 0,$$

and hence,

$$\langle I \rangle = 0.$$

This determines the first moment distribution function I.

The second moment distribution function is determined from the dependence

$$\left\langle I^2 \right\rangle = \left\langle \left(\sum_{s=1}^{N} \varepsilon_s \right)^r \right\rangle = \sum_{l} \sum_{s} \langle \varepsilon_l \varepsilon_s \rangle,$$

where l and s independently acquire all values from 1 to N. Their contribution to $\left\langle I^2 \right\rangle$ equals

$$\langle \varepsilon_l \varepsilon_s \rangle = \frac{1}{2} \left[(+\varepsilon)^2 + (-\varepsilon)^2 \right] = \varepsilon^2.$$

A double sum contains Nsummands of this type. If $l \neq s$, then $\langle \varepsilon_l \varepsilon_s \rangle = 0$. The latter can be illustrated by the behavior of a system consisting of two particles. This system has four possible states:

$$\langle s_1 s_2 \rangle = \frac{1}{4}[(+s)(+s) + (+s)(-s) + (-s)(+s) + (-s)(-s)] = 0.$$

Hence, terms with $l \neq s$ do not contribute to $\langle I^2 \rangle$, therefore, this parameter contains only N summands, each of them equal to ε^2,

$$\langle I^2 \rangle = N\varepsilon^2.$$

There exists a parameter characterizing a root-mean-square deviation

$$\sqrt{\langle I^2 \rangle} = \varepsilon\sqrt{N}.$$

It can be shown that the magnitude I has also a sharp maximum. To do it, we divide the root-mean-square deviation by its maximum value:

$$\frac{\varepsilon\sqrt{N}}{\varepsilon N} = \frac{1}{\sqrt{N}}.$$

Thus, we have shown that the number of particles in one m^3 of the flow is on the order of 10^{10}, and consequently, $\frac{1}{\sqrt{N}} = 10^{-5}$.

Chapter 4
System of Particles of Several Size Classes

Abstract A definition of entropy for critical two-phase flows is given. The most probable state of the system is defined. It is shown that a system is in its most probable configuration, if the number of its admissible configurations is maximal. Principal properties of this entropy are examined. The notions for chaotizing factor are formulated. A connection between statistical parameters of the system and parameters of separation curves affinization is validated from this standpoint. One more parameter, mobility factor of a two-phase flow is introduced. Statistical identities for such systems are examined. Entropy connection with governing characteristics of two-phase flows is established.

Keywords Entropy · System configuration · Ensemble of systems · Chaotizing factor · Mobility factor · Uncertainty of a system · Paradox · Irreversibility · Stratification · Identity

4.1 Interaction of Particles in a Flow

When examining a system consisting of particles of various size classes, we have to take into account an additional effect – mechanical interaction of particles in a flow. The presence of this effect was confirmed by a very simple experiment. On a plant presented schematically in Fig. 4.1, air flow velocity was selected in such a way as to create a suspended layer of balls with the diameter $d = 12 \div 15$ mm and density $\rho = 6{,}000\,\mathrm{kg/m^3}$ in its conical part. The layer was stabilized along the cone height. Then carbon slack of a low concentration $\mu \approx 0.1\,\mathrm{kg/m^3}$ and with the particle size $d < 0.25$ mm was fed into the flow from below. The flow transparency was not

E. Barsky, *Critical Regimes of Two-Phase Flows with a Polydisperse Solid Phase*,
Fluid Mechanics and Its Applications 93,
DOI 10.1007/978-90-481-8838-3_4,

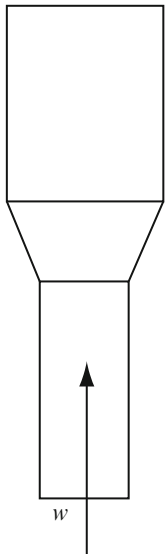

Fig. 4.1 Facility for demonstrating mechanical interaction of particles in a flow

deteriorated, but under the action of this slack, large heavy balls suspended in the cone were thrown out into the cylindrical part of the plant to the height up to 400 mm from the cone edge. This experiment visually demonstrated, first, the fact of mechanical interaction of particles in a flow, and secondly, the effect of this interaction on their behavior. To make conclusions, we use Fig. 3.1, where a section Δl long is marked out.

Under stationary separation regimes in a vertical counterflow, the material concentration is gradually reduced in both directions from the feeding zone. Therefore, this section should be large enough to hold a significant quantity of particles, but also small enough in comparison with the variation scale of disperse material velocity and concentration. It is clear that when the process is stationary, the quantity of solid particles in this section is constant. We consider the interaction of two size classes – fine and coarse.

We assume that

$$G = G_i + G_j$$

particles arrive at this section per unit time, where

G_i is the consumed part of i-th component, kg/s;

G_j is the consumed part of j-th component, kg/s.

We introduce the following notation:

$r_i; m_i; v_i$ are the radius, mass and mean axial velocity component for fine particles;

$r_j; m_j; v_j$ are similar parameters for coarse particles.

The weight of coarse particles within a unit length of the section under study amounts to:

$$\Delta g_j = \frac{G_j}{v_j}.$$

Over the entire section under study Δl, the weight of these particles is

$$\Delta G_j = \Delta g_j \cdot \Delta l = \frac{G_j \cdot \Delta l}{v_j}.$$

Similarly, for fine particles we can write:

$$\Delta G_i = \Delta g_i \cdot \Delta l = \frac{G_i \cdot \Delta l}{v_i}.$$

Irrespective of whether coarse particles move in or counter the direction of fine particles, they are constantly hit by fine particles. According to the separation curve, some of the fine particles move in the direction of the coarse product output and get into this product instead of getting into the fine product output. Therefore, we assume that coarse particles located in the volume under study hit only some of the fine particles,

$$\Delta G_i' = y \Delta G_i,$$

where y is a coefficient depending on the velocities and concentrations of fine and coarse particles, flow constraint conditions and regime of the medium motion $(y < 1)$.

It is known from mechanics that two particles can collide only if their encounter takes place within an area equal to the cross-section of collisions.

Since in the process under study bulk concentration of solid phase in the flow is insignificant $(\mu \approx 3\,\text{kg/m}^3; \beta \approx 0.001)$, we can assume that collisions with simultaneous participation of more than two particles are unlikely, and examine only pairwise interactions. In a unit of time, a coarse particle can collide with those fine particles whose centers are located at a given moment inside a cylinder with the base corresponding to the collisions cross-section and the height – to the difference between distances passed by these particles in a unit of time, that is,

$$h = v_i - v_j.$$

To determine the collision probability $P(x)$, coarse particles can be considered as motionless and fine ones as moving at relative velocities.

Collision probability can be defined as a ratio of all collision areas within one cross-section of the apparatus to the value of this cross-section, that is,

$$P(x) = \frac{4\sum S}{\pi D_e^2},$$

where $S = n_j'(r_i - r_j)^2\pi$; D_e is an equivalent diameter of the flow cross-section; n_j' is an average number of coarse particles in the flow cross-section. The average number of particles in the flow cross-section can be defined as follows:

$$n_j' = \frac{\Delta G_j \cdot 2r_j}{m_j g \cdot \Delta l}.$$

Only those fine particles that are 0 to h distance from this layer have a chance to collide with these particles in a unit of time. Their number can be determined to be

$$n_i' = \frac{\Delta G_i(v_i - v_j)}{m_i g \cdot \Delta l} y.$$

Besides, only some of the fine particles determined by the collision probability, that is

$$\Delta n_i' = n_i' \cdot P(x) = \frac{4(r_i + r_j)^2 n_i n_j (v_i - v_j) 2r_j y}{D_e^2}$$

can participate in collisions, but not all of them. The total number of collisions over the entire section under study amounts to

$$\Delta N = \frac{\Delta n_i' \cdot \Delta l}{2r_j} = \frac{4(r_i + r_j)^2 n_i n_j (v_i - v_j) y \cdot \Delta l}{D_e^2}.$$

In this dependence, n_i and n_j correspond to the number of particles of both classes per unit height of the flow under study.

$$n_i = \frac{\Delta G_i}{m_i g \Delta l}; \qquad n_j = \frac{\Delta G_j}{m_j g \Delta l}$$

Hence, taking into account previously obtained results,

$$n_i = \frac{G_i}{m_i g v_i}; \qquad n_j = \frac{G_j}{m_j g v_j}$$

We can pass from the number of particles to their concentration based on the following reasons. The medium flow rate is determined as

$$Q = F \cdot w\gamma_0,$$

where Q is the medium weight rate, kg/s; F is the apparatus cross-section area, m^2; w is the medium flow velocity, m/s; γ_0 is the medium specific weight, kg/m^3.

Output flow rates for each of the size classes under study can be represented in a similar way:

$$G_i = F \cdot v_i\gamma_i,\ G_j = F \cdot v_i\gamma_j$$

where $\gamma_i; \gamma_j$ have the physical meaning of the weight of respective solid particles in a unit volume occupied by these particles.

Relative degree of the flow loading with particles of respective size classes is

$$\mu_i^* = \frac{G_i}{Q} = \frac{v_i}{w} \cdot \frac{\gamma_i}{\gamma_0},\ \mu_j^* = \frac{G_j}{Q} = \frac{v_j}{w} \cdot \frac{\gamma_j}{\gamma_0}.$$

Local concentration per unit volume of the apparatus amounts to

$$\mu_i = \mu_i^* \cdot \frac{w}{v_i},\ \mu_j = \mu_j^* \cdot \frac{w}{v_j}.$$

Hence,

$$\gamma_i = \gamma_0\mu_i;\ \gamma_j = \gamma_0\mu_j.$$

Taking this into account,

$$n_i = \frac{F\gamma_0}{m_i g}\mu_i,\ n_j = \frac{F\gamma_0}{m_j g}\mu_j.$$

Finally we obtain the desired parameter as follows:

$$\Delta N = \frac{\pi(r_i + r_j)^2 V\gamma_0^2 y}{m_i m_j g^2}(v_i - v_j)\mu_i\mu_j,$$

where V is the volume of the zone under study, m^3

Hence, the total number of particles collisions within a certain volume is in direct proportion to their concentration in the flow, velocity difference for motions of different classes, and the magnitude of this volume. The total number of collisions in a unit volume of the apparatus amounts to

$$N = \frac{\pi(r_i + r_j)^2 \gamma_0^2 y}{m_i m_j g^2}(v_i - v_j)\mu_i\mu_j.$$

At the particle velocity fluctuation in any direction with respect to the mean value, the number of interactions acquires values within a certain range. We can assume that the obtained expression is its mathematical expectation.

It is of interest to determine the number of hits on the fine particles experienced, on the average, by one coarse particle. This value amounts to

$$N_j = \frac{N}{n_j} = \frac{\pi(r_i + r_j)^2 \gamma_0^2 y(v_i - v_j)\mu_i \mu_j m_j g}{m_i m_j g^2 \cdot F \cdot \gamma_0 \mu_j} = \frac{\pi(r_i + r_j)^2 \gamma_0 y(v_i - v_j)}{m_i g \cdot F}\mu_i.$$

If we know this value, we can calculate the mean distance traveled by a coarse particle between two interactions. During the time interval Δt, a particle traverses a certain zigzag path $v_j \Delta t$. The distance traveled by the particle between two collisions can be defined as a ratio of the total path traveled by the particle to the number of collisions experienced while traversing this path:

$$l_j = \frac{v_i \Delta t}{N_j \Delta t} = \frac{v_i m_i g \cdot F}{\pi(r_i + r_j)^2 \gamma_0 y(v_i - v_j)\mu_i}.$$

Let us combine all constant parameters into one. Note that the difference in the particles velocities can be written as

$$(v_i - v_j) = (w - w_{50(i)}) - (w - w_{50(j)}) = w_{50(j)} + w_{50(i)} = const.$$

Keeping this in mind, the obtained expression can be written as

$$l_j = c\frac{v_i}{\mu_i}. \tag{4.1}$$

Hence, the free path length of a particle of a certain size class under gravitational separation conditions is directly proportional to the velocity of particles of one class and inversely proportional to the concentration of particles of another class in this flow.

4.2 Forces Caused by Interactions of Particles of Various Classes

We assume that at a collision, a fine particle slows down its velocity in the axial direction, on the average, by a certain value Δv_j. Let us study the mechanism of velocities redistribution for two separate particles of different sizes. Since we are interested only in the axial velocity change, we restrict ourselves to forward collisions in the vertical direction. A collision of two bodies is considered forward if they do not rotate at the moment of the collision, and the velocities of their centers

c_1 and c_2 are directed along c_1c_2 line normal to contacting surfaces at the point of their contact.

Let two balls with the masses m_i and m_j collide at the moment of time t_0. During a very short time period $(t_1 - t_0)$ of the collision, the center line can be considered as motionless. We denote algebraic values of particles velocities before the collision by v_1 and v_2, and after the collision by $\overline{v_i}$ and $\overline{v_j}$. Let us analyze, in general, the phenomena taking place at the particles collision. Starting from the moment t_0, when the particles come into contact, they start deforming around the contact point and go on drawing together up to the moment t_1', when the distance between them becomes the smallest. During the time period $(t_1' - t_0)$ of the first stage of the particles interaction, a reaction tending to draw them apart arises. The work of these reactions during that time is negative, and the kinetic energy of the system decreases.

At the moment t_1' the velocities of both particles become equal, their centers do not get closer any more, and their deformation value is maximal. Starting from this moment, mutual reactions of both particles go on acting until they acquire their original shapes. At a certain moment of time t_1 they touch each other at only one point. During this second stage $(t_1 - t_1')$, the kinetic energy of the system increases because the work of the reaction forces becomes positive, which leads to a mutual separation of particles at velocities different from the initial ones.

In such collisions, rather significant forces are developed due to the smallness of the collision time. Gravity of the particles is, as a rule, neglected because of its insignificance. Therefore, a collision of two particles is considered as a system under the action of internal forces.

It follows from the theorem of a system center of gravity that the velocity of the common center of gravity has not changed, since there were no external collision momentums. Hence,

$$v_0 = \frac{m_i v_i + m_j v_j}{m_i + m_j} = \frac{m_i \overline{v_i} + m_j \overline{v_j}}{m_i + m_j},$$

and therefore

$$m_i v_i + m_j v_j = m_i \overline{v_i} + m_j \overline{v_j}.$$

Particle velocity after a collision is determined, in many respects, by elastic properties of colliding bodies. Usually all the bodies are subdivided into three groups – absolutely inelastic, absolutely elastic and possessing intermediate properties.

Absolutely inelastic bodies remain in contact after the collision, that is their velocities acquired as a result of the collision become identical:

$$\overline{v_i} = \overline{v_j}$$

or

$$\frac{m_i v_i + m_j v_j}{m_i + m_j} = \overline{v_i} = \overline{v_j}.$$

At the collision of absolutely elastic bodies, kinetic energy is not lost, that is,

$$\frac{m_i v_i^2}{2} + \frac{m_j v_j^2}{2} = \frac{m_i \overline{v_i^2}}{2} + \frac{m_j \overline{v_j^2}}{2}.$$

This expression, in combination with the previous one, allows unambiguous determination of particles velocities after the collision:

$$\overline{v_i} = v_j + \frac{m_j - m_j}{m_i + m_j}(v_i - v_j),$$

$$\overline{v_j} = v_i + \frac{m_i - m_j}{m_i + m_j}(v_i - v_j).$$

Velocity changes for both particles amount to

$$\Delta v_i = \overline{v_i} - v_i = \frac{2m_j}{m_i + m_j}(v_j - v_i),$$

and the value

$$\overline{v_i} - \overline{v_j} = v_j - v_i.$$

Thus, relative velocity of the pair of particles under study changes the sign, while its value remains unchanged.

Evidently, for real, that is non-absolutely elastic materials,

$$\overline{v_i} - \overline{v_j} = k(v_j - v_i),$$

where $0 \leq k \leq 1$. Proceeding from this expression, in combination with the momentum equation, we can obtain the following:

$$\Delta v_i = \frac{m_i(k+1)(v_j - v_i)}{m_i + m_j},$$

$$\Delta v_j = \frac{m_i(k+1)(v_i - v_j)}{m_i + m_j}.$$

The total collision momentum acting on a cluster of fine particles per unit time can be defined as

$$P = \Delta N m_i \Delta v_i,$$

where $\Delta N m_i$ is a mass of fine particles colliding with coarse ones. Taking into account the dependence for ΔN, we can write:

$$P = \frac{\pi(r_i + r_j)^2 \gamma_0^2 z \alpha (k+1)}{g^2(m_i + m_j)} (v_i - v_j)^2 \mu_i \mu_j,$$

where $\alpha < 1$. This coefficient takes into account the difference between an actual effect of particles collision and a forward collision.

We denote the combination of constant parameters in the last expression by

$$c_1 = \frac{\pi(r_1 + r_2)^2 \gamma_0^2 z \alpha (1+k)}{g^2(m_i + m_j)}.$$

Taking this expression into account,

$$P = c_1 \mu_i \mu_j (v_i - v_j)^2.$$

It has been shown that the difference in the velocities of particles is, on the average, a constant value independent of the flow velocity. It is determined only by the difference in hovering velocities of the particles to be compared, that is

$$v_i - v_j = const.$$

Thus, we can obtain

$$P = c_2 \mu_1 \mu_2.$$

This means that the total force due to the interaction of particles is only a function of concentrations of both kinds of particles in the flow.

Now that we have clarified the main regularities of particles interaction in a flow, we revert to the study of a system of particles consisting of two narrow size classes.

4.3 Two-Phase Flow Entropy in Critical Flow Regimes

The notion of entropy is crucial for the study of properties of mass systems. This notion was first formulated in thermodynamics and then extended to gaseous systems. To determine the entropy of any mass system, it is necessary to know

how to find the number of its admissible states. A state is considered admissible, if it is compatible with characteristics of the system. When a contact between two systems is established, an interesting situation arises. Let us examine the mechanisms of separation factors and lifting factors exchange.

The main problem of statistical mechanics is to study the most probable distribution between systems ensuring their mutual equilibrium.

We examine a system consisting of particles of one size class and mark particles of one part, for example, with paint or isotopes. We obtain two systems with different numbers of particles.

Let us determine the number of admissible states of the two systems and find the most probable configuration of a combined system. We consider their behavior in the system as follows. First we observe the particle of one class only, for instance, the marked ones. After we determine the number of states of such a system, we start observing the system of the second type of particles. Then we examine characteristics of the system consisting of particles of both groups.

Two interacting systems exchanging energies and particles eventually reach equilibrium with identical energy characteristics.

Let the realization of each system be defined by certain fixed nonzero values of separation factor z_1 and z_2. The number of admissible self-similar states of the first system with respect to their separation factor is $\phi_1(N_1; z_1)$, and each of these states can be realized side by side with any of $\phi_2(N_2; z_2)$ admissible self-similar states of the second system.

It is clear that the total number of states in a combined system is defined by a product

$$\phi_1(N_1; z_1)\phi_2(N_2; z_2).$$

We write

$$z = z_1 + z_2,$$

that is,

$$z_2 = z - z_1.$$

At a constant number of particles in the systems

$$N = N_1 + N_2 = const,$$

the realization of a combined system can be characterized completely enough by the product,

$$\phi_1(N_1; z_1)\phi_2[N_2(z - z_1)],$$

that is through the magnitude of one separation factor z_1.

To obtain the total number of all admissible states, it is sufficient to sum up the obtained expression over all possible values of z_1, that is,

$$\phi(N;z) = \sum_{z_1} \phi_1(N_1;z_1) \cdot \phi_2[N_2(z-z_1)].$$

As known, such a sum has a sharp maximum at a certain value of $z_1 \approx z_{m_1}$. This magnitude of the parameter determines the most probable realization of the combined system. Then the number of states in the most probable configuration equals

$$\phi_1(N_1;z_{m_1})\phi_2(N_2;z-z_{m_1}). \tag{4.2}$$

It is clear that if at least in one of the two systems the number of particles is very high, then this maximum is extremely sharp with respect to z_1 changes. The presence of a sharp maximum implies that the statistical properties of a combined system are determined by a relatively small number of configurations.

It is clear that for a distribution with a sharp maximum, averaged properties of the system are exactly determined by the most probable configuration. This means that the average value of a physical magnitude determined previously over all admissible configurations can be replaced with the value averaged only over the most probable configuration. Let us demonstrate the implications of this approximation for Eq. (4.2). Taking into account the obtained result, we can write:

$$\phi = \phi_1(N_1;z_1)\phi_2(N_2;z_2) = \phi_1(N_1;0)\phi_2(N_2;0)e^{\left(-\frac{2z_1^2}{N_1}-\frac{2z_2^2}{N_2}\right)}.$$

We examine this dependence as a function of z_1. Then Eq. (4.2) can be rewritten as:

$$\phi = Ae^{-\left[\frac{2z_1^2}{N_1}+\frac{2(z-z_1)}{N_2}\right]}. \tag{4.3}$$

Note that the function $\ln y(x)$ reaches its maximum at the same x value as the function $y(x)$. We obtain from Eq. (4.3):

$$\ln\phi = \ln A - \frac{2z_1^2}{N_1} - \frac{2z_2^2}{N_2}.$$

This magnitude has an extremum when the derivative with respect to z_1 equals zero.

For the first derivative, we obtain:

$$-\frac{4z_1}{N_1} + \frac{4(z-z_1)}{N_2} = 0.$$

The second derivative

$$-4\left(\frac{1}{N_1}+\frac{1}{N_2}\right)$$

is negative, and, consequently, the extremum represents a maximum. Thus, the most probable configuration is the one for which the relationship

$$\frac{z_1}{N_1}=\frac{z-z_1}{N_2}=\frac{z_2}{N_2} \tag{4.4}$$

is valid.

Thus, we have derived a very interesting relationship. Two systems are in the most probable state when the relative separation factor of the first system equals the relative separation factor of the second system. It testifies that the most probable state of a system is established in such a way that the separation factor equalizes a different number of particles in a flow. Thus, we have obtained a result indirectly confirming the experimentally determined invariance of fractional separation degree with respect to the original mixture composition. This conclusion shows the statistical essence of this empirical result that was obtained long ago, but has not been explained yet.

If z_1 and z_2 in the maximum of the product under study equal z_{m_1} and z_{m_2}, respectively, then the obtained relationship can be written as

$$\frac{z_{m_1}}{N_1}=\frac{z_{m_2}}{N_2}=\frac{z}{N},$$

hence,

$$(\phi_1\phi_2)_{\max}=\phi_1(N_1;z_{m_1})\phi_2(N_2;z-z_{m_1})=\phi_1(N_1;0)\phi_2(N_2;0)e^{-\frac{2z^2}{N}}.$$

We assume that

$$z_1=z_{m_1}+\varepsilon;\ z_2=z_{m_2}-\varepsilon.$$

Here ε is the measure of z_1 and z_2 deviation from their maximal values $z_{m_1}$and z_{m_2}.Therefore, it is clear that

$$z_1^2=z_1^2+2z_{m_1}\varepsilon+\varepsilon^2,$$

$$z_2^2=z_{m_2}^2-2z_{m_2}\varepsilon+\varepsilon^2.$$

Taking this into account,

$$\phi_1(N_1;z_1)\phi_2(N_2;z_2)=(\phi_1\phi_2)_{\max}e^{\left(-\frac{4z_1\varepsilon}{N_1}\right)-\left(\frac{2\varepsilon^2}{N_1}\right)+\left(\frac{4z_2\varepsilon}{N_2}\right)-\left(\frac{2\varepsilon^2}{N_2}\right)}.$$

In accordance with

$$\frac{z_{m_1}}{N_1} = \frac{z_{m_2}}{N_2},$$

the number of states in a configuration characterized by the deviation ε from the maximum equals

$$\phi_1(N_1; z_{m_1} + \varepsilon)\phi_2(N_2; z_{m_2} - \varepsilon) = (\phi_1\phi_2)_{\max} e^{\left(-\frac{2\varepsilon^2}{N_1}\right) - \left(\frac{2\varepsilon^2}{N_2}\right)}.$$

To see the effect of this dependence, we assume $N_1 = N_2 = 10^{10}$ and $\varepsilon = 10^6$. Hence, $\frac{\varepsilon}{N} = 10^{-4}$. For such an insignificant deviation from equilibrium, we obtain $\frac{2\varepsilon^2}{N_1} = \frac{2 \cdot 10^{12}}{10^{10}} = 200$.

The product $\phi_1\phi_2$ constitutes a portion equal to $e^{-400} \approx 10^{-179}$ of its maximal value. Therefore, it is clear that the decrease is very significant and, consequently, $\phi_1\phi_2$ should be a function of z_{m_1} with a very sharp peak.

Hence, practically always the most frequent values of z_1 and z_2 are very close to z_{m_1} and z_{m_2}.

It is natural to expect that in a small system appreciable relative deviations in its properties can take place. No theoretical difficulties arise when examining a small system in contact with a large one. The result obtained for the number of admissible states of two systems in contact can be generalized to the case of two systems taking into account the lifting factor.

Applying the same argumentation as previously, we obtain the following expression for the self-similarity of a combined system:

$$\phi(N; I) = \sum_{I_1} \phi_1(N_1 I_1)\phi_2(N_2; I - I_1),$$

where the summation is carried out over all I_1 values below or equal to I. Here $\varphi_1(N_1; I_1)$ is the number of admissible states of the system I at I_1. The configuration of the combined system is determined by I_1 and I_2 magnitudes. The number of admissible states is represented by the product $\phi_1(N_1; I_1)\phi_2(N_2; I_2)$, and the summing-up over all configurations gives $\phi(N; I)$. Let us find the greatest summand in this sum. It is necessary for the extremum that the respective differential was equal to zero:

$$d\phi = \left(\frac{\partial \phi_1}{\partial I_1}\right)_{N_1} \phi_2 dI_1 + \left(\frac{\partial \phi_2}{\partial I_2}\right)_{N_2} \phi_1 dI_2 = 0.$$

We take into consideration the fact that $dI_1 + dI_2 = 0$. We divide this equation by $\phi_1\phi_2$, and since $dI_1 = -dI_2$, we obtain

$$\frac{1}{\phi_1}\left(\frac{\partial \phi_1}{\partial I_1}\right)_{N_1} = \frac{1}{\phi_2}\left(\frac{\partial \phi_2}{\partial I_2}\right)_{N_2}.$$

Proceeding from the fact that

$$\frac{d}{dx}\ln y = \frac{dy}{ydx},$$

the previous expression can be rewritten as

$$\left(\frac{\partial \ln \phi_1}{\partial I_1}\right)_{N_1} = \left(\frac{\partial \ln \phi_2}{\partial I_2}\right)_{N_2}. \tag{4.5}$$

Here we have derived a very important relation for the statistical investigation of the problem under study and will revert to it more than once. At present, we can emphasize the following:

- First, the derivative of the logarithm of the number of self-similar states of each system with respect to the lifting factor determines the most probable configuration of the system; this is the most important feature of the relation (4.5)
- Secondly, two systems are in equilibrium when the combined system is in the most probable configuration, that is when the number of admissible states is maximal
- Thirdly, let us concentrate on the magnitude in the numerator of expression (4.5)

$$H = \ln \phi. \tag{4.6}$$

The obtained expression is surprisingly simple. According to L. Boltzmann's classical definition, this magnitude is nothing else but entropy. According to his definition, entropy is a measure of the system disorder or indefiniteness, that is, the higher H, the greater φ. This definition corresponds to the relation (4.6) in the sense that the more admissible self-similar states characterize the system, the higher is its entropy.

However, this entropy is not derived for an ideal gas as a function of its temperature. It is obtained for characterizing a two-phase flow in critical regimes.

Thus, we introduce a new notion into the theory of two-phase flows, which has a deep physical sense, and at the same time build a bridge to statistical mechanics of an ideal gas.

This mechanics has been based on the notion of gas molecules as ideal balls of the same diameter placed within a closed volume and possessing velocities unambiguously determined by the temperature of the medium. On the basis of such system and taking into account gas molecules collisions with each other and with the chamber walls, a harmonious statistical theory has been developed, which is confirmed by the totality of available data on gaseous systems. In recent years, the interest in this theory has sharply increased in two aspects.

On the one hand, many fundamental works expanding and deepening L. Boltzmann's theory have been published. On the other, the ideas of this theory have been rather successfully applied to non-gaseous systems in other fields of

research, for instance, to solids, nuclear matter, magnetism, quantum optics, polymerization, etc.

Let us apply certain ideas of statistical mechanics, naturally, binding them to specific conditions of the problem under study. At the same time, the specific character of a two-phase flow has required a basic revision of these ideas.

However, basic provisions of thermodynamics and ideal gas theory have been applied, because a sufficiently reliable notional and physical analogy between these processes can be tracked. Thus, some regularities recalling laws of thermodynamics by their structure are obtained. And although these regularities and the parameters involved have absolutely different physical meanings, they are named in a way that is traditional for statistical mechanics, for example, Gibbs factor, Boltzmann factor, entropy, statistical sum for a two-phase flow, etc.

With the account of these preliminary remarks, we expose below the main ideas of the method.

It is established that for the process under study entropy is a function of the number of particles in the system and of the lifting factor, that is,

$$H = f(N; I).$$

Later we examine the connection of entropy with other parameters of the process, and now we consider the main features of this new entropy.

4.4 Main Features of Entropy in Critical Regimes

We examine these features in a certain sequence.

1. Entropy equals zero when the state of the system is completely and unambiguously defined. It means that $\phi = 1$. In this case, $H = \ln \phi = 0$.
2. We try to determine the physical meaning of the expression (4.5). It is, in essence, a magnitude equal to the entropy derivative with respect to the lifting factor, which is equal for both systems, that is,

$$\frac{\partial H}{\partial I} = \frac{1}{\chi}.$$

By analogy with gas dynamics, the parameter χ plays the role of a chaotizing factor of the process. Since the entropy is dimensionless, the dimension of χ should be equal to that of the lifting factor, that is [kgm]:

$$\chi = \frac{m_0 w^2}{2},$$

where m_0 is the mass of the medium in the particle volume. Here the chaotizing factor acquires the meaning of the kinetic energy of the part of the flow equal to the volume of solid particles.

3. When the chaotizing factor of two systems in contact is exactly the same, the contact permits spontaneous changes in particles directions inside them, although the systems are in equilibrium. The number of the states of the first system equals ϕ_1, and each of them can be realized simultaneously with any of the admissible states of the second system equal to ϕ_2. Thus, the total uncertainty of two isolated systems is smaller than or equal to the uncertainty of a combined system.

   This means that

$$H_{\sum} \leq H_1 + H_2.$$

We can offer an illustrative example confirming this fact. Let us take two identical volumes with the same number of particles N in each of them. If the particles of one system differ at least in one feature (for example, in size or even color) from the particles of another system, at the mixing of these volumes the entropy grows.

Entropy of the mixture constitutes the probability logarithm, that is,

$$H = k \ln p.$$

Entropy of each part is zero, since $\ln 1 = 0$.

The probability of particle extraction from the mixture is

$$P = \frac{(N_1 + N_2)!}{N_1! N_2!}.$$

We rewrite this expression using the Stirling formula:

$$\ln N! = N \ln N - N.$$

Taking this into account,

$$\begin{aligned} H &= k[(N_1 + N_2)\ln(N_1 + N_2) - (N_1 + N_2) - N_1 \ln N_1 + N_1 - N_2 \ln N_2 + N_2] \\ &= k\{N_1[\ln(N_1 + N_2) - \ln N_1] + N_2[\ln(N_1 + N_2) - \ln N_2]\}. \end{aligned}$$

If the number of particles is the same, $N_1 = N_2$, then $\Delta H = 2N \ln 2$, which constitutes an entropy increment.

If, however, both volumes contain identical undistinguishable particles, there is no entropy increment, and $2N$ identical particles occupy the volume $2V$. This

phenomenon is known as Gibbs paradox. It testifies to an intricate character of the notion of entropy.

4. Entropy of a stationary process possesses the property of additivity. We know that $H = \ln(\phi_1\phi_2)$, hence $H = \ln\phi_1 + \ln\phi_2 = H_1 + H_2$. Let us analyze the validity of the property of additivity. We have established the number of states in the configuration characterized by a certain deviation ε. We assume, for the sake of convenience, that $N_1 = N_2 = \frac{N}{2}$. Then we can write that

$$\phi(N;z) = \sum_{\varepsilon} (N; z_m + \varepsilon)\phi_2[N_2(z_m - \varepsilon)] = (\phi_1\phi_2)_{\max} \int_{-\infty}^{+\infty} e^{-\left(\frac{8\varepsilon^2}{N}\right)} d\varepsilon$$

where summing over the deviations ε is replaced with an integral. We write $\frac{8\varepsilon^2}{N} = x^2$, then

$$\int_{-\infty}^{+\infty} d\varepsilon e^{-\left(\frac{8\varepsilon^2}{N}\right)} = \sqrt{\frac{N}{8}} \int_{-\infty}^{+\infty} e^{-x^2} dx = \sqrt{\frac{N}{8}}\sqrt{\pi} = \sqrt{\frac{\pi N}{8}}$$

and, consequently,

$$\ln\phi(N;z) = \ln(\phi_1\phi_2)_{\max} + \frac{1}{2}\ln\frac{\pi N}{8},$$

which differs from $\ln(\phi_1\phi_2)_{\max}$ value by a magnitude on the order of $\ln N$. We know that the order of $\ln(\phi_1\phi_2)_{\max}$ equals N, since $(\phi_1\phi_2)_{\max}$ is on the order of 2^N. It means that at $N \gg 1$, $\ln N$ can be neglected in comparison with N.

A conclusion follows that the entropy of a compound system can be considered equal to the sum of entropies of the constituting systems under the condition that the latter possess the most probable configuration.

5. It follows from the statements above that the sum of entropy changes cannot decrease. Omitting numerous consequences of this statement, we emphasize only one of them: Entropy increase in any processes distinguishes the future and the past, and therefore, the arrow of time exists.

If the entropy of the initial state H_0 is defined, then the entropy of an arbitrary state is

$$H_t = H_0 + \int_0^t \frac{dI}{d\chi}.$$

The difference between the infinitesimals dI, dz and $d\chi$ is that dI and dz are infinitesimal differences in comparison with a large number N, while $d\chi$ is simply an infinitesimal amount.

Usually, mass processes are basically irreversible. It is so, although it is not evident. Anyway, if there exists at least one system whose entropy spontaneously decreases without any external efforts, it can be used for decreasing the entropy of some other system. It means that a spontaneous decrease in the entropy of one system leads to a spontaneous decrease in the entropy of all the systems. Hence, either all mass processes are irreversible, or there are no irreversible processes at all. The process of irreversibility is usually identified by an expression of the following type:

$$dH \geq \frac{dI}{\chi}.$$

Irrespective of dI being positive or negative, entropy change in an irreversible process should be always positive.

Long ago, T. de Donde introduced the notion of local equilibrium. It can serve as an excellent approximation for computations in most hydrodynamic and chemical systems. Irreversible processes are usually described through mass forces and mass flows, the latter arising as a result of mass forces. In this sense, entropy change can be represented as

$$dH = F \cdot dX,$$

where F is a force determining the process direction, X is the flow determined by changes either in N or in I.

In the present formalism, mass force is a function of mass variables. Here the change in entropy is a sum of all changes caused by irreversible flows dX_k, which allows the following generalization:

$$dH = \sum_k F_k dX_k \geq 0$$

or

$$\frac{dH}{dt} = \sum_k \frac{F_k dX_k}{dt} \geq 0.$$

Such formulation has another important aspect; it is applicable not only to the entire system, but to all subsystems, as well. We successfully use this aspect considering only a narrow particle size class and extending the obtained results to other classes. All changes in a system occur in such a way that it is forced to approach the equilibrium state with an equalization of force irregularities.

By way of example, examine the following phenomenon. We analyze from this standpoint the behavior of a vertical ascending flow starting from the moment when a certain amount of polyfractional material enters this flow at a zero velocity.

We assume that in this case, particle size distribution is so broad that the flow velocity ensures the hovering velocity of a certain particle size within this distribution. For the sake of convenience, we take the total amount of material entering the flow as a unity. It is known in physics that any system evolves to an equilibrium state, which is equivalent to a state with the minimal potential energy. The equilibrium of particles moving in the flow ensues when the condition

$$v = w - w_{50}$$

is realized for each particle size. Therefore, immediately after placing the particles into the flow, the spatial volume occupied by them starts increasing in both directions. After some time, a certain number of particles acquire a velocity close or equal to the value corresponding to this expression. We call them stratified and introduce the following notations:

G is the total amount of non-stratified material after the time t elapsed since the beginning of the process; D is the amount of material stratified upwards from the feeding place; R is the amount of material stratified downwards. Evidently, at any time interval

$$G + D + R = 1.$$

It is necessary to emphasize once more that only the particles that have acquired a velocity close to the stationary one, and not all the particles that have left upwards or downwards, are considered as stratified.

According to the law of mass action, the number of particles stratified per unit time is proportional to the amount of non-stratified material, that is,

$$\frac{dD}{dt} = k_D G, \frac{dR}{dt} = k_R G,$$

where k_D, k_R are mass processes constants. We exclude the parameter of time out of these relations by dividing the first by the second:

$$\frac{dD}{dR} = \frac{k_D}{k_R}$$

and integrate the obtained expression:

$$D = \frac{k_D}{k_R} R + C.$$

Since at $t = 0$ the expressions $D = 0$ and $R = 0$, then $C = 0$ as well. Thus,

$$\frac{D}{R} = \frac{k_D}{k_R}.$$

If we sum up the principal expressions:

$$\frac{d(D+R)}{dt} = (k_D + k_R)G,$$

then

$$\frac{dG}{dt} = (k_D + k_R)t,$$

that is,

$$G = e^{-(k_D+k_R)t}.$$

Theoretically, at $t \to \infty$, the stratification is complete. In this case,

$$R = \frac{k_R}{k_D + k_R},\ D = \frac{k_D}{k_D + k_R}.$$

Time duration of the processes is limited, and therefore, the separation in real apparatuses is not complete and proceeds with a certain efficiency. Here some of the fine particles get into the coarse product and vice versa.

Thus, the process under consideration is based on the phenomenon of material stratification by particle sizes with respect to their stationary velocities under specific conditions, and not with respect to the apparatus volume.

Here the difference of particles velocities from equilibrium ones acts as a body force, and the occurring mass exchange – as a mass flow.

Similar forces and flows arise in two-phase flows depending on the irregularities of the solid phase concentration and continuum velocity drops. Surely, these parameters also affect particles stratification according to their velocities.

6. Let us establish the relationship between the main parameters. In any case, for a narrow size grade, the number of states of a system can be written as:

$$\phi = \frac{N!}{\frac{N}{2}!\frac{N}{2}!} e^{-\frac{2z^2}{N}},$$

hence

$$H = \ln \phi = \ln N! - 2\ln \frac{N}{2}! - \frac{2z^2}{N}.$$

Taking into account the Stirling formula,

$$\ln n! \approx n(\ln n - 1),$$

this expression can be reduced to the form

$$H = N(\ln N - 1) - N\left(\ln\frac{N}{2} - 1\right) - \frac{2z^2}{N}.$$

It follows that

$$H = N\ln 2 - \frac{2z^2}{N}. \tag{4.7}$$

By definition, the potential extraction is:

$$I = -2zgdm.$$

To write entropy in the form $H(N, I)$, let us square both parts of this expression:

$$I^2 = 4z^2(gdm)^2.$$

Hence,

$$z^2 = \frac{I^2}{4(gdm)^2}.$$

Substitute this expression into (4.7):

$$H(N,I) = H(N,0) - \frac{I^2}{2N(gdm)^2}. \tag{4.8}$$

It can be derived from the definition of the chaotizing factor that

$$\frac{1}{\chi} = \frac{\partial H}{\partial I} = -\frac{I}{N(gdm)^2},$$

whence we can express I through χ:

$$I = -\frac{N(gdm)^2}{\chi}. \tag{4.9}$$

Substituting this expression into (4.8), we obtain:

$$H(N,I) = H(N,0) - \frac{N(gdm)^2}{2\chi^2}.$$

It follows from two latter dependencies that with increasing chaotizing factor, the potential extraction and entropy increase. The mean value

$$\langle I \rangle = -2\langle z \rangle mgd.$$

Comparing this expression with (4.9),

$$-2\langle z \rangle mgd = -\frac{N(gdm)^2}{\chi},$$

hence,

$$\frac{2\langle z \rangle}{N} = \frac{gdm}{\chi} = \frac{gdm}{w^2 m_0} = \frac{gd(\rho - \rho_0)}{w^2 \rho_0}.$$

Consequently,

$$\frac{\langle z \rangle}{N} = \frac{gd(\rho - \rho_0)}{w^2 \rho_0} = B.$$

Here we obtain a confirmation of the fact that the parameter B determines the value of extraction. Let us revert to relation (4.9). If we examine the same system of particles in a different field (centrifugal, electric, magnetic, ultrasound, etc.), at a conserved entropy value we can write

$$H_0 - \frac{N(gdm)^2}{2\chi_1^2} = H_0 - \frac{N(adm)^2}{2\chi_2^2}.$$

It follows that

$$\frac{g^2}{\chi_1^2} = \frac{a^2}{\chi_2^2} \qquad \text{or} \qquad \frac{g}{a} = \frac{\chi_1}{\chi_2}$$

where a is an acceleration in the field of a different nature. We define the value of the specific potential extraction as

$$i(\chi) = \left(\frac{\partial I}{\partial \chi}\right)_{N=1}. \tag{4.10}$$

This is a relation between the potential and kinetic energy referred to one particle of a narrow size class. In this form, the parameter i is constant for particles of a certain size. For other particles, it is also constant, but its value is different, that is for each class, i has an individual value independent of χ.

4.5 Mobility Factor

In the previous section we examined the behavior of two systems that are in an immediate contact. It follows from this examination that the number of admissible states of a joint system is maximal when the chaotizing factors or flow velocities in both systems are equal.

Now we analyze a steady-state flow in a system represented in Fig. 4.2. A characteristic feature of this system is a longitudinal partition along the flow. This partition separates the system comprising particles of the same size grade into two isolated flows.

Let the first flow be characterized by the parameters N_1; I_1, and the second by N_2; I_2. Note that the dynamic conditions of the flow are not the same for both parts, that is,

$$\chi_1 \neq \chi_2 (w_1 \neq w_2).$$

For such steady-state statistical system the following relationships are valid:

$$N = N_1 + N_2,$$

$$I = I_1 + I_2.$$

The validity of the second sum follows from relation (4.4). For a stationary system at $N = N_1 + N_2$ it follows that $z = z_1 + z_2$, and the parameters I and z differ in a constant. After the removal of the partition, these relations remain.

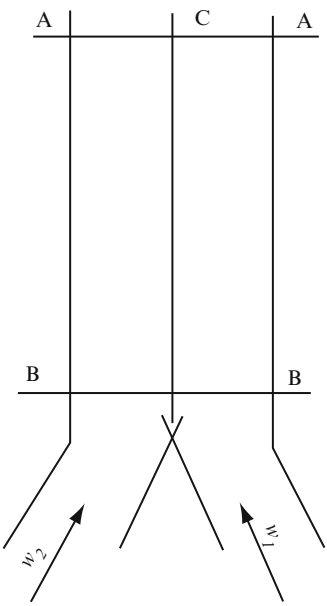

Fig. 4.2 Apparatus with a longitudinal partition

The total entropy change of the combined system after the removal of the partition occurs at the expense of the chaotizing factor equalization and particles exchange. It equals a sum of entropy change of each part caused by equilibrating flows and particles exchange, that is,

$$dH = -\frac{dI}{\chi_1} + \frac{dI}{\chi_2} = \left(\frac{1}{\chi_2} - \frac{1}{\chi_1}\right) dI.$$

Hence, it is clear that when the chaotizing factor in both parts is equalized, entropy generation becomes zero, while before that moment it exceeded zero, that is entropy was growing.

As we have already shown, the most probable configuration of the combined system is that with the maximal number of admissible states at the equality of chaotizing factors in both systems.

This maximal number can be determined by analyzing the product of the numbers of admissible states for separate systems with respect to independent variables characterizing both systems. From the relation

$$\phi = \phi_1 \phi_2 = \phi_1(N_1; I_1)\phi_2(N - N_1; I - I_1)$$

the extremum condition can be written as

$$d(\phi_1 \phi_2) = \left(\frac{\partial \phi_1}{\partial N_1} dN_1 + \frac{\partial \phi_1}{\partial I_1} dI_1\right)\phi_2 + \left(\frac{\partial \phi_2}{\partial N_2} dN_2 + \frac{\partial \phi_2}{\partial I_2} dI_2\right)\phi_1 = 0. \quad (4.11)$$

Taking (4.9) into account, we can write:

$$dN_2 = d(N - N_1) = -dN_1,$$

$$dI_2 = d(I - I_1) = -dI_1,$$

hence,

$$\frac{\partial \phi_2}{\partial N_1} = -\frac{\partial \phi_2}{\partial N_2}; \quad \frac{\partial \phi_2}{\partial I_1} = -\frac{\partial \phi_2}{\partial I_2}.$$

Dividing both sides of (4.11) by the product $\phi_1 \phi_2$ and taking into account the derived relations, we obtain:

$$\left(\frac{\partial \phi_1}{\phi_1 \partial N_1} - \frac{\partial \phi_2}{\phi_2 \partial N_2}\right) dN_1 + \left(\frac{\partial \phi_1}{\phi_1 \partial I_1} - \frac{\partial \phi_2}{\phi_2 \partial I_2}\right) dI_1 = 0.$$

This expression reflects the condition of mutual leveling or equilibrium of both systems. This dependence can be somewhat simplified:

$$\left(\frac{\partial \ln \phi_1}{\partial N_1} - \frac{\partial \ln \phi_2}{\partial N_2}\right) dN_1 + \left(\frac{\partial \ln \phi_1}{\partial I_1} - \frac{\partial \ln \phi}{\partial I_2}\right) dI_1 = 0. \tag{4.12}$$

Apparently, the condition of equilibration of the two systems is satisfied when the expressions in brackets acquire the zero value, since under equilibrium conditions the expression in the second brackets is zero, as established previously. Thus, we obtain from (4.12) that

$$\frac{\partial H_1}{\partial N_1} = \frac{\partial H_2}{\partial N_2}; \quad \frac{\partial H_1}{\partial I_1} = \frac{\partial H_2}{\partial I_2}.$$

The second condition is already known; it is reduced to $\chi_1 = \chi_2$, that is the values of chaotizing factors in both parts of the system are equalized. The first condition is new. We introduce a notation:

$$\frac{\partial H}{\partial N} = \frac{\tau}{\chi} \tag{4.13}$$

where τ is a parameter possessing the meaning of a mobility factor. $H$and N are dimensionless values, therefore, the right-hand side of Eq. (4.13) should be also dimensionless.

Thus, another condition of a stationary process is added. When two systems with equal flow velocities are combined, an additional new condition of a stationary flow acquires the form:

$$\frac{\tau_1}{\chi_1} = \frac{\tau_2}{\chi_2}, \tag{4.14}$$

that is, two systems that can exchange particles get equilibrated when the ratio of their mobility factors to the chaotizing factor become equal. We have assumed that the chaotizing factor is $\chi = w^2 m_0/2$. The mobility factor characterizes the behavior of a particle under specified flow conditions. The dimension of this parameter should be equal to that of the chaotizing factor, that is, [kgm].

Such characteristic of a particle is its vertical velocity component squared, multiplied by the particle mass

$$\tau = \frac{v^2 m}{2}.$$

The flow mobility acquires the meaning of the kinetic energy of solid particles. Using the parameters of the separation process, Eq. (4.14) can be written as follows:

$$\frac{v_1^2}{w_1^2} = \frac{v_2^2}{w_2^2} \qquad \text{i.e.,} \qquad \frac{v_1}{w_1} = \frac{v_2}{w_2}.$$

This ratio determines an extremely important aspect of critical flows. Equilibrium expressed in this way explains the reason of equal extractability of particles of various sizes within the same apparatus, that is offers a statistical substantiation of the separation curves affinization. In fact, it is known that in a deterministic case

$$v = w - w_{50}.$$

Taking this into account, the previous expression can be written as:

$$\frac{(w_1 - w_{50_1})^2}{w_1^2} = \frac{(w_2 - w_{50_2})^2}{w_2^2}$$

or

$$\left(1 - \frac{w_{50_1}}{w_1}\right)^2 = \left(1 - \frac{w_{50_2}}{w_2^2}\right)^2.$$

Taking into consideration the fact that

$$w_{50} = \sqrt{\frac{4}{3}\frac{gd(\rho - \rho_0)}{\lambda\rho_0}},$$

we obtain

$$\left(1 - \sqrt{\frac{8}{3}B_1}\right)^2 = \left(1 - \sqrt{\frac{8}{3}B_2}\right)^2$$

and since $B > 1$ is always valid, it follows that

$$B_1 = B_2 = const.$$

If the solid phase consists of a powder of one and the same density $\rho = const$, this expression becomes

$$Fr_1 = Fr_2 = const.$$

This dependence expresses the condition of equal extractability of particles and explains the reason for separation curves affinization.

An additional condition follows for the equilibrium of two systems that can exchange particles. Such systems are in equilibrium if the equal extractability conditions are satisfied in both of them.

Let us consider a non-equilibrium case. Let $\tau_2 > \tau_1$. At the transition of ΔN particles from system 2 into system 1, the entropy change, according to condition (4.12) is

$$dH = d(H_1 + H_2) = \left(\frac{\partial H_1}{\partial H_1}\right)_{I_1} \cdot dN - \left(\frac{\partial H_2}{\partial I_2}\right)_{I_2} \cdot dN$$
$$= \left(-\frac{\tau_1}{\chi_1} + \frac{\tau_2}{\chi_2}\right) \cdot dN. \tag{4.15}$$

In this expression, the statistical force of the process is $(-\tau_1/\chi_1 = \tau_2/\chi_2)$, and the statistical flow is the particles redistribution. These statistical force and flow form the basis of entropy generation. At the onset of equilibrium, that is at

$$\frac{\tau_1}{\chi_1} = \frac{\tau_2}{\chi_2} \tag{4.16}$$

the directional transverse flow of particles ceases, and entropy generation becomes zero. At the equilibrium, $\chi_1 = \chi_2$ and $\tau_1 = \tau_2$, while $dH = 0$. Hence,

$$\frac{\tau}{\chi_1} = \frac{\tau}{\chi_2}.$$

This is equivalent to

$$\frac{v_1^2}{w_1^2} = \frac{v_2^2}{w_2^2},$$

therefore, we can obtain from (4.16)

$$B_1 = B_2 = const.$$

It has turned out that this complex is universal for critical regimes of two-phase flows. Its application for processing experimental data is described in detail in Chapter 1.

Running a few steps forward (Chapter 8), it follows from the structural model that the separation coefficient

$$k = \frac{v}{w}.$$

Taking this into account, the latter expression can be written as

$$k = \sqrt{2}\frac{z}{N}.$$

This expression reflects correctly the meaning of the separation coefficient.

4.6 Statistical Identities

We examine solid particles interaction in a flow in the critical regime. The gravitational field regulates the motion of particles directing them downwards, and the chaotizing factor prevents this process from disordering the system. We mentally choose a segment in the vertical channel limiting a certain volume by two planes located at a distance l normal to the channel axis. Let us analyze the process in this segment. It is of no importance whether the solid bulk material enters this segment from below – along with the flow, from above – against the flow, or through holes in the lateral side of the segment. We assume that at a certain moment of time, there are N particles of various sizes in this segment:

$$N_n = \sum_n N_i.$$

We select a particular size class out of the flow of particles and examine its behavior. The flow affects this class with a specific force $f[\mathrm{kg/m^2}]$, which allows a certain number of these particles to overcome the gravity force. The flow rate of the medium through this volume is $\mathrm{Vm^3/s}$. Here the chaotizing factor is χ kgm. The number of particles in this volume is proportional to the volume V, specific force f and inversely proportional to the chaotizing factor, that is the higher the latter, the faster the particles leave this volume. Hence, we can write:

$$\frac{fV}{\chi} = \sigma_i N_i,$$

where σ_i is a certain dimensionless proportionality factor.

This relation will be derived later from the process parameters. For all the particles, this dependence can be written as

$$\frac{Vf}{\chi} = \sum_n \sigma_i N_i.$$

If this equality holds for at least one i-th size class out of the total particles distribution, a critical regime of two-phase flow is provided.

The magnitude of f should ensure the gravity force overcoming by particles of a certain size within their distribution and aerodynamic resistance of the rest of the particles to the flow. It can be achieved only at the expense of the energy of the flow equilibrating or exceeding the particles weight. This issue is discussed in detail in Chapter 8.

This parameter can be called flow intensity, and the magnitude fV – potential energy of a moving medium. If for all classes of particles

$$\frac{Vf}{\chi} > \sigma_i N_i,$$

we are dealing with the pneumatic transport regime. At $\frac{Vf}{\chi} < \sigma_i N_i$ for all classes of particles, a descending layer or a motionless layer on a grate blown through from below is realized.

The entropy of this process is a function of the lifting factor, volume and the number of particles $(I; V; N)$. It can be written as a function of several variables:

$$dH = \left(\frac{\partial H}{\partial I}\right)_{V;N} \cdot dI + \left(\frac{\partial H}{\partial V}\right)_{I;N} \cdot dV + \left(\frac{\partial H}{\partial N}\right)_{I;V} \cdot dN. \tag{4.17}$$

Recall the two determinative relations that we have found:

$$\frac{\partial I}{\partial H} = \chi \qquad \text{and} \qquad \frac{\partial H}{\partial N} = \frac{\tau}{\chi}.$$

Multiplying left-hand and right-hand sides of these expressions, we obtain

$$\frac{\partial I}{\partial N} = \tau,$$

whence

$$\partial I = \tau dN.$$

From the first expression, $\partial I = \chi dH$.

We determine the influence of the volume V and flow intensity f on the lifting factor. Examine a certain number of self-similar systems with the same entropy H, volume V, lifting factor I and the same f.

We mentally perform a slow quasi-stationary increase of the volume of one of these systems from V to $V + \Delta V$. The change is so slow that the system remains in its initial equilibrium state, that is its entropy H and the number of particles N remain unchanged. In these conditions, such change is reversible.

All equations of mechanics can be derived using the principle of least action (principle of the potential energy minimum). This is a generally accepted fact established long ago. All systems in nature spontaneously evolve towards their equilibrium states, in which entropy reaches its characteristic extreme values. If physical magnitudes acquire minimal or maximal possible values, it means that they reach their characteristic extreme values. As known, at constant I and V, a system evolves to a state with maximal entropy. At the same time, by analogy with the second law of thermodynamics, at constant H and V, a system evolves to a state with minimal I. In the case under study, at a constant H, the lifting factor changes from $I(V)$ to $I(V + \Delta V)$. at increasing volume.

We expand the lifting factor in series to the accuracy of terms of the first order with respect to ΔV

$$I(V + \Delta V) = I(V) + \frac{\partial I(V)}{\partial V} \cdot \Delta V + \cdots.$$

If, in this case, I decreases, then, apparently,

$$\frac{\partial I(V)}{\partial V} = -f,$$

while a general expression is written as

$$I(V + \Delta V) = I(V) - \Delta V f.$$

Taking this into account and using the general relation

$$dI = \chi dH - f dV + \tau dV,$$

we can write

$$dH = \frac{dI}{\chi} + \frac{f}{\chi} dV - \frac{\tau}{\chi} dN.$$

Reducing the latter expression to a common denominator, we can write

$$\chi dH = dI - \tau dN + f dV. \tag{4.18}$$

This expression can be named as a statistical identity for the critical regime of a two-phase flow. It follows from the comparison of (4.17) and (4.18) that

$$\left(\frac{\partial H}{\partial I}\right)_{V,N} = \frac{1}{\chi}; \quad \left(\frac{\partial H}{\partial V}\right)_{I,N} = \frac{f}{\chi}; \quad \left(\frac{\partial H}{\partial N}\right)_{I,V} = -\frac{\tau}{\chi}.$$

For any multivariable function, mixed derivatives should be independent of the order of differentiation, that is equalities of the following type are valid:

$$\frac{\partial^2 H}{\partial V \partial I} = \frac{\partial^2 H}{\partial I \partial V}.$$

It means that

$$\left(\frac{\partial}{\partial V} \cdot \frac{1}{\chi}\right)_{I,N} = \left(\frac{\partial}{\partial I} \cdot \frac{f}{\chi}\right) \qquad \text{and} \qquad \left(\frac{\partial}{\partial V} \cdot \frac{\tau}{\chi}\right) + \left(\frac{\partial}{\partial N} \cdot \frac{f}{\chi}\right) = 0.$$

Similarly, we can derive other important relations of the same type. It is possible because entropy is a function of the system state. Besides, entropy is directly proportional to the system dimensions, that is, V, since it is an extensive variable. It means that entropy is a homogeneous function of the first power of variables $I; V; N$, that is possesses the property

$$H(\alpha I; \alpha V; \alpha N) = \alpha H(I; V; N).$$

Differentiating this expression with respect to α and then assuming that $\alpha = 1$, we can obtain the Euler theorem for homogeneous functions:

$$H = \left(\frac{\partial H}{\partial I}\right)_{V,N} \cdot I + \left(\frac{\partial H}{\partial V}\right)_{I,N} \cdot V + \left(\frac{\partial H}{\partial N}\right)_{I,V} \cdot N.$$

All parameters in this formula except the lifting factor can be readily determined experimentally. However, the magnitude I can be determined as a function of the parameters $\chi; V; N$. Entropy can be also expressed through these readily determinable parameters. As follows from (4.18),

$$\begin{aligned} \chi dH &= dI + f dV - \tau dN \\ &= \left(\frac{\partial I}{\partial \chi}\right)_V \cdot d\chi + \left(\frac{\partial I}{\partial V}\right)_\chi \cdot dV + f dV - \tau dN + \left(\frac{\partial I}{\partial N}\right)_{V,\chi} \cdot dN, \end{aligned}$$

that is,

$$dH = \frac{1}{\chi}\left[\left(\frac{\partial I}{\partial V}\right)_\chi + f\right] + \frac{1}{\chi}\left(\frac{\partial I}{\partial \chi}\right)_V \cdot d\chi - \frac{\tau}{\chi} \cdot dN + \left(\frac{\partial I}{\partial N}\right)_{V\chi} \cdot dN.$$

Examining these two relations, we can obtain:

$$\left(\frac{\partial H}{\partial V}\right)_{\chi,N} = \frac{1}{\chi}\left(\frac{\partial I}{\partial V}\right)_\chi + \frac{f}{\chi},$$

$$\left(\frac{\partial H}{\partial \chi}\right)_{V,N} = \frac{1}{\chi}\left(\frac{\partial I}{\partial \chi}\right)_{V} = \frac{i}{\chi},$$

$$\left(\frac{\partial H}{\partial N}\right)_{V,\chi} = -\frac{\tau}{\chi} + \left(\frac{\partial I}{\partial N}\right)_{V,\chi} \cdot \frac{1}{\chi},$$

where i is a specific value of the lifting factor. Similarly, we can derive relations for I

$$dI = \chi H - fdV + \tau dN.$$

By analogy with thermodynamics, this dependence, like (4.18), can be called a statistical identity for a two-phase flow. The physical meaning of this identity becomes visual, if we write it as

$$\chi dH + \tau dN = dI + fdV.$$

The left-hand side of this identity contains the kinetic energy of a flow of particles, and the right-hand side – their potential energy. However, this identity is not a conservation law, since it does not comprise the entire flow energy and the entire potential energy of the solid phase.

In critical regimes of two-phase flows, a novel unusual property arises – negative entropy generation, – which is connected with solid phase behavior in a flow. If a polyfractional material gets into an ascending flow, then a certain ordering of particles by size occurs as a result of the phenomenon of stratification. This phenomenon is opposite to mixing. If we conceive that a mixture of particles can be characterized by the entropy of composition, the process of separation leads to a decrease in this entropy component.

In conclusion of this chapter, we discuss one more relation. The specific pressure of a flow can be found from the dependence

$$\frac{fV}{\chi} = \sigma N.$$

Hence,

$$f = \frac{\sigma N S w^2 \rho_0}{2V}.$$

We write

$$\beta = \frac{NS}{V}$$

where β is the specific volume of the solid phase in a flow; S is the volume of an individual particle. Taking this into account,

$$f = \frac{1}{2}\sigma\beta w^2\rho_0.$$

Here we observe an analogy with the quadratic law of the resistance, since f is proportional to $w^2\rho_0$, which is perfectly true from the standpoint of physics of two-phase flows.

Chapter 5
Principal Statistical Relations of Mass Transfer in Critical Flow

Abstract Principal regularities of mass exchange between the zone and apparatus are defined; the notion of large statistical sum is validated; a method of determining average values is presented. Entropy value for the zone and apparatus is determined based on these. On the basis of obtained results, distribution of solid phase of low concentration is examined. General regularities for the zone are formulated.

Keywords Zone · Apparatus · Cell · Large statistical sum · Canonical distribution · Impact factor · Entropy

5.1 Mass Exchange Between the Zone and the Apparatus

We analyze a system that comprises a constant number of particles N_α in the static state. At a definite flow velocity of the medium (w), the lifting factor of this system is characterized by the magnitude I_α.

We conventionally divide this system into two parts and call the larger part an apparatus and the smaller one a zone. The zone implies a part of the vertical channel volume of a moderate height covering the entire cross-section of the channel. The zone height is accepted to be small, but sufficient for holding a large number of particles, and insufficient for appreciable changes in the composition, particles concentration and other parameters of the process. For the sake of convenience, we locate the selected zone on the upper edge of the system, although it can be located in any part of the apparatus, which will not affect the character of the obtained results.

We introduce another limitation of the zone height. It is chosen so small that all the particles moving upwards leave its limits, that is are removed out of the apparatus. We examine statistical properties of such a zone taking into account its contact with the apparatus. The latter means that they possess an unlimited possibility to exchange particles, and the flow velocities therein are either equal or rigidly bound, which is stipulated only by the ratio of the corresponding orifices.

E. Barsky, *Critical Regimes of Two-Phase Flows with a Polydisperse Solid Phase*,
Fluid Mechanics and Its Applications 93,
DOI 10.1007/978-90-481-8838-3_5,

Besides, in this context, one should accept the equality of mobility factors, since we are dealing with particles of a narrow size class. If the number of particles in the zone equals N ($N \ll N_\alpha$), their number remaining in the apparatus equals $N_\alpha - N$; if the zone possesses a lifting factor E, then the respective parameter for the apparatus equals $(I_\alpha - E)$. Our task is to determine statistical properties of a system consisting of two parts. Therefore, we use in full measure the results obtained in Chapter 4.

We determine first the probability for the zone to be found in the i-th state with the lifting factor E_i and to comprise N particles. The probability $P(E_i; N)$ is proportional to the number of admissible states of the apparatus, and not of the zone, since if the zone state is fixed, the number of admissible states of the entire system is equal to the number of admissible states of the apparatus.

As noted above, in this state the apparatus contains ($N_\alpha - N$) particles and possesses the lifting factor $(I_\alpha - E)$. The desired probability is:

$$P(N; E_\mathrm{i}) \approx \phi[(N_\alpha - N); (I_\alpha - E_i)].$$

In this relationship the proportionality coefficient is unknown. To find this coefficient, we apply a method usually used for overcoming this difficulty – determine the ratio of the probabilities for the zone to be in two states:

$$\frac{P(N_1; E_1)}{P(N_2; E_2)} = \frac{\phi(N_\alpha - N_1; I_0 - E_1)}{\phi(N_\alpha - N_2; I_0 - E_2)}. \tag{5.1}$$

By the definition of entropy for the entire apparatus, we can write:

$$\phi(N_\alpha; I_\alpha) = e^{H(N_\alpha; I_\alpha)}.$$

Taking the latter into account, the expression (4.17) can be written as a difference of entropies:

$$\frac{P_1[N_1; E_1]}{P_2[N_2; E_2]} = e^{[H(N_\alpha - N_1; I_\alpha - E_1)] - H(N_\alpha - N_2; I_\alpha - E_2)}. \tag{5.2}$$

The exponent in expression (5.2) can be expanded into a Taylor's series:

$$H(N_\alpha - N; I_\alpha - E) = H(N_\alpha; I_\alpha) - \left(N\frac{\partial H}{\partial N_\alpha}\right)_{I_\alpha} - E\left(\frac{\partial H}{\partial I_\alpha}\right)_{N_\alpha} + \cdots$$

We can write the entropy difference to within the first order as follows:

$$\begin{aligned}\Delta H &\approx [(N_\alpha - N_1) - (N_\alpha - N_2)]\left(\frac{\partial H}{\partial N_\alpha}\right)_{I_\alpha} + [(I_\alpha - E_1) - (I_\alpha - E_2)]\left(\frac{\partial H}{\partial I_a}\right)_{N_\alpha} \\ &= -(N_1 - N_2)\left(\frac{\partial H}{\partial N_0}\right)_{I_a} - (E_1 - E_2)\left(\frac{\partial H}{\partial I_\alpha}\right)_{N_0}.\end{aligned}$$

Using the definition of the newly introduced factors

$$\frac{1}{\chi} = \left(\frac{\partial H}{\partial I}\right)_N; -\frac{\tau}{\chi} = \left(\frac{\partial H}{\partial N}\right)_I,$$

we rewrite the derived expression in the form

$$\Delta H = \frac{(N_1 - N_2)\tau}{\chi} - \frac{(E_1 - E_2)}{\chi}. \tag{5.3}$$

It is noteworthy that ΔH refers to the apparatus, whereas N_1; N_2; E_1; E_2 – to the zone.

Thus, the changes taking place in the zone predetermine the entropy change of the entire apparatus. This is intuitively clear, since everything that leaves the zone and only that determines the sought fractional separation value.

Taking this into account, the dependence (5.3) gives an extremely important relationship from the standpoint of a statistical approach to the problem:

$$\frac{P_1[N_1; E_1]}{P_2[N_2; E_2]} = \frac{\exp[(N_1\tau - E_1)/\chi]}{\exp[(N_2\tau - E_2)/\chi]}.$$

The structure of each exponential term in this dependence is similar to the ratio obtained by Gibbs when studying the thermodynamics of elementary particles in an ideal gas. Although it comprises absolutely different parameters determining the process under study, we will call it Gibbs' factor for a two-phase flow.

Another well-known thermodynamic ratio is called Boltzmann's factor. It can be obtained from Gibbs' factor at a fixed number of particles ($N_1 = N_2 = N$). In this case, this expression is written as

$$\frac{P_1(I_1)}{P_2(I_2)} = \frac{e^{-E_1/\chi}}{e^{-E_2/\chi}} = e^{-(E_1 - E_2)/\chi}.$$

This dependence shows the ratio of probabilities for the zone to be in two states having lifting factors E_1 and E_2 at a constant number of particles N in the zone.

The parameter of $e^{-E/\chi}$ form is called Boltzmann's factor; Gibbs has named this expression a canonical distribution.

The obtained results allow us to make further steps in drawing an analogy between the process under consideration and thermodynamics. Let us consider some more parameters of exceptional importance.

If we summarize the dependence characterizing Gibbs' factor over all the states of the zone and over all particles, we derive an expression called a large statistical sum:

$$Z(\tau; \chi) = \sum_N \sum_i e^{(N\tau - E_i)/\chi}.$$

Such sum is a normalization factor transforming relative probabilities into absolute ones, that is, it plays the part of the previously unknown proportionality coefficient. Now it is clear that the system in the state with $N_1; I_1$ has a probability determined by Gibbs' factor divided by the large sum:

$$P(N_1; I_1) = \frac{e^{(N\cdot\tau - I)/\chi}}{Z}.$$

One can readily see that the sum of this probability over all N and I equals unity.

In chemical kinetics, a large statistical sum is often expressed using a so-called absolute activity parameter. In our case, it is written as:

$$\lambda = e^{\tau/\chi}$$

and we call it, by analogy, an absolute mobility parameter of the system, and the large sum in this case is

$$Z = \sum_N \sum_i \lambda^N e^{-(E_i/\chi)}.$$

Using these ideas, we can establish that the probability for the zone to be in the i-th state is determined as

$$P(N_i; I_i) = \frac{e^{N[E_i\tau - I_i]/\chi}}{Z}.$$

From this standpoint, we can determine a number of important parameters, for example, the average number of particles in the zone.

5.2 Determination of Average Values

The formation of the large sum value makes it possible to determine average values of determining parameters. We seek an average value of a certain physical quantity C taken over an ensemble of systems and denote this average value as $<C>$. If $C(N; i)$ is the value of C for a system of N particles with the zone being in the i-th state, we can write the following:

$$<C> = \sum_N \sum_i C(N; i) P(N; I_i) = \frac{\sum\limits_N \sum\limits_i C(N; i) e^{(N\tau - I_i)/\chi}}{Z} \tag{5.4}$$

Using this approach, we can determine a number of important parameters, for example, the average number of particles in the zone. In principle, the number of particles in the zone can vary because it is in contact with the apparatus, and a number of particles leave the zone moving upwards.

To obtain the average value, each Gibbs' factor in the large sum should be multiplied by N, and in compliance with (5.4), we can write:

$$<N> = \frac{\sum\limits_{N}\sum\limits_{i} N e^{\frac{N\tau - E_i}{\chi}}}{Z}. \tag{5.5}$$

Expression (5.5) can be written in a form that is more convenient for calculations.

By definition of the large sum,

$$\frac{\partial Z}{\partial \tau} = \frac{1}{\chi}\sum_{N}\sum_{i} N e^{\frac{N\tau - E_i}{\chi}}.$$

In this expression, the numerator of Eq. (5.5) is under the signs of sum, therefore, we can write:

$$<N> = \frac{\chi}{Z}\frac{\partial Z}{\partial \tau} = \chi \frac{\partial \ln Z}{\partial \tau}. \tag{5.6}$$

Taking into account previous results,

$$\lambda = e^{\frac{\tau}{\chi}},$$

the large sum can be written as

$$Z = \sum_{N}\sum_{e} \lambda^N e^{-\frac{E_i}{\chi}}.$$

Hence, the average over an ensemble of states can be written as

$$<N> = \lambda \frac{\partial}{\partial \lambda} \ln Z = N. \tag{5.7}$$

This relationship will be used later. The average value of the lifting factor of the zone can be determined as

$$<E> = \frac{\sum\limits_{N}\sum\limits_{i} E_i e^{(N\tau - E_i)/\chi}}{Z}. \tag{5.8}$$

We write $\alpha = \frac{1}{\chi}$ and differentiate the large sum with respect to α:

$$\frac{\partial Z}{\partial \alpha} = \sum_{N}\sum_{i} E_i (N\tau - E_i).$$

Based on (5.8), we can write

$$\langle N\tau - E_i \rangle = \frac{1}{Z}\frac{\partial Z}{\partial \alpha} = \frac{\partial \ln Z}{\partial \alpha}. \tag{5.9}$$

Combining (5.6) and (5.9), we obtain

$$E = \left(\chi\tau\frac{\partial}{\partial \tau} - \frac{\partial}{\partial \alpha}\right)\ln Z. \tag{5.10}$$

If the number of particles in the zone is constant, a quantity analogous to Boltzmann's factor

$$Z_s = \sum_i e^{-E_i/\chi} \tag{5.11}$$

can be taken as a normalizing sum. It is called a statistical sum. It also plays the part of proportionality coefficient between the probability and Boltzmann's factor, that is,

$$P(E_i) = \frac{e^{-E_i/\chi}}{Z_s}. \tag{5.12}$$

At a fixed number of particles, the average value of the lifting factor in the zone amounts to

$$<E_i> = \frac{\sum_i E_i e^{-E_i/\chi}}{Z_s} = \frac{\chi^2 \partial Z_s}{Z_s \partial \chi} = \chi^2 \frac{\partial \ln Z_s}{\partial \chi}. \tag{5.13}$$

Averaging is performed here over the ensemble of states of the zone that is in contact with the apparatus, but comprises a constant number of particles in a stationary process.

5.3 Cell and Apparatus, Entropy

As established, the lifting factor is a homogeneous function of two parameters $I(\chi; N)$. Therefore, we can write

$$I(\chi; N) = NI(\chi),$$

where $I(\chi)$ is the potential extraction probability for one particle.

To understand mass exchange with the cell, we examine a limiting case, where only one particle of a certain fixed size class is constantly located in the zone. Then we pass to the examination of N identical independent particles of the same class.

Let us determine a statistical sum for one particle. Evidently, one particle has only two possible states with its velocity oriented upwards or downwards. The large sum for these two possible states is

$$Z = 1 + e^{-E/\chi}. \tag{5.14}$$

The average lifting factor value for one particle is:

$$<E> = \frac{0 \cdot 1 + Ee^{-E/\chi}}{Z} = \frac{Ee^{-E/\chi}}{1 + e^{-E/\chi}}.$$

The average value for a system of N particles is N-fold greater and amounts to

$$<E> = \frac{NEe^{-E/\chi}}{1 + e^{-E/\chi}} = \frac{NE}{e^{E/\chi} + 1}. \tag{5.15}$$

These relations lead us to the necessity of introducing another element of the model under study – its cell. Let us try to define entropy from this standpoint.

We write the Boltzmann's factor as

$$P_i = \frac{e^{E_i/\chi}}{Z}$$

and take the logarithm of this expression:

$$\ln P_i = -\frac{E_i}{\chi} - \ln Z. \tag{5.16}$$

Hence,

$$E_i = -\chi(\ln P_i + \ln Z). \tag{5.17}$$

The latter is valid only for a stationary state of the system. Taking $\sum_i E_i dP = \kappa dH$ into account, we obtain

$$\chi dH = \sum_i E_i dP_i = -\chi \sum_i (\ln P_i) dP_i - \chi \ln Z \sum_i dP_i. \tag{5.18}$$

However, the probabilities are normalized to unity, that is,

$$\sum_i P_i = 1,$$

and therefore,

$$\sum_i dP_i = 0.$$

Hence, we can obtain

$$\chi dH = -\chi \sum_i (\ln P_i) dP_i,\ d\sum_i (P_i \ln P_i) = \sum_i (\ln P_i) dP_i = \sum_i \ln(P_i) dP_i.$$

Taking this into account, we can write

$$\chi dH = \sum_i E_i dP_i = \chi d\left(-\sum_i P_i \ln P_i \right).$$

We obtain the following expression for the entropy change:

$$dH = d\left[-\sum_i P_i \ln P_i \right] \tag{5.19}$$

and entropy

$$H = -\sum_i P_i \ln P_i. \tag{5.20}$$

For a particle oriented upwards $P_\mathrm{i} = 1$, and downwards $-P_\mathrm{i} = 0$. Therefore, $H = -1 \cdot \ln 1 = 0$. Hence, it is clear that no additional constants appear at the transition from (5.19) to (5.20). Note that (5.20) is entropy definition according to Boltzmann. If a zone possesses φ equiprobable admissible states, then

$$P_i = \frac{1}{\phi}$$

is valid for each of them, and hence

$$-P_i \ln P_i = -\frac{1}{\varphi} \ln \frac{1}{\varphi} = -\frac{1}{\varphi} (\ln 1 - \ln \varphi) = \frac{1}{\varphi} \ln \varphi$$

and

$$H = \sum_i^{\varphi} \frac{1}{\varphi} \ln \varphi = \ln \varphi$$

which totally coincides with the original definition of entropy.

5.4 Separation at Low Concentrations

Let us estimate the influence of the chaotizing factor and the value of narrow class extraction on the change in entropy. The number of states of a system as a function of the number of particles is

$$\phi(N) = \frac{N!}{(N - N_a) N_a!},$$

where N is the total number of particles in the system, N_a is the number of particles oriented upwards.

By the definition of entropy,

$$H = \ln \phi(N) = \ln N! - \ln(N - N_a)! - \ln N_a!.$$

Using Stirling's approximation, we can rewrite this expression as

$$\begin{aligned} H(N) &= N \ln N - N - (N - N_a) \ln(N - N_a) \\ &\quad + N - N_a - N_a \ln N_a + N_a \\ &= N \left[\ln N - \left(1 - \frac{N_a}{N}\right) \ln(N - N_a) - \frac{N_a}{N} \ln N_a \right] \\ &= -N \left[\left(1 - \frac{N_a}{N}\right) \ln\left(1 - \frac{N_a}{N}\right) - \frac{N_a}{N} \ln \frac{N_a}{N} \right]. \end{aligned}$$

According to (3.2a), $\frac{N_a}{N} = \varepsilon_f$. Taking this into account, we can write

$$H(N) = -N\left[\left(1 - \varepsilon_f\right) \ln\left(1 - \varepsilon_f\right) + \varepsilon_f \ln \varepsilon_f\right]. \tag{5.21}$$

The dependence $H(N) = f\left(\varepsilon_f\right)$ is plotted in Fig. 5.1. Its characteristic feature is the presence of optimum. We determine the value of ε_f corresponding to the optimum value of $H(N)$:

$$\frac{\partial H(N)}{\partial \varepsilon_f} = -N \left[-1 \cdot \ln\left(1 - \varepsilon_f\right) - \frac{1 - \varepsilon_f}{1 - \varepsilon_f} + \ln \varepsilon_f + 1 \right] = 0.$$

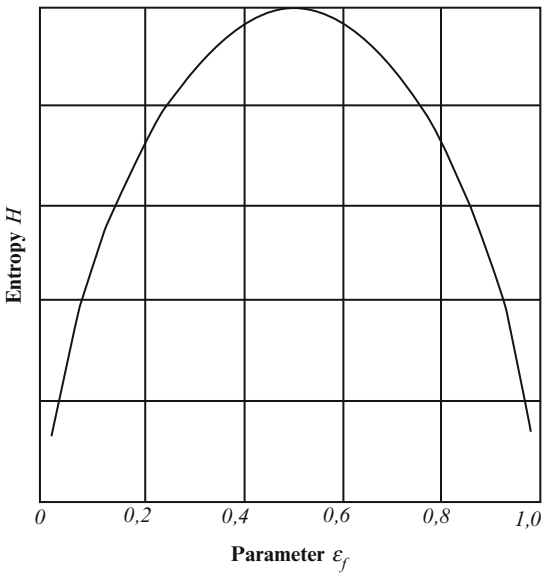

Fig. 5.1 Entropy dependence on ε_f parameter value

Hence, $\log(1-\varepsilon_f) = \log \varepsilon_f$. The only value

$$\varepsilon_f = \frac{1}{2}$$

corresponds to this condition.

Naturally, ε_f is proportional to κ. At the point $\varepsilon_f = 0$, all the particles fall downwards, although κ can be nonzero. With increasing κ, ε_f starts growing, the uncertainty in the particles behavior increases, and entropy grows. This growth with increasing κ continues until ε_f reaches the value $\varepsilon_f = \frac{1}{2}$, and at this moment $H(N)$ reaches its maximum. Here a specific equilibrium is established in the distribution of particles, half of which is oriented upwards, and another half downwards. With further increase in κ, the value of ε_f grows, a larger number of particles acquires a definite direction of motion, and therefore the total uncertainty starts decreasing and the entropy value drops.

At the point $\varepsilon_f = 0$, the magnitude κ has the meaning of the descending layer velocity, while at the point $\varepsilon_f = 1$, the parameter κ acquires the meaning of the critical pneumatic transport velocity. In this case, the entropy reaches the minimal possible value. These two limiting cases correspond to $z = \pm\frac{N}{2}$, and $z = 0$ corresponds to the optimal case.

To determine the value of the optimally attainable entropy, we make use of relation (3.15) and rewrite it in the form

$$H(N,z) = H(N,0) - \frac{2z^2}{N}.$$

For the optimal value,

$$H(N,0) = \frac{N!}{\frac{N}{2}!\frac{N}{2}!} = N\ln N - N - N\ln\frac{N}{2} + N = N\ln N - N\ln N + N\ln 2$$
$$= N\ln 2. \tag{5.22}$$

The minimal value of entropy is

$$H_{\min} = N\ln 2 - \frac{2(N/2)^2}{N} = N\left(\ln 2 - \frac{1}{2}\right). \tag{5.23}$$

It is clear that the absolute value of entropy depends on the logarithm base value. For a natural logarithm, the maximally attainable value is $H_{\max} = 0.693N$, and the minimally possible one is $H_{\min} = 0.193N$. Proceeding from the fact of the solid phase distribution into two products, we can assume that the logarithm base is 2. Then $H_{\max} = N$ and $H_{\min} = 0.5N$. This shows the order of entropy change in the entire range of its values.

The kinetic energy of the flow (κH) characteristic of the volume occupied by the solid phase particles does not have an optimal value. As follows from Fig. 4.2, at a monotonic growth of the chaotizing factor κ, the entropy increases from its minimal to optimal value. The starting point of its growth depends on the dimension and density of the solid particles and takes place, as a rule, at $\kappa > 0$.

With further increase in κ, the entropy value starts decreasing, and this decrease continues until the initial minimal value of entropy is reached. Further increase in κ cannot change this value.

We examine actual conditions that may affect the obtained results. In the zone that is in contact with the apparatus, the number of particles is not constant. The average number of particles is defined as $<N> = \frac{\chi}{z}\frac{\partial z}{\partial \tau}$, and we can show that $<N^2> = \frac{\chi^2}{z}\frac{\partial^2 z}{\partial^2 \tau}$.

Root-mean-square deviation ($<\Delta N>^2$) of the number of particles N from $<N>$ is determined by an expression $N^2 - 2N<N> + <N>^2$, and $<(\Delta N)^2> = <(N - <N>)^2> = <N^2> - 2<N><N> + <N>^2 = <N^2> - <N>^2$

The latter relationship, with the account of the previous ones, amounts to

$$<(\Delta N)^2> = \chi^2\left[\frac{1}{z}\frac{\partial^2 z}{\partial \tau^2} - \frac{1}{z^2}\left(\frac{\partial z}{\partial \tau}\right)^2\right].$$

It can be also shown that

$$<(\Delta N)^2> = \chi\frac{\partial <N>}{\partial \tau}.$$

We have already demonstrated that $\frac{<(\Delta N)^2>}{<N>^2} = \frac{1}{<N>}$. The value of $<N>$ is very high, and therefore fluctuations in the number of particles are very small. Hence, it is necessary to conclude that the number of particles in the zone is a well-defined value, although it is not maintained rigorously constant.

Regarding the lifting factor fluctuations, we can write, proceeding from previously obtained results,

$$<(E - <E>)^2> = \chi^2\left(\frac{\partial I}{\partial \chi}\right).$$

We know that

$$\frac{1}{\chi} = \left(\frac{\partial H}{\partial I}\right)_N,$$

where the right-hand side is calculated for the most probable or equilibrium configuration of a system.

Consequently, at a constant flow velocity, the lifting factor can somewhat fluctuate.

5.5 General Regularities for the Zone

At a constant number of particles, entropy depends on the lifting factor and volume, that is,

$$H = f(I; V),$$

hence, the entropy differential acquires the form:

$$dH = \left(\frac{\partial H}{\partial I}\right)_V \cdot dI + \left(\frac{\partial H}{\partial V}\right)_I \cdot dV. \tag{5.24}$$

In processes taking place at a constant entropy, $dH = 0$. Dividing both parts of Eq. (5.24) by dV, we obtain:

$$\left(\frac{\partial H}{\partial V}\right) = 0 = \left(\frac{\partial H}{\partial I}\right)_V \cdot \left(\frac{dI}{dV}\right)_H + \left(\frac{\partial H}{\partial V}\right)_I. \tag{5.25}$$

Using the relationship (5.24) and the definition of the chaotizing factor, we can write:

$$0 = -\frac{f}{\chi} + \left(\frac{\partial H}{\partial V}\right)_I,$$

which finally results in

$$\frac{f}{\chi} = \left(\frac{\partial H}{\partial V}\right)_{N;I}. \tag{5.26}$$

The latter relationship connects the influence factor with entropy dependence on the volume. Now we consider a total differential of entropy:

$$dH = \left(\frac{\partial H}{\partial I}\right)_{V;N} \cdot dI + \left(\frac{dH}{\partial N}\right)_{I;V} \cdot dN + \left(\frac{dH}{\partial V}\right)_{I;N} \cdot dV. \tag{5.27}$$

Using definitions of τ, χ and f, this expression can be rewritten in the form:

$$dH = \frac{1}{\chi} dI - \frac{\tau}{\chi} dN + \frac{f}{\chi} dV. \tag{5.28}$$

By analogy, the total differential for the lifting factor can be written as

$$dI = \left(\frac{\partial I}{\partial H}\right)_{N;V} \cdot dH + \left(\frac{\partial I}{\partial N}\right)_{H;V} \cdot dN + \left(\frac{\partial I}{\partial V}\right)_{H;N} \cdot dV. \tag{5.29}$$

We can obtain from (5.29):

$$dI = \chi dH + \tau dN - fdV. \tag{5.30}$$

Comparing Eqs. (5.29) and (5.30), we can write:

$$\left(\frac{\partial I}{\partial H}\right)_{N;V} = \chi;\ \left(\frac{\partial I}{\partial N}\right)_{H;V} = \tau;\ \left(\frac{\partial I}{\partial V}\right)_{N;H} = -f. \tag{5.31}$$

Since the second derivative has the property

$$\frac{\partial^2 I}{\partial V \cdot \partial H} = -\frac{\partial^2 f}{\partial H \partial V}, \tag{5.32}$$

hence,

$$\left(\frac{\partial \chi}{\partial V}\right)_{H;N} = -\left(\frac{\partial I}{\partial H}\right)_{V;N}. \tag{5.33}$$

These ratios are in many respects analogous to well-known Maxwell relations for gases, which testifies to the validity of the analogy between gaseous systems and two-phase flows in the critical flow regime.

Chapter 6
Correlation Between the Apparatus and the Cell

Abstract Cellular model validation. Relation between the lifting factor and cell occupancy probability. For coarse particles, the cell occupancy probability is similar to fermion gas regularities. For fine particles, such dependence is similar to boson gas. Mass transfer parameters are determined on the basis of cell occupancy probability. Cellular model for separation process is examined. Entropy of a cellular stationary system is determined. Physical meaning of principal separation parameters is examined from this standpoint.

Keywords Cellular model · Fine particles · Coarse particles · Fermion gas · Boson gas · Cell occupancy probability · Limiting distribution function · Discrete volume · Impact factor · Entropy

6.1 Coarse Particles Separation

In the course of the study of the behavior of an isolated particle in the zone, it was concluded that it is necessary to consider a cellular model. Let us assume that the entire volume of the apparatus is subdivided into rectangular cells in such a way that the volume of each cell holds at most one particle. If the size class under consideration comprises N particles, we can assume that N cells in the apparatus are occupied, and all the rest are free.

It is assumed that the number of cells greatly exceeds the number of particles. Let us examine a system consisting of one cell. Suppose that the cell is located in the apparatus zone and possesses the properties of the zone. It means that a particle located in this cell leaves the apparatus in case of upwards orientation, that is, is extracted into the fine product. We assume that all the rest except this cell is the apparatus. If the cell is not occupied, its $E = 0$. If the cell is occupied, its lifting factor has a certain value corresponding to the probability of its upward orientation.

E. Barsky, *Critical Regimes of Two-Phase Flows with a Polydisperse Solid Phase*,
Fluid Mechanics and Its Applications 93,
DOI 10.1007/978-90-481-8838-3_6,

It follows from the definition of a large sum for one cell that

$$Z = 1 + \lambda e^{\frac{-E}{\chi}}. \tag{6.1}$$

The first summand corresponds to the case of a non-occupied cell with a zero lifting factor; the second summand corresponds to an occupied cell with $n = 1; E \neq 0$.

Average occupancy of a cell is equal to the ratio of the large sum term with $n = 1$ to a sum of summands with $n = 0$ and $n = 1$.

$$<n(E)> = \frac{\lambda e^{\frac{-E}{\chi}}}{1 + \lambda e^{\frac{-E}{\chi}}} = \frac{1}{\lambda^{-1} e^{\frac{E}{\chi}} + 1}. \tag{6.2}$$

We introduce a simpler notation for the average occupancy of a cell:

$$<n(E)> = f(E). \tag{6.3}$$

Recall that $\lambda = e^{\frac{\tau}{\chi}}$. Taking this into account, (6.2) can be written as

$$f(E) = \frac{1}{e^{\frac{E-\tau}{\chi}} + 1}, \tag{6.4}$$

the value $f(E)$ always being between zero and unity.

The form of this dependence recalls the Fermi–Dirac distribution function for a fermion gas. It allows interesting conclusions from the standpoint of statistical properties of the process under study.

6.2 Fine Particles Separation

As regards fine particles, it is necessary to accept the condition that several particles can be simultaneously located in a cell. If we introduce a comparable ratio of the sizes of fine and coarse particles, then the number of fine particles in one cell can be rather significant. We examine one cell in the apparatus zone. The number of fine particles in the cell is n. We emphasize again that from the standpoint of the behavior of coarse particles, a cell can be either occupied or empty, while in case of fine particles it can be either empty or occupied, with n varying within a broad range.

The large sum for fine particles can be written as

$$Z = \sum_n \lambda^n e^{\frac{-nE}{\chi}} = \sum_n \left(\lambda e^{\frac{-E}{\chi}}\right)^n. \tag{6.5}$$

We denote the expression in brackets as

$$\lambda e^{\frac{-E}{\chi}} = y. \tag{6.6}$$

Then at $y < 1$ the following is valid for (6.6):

$$Z = \sum_n y^n = \frac{1}{1-y} = \frac{1}{1-\lambda e^{\frac{-E}{\chi}}}. \tag{6.7}$$

By the definition of the average and taking (6.7) into account, the average number of particles in a cell is

$$<n(N)> = \frac{\sum_n n y^n}{\sum_n y^n}. \tag{6.8}$$

Transforming this dependence, we obtain

$$<n(E)> = \frac{y}{1-y} = \frac{1}{y^{-1}-1} = \frac{1}{\lambda^{-1} e^{\frac{E}{\chi}} - 1}.$$

Hence, we can finally write

$$<n(E)> = \frac{1}{e^{\frac{E-\tau}{\chi}} - 1}. \tag{6.9}$$

This relationship recalls the Bose–Einstein distribution function for a boson gas.

Expressions (6.4) and (6.9) differ in that +1 in the denominator of the first equation is substituted with –1 in the second, but their physical meaning is basically different.

Thus, a common statistical dependence for all particles is expressed by the relation

$$f(E) = \frac{1}{e^{\frac{E-\tau}{\chi}} \pm 1}. \tag{6.10}$$

6.3 Definition of Mass Transfer Parameters

The distribution function (6.10) is related to both fine and coarse particles. It should be taken into account that formally the lifting factor E is related only to the cell, and not to the entire apparatus. If we sum it over the zone, it is equivalent to summing over the apparatus, since particles are extracted only from the zone where the cells are located. Since we analyze averaged behavior of a cell, the results of such analysis can be extended over all the cells of the zone, that is over the entire apparatus.

As follows from Chapter 1, a classical separation regime begins when some size classes totally or partially settle against the flow direction.

Particles settling against the flow direction is possible when their hovering velocity considerably exceeds the flow velocity, that is when

$$w_{50} \gg w_i.$$

For the conditions of air-assisted separation, the ratio

$$\frac{\rho}{\rho_0} \gg 1.$$

Therefore, a part of the denominator in (6.10)

$$e^{\frac{E-\tau}{\chi}} \gg 1.$$

In this case, we can write relationship (6.10) without taking ± 1 into consideration, that is in the form

$$f(E) \approx e^{\frac{\tau-E}{\chi}}. \tag{6.11}$$

The dependence (6.11) is a limiting case for the distribution of coarse and fine particles within the cellular model. The physical meaning of this case is that the average probability of the occupancy of any cell irrespective of the particle size is always below unity.

This condition fully corresponds to fractionating regimes at the solid component concentration in gas up to $\mu = 2\,\mathrm{kg/m^3}$. For example, at the particles density $\rho = 2{,}000\,\mathrm{kg/m^3}$, bulk occupancy of the space amounts to only

$$\beta = \frac{\mu}{\rho} = 0.001.$$

If we assume, in compliance with particles size, that the cell volume is one cubic millimeter, then one cubic meter comprises

$$N_\alpha = 10^9 \text{ cells}.$$

If the particles are supposed to be round, 1 mm in size, their number equals

$$N = \frac{6G}{\pi D^3 \rho} = 2 \cdot 10^6.$$

Thus,

$$n = \frac{10^9}{2 \cdot 10^6} = 500 \text{ cells}$$

correspond to each particle, that is actual occupancy of cells is very low.

Thus, a dependence of (6.11) type is a distribution limit for coarse and fine particles at the average cell occupancy much smaller than unity. In the statistical theory of gases, such an expression is usually called a statistical limit.

It is noteworthy that the limiting distribution function can be used for finding the probable average of such process parameters as the number of particles, their concentration, potential extraction, specific flow pressure and even particles distribution in velocities.

The total number of particles can be obtained from the distribution function by summing over all the cells:

$$N = \sum_i f(E_i),$$

that is the total number of particles equals the sum of their average contents in each cell.

Substitute the sum with an integral:

$$N = \int_0^\infty e^{\frac{\varepsilon - E}{\chi}} dE = \lambda \int_0^\infty e^{\frac{-E}{\chi}} dE = \lambda\chi.$$

Hence, we obtain a compact expression for the absolute mobility parameter

$$\lambda = \frac{N}{\chi}. \tag{6.12}$$

If we pass to specific separation conditions, they usually use the concentration parameter in kg/m^3 without resorting to the notion of the quantity of particles.

Therefore, the possibility of determining concentration as the quantity of particles per cubic meter is a step forward. Hence, we can write

$$N = \mu \cdot V, \tag{6.13}$$

where μ is the particles concentration; V is the volume occupied by the particles.

Which volume is implied here?

It is clear that the stationary volume of the apparatus can pass different quantities of particles per unit time depending on the value of the chaotizing factor (or flow velocity). It is necessary to formulate a certain volume normalized to the chaotizing factor. Such volume can be assumed as

$$V_1 = \frac{Vgdm}{\chi}, \tag{6.14}$$

where V is the volume of the apparatus; χ is the chaotizing factor; g is gravitational acceleration, and d is particle size.

In this case, the dimension of V_1 is that of volume – $[\mathrm{m}^3]$.

Taking into account Eqs. (6.12) and (6.13), the dependence (6.14) can be written as

$$\lambda = \mu \frac{V_1}{gdm}.$$

We call the parameter $V_Q = \frac{V_1}{gdm}$ a discrete volume for critical two-phase flows. Hence, we can write:

$$\lambda = e^{\frac{\tau}{\chi}} = \mu V_Q. \tag{6.15}$$

This dependence characterizes absolute activity of particles in a flow.

Taking this into account, a classical distribution function acquires the form

$$f(E) = \mu V_Q e^{\frac{-E}{\chi}}. \tag{6.16}$$

In our interpretation, we can write

$$f(E) = \mu V_Q e^{-CB},$$

where B is a universal parameter of separation curves; C is a proportionality factor. This expression agrees with the results of empirical processing of a large array of experimental data.

It follows from (6.15) that

$$\frac{\tau}{\chi} = \ln \mu + \ln V_Q. \tag{6.17}$$

In this expression, the concentration parameter is under the sign of its logarithm, which explains experimental results. The values of concentration in separation processes are rather small, down to $2 \div 3\ \mathrm{kg/m}^3$, and logarithms of these values are small and very close to each other. Therefore, the effect of this parameter on the process results cannot be revealed experimentally. Thus, for actual conditions, we can write to a sufficient degree of accuracy that

$$\tau \approx \chi \ln \frac{V_1}{\chi}.$$

Finally, we obtain the following τ for a unit volume:

$$\tau \approx \chi - \ln \chi. \tag{6.18}$$

Hence, the mobility parameter τ is smaller than the chaotizing factor by the value of its logarithm. It has the same dimension as the chaotizing factor.

This differs from the idealized particle velocity value. In actual flows, due to the interaction of coarse and fine particles, their velocity is somewhat leveled, since fine particles accelerate coarse ones, while coarse particles slow down fine ones. Therefore, the actual velocity of both kinds differs from the idealized value

$$v = w - w_0.$$

The expression (6.18) reflects a realistic relation between the velocities of particles and the flow affected by a great number of random factors of a two-phase flow. It also reflects, to a certain extent, their idealized relation.

The total value of the lifting factor for the case under study amounts to

$$I = \sum_i E_i f(E_i) = \lambda \sum_i e^{\frac{-E}{\chi}}.$$

We substitute the sum with an integral and take it for all cells:

$$I = \lambda \int_0^\infty E e^{\frac{-E}{\chi}} dE = \lambda \chi^2.$$

Taking (6.12) into account, we can write:

$$I = N\chi = \mu V_Q \chi. \tag{6.19}$$

Hence, the lifting factor is proportional to the chaotizing factor value, particles concentration and discrete volume. However, within the working interval of concentrations, the two latter parameters affect the separation process only slightly. Let us determine the entropy value from this standpoint. By definition, we can write

$$\left(\frac{\partial H}{\partial N}\right)_I = -\frac{\tau}{\chi}. \tag{6.20}$$

On the other hand, we have established that

$$\frac{\tau}{\chi} = \ln \mu V_Q = \ln N.$$

In this equation, N is the number of particles in a discrete volume. Taking this into account, Eq. (6.20) can be written as follows:

$$\int_0^N dH = \int_0^N dN \left(-\frac{\tau}{\chi}\right) = \int_0^N dN \ln N = N \ln N - N,$$

i.e.,

$$H = N(\ln N - 1). \tag{6.21}$$

Hence, we derive the following sufficiently simple dependence for entropy:

$$H = N(\ln \mu V_Q - 1) = N(\ln V_Q + \ln \mu - 1).$$

In the practice of separation, concentration varies within a small range of values, therefore its logarithm is practically constant.

Taking this into account, we can write:

$$H = N(\ln V_Q + const). \tag{6.22}$$

With the account for previously found relationship

$$\frac{\partial H}{\partial V} = \frac{f}{\chi}.$$

we can obtain from Eq. (4.18):

$$\frac{N}{V_Q} = \frac{f}{\chi}. \tag{6.23}$$

Hence,

$$\frac{V_Q f}{\chi} = N. \tag{6.24}$$

This dependence is obtained for a two-phase flow in the separation regime.

We have examined this relation in Chapter 4, and here it is derived taking into account some qualifying details, and it has turned out that for a discrete volume $\sigma = 1$. If this result seems insufficiently correct, a similar result can be obtained from a somewhat different standpoint.

6.4 Cellular Model of Separation

We can obtain similar results and some additional information by analyzing stationary states of the system under consideration from a somewhat different standpoint. Let us divide the apparatus into N_0 cells and assume, for the sake of simplicity, that these cells are of cuboid shape and sufficient for placing one particle into each. We also assume that N particles are distributed at random over these cells. The number of particles $N \gg 1$, and the number of cells greatly exceeds the number of particles, that is, $N_0 \gg N$. We denote an occupied cell by Θ, and an empty one by O.

The magnitude $(\Theta + \mathrm{O})^{N_0}$ is analogous to previously used notations of $(\uparrow + \downarrow)^{N_0}$ type.

It is clear that the number of various arrangements of N particles in N_0 cells is

$$\phi(N_0; N) = \frac{N_0!}{(N_0 - N)!N!}. \tag{6.25}$$

This value shows the number of stationary states of a system under the condition that each cell can hold at most one particle.

This dependence resembles Eq. (3.8), but it is perfectly clear that the meaning of the parameter N differs from that of the separation factor z.

Denoting by $k = \frac{N}{N_0}$ the share of cells occupied by particles, we can show that for the model under consideration,

$$\tau = \chi \ln k. \tag{6.26}$$

To prove it, let us consider an apparatus consisting of cells and divided into two parts by a vertical partition. For the sake of simplicity, we assume that each part comprises N_0 cells, and the total number of particles in each part is N. Particles in both parts of the apparatus are identical.

If a particle is in a cell of the first part of the apparatus, its separation factor is E_1, and if it is in a cell of the second part of the apparatus, this value is, respectively, E_2. A large sum for one cell of the first part of the apparatus is

$$Z_1 = 1 + \lambda e^{\frac{-E_1}{\chi}}.$$

By analogy with previous derivations, we can obtain for the first apparatus,

$$k_1 = \frac{\lambda e^{\frac{-E_1}{\chi}}}{1 + \lambda e^{\frac{-E_1}{\chi}}} = \frac{1}{\lambda^{-1} e^{\frac{-E_1}{\chi}} + 1} = \frac{\lambda}{e^{\frac{-E_1}{\chi}} + \lambda}. \tag{6.27}$$

For the second apparatus,

$$Z_2 = 1 + \lambda e^{\frac{-E_2}{\chi}}$$

and

$$k_2 = \frac{1}{\lambda^{-1} e^{\frac{-E_2}{\chi}} + 1} = \frac{\lambda}{e^{\frac{-E_2}{\chi}} + \lambda}. \tag{6.28}$$

One can readily see that λ is the same in both formulas, since the cells and particles are identical and χ is the same, too. Let us determine the ratio of the obtained parameters:

$$\frac{k_1}{k_2} = \frac{e^{\frac{-E_2}{\chi}} + \lambda}{e^{\frac{-E_1}{\chi}} + \lambda}.$$

Since we have assumed that in both parts the total number of particles is N, we can write:

$$N = (k_1 + k_2)N_0. \tag{6.29}$$

We have assumed that $N_0 \gg N$, that is there are very few occupied cells. This means that

$$Z \approx 1,$$

and, hence, we can write, based on (6.27) and (6.28), that

$$\left.\begin{aligned} k_1 &\approx \lambda e^{\frac{-E_1}{\chi}} \\ k_2 &\approx \lambda e^{\frac{-E_2}{\chi}} \end{aligned}\right\}. \tag{6.30}$$

According to (6.29), we can write:

$$N \approx \lambda\left(e^{\frac{-E_1}{\chi}} + e^{\frac{-E_2}{\chi}}\right)N_0.$$

Solving (6.30) with respect to λ, we obtain

$$\begin{aligned} \ln k_1 &= \ln \lambda - \tfrac{E_1}{\chi}, \\ \ln k_2 &= \ln \lambda - \tfrac{E_2}{\chi}. \end{aligned} \tag{6.31}$$

By definition,

$$\tau = \chi \ln \lambda.$$

We reduce Eq. (6.31) to a common denominator:

$$\chi \ln k_1 = \chi \ln \lambda - E_1,$$

$$\chi \ln k_2 = \chi \ln \lambda - E_2,$$

and obtain

$$\tau_1 = \chi \ln k_1 + E_1,$$

$$\tau_2 = \chi \ln k_2 + E_2.$$

Obviously, $\tau_1 = \tau_2$, since both parts constitute one apparatus, that is in a general case

$$\tau = \chi \ln k + E.$$

For a cellular stationary system, entropy is expressed by a dependence

$$H(N_0;N) = \ln \phi(N_0;N) = \ln \frac{N_0!}{(N_0-N)!N!}. \tag{6.32}$$

Using Stirling's formula, we can obtain:

$$H(N_0;N) \approx N_0 \ln N_0 - (N_0-N)\ln(N_0-N) - N \ln N. \tag{6.33}$$

As follows from previous statements, the impact factor is connected with entropy by a relationship:

$$\frac{f}{\chi} = \left(\frac{\partial H}{\partial V}\right)_{N;I} = \left(\frac{\partial H}{\partial N_0}\right)_{N;I} \cdot \frac{dN_0}{dV}. \tag{6.34}$$

Proceeding from Eq. (6.33), we can write

$$\left(\frac{\partial H}{\partial N_0}\right)_{N;I} = \ln \frac{N_0}{N_0-N} + \frac{N}{N_0},$$

but according to initial conditions, it was accepted that $\frac{N}{N_0} \ll 1$; then, finally,

$$\left(\frac{\partial H}{\partial N_0}\right)_{N;I} = -\ln\left(1-\frac{N}{N_0}\right).$$

Under the condition $\frac{N}{N_0} \ll 1$, the logarithm can be expanded in series, that is,

$$\left(\frac{\partial H}{\partial N_0}\right)_{N;I} = \frac{N}{N_0}. \tag{6.35}$$

The number of cells is connected with their concentration and apparatus volume:

$$N_0 = n_0 V,$$

hence,

$$\frac{dN_0}{dV} = n_0. \tag{6.36}$$

Using Eqs. (6.34), (6.35), (6.36), we can write

$$\frac{f}{\chi} = \left(\frac{N}{N_0}\right) n_0 = \frac{N}{n_0 V} \cdot n_0 = \frac{N}{V},$$

and finally

$$\frac{fV}{\chi} = N. \tag{6.37}$$

Thus, we obtain the same result.

The dependence (6.37) resembles the Clapeyron law for an ideal gas. The physical meaning of all these parameters is absolutely identical to the parameters of Clapeyron's relation.

6.5 Physical Meaning of Separation Factors

6.5.1 Chaotizing Factor

It has been shown that the chaotizing factor of the process equals

$$\chi = \frac{w^2 m_0}{2},$$

where w is the flow velocity; m_0 is the mass of the medium within the particle volume connected with the Archimedes force.

6.5.2 Flow Mobility

This parameter predetermines diffusion processes. However, under the conditions of separation, where the effect of concentration is leveled, its value is mainly determined by the air flow velocity and the particle mass. It is clear from the physical meaning of the process and even at a purely intuitive level that it corresponds to

$$\tau = \frac{v^2 m}{2},$$

where v is the local velocity of a particle; m is the particle mass.

6.5.3 Separation Factor

It is found that the lifting factor is expressed by a simple relation

$$I = -\frac{N(gdm)^2}{\chi}. \tag{6.38}$$

On the other hand, by definition, it equals

$$I = -2zgdm.$$

From these two expressions we can obtain

$$2zgdm = \frac{2N(gdm)^2}{m_0 w^2}.$$

The latter dependence can be transformed into

$$\frac{z}{N} = -\frac{gd(\rho - \rho_0)}{w^2 \rho_0} = B. \tag{6.39}$$

This amazingly simple dependence means that by specifying the values of the regime parameter B, we can control the relative extraction irrespective of the particles size and density, which ensures the affinization of the separation curves. This hyperbolic dependence of the universal separation curve on the parameter B complies with experimental data.

6.5.4 Concentration Effect

It has been obtained that for a constant number of particles

$$dI = \chi dH - fdV,$$

hence,

$$\chi dH = dI + fdV.$$

In the relation, we express dI as a function of V and χ,

$$\chi dH = \left(\frac{\partial I}{\partial V}\right)_{\chi} dV + \left(\frac{\partial I}{\partial \chi}\right)_{V} d\chi + fdV. \tag{6.40}$$

It is clear that changes in the potential extraction are independent of the volume. Therefore,

$$\left(\frac{\partial I}{\partial V}\right)_{\chi} = 0.$$

The magnitude $\frac{\partial I}{\partial \chi} = iN$. Taking this into account, the general equation can be written as

$$dH = \frac{iN}{\chi} d\chi + f \frac{dV}{\chi}. \tag{6.41}$$

The parameter f can be determined from the relation

$$fV = N\chi.$$

Taking this into account,

$$dH = \frac{iN}{\chi} d\chi + N \frac{dV}{V}.$$

Let us take an integral of this expression:

$$H = iN \ln \chi + N \ln V + c = N(\ln \chi + \ln V + s) \tag{6.42}$$

where c is the integration constant, $s = \frac{c}{N}$. Here the volume $V$is not defined. In this expression i is referred to a single particle. To obtain a correct sum, we should refer the volume to a single particle, too, that is write

$$H = N\left(i \ln \chi + \ln \frac{V}{N} + s\right).$$

The magnitude $\frac{V}{N} = \mu$ is the concentration of particles. Therefore, we finally obtain

$$H = N(i \ln \chi - \ln \mu + s).$$

The concentration value affects entropy only slightly, since it appears in this relation under the sign of its logarithm. Here the number of particles exerts a determining influence.

As for the potential extraction and extraction in general, proceeding from equation

$$\frac{\partial H}{\partial I} = \frac{1}{\chi},$$

we can derive

$$I = N\chi(i \ln \chi - \ln \mu + s).$$

Since the solid phase concentration in the processes of separation is rather low (weight concentration amounts to 2–3 kg/m^3 and volume – to $\beta = 0.001$), and its influence manifests itself through its logarithm, separation results are independent of μ value, which has been established in numerous experiments.

Two parameters, chaotizing factor and the number of particles, exert a determining effect on the potential extraction. The value of the chaotizing factor is not the same over the channel cross-section. From the standpoint of energy minimization, all the particles should be concentrated near the channel walls, where the velocity is minimal. However, it is not the case. As measurements show, particles of all size classes are distributed nearly uniformly over the entire cross-section. It does not seem clear. Maybe this problem is similar to that of a coffee and milk mixture. Namely, milk particles, whose density is smaller than that of coffee, do not float upwards. Apparently, the reason is that the entropy is higher when the particles are uniformly distributed in space, and equilibrium is characterized by entropy maximization.

6.5.5 Potential Extraction

As already shown, potential extraction is mainly determined by the chaotizing factor and the number of particles,

$$I(\chi, N) = Ni(\chi).$$

For a polyfraction mixture, we can write

$$I(\chi, N) = \sum_k i_k(\chi) N.$$

For a narrow size class, a total differential for I is

$$dI = \left(\frac{\partial I}{\partial \chi}\right)_{V,N} d\chi + \left(\frac{\partial I}{\partial V}\right)_{\chi,N} dV + \left(\frac{\partial I}{\partial N}\right)_{V,\chi} dN. \tag{6.43}$$

If the system under study consists of n narrow classes containing N_1; $N_2; N_3; \ldots; N_n$ particles each, the potential extraction is connected with them as follows:

$$dI = \chi dH - f dV + \tau_1 dN_1 + \tau_2 dN_2 + \tau_3 dN_3 + \cdots + \tau_n dN_n.$$

In the general form, this relation can be written as

$$dI = \chi dH - f dV + \sum_n \tau_k dN_k.$$

We know that the examination of cumulative extraction of various classes is not of interest, since only the extraction of narrow classes is invariant. Therefore, we concentrate on the potential extraction of a narrow class keeping in mind that in critical regimes, each narrow class contributes not only into I, but also into the system entropy. For a narrow class, we can write

$$dI = \chi dH - fdV + \tau dN.$$

Using Euler's theorem for homogeneous functions, we can write

$$I = H\chi - fV + \tau N.$$

Hence, the entropy in the explicit form is

$$H = \frac{I}{\chi} + \frac{fV}{\chi} - \frac{\tau}{\chi}N.$$

The two latter expressions are of determining importance for the process under study.

6.6 Extraction from a Cell Located in the Zone

Now we analyze the character of particles extraction from one cell of the zone depending on the ratio of the main distribution parameters.

We revert to Eq. (6.5) for the average cell occupancy:

$$f(E) = \frac{1}{e^{\frac{E-\tau}{\chi}} + 1}.$$

This dependence varies from 0 to 1 and is connected with the fractional separation parameter as follows:

When the kinetic and potential energies of the particle are equal ($E = \tau$), we obtain

$$f(E) = \frac{1}{2}.$$

This corresponds to the separation in optimal conditions.

At $E > \tau$, we obtain

$$f(E) < \frac{1}{2},$$

and at $E<\tau$,

$$f(E)>\frac{1}{2}.$$

All these parameters exactly correspond to the curve of the type

$$F_f(x) = f(B).$$

This is visually confirmed by designed curves of the dependence

$$f(E) = f\left(\frac{v}{w_i}\right)$$

presented in Fig. 6.1, where w_i is the velocity in a specific point of the cross-section, v is the particle velocity. The ratio $\frac{v}{w_i}$ is directly affected by the value of the chaotizing factor χ.

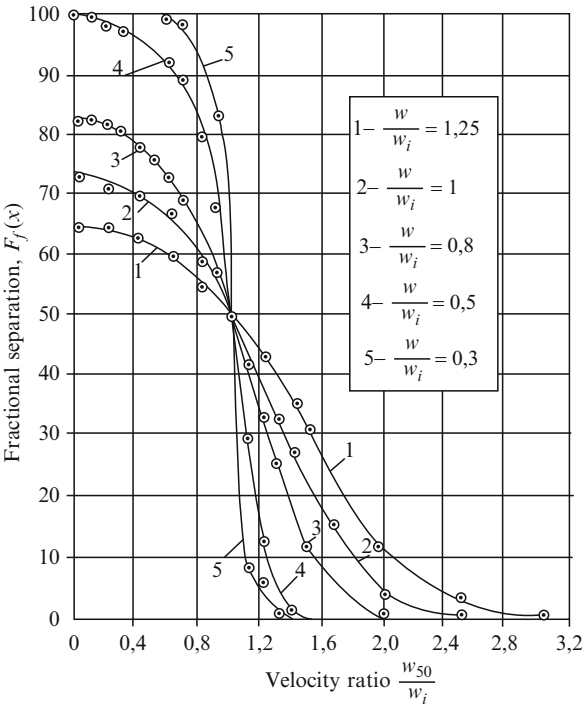

Fig. 6.1 Dependence of fractional separation of a narrow size class on the ratio $\frac{w_{50}}{w_i}$ characteristic of one point of the cross-section

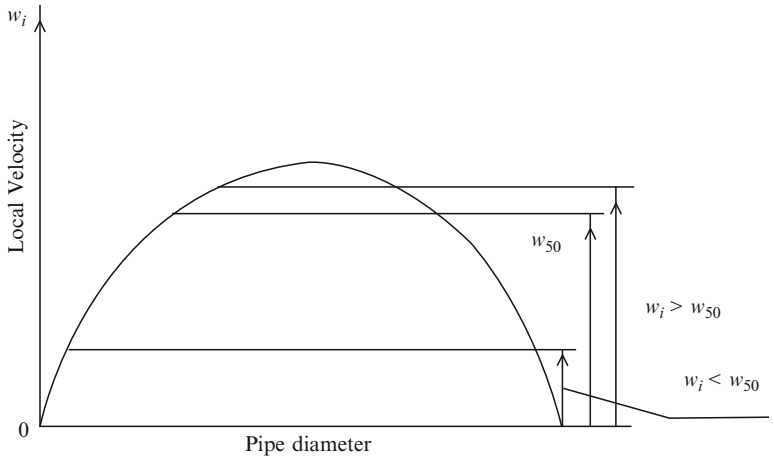

Fig. 6.2 Character of flow structure and principal ratios for a critical flow

The indirect influence on this ratio is determined by the character of velocity profile in the channel cross-section. Figure 6.2 shows a typical characteristic of such a profile. The condition of particles extraction upwards or downwards, features of the behavior of the same particles in the center of the flow or on its periphery depend on the velocity ratio in the profile. Hence, it is necessary to examine the influence of the flow structure on mass distribution in critical regimes. This will be considered in detail in Chapter 7.

Chapter 7
Structural Model of Mass Transfer in Critical Regimes of Two-Phase Flows

Abstract Physics of a two-phase flow motion is examined. The notion of distribution coefficient is substantiated. Balance and structural mathematical models of such flows are developed. Distribution coefficient formation is considered in laminar, transient and turbulent flow regimes. Analysis of this parameter is performed. It has allowed us to formulate a mathematical definition of distribution coefficient for the three flow regimes. Structural model adequacy to experimental data is demonstrated. It allows a prognostic estimation of the process of mass distribution of polyfractional mixture of particles in a flow.

Keywords Flow structure · Distribution coefficient · Cross-section geometry · Flow rate · Velocity profile · Reynolds criterion · Froude criterion · Archimedes criterion · Level lines · Flow profile · Velocity gradient

7.1 Validation of the Distribution Coefficient

Any apparatus, even a hollow one, can be conventionally represented as comprising a certain number of stages with a directional mass exchange between them. A cascade classifier comprising stages of the same or different construction gives the simplest idea of the staged character of the process.

The quantity characterizing redistribution of a narrow size class at a single stage can be presented in the form

$$k = \frac{r_i^*}{r_i}, \tag{7.1}$$

where r_i is the initial contents of narrow size-class particles at a certain i-th stage of the apparatus; r_i^* – quantity of the same particles passing from the i-th stage to the overlying $(i-1)$th stage; K or k – distribution coefficient.

E. Barsky, *Critical Regimes of Two-Phase Flows with a Polydisperse Solid Phase*, Fluid Mechanics and Its Applications 93,
DOI 10.1007/978-90-481-8838-3_7,

A general schematic diagram of particles distribution over the apparatus height at their feeding to the i^*-th stage is presented in Fig. 7.1a. In case of one stage, the process pattern is rather simple (Fig. 7.1b).

We take the initial content of particles of the same narrow class as a unity being clearly aware of the fact that it is fed to be classified in a mixture with other particles.

Fractional extraction degree for the entire apparatus is expressed by a function

$$F_f(x) = \frac{r_f}{r_s}\gamma_s, \tag{7.2}$$

where r_f is the narrow class quantity in the fine product output; r_s – quantity of the same class in the initial material to be classified; γ_s – fine product output.

It was proved that the value of fractional extraction into fine product j is described for any size class by the dependence

$$F_f(x_j) = \begin{cases} \dfrac{1-\sigma^{z+1-i^*}}{1-\sigma^{z+1}}; & k \neq 0.5, \\ \dfrac{z+1-i^*}{z+1}; & k = 0.5, \\ 0; & k = 0, \end{cases} \tag{7.3}$$

where $\sigma = \frac{1-k}{k}$; i^* is the number of the stage of material input into the apparatus.

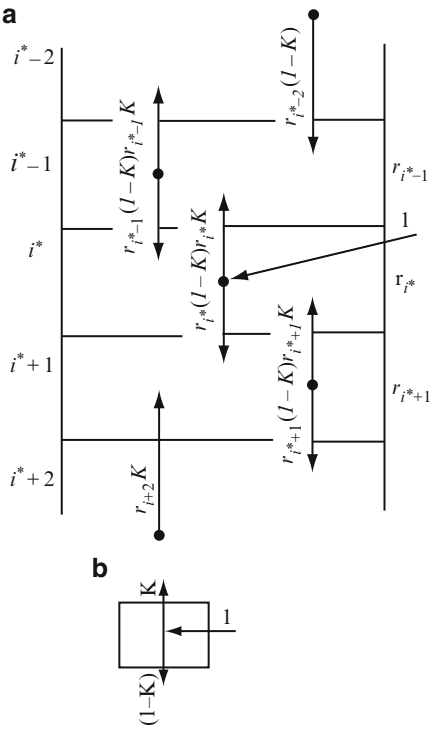

Fig. 7.1 Schematic diagram of flows of a narrow size class: (**a**) in a regular cascade; (**b**) in one stage of a cascade

The dependence (7.3) may serve the basis for designing equilibrium and cascade classifiers, if we manage to establish the dependence of the parameter k on its regime and structural properties of the process.

7.2 Physical Meaning of the Distribution Coefficient

When developing a structural model of the distribution coefficient, we make certain assumptions, namely:

1. Particles are spherical.
2. Distribution of particles of any narrow size class over the cross-section of the apparatus is uniform due to their intense interaction with each other and with the apparatus walls and internal facilities.
3. Ascending two-phase flow should be considered as a continuum with elevated density. As established, carrying capacity of dust-laden flow is higher than that of pure medium. It can be conventionally taken into account by increasing the effective flow density. The distribution of local velocities of the solid phase is a function of geometrical characteristics of the channel cross-section. It can be written in a general form as

$$u_r = w \cdot f\left(\frac{r}{R}\right) \tag{7.4}$$

where $f\left(\frac{r}{R}\right)$ is a function connected with the cross-section geometry; r is a characteristic coordinate of a certain point of the apparatus cross-section; R is a characteristic limiting dimension of the apparatus cross-section; u_r is the local velocity of the continuous phase in a point with the coordinate r; w is the mean flow velocity. Thus, the dependence (7.4) takes into account the shape of the channel cross-section.

According to the Newton–Rittinger law, the dynamic impact of a flow on an isolated particle is described by the relationship

$$F_r = \lambda \frac{\pi d^2}{4} \rho_n \frac{(u_r - v_r)}{2},$$

where λ is the resistance coefficient of a particle; $\frac{\pi d^2}{4}$ is the midlength section area of a particle; ρ_n is flow density; v_r is an absolute local velocity of a particle; $(u_r - v_r)$ is the particle velocity with respect to the flow.

The difference of absolute velocities is algebraic. The flow direction is chosen as a positive direction of u_r and v_r velocities.

If we take the total number of particles of a given mono-fraction in the cross-section under study as a unity, the distribution coefficient can be written as $K = n$, which is a relative number of particles of a specified narrow size class having the absolute velocity above or equal to zero $(v \geqslant 0)$.

Considering the equilibrium of an isolated particle at the distance r_0 from the axis, we obtain

$$\frac{\pi d^3}{6}(\rho - \rho_0) = \lambda \frac{\pi d^2}{4} \rho_0 \frac{(u_r - v_r)^2}{2}. \tag{7.5}$$

Hence,

$$u_r - v_r = w\sqrt{\frac{4}{3\lambda} \cdot B}, \tag{7.6}$$

where $B = \frac{qd(\rho - \rho_0)}{w^2 \rho_0}$.

Let us examine the regime of turbulent overflow of a particle characterized by a constant resistance coefficient λ. In this case, the Reynolds criterion for a particle is

$$\mathrm{Re}_r = \frac{(u_r - v_r) d \rho_o}{\mu} \geqslant 500,$$

where μ is the dynamic viscosity of the medium. Taking (7.6) into account, we obtain

$$\frac{w\sqrt{\frac{4}{3\lambda} \cdot B} \cdot d\rho_0}{\mu} \geqslant 500.$$

This condition corresponds (at $\lambda = 0.5$) to the expression

$$\sqrt{\frac{8}{3} Ar} \geqslant 500,$$

where Ar is the Archimedes criterion:

$$Ar = \frac{qd^2 \cdot \rho \cdot \rho_0}{\mu^2}.$$

Thus, we can determine the limiting size of particles, above which the overflow of particles is certainly turbulent.

Now we examine some properties of laminar overflow of particles. In this case,

$$\mathrm{Re}_p = \frac{(u_r - v_r) d \rho_0}{\mu} \leqslant 1.$$

It follows from equilibrium conditions that

$$\frac{\pi d^3}{6} q\rho = 3\pi\mu(u_r - v_r)d.$$

Taking previous results into account, an expression for this case can be written as

$$Ar = 18\mathrm{Re}.$$

It is known that at a laminar overflow, the resistance coefficient of particles is

$$\lambda = \frac{24}{\mathrm{Re}} = \frac{24\mu}{(u_r - v_r)d\rho_0}.$$

Let us single out the following ratio from (7.5):

$$\frac{u_r - v_r}{w} = \sqrt{\frac{4}{3} B \frac{(u_r - v_r)d\rho_0}{24\mu}},$$

hence,

$$\frac{u_r - v_r}{w} = \frac{1}{18}\mathrm{Re}_w B,$$

where Re_w is the Reynolds number estimated through the mean flow velocity.

Now we can revert to the relation (7.6). For particles of a narrow class with absolute velocity $v_r \geqslant 0$, we can write:

$$u_r \geqslant w\sqrt{\frac{4B}{3\lambda}}.$$

Substituting this into (7.4), we obtain

$$f\left(\frac{r}{R}\right) \geqslant \sqrt{\frac{4}{3\lambda} \cdot B}. \tag{7.7}$$

Similarly, for particles with $v_r \leqslant 0$,

$$f\left(\frac{r}{R}\right) \leqslant \sqrt{\frac{4B}{3\lambda}}. \tag{7.8}$$

Inequalities (7.7) and (7.8) enclose the following limiting cases:

1. For any coordinate

$$f\left(\frac{r}{R}\right) > \sqrt{\frac{4B}{3\lambda}}.$$

In this case, the distribution coefficient $K = 1$;

2. Respectively, at $f\left(\frac{r}{R}\right) < \sqrt{\frac{4B}{3\lambda}}$, for any coordinate r, $K = 0$ is valid

An intermediate case is characterized by level lines formed by certain coordinates according to the equality

$$f\left(\frac{r_0}{R}\right) = \sqrt{\frac{4B}{3\lambda}}. \tag{7.9}$$

We assume that this equation has one real root:

$$\frac{r_0}{R} = f^{-1}\left(\frac{4B}{3\lambda}\right). \tag{7.10}$$

Taking this into account, we find a corresponding area ω_{r_0} for which the following is valid:

$$f\left(\frac{r_i}{R}\right) \geqslant f\left(\frac{r_0}{R}\right).$$

Then the distribution coefficient can be written as

$$K = \frac{\omega_{r_0}}{\omega_R} = c\left(\frac{r_0}{R}\right) \text{ for a convex profile } f\left(\frac{r}{R}\right),$$

$$K = C\left[1 - \left(\frac{r_0}{R}\right)^2\right] \text{ for a concave profile } f\left(\frac{r}{R}\right).$$

The coefficient C characterizes the shape of level lines and cross-section. For example, for a circle, $C = 1$. Substituting dependence (7.7) into the derived equations, we finally obtain

$$K = \phi\left(\frac{B}{\lambda}\right).$$

A similar dependence is valid for two or more roots of Eq. (7.8), which takes place in the case of complicated profiles $f\left(\frac{r}{R}\right)$. For example, in the case of a profile shown in Fig. 7.2, for a certain mono-fraction Eq. (7.8) has three real roots: $r_{0_1}; r_{0_2}; r_{0_3}$. The latter form isotaches with the account for the shape of the apparatus cross-section. Isotaches determine a corresponding total area $\sum \omega_{r_{oi}}$ for which the following is valid:

$$f\left(\frac{r}{R}\right) \geqslant f\left(\frac{r_{oi}}{R}\right).$$

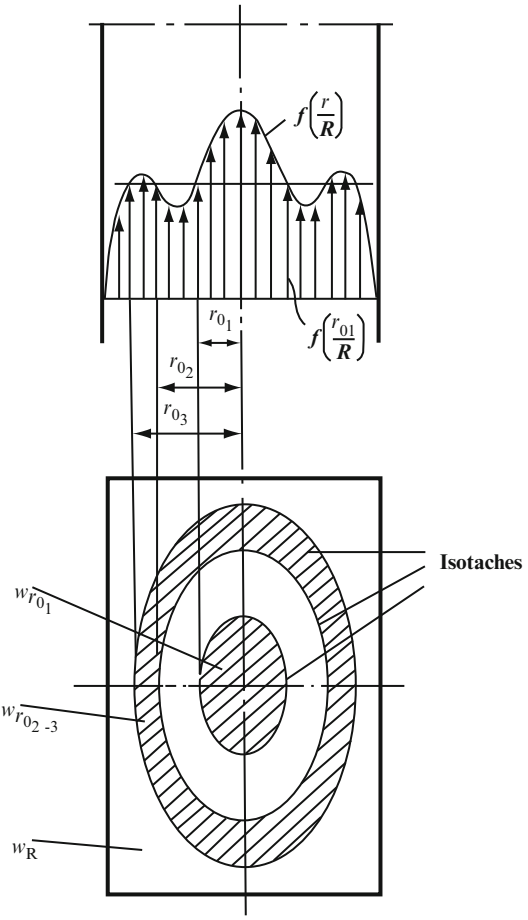

Fig. 7.2 Formation of distribution coefficient in case of a complicated transverse structure of a flow

Thus, for the present case,

$$\sum \omega_{r_{0i}} = \omega_{r_{01}} + \omega_{r_{02}} + \omega_{r_{03}}$$

and the distribution coefficient can be written as

$$K = \frac{\sum \omega_{r_{0i}}}{\omega_R}.$$

Since $\sum \omega_{r_{0i}}$ can be unambiguously expressed through r_{0i}, which are roots of Eq. (7.8), the final expression of the distribution coefficient has the form

$$K = \phi\left(\frac{B}{\lambda}\right). \tag{7.11}$$

A concrete expression of the distribution coefficient can be obtained using a concrete profile of the continuum over the apparatus cross-section. Now we examine step by step possible cases of flow interaction with particles.

7.2.1 *Turbulent Overflow of Particles and Turbulent Regime of the Medium Motion in the Apparatus*

Velocity distribution of a continuum over the radius in equilibrium apparatuses of circular cross-section is usually expressed empirically as

$$u_r = w\frac{(n+1)(n+2)}{2}\cdot\left(1-\frac{r}{R}\right)^n = wf\left(\frac{r}{R}\right) \tag{7.12}$$

where n is a parameter depending on the regime of the medium motion and on the roughness of pipe walls $(n<1)$.

Using Eq. (7.9), we can find the coordinate of isotach where the absolute velocity of a fixed monofraction is zero:

$$\frac{(n+1)(n+2)}{2}\cdot\left(1-\frac{r_0}{R}\right)^n = \sqrt{\frac{4B}{3\lambda}},$$

and hence,

$$\frac{r_0}{R} = 1-\left[\frac{2}{(n+1)(n+2)}\sqrt{\frac{4B}{3\lambda}}\right]^{\frac{1}{n}}. \tag{7.13}$$

Here, the cross-section area for which

$$f\left(\frac{r}{R}\right) \geqslant f\left(\frac{r_0}{R}\right)$$

amounts to $\omega_{r_0} = \pi r_0^2$.

Hence, the distribution coefficient is expressed by the ratio

$$K = \left(\frac{r_0}{R}\right)^2.$$

Then, taking Eq. (7.13) into account, we obtain

$$K = \left\{1-\left[\frac{2\cdot\sqrt{4B/3\lambda}}{(n+1)(n+2)}\right]^{\frac{1}{n}}\right\}^2.$$

Instead of dependence (7.12), we can examine a different profile of velocity distribution of a continuum over the radius:

$$u_r = \frac{n+2}{n} \cdot w\left[1 - \left(\frac{r}{R}\right)^n\right] \tag{7.14}$$

where n is the flow turbulization degree $(n = 2 \div \infty)$.

Let us analyze the following cases:

1. Velocity gradient on the flow axis

   The following relationship is valid for the dependence (7.14)

$$\frac{du}{dr} = -(n+2) \cdot \frac{w}{R}\left(\frac{r}{R}\right)^{n-1} \tag{7.15}$$

   and for the dependence (7.13)

$$\frac{du}{dr} = -\frac{w}{R} \cdot \frac{n(n+1)(n+2)}{2(1 - r/R)^{1-n}}. \tag{7.16}$$

   Then according to Eq. (7.15), we obtain for Eq. (7.14):

$$\left(\frac{du}{dr}\right)_{r=0} = 0.$$

   Respectively, we obtain for Eq. (7.12) from Eq. (7.16):

$$\left(\frac{du}{dr}\right)_{r=0} = -\frac{f(0) \cdot n}{R}.$$

   Thus, Eq. (7.12), in contrast to Eq. (7.14), describes a function discontinuous on the flow axis.

2. Velocity gradient on the pipe wall

   It follows from Eq. (7.15) for the function (7.14) that

$$\left(\frac{du}{dr}\right)_{r=R} = -(n+2) \cdot \frac{w}{R} = -\frac{f(0) \cdot n}{R},$$

   that is, the higher flow turbulization degree and mean velocity, the greater the gradient.

   For the dependence (7.12) we obtain, according to Eq. (7.16),

$$\left(\frac{du}{dr}\right)_{r=R} = \infty,$$

which points to the transfer of infinite momentum and corresponds to infinite friction force.

3. The expression (7.14), in contrast to (7.12), combines all regimes of motion up to laminar. Based on Eq. (7.10), the radius forming the distribution coefficient is

$$\frac{r_0}{R} = \left[1 - \frac{n}{n+2} \cdot \sqrt{\frac{4B}{3\lambda}}\right]^{\frac{1}{n}}.$$

Hence, we obtain an expression for the distribution coefficient:

$$K = \left[1 - \frac{n}{n+2} \cdot \sqrt{\frac{4B}{3\lambda}}\right]^{\frac{2}{n}}.$$

7.2.2 *Laminar Overflow Regime*

In this case, the regime of medium motion in a channel is based on the dependence (7.14) for the flow structure. Thus, at $n = 2$ we deal with a parabolic velocity profile, at $n > 8$ – with a turbulent motion, at $2 < n < 8$ – with a transient regime. Then, according to Eq. (7.10),

$$\frac{n+2}{n}\left[1 - \left(\frac{r_0}{R}\right)^n\right] = \sqrt{\frac{4B}{3\lambda}}. \tag{7.17}$$

Using the expression for the resistance coefficient in this equation, we obtain

$$\frac{n+2}{n}\left[1 - \left(\frac{r_0}{R}\right)^n\right] = \sqrt{\frac{4}{3} \cdot \frac{u_{r_0} d\rho_0 B}{24\mu}}$$

or

$$\frac{n+2}{n}\left[1 - \left(\frac{r_0}{R}\right)^n\right] = \sqrt{\frac{\frac{n+2}{n} \cdot w\left[1 - \left(\frac{r_0}{R}\right)^n\right] d\rho_0}{18\mu} \cdot B}.$$

Simplifying, we obtain

$$\frac{n+2}{n}\left[1 - \left(\frac{r_0}{R}\right)^n\right] = \frac{\mathrm{Re}_w B}{18}.$$

Taking into account the fact that the distribution coefficient $K = \left(\frac{r_0}{R}\right)^2$ and $Re^2B = Ar$, we finally obtain the expression

$$K = \left[1 - \frac{\sqrt{Ar \cdot B}}{18} \cdot \frac{n}{n+2}\right]^{\frac{2}{n}}.$$

For a parabolic profile $(n = 2)$,

$$K = 1 - \frac{\sqrt{Ar \cdot B}}{36}.$$

7.2.3 *Intermediate Regime of Overflow*

Using a well-known dependence of the resistance coefficient on the criteria Re and Ar,

$$\lambda = \frac{4}{3} \cdot \frac{Ar}{\mathrm{Re}^2}$$

and an interpolation formula that is valid for all overflow regimes

$$\mathrm{Re} = \frac{Ar}{18 + 0.61\sqrt{Ar}},$$

we obtain

$$\lambda = \frac{4}{3} \cdot \frac{\left(18 + 0.61\sqrt{Ar}\right)^2}{Ar}.$$

Substituting the latter into Eq. (7.17) and passing to the distribution coefficient, we can define

$$\frac{n+2}{n}\left(1 - k^{\frac{n}{2}}\right) = \frac{\sqrt{Ar \cdot B}}{18 + 0.61\sqrt{Ar}}.$$

A generalized dependence of the distribution coefficient in an arbitrary regime of the medium motion and of an arbitrary regime of particles overflow acquires the form

$$K_{\sum} = \left[1 - \frac{n}{n+2} \cdot \frac{\sqrt{Ar \cdot B}}{\left(18 + 0.61\sqrt{Ar}\right)}\right]^{\frac{2}{n}}. \tag{7.18}$$

7.3 Analysis of Distribution Coefficient

We analyze Eq. (7.18) for turbulent regimes ($Ar \geqslant 10^5$). Under such conditions, the summand 18 in the denominator can be neglected, and the formula is reduced to an expression

$$K = \left(1 - \frac{n}{n+2} \cdot \sqrt{\frac{8}{3} \cdot B}\right)^{\frac{2}{n}}.$$

With the account for the mathematical model of the regular cascade (7.3), this expression well agrees with experimentally obtained dependences.

Two approaches to the study of suspension-bearing flows are the most widespread. The first one considers a two-phase flow as a continuum with averaged properties. Such a dispersoid is characterized by a certain mean velocity, density, etc.

As it is, this approach is unacceptable for a critical flow, since we have to divide the dispersoid into separate phases, because the process result is the separation of each monofraction, which constitute, in total, a discrete phase. Therefore, this approach can be successfully used, for example, for the description of such processes as pneumatic transport, and not for classification.

The second approach consists in a separate analysis of the behavior of each phase. Here, the classification process should take into account numerous random factors. This causes insuperable difficulties in the quantitative description of the results in an explicit form. Therefore, the applicability of this approach is limited. It allows solving the simplest problems of the behavior of two-phase flows and is absolutely inapplicable for describing the classification process on the whole.

As for the classification process, it seems expedient to apply a combined method. Its essence is a transition to a dispersoid with an effective carrying capacity on the basis of the evaluation of the continuum impact on a discrete phase and of the behavior and interaction of individual monofractions. Thus, both the continuum and each separate monofraction participate in the dispersoid formation, and the latter, in turn, affects the behavior of particles of each narrow size class. This implicitly reflects intraphase and interphase interactions on the basis of the continuum.

To substantiate the transition to a "divided" dispersoid, we evaluate the density of monofractions flow. The quantity of particles of a fixed monofraction passing through the apparatus cross-section per unit time can be expressed as

$$Q_{\sum} = \frac{G \cdot r_s \cdot r_i}{P} \tag{7.19}$$

where G is the monofraction mass;

P is the mass of an isolated particle of a specified narrow size class.

Here an ascending flow of monofraction particles is written as

$$Q_a = \frac{G_f \cdot r_s \cdot r_i \cdot K}{P} \tag{7.20}$$

where $r_i \cdot K$ is a relative flow of the particles under study from section i to the overlying section. The resulting ascending flow of the given monofraction is

$$Q_r = \frac{G_f \cdot r_s \cdot F_f}{P}. \tag{7.21}$$

According to the regular cascade model, expressions (7.19), (7.20) depend on $K, z, i^*, i,$ whereas Eq. (7.21) is independent of the section under study.

Assuming a uniform distribution of particles over the apparatus cross-section, we obtain expressions for the flow density of particles of a fixed narrow size class:

$$q_1 = \frac{G_f \cdot r_s}{F \cdot P}$$

for an isolated relative flow and

$$q = q_1 \cdot F_f \tag{7.22}$$

for a resulting flow.

We transform the obtained expressions multiplying both the numerator and the denominator of the right-hand side by the volumetric flow of the continuous phase V

$$q = \frac{G_f \cdot r_s \cdot V}{V \cdot F \cdot P} = \frac{\mu \cdot r_s \cdot V}{F \cdot P} = \frac{\mu \cdot r_s \cdot w}{P}. \tag{7.23}$$

Let us examine the dependencies (7.22) and (7.23) on a concrete example. Thus, at the separation of periclase ($\rho = 3{,}600\,\text{kg/m}^3$) on an equilibrium apparatus in the regime of $w = 2.83\,\text{m/s}$ and at a consumed concentration $\mu = 1.5\,\text{kg/m}^3$, fine product output amounted to about 20%.

Granulometric composition of the initial material, fractional extraction degrees and particle density flows calculated using Eqs. (7.22) and (7.23) are given in Table 7.1.

These data point to the fact that the densities of particle flows (especially of fine particles) in the apparatus are sufficiently high, although the fine product yield is low. It can be attributed to the fact that fine particles, catching up with coarse ones,

Table 7.1 Flow densities of particles of different monofractions calculated by Eqs. (7.22) and (7.23)

Narrow size class (mm)	0.14	0.2 + 0.14	0.3 + 0.2	0.5 + 0.3
Average size d (mm)	0.07	0.17	0.25	0.40
r_s%	10.93	13.51	15.75	26.59
F_f%	93	45.5	8.0	2.0
$q(\text{cm}^2 \times \text{s})^{-1}$	71.8×10^3	6.2×10^3	2.3×10^3	0.94×10^3
$q_{\sum}\,(\text{cm}^2 \times \text{s})^{-1}$	66.8×10^3	2.8×10^3	184	19

exert additional impact on them in comparison with a continuum. Besides, the high density of particles averages and levels out this effect in time. This allows us to pass to the carrying capacity of the flow on the whole (to a dispersoid) and estimate its effect on particles of each narrow size class individually (a divided dispersoid).

It seems reasonable to compare the quantitative value of the particles flow density with experimental data. Thus, Razumov presents experimental data (under the conditions of vertical pneumatic transport) on the number of collisions between the suspension-carrying flow containing a mono-fraction of the size $d = 2.3\,\text{mm}$ and the motionless surface with the area $1\,\text{cm}^2$. The characteristic parameters of the experimental conditions were as follows:

- Density of the medium $\rho_0 = 1.29\,\text{kg/m}^3$
- Density of the particles material $\rho = 1{,}200\,\text{kg/m}^3$
- Initial mass concentration $3.5\,\frac{\text{kg/h}}{\text{kg/h}}$, which corresponds to $\mu = 4.515\,\text{kg/m}^3$
- $r_s = 100\%$, since the experiment was performed on a monofraction
- Mean velocity of the medium flow varied within the limits of $10 \div 17.5\,\text{m/s}$

In the course of the experiments, 300–1,300 collisions were registered per second per $1\,\text{cm}^2$ of surface placed into the ascending flow. Apparently, proceeding from experimental conditions, the number of collisions corresponds to the density of particles flow described by Eq. (7.22). Assuming, on the average, $w = 14\,\text{m/s}$, we obtain $N = q = 827\,\frac{1}{\text{cm}^2\cdot\text{s}}$, which is close to the average number of collisions registered in the experiment. For the velocities $w = 10\,\text{m/s}$ and $w = 15\,\text{m/s}$, the numbers of collisions determined by Eq. (7.22) are 590 and $1{,}033\,\frac{1}{\text{cm}^2\cdot\text{s}}$, respectively. Apparently, these results give rather satisfactory estimations.

To pass to a divided dispersoid, which is different for particles of each narrow size class, we have to evaluate its important parameter – density ρ_{n_j} (dispersoid density for particles of the j-th narrow size class).

Let us examine two monofractions with particle masses m and M. We assume that N fine particles inelastically collide with one coarse particle imparting their momentum to it. To the first approximation, the quantity N can be evaluated through the ratio of flow densities of the monofractions under study.

$$N = \frac{q_m}{q_M} = \frac{r_m}{r_M} \cdot \left(\frac{d_m}{d_M}\right)^3. \tag{7.24}$$

As a result of inelastic collisions, the ensembles of fine and coarse particles acquire the same velocity $v_{Km} = v_{KM}$, the velocity of fine particles having decreased from v_{Hm} to v_{KM}, and that of coarse particles – increased from v_{HM} to v_{KM}. The change in the momentum of the fine particles ensemble amounts to

$$\Delta L_m = Nm(v_{Hm} - v_{Km}),$$

and that of coarse particles – to

$$\Delta L_M = M(v_{KM} - v_{HM}).$$

Obviously, $\Delta L_m = \Delta L_M$. This stipulates the following:

$$v_{Km} = v_{KM} = \frac{Nmv_{Hm} + Mv_{HM}}{Nm + M}. \tag{7.25}$$

The conditions of a uniform motion of fine and coarse particles with initial velocities are as follows:

$$(u - v_{Hm})^2 = \frac{3}{4\lambda} \cdot \frac{\rho}{\rho_0} \cdot gd_m, \tag{7.26}$$

$$(u - v_{HM})^2 = \frac{3}{4\lambda} \cdot \frac{\rho}{\rho_0} \cdot gd_M. \tag{7.27}$$

The conditions of a uniform motion of a coarse particle with a final velocity in a dispersoid is, respectively:

$$(u - v_{KM})^2 = \frac{3}{4\lambda} \cdot \frac{\rho}{\rho_0} gd_M. \tag{7.28}$$

Having divided term-by-term the expression (7.27) by (7.28), we obtain

$$\frac{\rho}{\rho_0} = \left(\frac{u - v_{KM}}{u - v_{Km}}\right)^2 \tag{7.29}$$

From Eq. (7.25),

$$u - v_{KM} = u - \frac{Nmv_{Hm} + mv_{HM}}{Nm + M}. \tag{7.30}$$

After simple transformations, this expression acquires the form

$$u - v_{KM} = \frac{Nm(u - v_{Hm}) + M(u - v_{HM})}{Nm + M}. \tag{7.31}$$

Using Eq. (7.29)

$$\frac{\rho_n}{\rho_0} = \frac{(Nm + M)^2}{\left(Nm\frac{u - v_{Hm}}{u - v_{HM}} + M\right)^2} \tag{7.32}$$

or, taking into account both (7.26) and (7.27),

$$\frac{\rho_n}{\rho_0} = \frac{(Nm + M)^2}{\left(Nm\sqrt{\frac{d_m}{d_M}} + M\right)^2} = \left(\frac{N\frac{m}{M} + 1}{N\frac{m}{M}\sqrt{\frac{d_m}{d_M}} + 1}\right)^2. \tag{7.33}$$

Using Eq. (7.24) and taking into account the fact that $\frac{m}{M} = \left(\frac{d_m}{d_M}\right)^3$, we obtain

$$\frac{\rho_n}{\rho_0} = \left(\frac{\frac{r_m}{r_M} + 1}{\frac{r_m}{r_M}\sqrt{\frac{d_m}{d_M}} + 1} \right)^2. \tag{7.34}$$

Since $\rho_n = \rho_0 + \Delta\rho_n$, a relative increase in the dispersoid density is

$$\frac{\Delta\rho_n}{\rho_0} = \frac{\rho_n}{\rho_0} - 1.$$

With the account of n mono-fractions under study, which transfer the momentum to a coarser particle, relative increase in the dispersoid density is

$$\frac{\rho_n}{\rho_0} = \sum_{j=1}^{n} \left(\frac{\rho_n}{\rho_0}\right)_j - n + 1.$$

With the account for Eq. (7.34), the final expression for the dispersoid density is

$$\rho_n = \rho_0 \left[\sum_{j=1}^{n} \left(\frac{\frac{r_m}{r_M} + 1}{\frac{r_m}{r_M}\sqrt{\frac{d_m}{d_M}} + 1} \right)^2 + 1 - n \right]. \tag{7.35}$$

To check the above-mentioned experiment on periclase classification using Eq. (7.35), we have calculated dispersoid flow densities for the mentioned mono-fractions

$$\begin{aligned} d_m &= 0.40\,\text{mm} \quad \rho_n = 2.29\,\text{kg/m}^3 \\ d_m &= 0.25\,\text{mm} \quad \rho_n = 2.06\,\text{kg/m}^3 \\ d_m &= 0.17\,\text{mm} \quad \rho_n = 1.70\,\text{kg/m}^3 \end{aligned}$$

The obtained results point to an insignificant change in the flow density of the dispersoid affecting individual narrow classes of particles. On the average, in the present case we can assume $\rho_n = 2.0\,\text{kg/m}^3 = const$ as a first approximation for all monofractions. It is noteworthy that for materials without sharp granulometric differences, the difference in the mean flow density is insignificant. For more exact estimations (or for materials with extremely different compositions), it is recommended to use Eq. (7.35) for each monofraction.

Another important issue arising at a transition to the dispersoid is to evaluate its structure, the profile of its velocity distribution over the apparatus cross-section. Equations (7.26) and (7.27) implied a dispersoid with local effective velocities u. A transition to ρ_n was realized at the expense of the momentum transfer from fine

particles to coarse ones. The flow density ρ_n was assumed to remain unchanged over the apparatus cross-section owing to the assumption of a uniform distribution of particles. Since the local carrying capacity per unit area is characterized by the product $\rho_n u^2$, its profile should be affine or uniform with respect to the distribution of squared dispersoid velocities in the cross-section. Taking into account its affine transformation with the scale factor 0.5 and nonlinear square-root transformation, we obtain the profile of effective dispersoid velocities close to a parabolic one. Since the volume flow rate of a dispersoid should be equal to a continuum volume flow rate, the equation of dispersoid velocity distribution should be written as

$$f\left(\frac{r}{R}\right) = 2w\left[1 - \left(\frac{r}{R}\right)^2\right], \tag{7.36}$$

which corresponds to the parameter $n = 2$.

Obviously, the above-stated estimation should be considered as approximate, because it is based on a number of assumptions.

Substituting $n = 2$ in Eq. (7.19) and replacing ρ_0 with ρ_n, we obtain

$$K = 1 - \sqrt{0.4 \cdot B}. \tag{7.37}$$

The obtained expression reflects adequately enough $B_{\max} = 2.5$ and agrees sufficiently well with the description of experimental separation curves $F_f(d)$ based on a cascade model (for turbulent regimes). In the case of an arbitrary regime of particles overflow, we derive from Eq. (7.19):

$$K = 1 - \frac{\sqrt{Ar \cdot B}}{36 + 1.575\sqrt{Ar}}. \tag{7.38}$$

Equations (7.37) and (7.38) are valid for $\rho_0 = 1.2\,\mathrm{kg/m^3}$and $\rho_n = 2.0\,\mathrm{kg/m^3}$ appearing in the coefficients, and the criterion Ar and B are expressed, as before, through ρ_0.

7.4 Analysis of Experimental Dependencies from the Standpoint of Structural Models

Principal regularities of the gravitational classification process were revealed experimentally on various cascade apparatuses. Now it has become possible to explain experimental facts from the standpoint of structural and cascade models.

First of all, it follows directly from Eqs. (7.37) and (7.19) that it is possible to plot a separation curve $F_f(x)$ in any regime.

The same expressions allow us to take into account separation results depending on the number of stages in a cascade apparatus (classifier height) and on the material feeding place.

The effect of structural differences of various apparatuses on the fractioning process is taken into account by the application of different cascade models.

To check fractional separation curves for particles of different narrow size classes depending on the classification regime, as well as other regularities, respective estimations were performed for a shelf-type cascade apparatus comprising four stages $(z = 4)$ in the case of initial material feed from above $(i^* = 1)$. Experimental data on quartzite separation in it $(\rho = 2650\,\mathrm{kg/m^3})$ are presented in Fig. 7.3. The comparison of computation results $F_f(d_j, w)$ obtained using Eqs. (7.37) and (7.19) with experimental data is presented in the same figure.

According to Eq. (7.37), the velocity w_0 of the onset of fixed monofraction extraction (intersection of $F_f[d_i, w]$ curve with the abscissa axis) is determined from the condition

$$K = 0 = 1 - \sqrt{0.4 \cdot B}.$$

Hence, neglecting ρ_0 value in comparison with ρ_f, we obtain

$$w_0 = \sqrt{0.4 \cdot \frac{\rho}{\rho_0} gd}.$$

This makes it possible to predict the ratio of the velocity w_0 to the final settling velocity v_0 of an individual particle of the specified size class in air. As known,

$$v_0 = \sqrt{\frac{4}{3\lambda} \cdot \frac{\rho}{\rho_0} \cdot gd}. \tag{7.39}$$

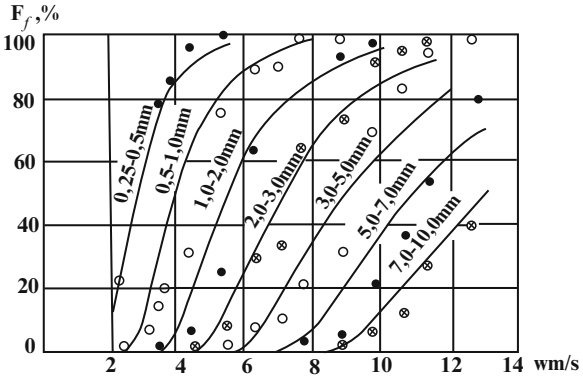

Fig. 7.3 Fractional separation dependence on the air flow rate: ○ ● ⊗ – experimental points; —— – estimated curve

At the aerodynamic resistance factor $\lambda = 0.5$, we obtain

$$\frac{v_0}{w_0} = \sqrt{\frac{4}{3 \cdot 0.5 \cdot 0.4}} = 2.59. \tag{7.40}$$

To check this ratio, w_0 velocities were calculated using Eq. (7.39) for particles of all narrow size classes examined in the previous example, and compared with experimental w_0 values. The aerodynamic resistance factor in Eq. (7.39) was determined using an adjusted dependence

$$\lambda = 0.5 + \frac{29.2}{\sqrt{Ar}} + \frac{430}{Ar}.$$

The comparison of the computed dependence (7.40) with experimental data is shown in Fig. 7.4.

A characteristic property of separation curves is their affinity. Its consequence is a unitary character of $F_f\left(\frac{w}{w_{50}}\right)$ curve for all monofractions. A combined analysis of cascade and structural models confirms this fact. Thus, the distribution factor K_{50} for any 50%-extractable monofraction is determined from the equation

$$\frac{1 - [(1 - K_{50})/K_{50}]^{z+1-i^*}}{[(1 - K_{50})/K_{50}]^{z+1}} = 0.5. \tag{7.41}$$

Substitute K_{50} value found from Eq. (7.41) into Eq. (7.37):

$$K_{50} = 1 - \sqrt{0.4 \frac{\rho}{\rho_0} \cdot \frac{gd}{w_{50}^2}}.$$

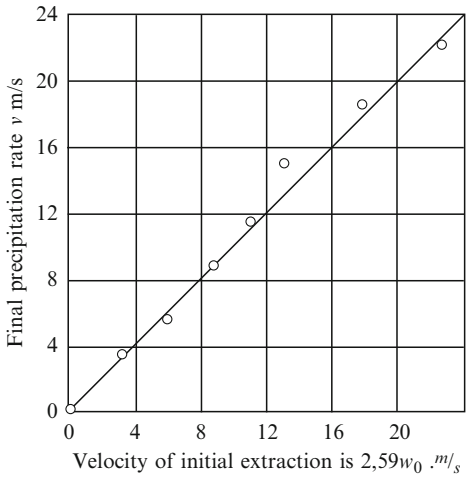

Fig. 7.4 Correlation between the final precipitation velocity and the velocity of initial extraction of various monofractions ensuring $F_f(x) = 0$

Hence,

$$0.4\frac{\rho}{\rho_0}\cdot gd = (1-K_{50})^2 w_{50}^2.$$

We substitute the obtained value $0.4\frac{\rho}{\rho_0}gd$ into Eq. (7.37) for an arbitrary distribution factor

$$K = 1 - \frac{w_{50}}{w}(1-K_{50}).$$

Substitute the latter into Eq. (7.19):

$$F_f\left(\frac{w}{w_{50}}\right) = \frac{1-\left\{1/\left[\left(\frac{1}{1-K_{50}}\right)\frac{w}{w_{50}}-1\right]\right\}^{z+1-i^*}}{1-\left\{1/\left[\left(\frac{1}{1-K_{50}}\right)\frac{w}{w_{50}}-1\right]\right\}^{z+1}}. \tag{7.42}$$

The obtained expression (7.42) satisfies the unitary character of $F_f\left(\frac{w}{w_{50}}\right)$ curve, whose plotting requires successive solution of Eq. (7.41), and then Eq. (7.42). In particular, for the case under study $(z=4, i^*=1)$, we derive from Eq. (7.41):

$$K_{50} = 0.342;\ 1-\frac{1}{K_{50}} = 1.519.$$

In this case, the dependence (7.42) acquires the form

$$F_f\left(\frac{w}{w_{50}}\right) = \frac{1-\left[1/\left(1.519\frac{w}{w_{50}}-1\right)\right]^4}{1-\left(\frac{1}{1.519}\frac{w}{w_{50}}-1\right)^5}. \tag{7.43}$$

The comparison of results computed by Eq. (7.43) with experimental data is presented in Fig. 7.5.

As previously, the affinity of separation curves $F_f(x)$ results in a unitary character of $F_f\left(\frac{d}{d_{50}}\right)$ curve for all velocities. Using the solution of Eq. (7.41) with respect to K_{50} in (7.37), we obtain for an arbitrary regime:

$$K_{50} = 1 - \sqrt{0.4\frac{\rho}{\rho_0}\cdot\frac{gd_{50}}{w^2}}, \tag{7.44}$$

$$\frac{(1-K_{50})^2}{d_{50}} = 0.4\frac{\rho}{\rho_0}\cdot\frac{g}{w^2}. \tag{7.45}$$

Passing to an arbitrary distribution factor, we obtain

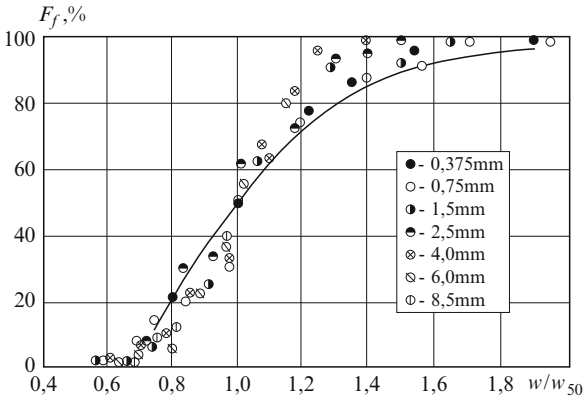

Fig. 7.5 Fractional separation dependence on the relative velocity:○ ● ◓ ◑ ⦸ ⊗ ⦶ – experimental points; —— – estimated curve

$$K = 1 - (1 - K_{50}) \cdot \sqrt{\frac{d}{d_{50}}}. \tag{7.46}$$

Then the expression (7.19) acquires the form:

$$F_f\left(\frac{d}{d_{50}}\right) = \frac{1 - \left[\frac{(1-K_{50})\sqrt{\frac{d}{d_{50}}}}{1-(1-K_{50})\frac{d}{d_{50}}}\right]^{z+1-i^*}}{1 - \left[\frac{(1-K_{50})\sqrt{\frac{d}{d_{50}}}}{1-(1-K_{50})\sqrt{\frac{d}{d_{50}}}}\right]^{z+1}}. \tag{7.47}$$

Experimental check of the dependence (7.47) at $z = 4; i^* = 1$ is presented in Fig. 7.6.

It is noteworthy that we can prove in a similar way the unitary character of $F_f\left(\frac{d}{d_{50}}\right)$ and $F_f\left(\frac{w}{w_{s0}}\right)$ curves for an arbitrary fractional separation value.

Experimentally established universality of $F_f(Fr)$ curve for various regimes and different monofractions can be directly revealed from the structural and cascade models. In fact, for a specific apparatus $(z; i^*)$ and the density of material particles ρ, fractional extraction is unambiguously determined by the parameter $\frac{gd}{w^2}$. The comparison of the curve calculated by Eqs. (7.37) and (7.19) with experimental data in the case under study $(z = 4; i^* = 1;\ 2{,}500\,\mathrm{kg/m^3})$ is presented in Fig. 7.7.

In a more general case, when the densities of materials to be classified differ, a universal dependence is a function of the generalized classification parameter $F_f(B)$. This fact also follows directly from Eqs. (7.37) and (7.19). In particular, computed $F_f(B)$ values and experimental data for the separation of different materials in an equilibrium apparatus of circular cross-section $(D = 100\,\mathrm{mm};\ z = 9;\ i^* = 6;\ \mu = 1.5\,\mathrm{kg/m^3})$ are presented in Fig. 7.8.

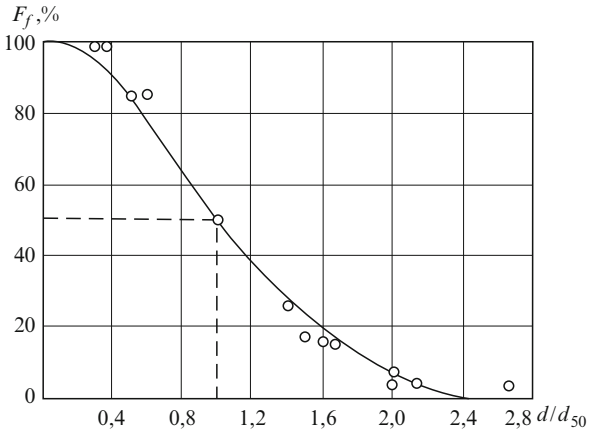

Fig. 7.6 Fractional separation dependence on the relative size: ○ – experimental points; —— – estimated curve

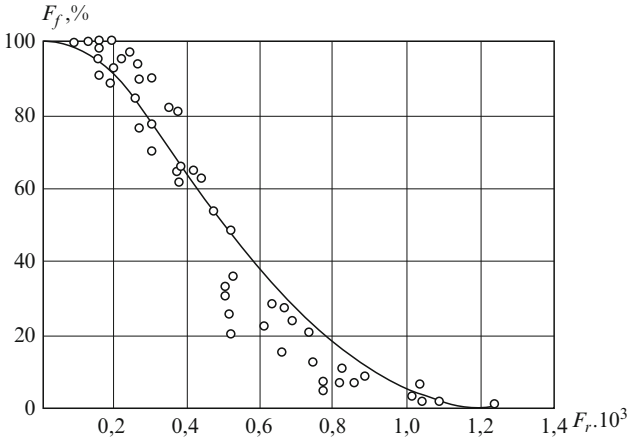

Fig. 7.7 Fractional separation dependence on the Froude criterion: ○ – experimental points; —— – estimated curve

To check the compliance of the structural model with the empirical dependence, we express the value of the parameter Fr_{50} using Eq. (7.19):

$$K_{50} = 1 - \sqrt{0.4 \frac{(\rho - \rho_0)}{\rho_0} \cdot Fr_{50}}.$$

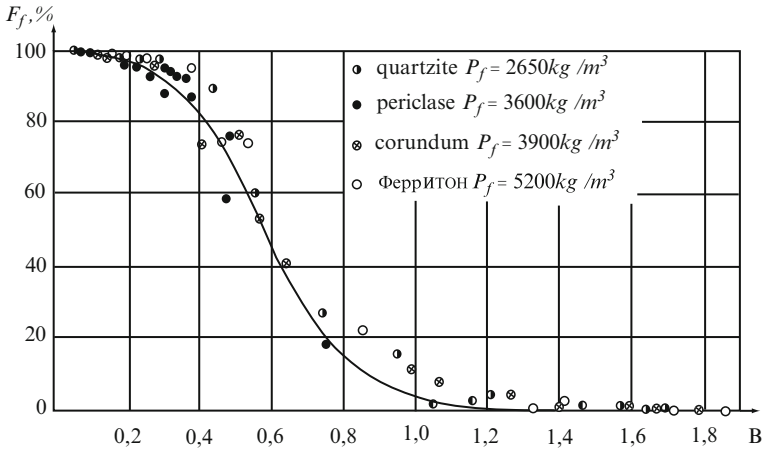

Fig. 7.8 Fractional separation dependence for materials of various densities on the parameter B: ○ ● ◑ ⊗ – experimental points; —— – estimated curve

Hence,

$$Fr_{50} = \frac{(1 - K_{50})^2}{0.4} \cdot \frac{\rho_0}{(\rho - \rho_0)}.$$

With the account for the fact that in this example $K_{50} = 0.342$, we obtain:

$$Fr_{50} = 1.08 \frac{\rho_0}{(\rho - \rho_0)},$$

which is close to the experimental correlation.

On the whole, all the examples studied clearly point to the predominance of flow structure in the process of gravitational classification. The advantages of this approach are its simplicity and satisfactory compliance with basic experimental dependencies related to the gravitational classification process accumulated by today.

7.5 Check of the Structural Model Adequacy

The account for the flow structure allows a more objective approach to the prediction of fractionating results on apparatuses of different constructions. Without dwelling on extremely complicated patterns of flow formation in actual apparatuses, for their roughest examination we should single out three characteristic properties of a moving flow that can be connected with the apparatus construction:

– Character of the change in the continuous phase velocity field along the apparatus height

– Presence of stagnant zones and the rate of the apparatus cross-section filling with the moving flow
– Character of the material motion at the first stage of the process (at the feeding stage), intensity of its interaction with the flow and internal elements promoting concentration leveling and reduction of skips and depressions

Thus, for example, a velocity field of a continuum can be both uniform and nonuniform along its height. Operation of hollow (equilibrium) apparatuses of a constant cross-section is the closest to the former case. A uniform velocity field stipulates for an identical regime of flow interaction with particles at any level of the cross-section and predetermines the invariability of the distribution factor over the apparatus height. The model of regular cascade satisfies most completely such conditions of the process organization.

The intensity of the continuum interaction with particles depends not only on the nonuniform velocity field over the apparatus height, but also on its nonuniformity over the cross-section. For an apparatus of a circular cross-section, the structural model takes into account the influence of transverse nonuniformity of the flow. It is assumed obvious that the rate of filling the apparatus cross-section with a moving continuous phase amounts to 100%. The matter is different with apparatuses of square and rectangular cross-sections, where stagnant zones are formed in the corners, reducing to zero the effect of the continuum on the removal of particles. If we assume that the line of zero flow velocity in an apparatus of square cross-section can be approximated by a circumference inscribed into the square, the rate of filling such cross-section with an ascending flow amounts to

$$C_{sq} = \frac{F_{cir}}{F_{sq}} = \frac{\pi}{4}.$$

Since the distribution factor (proceeding from the structural model) is determined through the ratio of areas, when estimating this factor for a square cross-section, a correction factor

$$C_{sq} = \frac{\pi}{4}$$

should be introduced. Taking it into account,

$$k_{sq} = \frac{\pi}{4} \cdot K_0, \tag{7.48}$$

where K_0 is the distribution factor for an apparatus of circular cross-section.

If we accept an inscribed ellipse as the zero velocity line for an apparatus of rectangular cross-section, the expression (7.48) will be also valid for determining k_{rec}, since

$$C_{rec} = \frac{F_{el}}{F_{rec}} = \frac{\pi}{4}. \tag{7.49}$$

The expression (7.49) for square and rectangular cross-sections is recommended only as a first approximation, since actual filling rates are somewhat higher.

Finally, at the first stage of the process, a significant fall of the majority of particles with respect to the level of their inlet is observed in the absence of intense interaction of particles with internal components of the apparatus and in the presence of stagnant zones. Apparently, the most favorable conditions for their skip are realized in a hollow apparatus of square or rectangular cross-section.

In the light of the statements above, we have made an attempt to predict quantitative results of fractionating process for several apparatuses of various designs. Computation results are presented in respective figures in comparison with experimental data.

Figure 7.9 shows an estimated curve and experimental data obtained at the classification of periclase with the density $\rho = 3{,}600\,\text{kg/m}^3$ in an equilibrium apparatus of circular cross-section ($D = 100\,\text{mm}$). The number of conventional sections $z = 9$, feed sections $i^* = 6$. Consumed concentration of the material is $\mu = 1.5\,\text{kg/m}^3$. Computations were carried out using the model of regular cascade (7.3) and structural model according to Eqs. (7.19) and (7.37). Average deviation of the estimated curve of $F_f(B)$ dependence from experimental points in Fig. 7.9 amounts to $+1.8\% \div 2.1\%$.

Figure 7.10 shows $F_f(B)$ dependence at the classification of quartzite with the density $\rho = 2{,}650\,\text{kg/m}^3$ in an equilibrium apparatus of square cross-section with the dimensions $100 \times 100\,\text{mm}^2$. The number of conventional sections $z = 6$, feed sections $i^* = 3$. Consumed concentration of the material is $\mu = 2\,\text{kg/m}^3$.

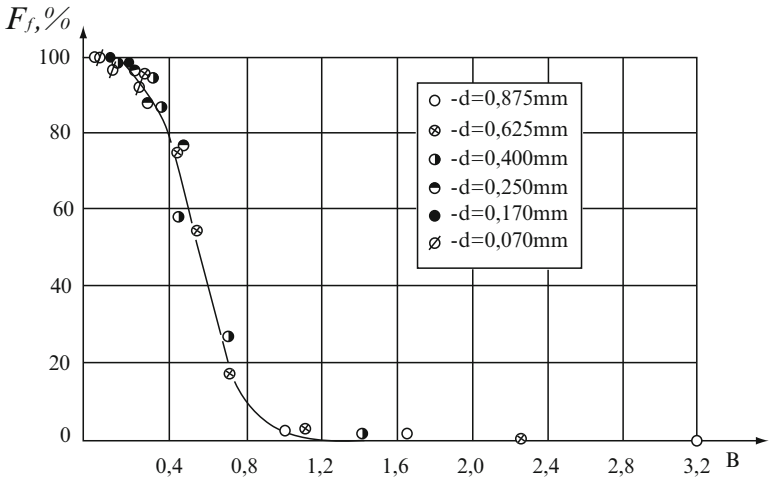

Fig. 7.9 Dependence $F_f(x) = f(B)$ for a cascade apparatus of circular cross-section. ○ ⊗ ◑ ◓ ● ∅ – experimental points; —— – estimated curve

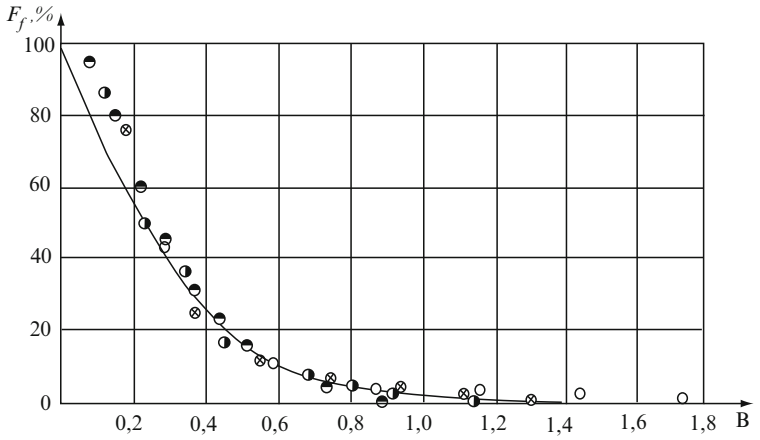

Fig. 7.10 Dependence $F_f(x) = f(B)$ for a cascade apparatus of square cross-section: ● ◓ ◑ ⊗ – experimental points; —— – estimated curve

Computations were carried out using the model of a regular cascade with a skip by 1.5 conventional sections.

$$F_f = \frac{1 - \sigma^{2,5}}{1 - \sigma^7}.$$

The distribution factor was determined with a correction for square cross-section according to Eq. (7.48)

$$k_{sq} = \frac{\pi}{4}\left[1 - \sqrt{0.4 \cdot B}\right].$$

Maximal deviation of the estimated curve from experimental points does not exceed 15%.

Figure 7.11 shows $F_f(B)$ dependence at the classification of quartzite with the density $\rho = 2650\,\text{kg/m}^3$ in an apparatus of rectangular cross-section of zigzag type. The number of sections $z = 6; i^* = 3$. Consumed concentration is $\mu = 2.0\,\text{kg/m}^3$. Computations were carried out using the model of a regular cascade:

$$F_f = \frac{1 - \sigma^4}{1 - \sigma^7}.$$

The distribution factor was determined with a correction for square cross-section.

$$k_{sq} = \frac{\pi}{4}\left[1 - \sqrt{0.4 \cdot B}\right].$$

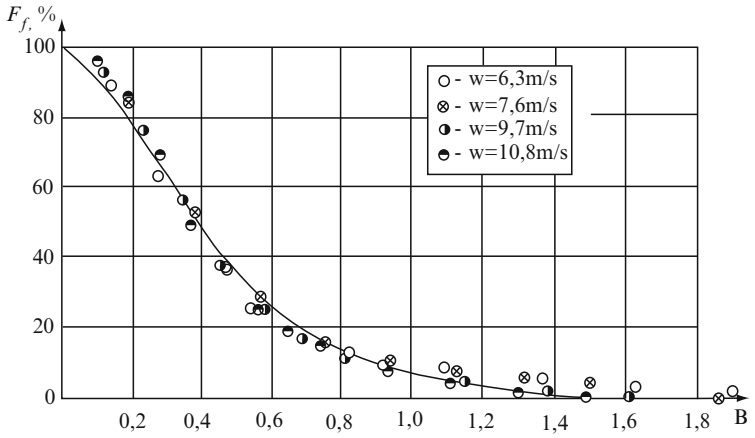

Fig. 7.11 Dependence $F_f(x) = f(B)$ for a cascade apparatus of square cross-section of "Zigzag" type: ○ ◓ ◑ ⊗ – experimental points; —— – estimated curve

In all the cases, maximal deviation of the estimated curve from experimental points does not exceed 7%, which is within the limits of experimental accuracy.

7.6 Correlation Between the Structural and Cellular Models of the Process

Equation (7.6) can be written for a cell as follows:

$$u_r - v_r = u_r \sqrt{\frac{4B}{3\lambda}},$$

since here we examine hydrodynamic conditions practically in one point of the flow. Hence,

$$1 - \frac{v_r}{u_r} = \sqrt{\frac{4B}{3\lambda}}$$

or

$$\frac{v_r}{u_r} = 1 - \sqrt{\frac{4B}{3\lambda}}.$$

According to (7.37), in this case we can write

$$\frac{v_r}{u_r} = \frac{v_r}{w} = k.$$

Then the limiting expression for coarse and fine particles extraction from a cell can be written as

$$f(E) = e^{\frac{\tau - E}{\chi}} = e^{\frac{\rho v^2}{\rho_0 w^2} - \frac{gd\rho}{w^2 \rho_0}}.$$

Then we obtain

$$f(E) = e^{\frac{\rho}{\rho_0} k^2} - B.$$

Since $k = 1 - \sqrt{\frac{4B}{3\chi}}$, this dependence can be finally written as

$$f(E) = A \cdot e^{-\phi(B)}$$

where A is a constant value $A = e^{\frac{\rho}{\rho_0}}$; $\phi(B)$ is a function of the parameter B.

This dependence totally complies with empirical dependencies for actual separation curves, which were confirmed over and over again, but have not found as yet a clear theoretical justification.

Chapter 8
Correlation Between Statistical and Empirical Results

Abstract Taking into account the results of statistical and structural models of the process, a method of comprehensive calculation of the process is developed. Fractional separation dependence on such process parameters as medium flow velocity, apparatus height and cross-section is found. The notion of "separation completeness" is formulated. Physical causes of equal extractability of different size classes are examined and validated, since when using affinization criteria, all equal values of fractional separation of different size classes meet at one point in the universal curve.

Keywords Approximation · Separation efficiency · Affinity · Separation curves · Universal curve · Equal extractability · Separability · Separation completeness · Optimal regime · Semi-logarithmic coordinates

8.1 Approximation of Universal Separation Curve

The analysis carried out in the previous chapter has made it possible to develop an exhaustive method of estimating process results on the basis of structural and cascade models. However, this method is somewhat intricate and not always easy-to-use. Therefore, we are making an attempt to develop a simpler approximation of separation curves, which covers both cascade and equilibrium processes, making use of a statistical approach.

It is established in Chapter 6 that the Boltzmann factor for a zone at a constant number of particles $N_1 = N_2 = N$ is determined by an expression $e^{-\frac{E}{\chi}}$. On such conditions, the statistical sum should be written as

$$Z = \sum_i e^{-\frac{E_i}{\chi}}.$$

E. Barsky, *Critical Regimes of Two-Phase Flows with a Polydisperse Solid Phase*, Fluid Mechanics and Its Applications 93,
DOI 10.1007/978-90-481-8838-3_8,

This sum is a proportionality factor connecting the probability $P(E_i)$ with the Boltzmann factor, that is,

$$P(E_i) = \frac{e^{-\frac{E_i}{\chi}}}{Z}.$$

By the definition of a zone, this probability is proportional to the fractional separation degree for a narrow size class. To understand the influence of the proportionality, we analyze the ratio of these probabilities.

For a zone adjoining the apparatus, we can derive the following ratio for the occupancies of two states:

$$\frac{P_1}{P_2} = e^{-\frac{(E_1 - E_2)}{\chi}}, \tag{8.1}$$

and the ratio of particles oriented in both directions can be written as

$$\frac{P(\uparrow)}{P(\downarrow)} = e^{-\frac{E}{\chi}}. \tag{8.2}$$

The numerator of the exponent in expressions (8.1) and (8.2) contains the value of the lifting factor or a difference of its values.

As already shown, the lifting factor is functionally connected with hydrodynamic particle size or with hovering velocity:

$$E = gdm.$$

Taking this into account, the dependence (8.2) can be written as

$$e^{-\frac{E}{\chi}} = e^{-\frac{gdm}{w_0^2 m_0}} = e^{-B}.$$

The extraction $F_f(x)$is proportional to the probability P. The parameter B is analogous to the Froude criterion at $\rho = const$, that is when only one material takes part in the process. This suggests a simplified method of approximating universal separation curves and analyzing process results.

Experimental dependence presented in Fig. 1.11 is reliably rectified in semilogarithmic coordinates, as shown in Fig. 8.1. According to this dependence, we can write:

$$\lg F_f(x) = A - sB.$$

We express the value A in this equation through a coefficient s equal to $tg\alpha$ (α being the angle of the approximating straight line intersection with the abscissa axis). It is usually assumed that $F_f(x) = 50\%$ is the optimal value of the degree of fractional separation. Therefore, we express A through B_{50}:

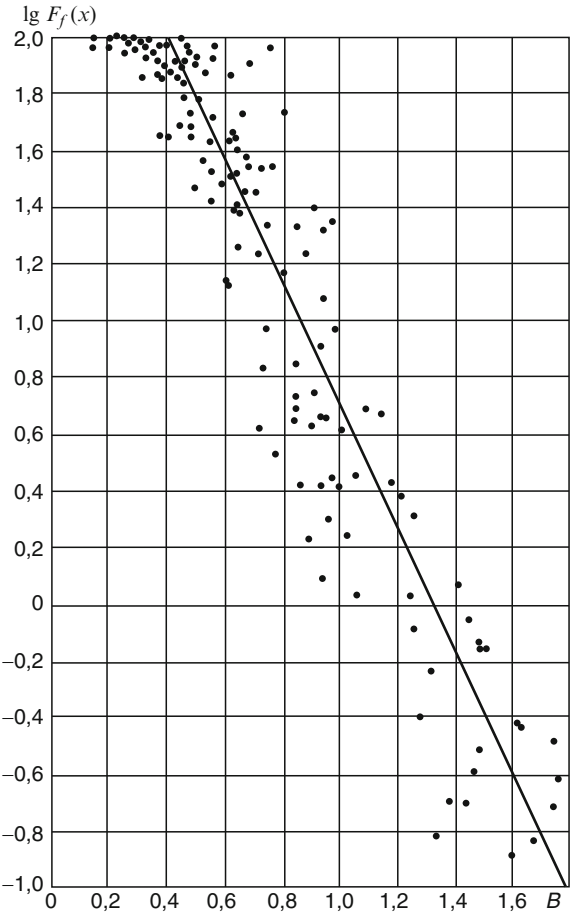

Fig. 8.1 Semi-logarithmic dependence: lg $F_f(x) = f(B)$

$$A = \lg 50 + B_{50} tg\alpha = \lg 50 + sB_{50}.$$

Taking this into account, the approximating dependence is written as

$$\lg F_f(x) = \lg 50 + sB_{50} - sB.$$

We finally obtain:

$$F_f(x) = 50e^{-2.3s(B-B_{50})} \tag{8.3}$$

where B_{50} is the value of the parameter B ensuring equal (50%) extraction of different size classes; s is a constant depending on the apparatus design, as well as on boundary conditions (place of material feed into the apparatus, fine and coarse products output, air inlet into the apparatus, conditions of the walls, internal facilities, etc.).

At the same material density, this dependence can be simplified and reduced to

$$Ff(x) = 50e^{-2,3s(Fr-Fr_{50})}.$$

8.2 Principal Separation Parameters Depending on the Apparatus Height

Using this approximation, we analyze the available experimental material. It should be emphasized that more than a 100 types of gravitational classifiers were experimentally studied, and the treatment of the results has not revealed any cases of considerable deviation of experimental dependence from Eq. (8.3).

Seven sets of experiments were carried out with cascade classifiers (Fig. 1.2). All the apparatuses were of counter-flow type, that is the material was fed to the upper shelf, while the air was introduced from below. The number of stages in the apparatuses varied as follows: 1; 2; 4; 6; 8; 12; 14.

Principal results of this set of experiments are presented in Table 8.1.

For the sake of comparison, a variety of tests with hollow apparatuses of different heights with removed pour-over shelves were performed. The height of each stage remained unchanged. Principal separation parameters determined on the basis of these studies are shown in Table 8.2.

In addition to these studies, another set of experiments was performed on a zigzag separator (Fig. 8.1b) of various heights.

In these experiments, a gravitational separator column was assembled of 2, 4, 6 and 8 stages, respectively. In all the experiments, the source material was fed to the uppermost stage. Principal parameters of the separation process revealed in these experiments are presented in Table 8.3.

Table 8.1 Dependence of Fr_{50} and s parameters on the number of stages of a cascade classifier with inclined shelves

Number of stages n	1	2	4	6	8	12	14
$Fr_{50} \times 10^2$	0.0345	0.04	0.0445	0.049	0.052	0.056	0.058
$s \times 10^{-2}$	29.4	24	21.9	20.2	20	18.2	17.6

Table 8.2 Dependence of Fr_{50} and s parameters on the height of equilibrium gravitational apparatus

Number of stages n	1	2	4	6	8
$Fr_{50} \times 10^2$	0.0275	0.022	0.0175	0.015	0.014
$s \times 10^{-2}$	21.3	30	43.3	53	60

Table 8.3 Dependence of Fr_{50} and s parameters on the number of stages of a zigzag separator

Number of stages n	2	4	6	8
$Fr_{50} \times 10^2$	0.0385	0.0255	0.0185	0.016
$s \times 10^{-2}$	17.8	29.6	47.5	53

Figure 8.2 summarizes all the curves obtained for one narrow size class on cascade separators of different heights. Since the separation efficiency is determined by the curve steepness, it follows from this figure that the efficiency monotonically grows with increasing apparatus height. Similar dependences are characteristic of other types of classifiers, as well.

The dependence of the parameter Fr_{50} value on the apparatus height for all the three types of classifiers is shown in Fig. 8.3. The parameter Fr_{50} determines optimal regimes of the medium flow.

It is of great interest to find a way of obtaining a generalized quantitative characteristic of a process from separation curves. Affine transformation of these curves in a semi-logarithmic scale gives a linear dependence. The arrangement of

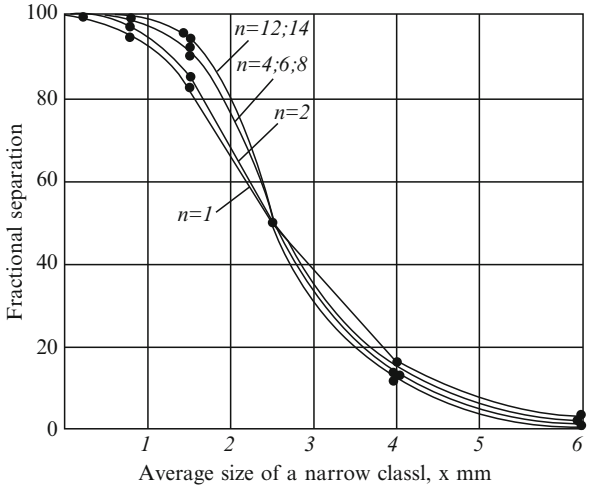

Fig. 8.2 Fractional separation dependence for apparatuses of different heights in optimal regimes

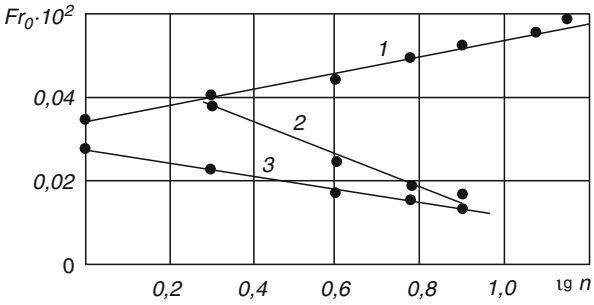

Fig. 8.3 Dependence $Fr_{50} = f(n)$ for various classifiers: 1 – cascade shelf classifier; 2 – classifier of "Zigzag" type; 3 – hollow pipe

these curves contains information on the separation process quality. Besides the parameter Fr_{50}, another important characteristic of the dependence under study is the coefficient s.

The mere parameters Fr_{50} and s cannot characterize the separation completeness, since the approximating straight lines do not intersect in the point corresponding to the separation optimum. For graphic dependences of

$$F_f(x) = f(Fr)$$

type under study to intersect in one point, they should be transformed by changing the abscissa axis.

Let us examine the effect of this transformation on the values of the coefficient s (Fig. 8.4).

Whereas before the transformation the dependence is

$$y = b - s_1 x_1,$$

after the transformation

$$y = b - s_2 x_2.$$

For any fixed ordinate value, we can write:

$$s_1 x_1 = s_2 x_2,$$

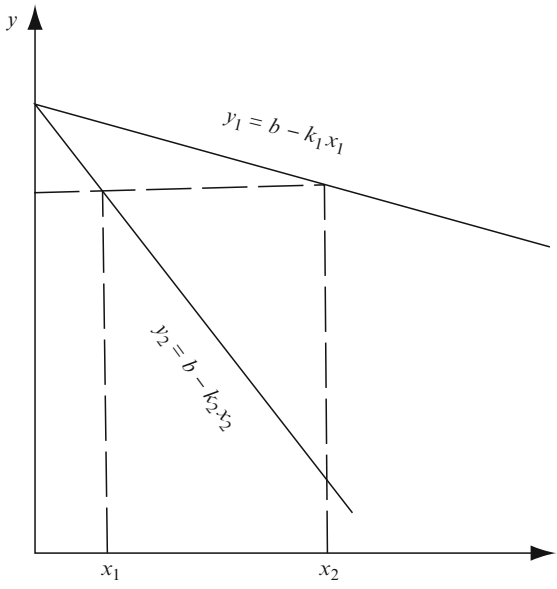

Fig. 8.4 Schematic diagram of affine transformation

hence,

$$s_2 = \frac{s_1 x_1}{x_2} = \frac{s \cdot Fr_{50}}{Fr_2}.$$

Assuming $Fr_2 = 1$, the parameter $s \cdot Fr_{50} = \psi$ unambiguously characterizes the separating capability of a separator and has a clear geometrical and physical sense.

Values of coefficients ψ determined for various apparatuses on the basis of Tables 8.1 through 8.3 are summarized in Table 8.4.

It follows from the Table that ψ values exactly reflect qualitative ratios between various apparatuses revealed by the comparison of their separation results. These ratios hold both in columns and lines of Table 8.4, which points to a general and objective nature of the introduced parameter – separation completeness ψ.

It is noteworthy that this parameter was also successfully applied when examining and comparing other types of separating devices. It reflects not only the steepness of the universal separation curve, but also its position in the coordinate system. From the geometrical standpoint, this parameter shows not only the slope angle of the universal curve, which is insufficient for evaluating separation quality, but also the parameter Fr_{50} value. Only the combination of these two parameters gives an objective evaluation.

The following conclusions can be made from the statements above:

1. Separating capacity of any separating facility can be unambiguously characterized by the position of the approximating straight line in the coordinate system.
2. To know the parameters of this straight line is a prerequisite for calculating optimal and other separation regimes and for predicting compositions of separation products.
3. The obtained dependence leads to a conclusion on the necessary limiting information about the process.

In principle, it can be obtained in a single experiment, since the results of sieve analysis of the source product and separation products give several points at the same w value. It is sufficient for restoring all the dependence and calculating any parameters of the process.

Thus, the parameter ψ characterizes completely and in detail the apparatus separating capacity. This parameter allows one to compare various separation facilities in an unambiguous and objective manner.

Table 8.4 Values of coefficients ψ for various separators

Number of stages Type of separator	1	2	4	6	8	12	14
Cascade separator	0.935	0.96	0.975	1.00	1.01	1.02	1.025
Zigzag separator	–	0.684	0.785	0.83	0.945	–	–
Equilibrium separator	0.585	0.66	0.755	0.8	0.84	–	–

As for the evaluation of optimality of material separation, it requires a somewhat different approach substantiated in the next chapter.

In technical literature, the efficiency of separators is evaluated by the results of the source material distribution into both outlets. Here, however, the notions of the apparatus operation efficiency and material separation efficiency are distinguished for the first time. The separating capacity of a separator is determined by its configuration and boundary conditions, whereas the material separation efficiency is primarily determined by its initial composition and only in the second place by the apparatus design.

8.3 Equal Extractability of Various Size Classes

Usually, serious attention in the theory and practice of separation is paid to optimality conditions for boundary-size particles. It is known that these conditions are satisfied if $F_f(x) = 50\%$ is valid for these sizes. It follows from the unified curve (Fig. 7.8) that all these conditions are unambiguously determined for a specific apparatus at $B_{50} = const$. However, the same curve shows that not only optimal, but any other separation, as well, for example, $F_f(x) = 20\%; 30\%; 60\%; 70\%$, etc. is also unambiguously determined by the constancy of the respective parameters $B_{20}; B_{30}; B_{60}; B_{70}$ etc. The nature of this mechanism, which makes it possible to obtain finally a strictly deterministic regularity in a chaotic separation process with an immense number of random factors, remains unclear.

It has been shown from the standpoint of statistical analysis that the conditions of equal extractability are determined by the ratio

$$\frac{\tau}{\chi} = const$$

for all size classes and flow velocities. Let us try to clarify the physical nature of this phenomenon

First we examine a simple precipitation of a particle in an unlimited medium. The character of precipitation of a solid round particle is determined by a system of forces consisting of the particle weight in the medium under study and the medium resistance to the precipitation. The particle weight equals

$$G = mg_0,$$

where m is the particle mass; g_0 is the free fall acceleration in a moving medium:

$$g_0 = g\frac{\rho - \rho_0}{\rho},$$

where g is gravity acceleration; ρ, ρ_0 are densities of the solid particle and the medium.

The medium resistance to the particle motion is determined, in the general form, by the dependence

$$R = \lambda F \frac{v^2}{2} \rho_0,$$

where λ is the medium resistance coefficient; F is the midlength section of a particle; ρ_0 is the medium density; v is the particle velocity.

Thus, we can write an equation of a particle motion at its precipitation in a motionless medium:

$$m \frac{dv}{dt} = -mg_0 + \frac{1}{2} \lambda F v^2 \rho_0.$$

This equation can be solved in the general form by changing variables:

$$v = -\frac{u'}{ku}, \text{ where } k = \frac{\lambda F \rho_0}{2m}.$$

After collecting similar terms,

$$\frac{d^2u}{dt^2} - g_0 k u = 0.$$

A general solution of this equation is

$$u = c_1 e^{t\sqrt{g_0 k}} + c_2 e^{-t\sqrt{g_0 k}}.$$

Taking into account the performed change of variables, we can find

$$v = -\sqrt{\frac{g_0}{k}} \cdot \frac{c_1 e^{t\sqrt{g_0 k}} - c_2 e^{-t\sqrt{g_0 k}}}{c_1 e^{t\sqrt{g_0 k}} + c_2 e^{-t\sqrt{g_0 k}}}. \tag{8.4}$$

It follows from the initial conditions

$$v_{t=0} = 0$$

that $c_1 = c_2$. We obtain from dependence (8.4):

$$v = -\sqrt{\frac{g_0}{k}} th t\sqrt{g_0 k}. \tag{8.5}$$

Theoretically, the limit (8.5) is reached after infinite time. However, we can assume, to a practically sufficient precision, that a hyperbolic tangent reaches its

limiting value at the argument equal to 2.5. Hence, the time of a transitory process at the particle precipitation can be defined as

$$t\sqrt{g_0 k} = 2.5$$

or

$$t = \frac{2.5}{\sqrt{\frac{(\rho-\rho_0)}{\rho} \cdot \frac{\lambda F \rho_0}{2m}}}.$$

After the lapse of this time period, an isolated particle acquires a stationary velocity that is called final precipitation velocity. It follows from (8.5) that

$$v_0 = \sqrt{\frac{g_0}{k}} = \sqrt{\frac{(\rho-\rho_0)2m}{\rho\lambda F \rho_0}}.$$

For a round particle,

$$m = \frac{\pi d^3}{6} \cdot \rho,\ F = \frac{\pi d^2}{4},$$

where d is the particle diameter. Finally, we can write:

$$v_0 = \sqrt{\frac{4gd(\rho-\rho_0)}{3\lambda\rho_0}}. \tag{8.6}$$

Let us examine a general equation of a particle motion in a flow. The determining parameter is the resistance coefficient. Its value determines the thickness of the boundary layer on the particle, the place of this layer breakaway, velocity profile in the boundary layer and the character of its variation. All these physical parameters are determined by the Reynolds number calculated for a particle.

There are many ways of determining λ. For fine particles under laminar overflow conditions

$$\lambda = \frac{24}{\mathrm{Re}}.$$

For coarse particles under turbulent overflow conditions, the resistance becomes constant and amounts to

$$\lambda \approx 0.5.$$

In transient regimes (between turbulent and laminar ones)

$$\lambda = \frac{24}{\mathrm{Re}} + 0.5.$$

At a simple precipitation of particles, the velocity of their overflow by the medium constitutes the fall velocity

$$w_x = -v.$$

In a moving flow, the overflow velocity is

$$w_x = w - v,$$

where w is the ascending flow velocity.

Taking into account the remarks related to the previous derivation, a general equation of the particle motion can be written as

$$m\frac{dv}{dt} = -mg + \frac{1}{2}\lambda F\rho_0(v-w)^2, \tag{8.7}$$

where w is flow velocity. This expression can be transformed into the following:

$$\frac{dv}{dt} = -g_0 + k(v-w)^2,$$

where $k = \frac{\lambda F\rho_0}{2m}$. In this form, it represents an equation of Riccatti type, which can be reduced to a differential equation of the second order,

$$\frac{d^2u}{dt^2} + 2kw\frac{du}{dt} + k(-g_0 + kw^2) = 0,$$

where $v = \frac{-u'}{ku}$. The solution of this equation gives the following:

$$v = w - \sqrt{\frac{g_0}{k}} \cdot \frac{c_1 e^t\sqrt{g_0 k} - c_2 e^{-t}\sqrt{g_0 k}}{c_1 e^t\sqrt{g_0 k} + c_2 e^{-t}\sqrt{g_0 k}}. \tag{8.8}$$

It follows from the comparison of (8.4) and (8.8) dependences that at any comparable moment of time, the theoretical averaged particle velocity in a counterflow equals its precipitation velocity in a motionless medium plus the velocity of the flow itself.

The second multiplier in expression (8.8) is, under respective initial conditions, a hyperbolic tangent asymptotically tending to its limit. After the lapse of a certain time interval, the particle velocity becomes practically constant and is determined by the dependence

$$v = w - \sqrt{\frac{g_0}{k}}.$$

Finally, it can be written as

$$v = w - \sqrt{\frac{4gd(\rho - \rho_0)}{3\lambda\rho_0}} = w - w_{50}.$$

The resistance to a particle motion in a moving flow is determined as

$$R = \lambda F \frac{(w - v)^2}{2}\rho_0.$$

For hovering conditions, the balance of the weight and resistance constitutes

$$mg = \lambda F \frac{w_{50}^2}{2}\rho_0,$$

hence,

$$\frac{\lambda F \rho_0}{2} = \frac{mg}{w_{50}^2}.$$

Taking this into account, we can finally obtain the minimal value of the resistance to the particles in a flow, which can ensure the appearance of the lifting factor in the form

$$R = mg \frac{(w - v)^2}{w_{50}^2}.$$

It is noteworthy that the obtained relation contains all parameters that can be easily determined experimentally and does not contain explicitly the resistance coefficient λ, which is always difficult to choose.

We have shown that a particle sliding with respect to the flow is determined by its hovering velocity, that is a particle always lags behind the flow by the magnitude of its hovering velocity. Hence,

$$w = w_{50} + v. \tag{8.9}$$

In this case, a general expression for the parameter B can be written as

$$B = \frac{gd}{w^2} \cdot \frac{(\rho - \rho_0)}{\rho_0} = \frac{gd(\rho - \rho_0)}{(w_{50} + v^2)\rho_0} = \frac{3}{4}\lambda,$$

whereas it is known that the hovering condition is:

$$B_{50} = \frac{gd}{w_{50}^2} \cdot \frac{(\rho - \rho_0)}{\rho_0} = \frac{3}{4}\lambda_{50}.$$

We divide the second expression by the first:

$$\frac{B_{50}}{B} = \frac{\lambda_{50}}{\lambda} = \frac{w^2}{w_{50}^2}.$$

Consequently, the ratio of the flow velocity to the hovering velocity predetermines equal extractability rate, and this parameter is of universal nature.

While a function of $F_f(x) = f(B)$ type is universal for turbulent flows only, a dependence of $F_f(x) = f\left(\frac{B_{50}}{B}\right)$ type acquires a universal character for any regimes of medium motion.

A specific example of fractionating a finely disperse aluminum powder with the density of $2{,}700\,\mathrm{kg/m^3}$, which is used for producing paints, can serve as an illustration. Grain size composition of aluminum powder in partial residues is given in Table 8.5. Here d (mm) is the boundary size, r (%) – partial residues.

The experiments were performed on a cascade air classifier consisting of nine stages with an average inlet ($z = 9; i = 5$). Air flow velocities varied within the range of 0.29–1.46 m/s at tested concentrations of the material, which did not affect the results of separation. The results of this set of experiments treated using the system $F_f(x) = f(B)$ are shown in Fig. 8.5. As follows from this figure, the obtained curves do not become affine. It is noteworthy that at elevated velocities equal to 1.46 and 1.19 m/s they get practically merged, but at lower velocities they diverge, and the extent of this divergence grows with decreasing flow velocity.

Table 8.5 Granulometric composition of aluminum powder in partial residues

d (mm)	0.4	0.315	0.2	0.16	0.125	0.1	0.08	0.063	0.05	0.045	0.04	0.035	0.03
r (%)	6.5	6.9	14.3	7.8	6.5	6.7	7.8	8.2	3.5	4.2	4.2	4.2	4.8
0.025	0.02	0.015	0.01	0.005	bottom								
4.2	3.0	1.8	1.6	3.5	0.3								

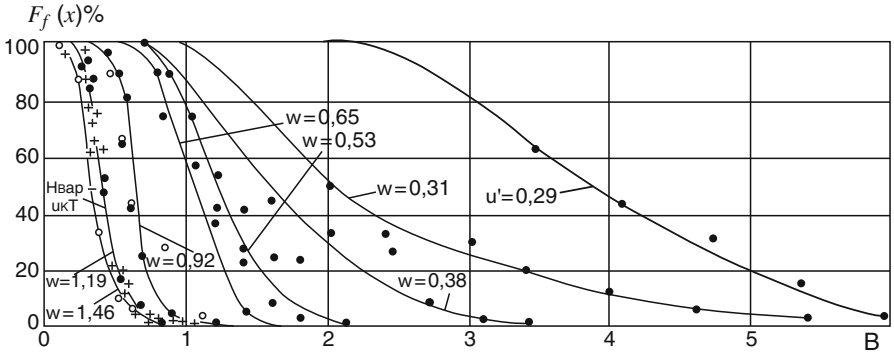

Fig. 8.5 Dependence $F_f(x) = f(B)$

Based on experimental data, we have first plotted a dependence of $F_f(x) = f(x)$ type and used it to determine x_0 value for each flow velocity. A B_0 value was determined for each flow velocity from Fig. 8.5. The results of all these operations are presented in Table 8.6.

To obtain the broadest possible range in the experiments on this apparatus, additional experiments were performed on quartzite powder $(\rho = 2670\,\mathrm{kg/m^3})$ with particle size from 0.1 to 3 mm at flow velocities equal to 4.7; 5.57; 6.67; 7.3 and 7.89 m/s. All these curves give an affine dependence in the plot of Fig. 8.5, which coincides with curves obtained at air flow velocities equal to 1.46 and 1.19 m/s.

On the basis of these data, an experimental dependence of

$$B_{50} = f(\mathrm{Re}_{50})$$

type shown in Fig. 8.6 was obtained. It completely corresponds to the character of a well-known Rayleigh curve of $\lambda = f(\mathrm{Re})$ type for an isolated particle. This confirms the validity of our conclusions on the connection between B and λ. At higher Re values, the parameter B_{50} is constant. It is a turbulent region, which corresponds to unambiguous affinization of separation curves by the parameter B. At a transition to laminar processes, such regularity is violated, and the affinization by this

Table 8.6 Principal parameters obtained during the separation of aluminum powder on a cascade apparatus (z = 9, i = 5)

Air flow velocity, w m/s	1.46	1.19	0.92	0.65	0.53	0.38	0.31	0.29
B_{50}	0.35	0.41	0.65	1.1	1.23	1.6	2.0	3.9
Reynolds number Re_{50}	8.14	4.76	3.28	1.99	1.21	0.54	0.33	0.26

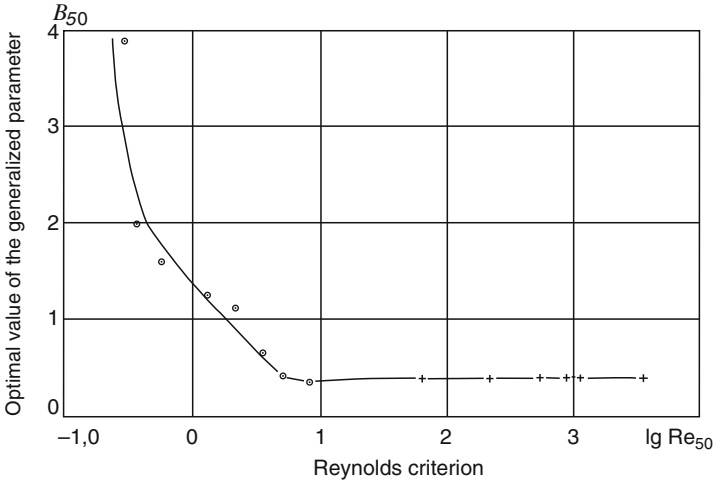

Fig. 8.6 Dependence $B_{50} = f(\mathrm{Re}_0)$

parameter is not observed. A transition from one regime to another is realized in this apparatus at $\mathrm{Re}_{50} \approx 4.76$, which corresponds to the boundary size of about 0.056 mm for the specified material ($\rho = 2{,}700\,\mathrm{kg/m^3}$). Obviously, for other materials and apparatuses, this transition can occur at other sizes. Taking into account a generalizing character of the parameter B, we can determine this value for any material.

Using the obtained regularity, we can plot a dependence of

$$F_f(x) = f\left(\frac{B}{B_{50}}\right) \tag{8.10}$$

type for all above-mentioned experiments.

Such dependence is shown in Fig. 8.7. As follows from this figure, in this case a complete affinization of separation curves is obtained. This means that a unified common regularity is established for the process of separation of powders within the range from 10 mm to 10 μm.

The dependence presented in Fig. 8.5 can be well approximated in semi-logarithmic coordinates, as shown in Fig. 8.8. According to this figure, we can write

$$F_f(x) = e^{\psi - s\frac{B}{B_{50}}}. \tag{8.11}$$

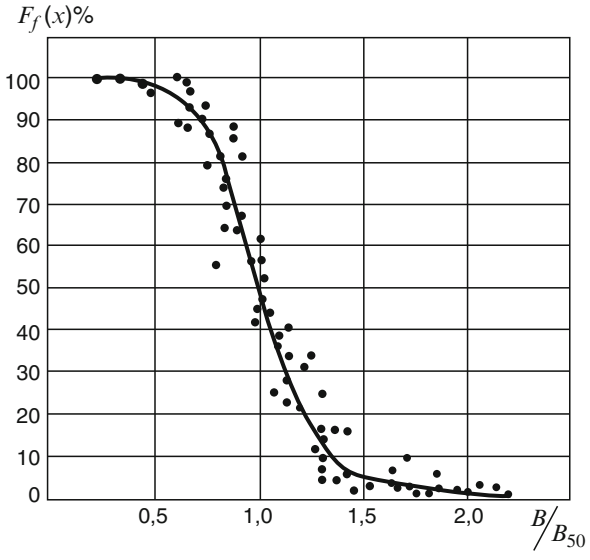

Fig. 8.7 Dependence $F_f(x) = f\left(\frac{B}{B_{50}}\right)$

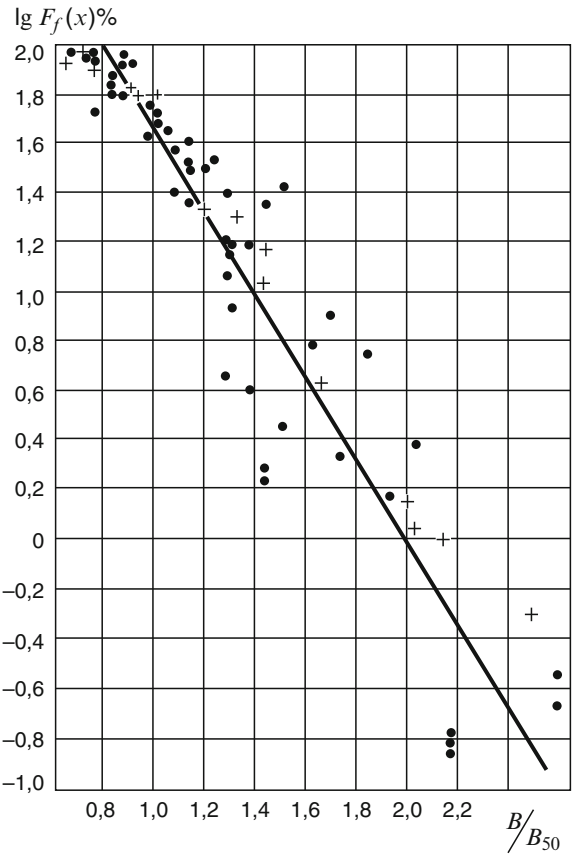

Fig. 8.8 Dependence $\lg F_f(x) = f\left(\frac{B}{B_{50}}\right)$

This dependence reveals the desired general connection between all the parameters of the process under study. For turbulent regimes of the medium motion, it is somewhat simplified:

$$F_f(x) = Ae^{\psi - sB}.$$

Chapter 9
Entropy of Composition: Optimization Criterion

Abstract It has been assumed that entropy characterizes dynamic systems only. It turned out that such a stationary system as a solid phase can be also characterized by composition entropy. It reflects the uncertainty of granulometry based on a probabilistic characteristic. Composition entropy, in contrast to thermodynamic entropy, has a tendency to a decrease in critical regimes of motion. Ordering of compositions because of fine and coarse particles distribution into different directions gives grounds for unbiased unambiguous optimization of separation process by entropy decrease value. Optimality conditions are determined.

Keywords Composition heterogeneity · Composition entropy · Separation · Efficiency · Information · Binary separation · Multiproduct separation · Unequivocal estimation · Equal extraction

9.1 Entropy and Particles Stratification

In the classical representation, entropy of a system is formed under two different impacts exerted on the system, that is,

$$dH = d_eH + d_iH$$

where d_eH is a part of entropy due to the impact of an external medium in respect of the system, d_iH is a part of entropy due to irreversible internal changes in the system itself in the course of the process.

In the classical representation, the part of entropy d_eH can grow, be zero and even take on a negative value under certain conditions. As for d_iH, it is accepted that it always grows, that is, $d_iH > 0$. In any case, the change in both components is such that $d_eH + d_iH > 0$.

E. Barsky, *Critical Regimes of Two-Phase Flows with a Polydisperse Solid Phase,*
Fluid Mechanics and Its Applications 93,
DOI 10.1007/978-90-481-8838-3_9,

Irreversible processes can be described in terms of mass forces and mass flows, the flows arising as a result of forces. For example, a gradient of concentrations or flow velocities in different parts of the system is a mass force. In this case, a flow can imply dN – the number of particles displaced (transformed) between these parts during the time interval dt. In this case, entropy change can be represented as

$$d_i H = F dN$$

where F is the mass force. For open systems

$$d_e H = \frac{dI + f dV}{\chi}.$$

The value $d_e H$ denotes entropy change caused by a flow of particles entering the system and leaving it in the opposite direction. The mobility factor plays a crucial role here. The total entropy for a narrow size class is written as

$$dH = \frac{dI + f dV}{\chi} - \frac{\tau dN}{\chi}.$$

Clearly, in this dependence

$$d_{i1} H = -\frac{\tau dN}{\chi}.$$

The total number of particles of a narrow class in the process is determined by their entry into the system, exit from the system and internal displacement. It means that we can write

$$dN = d_e N + d_i N.$$

It has been shown that potential extraction of a narrow size class is determined by the number of particles and the chaotizing factor magnitude, that is,

$$I(\chi; N) = N I(\chi)$$

where $I(\chi)$ is the potential extraction probability for one particle. By analogy, we can write the following for a polyfractional mixture:

$$I(\chi; N) = \sum_i I_i(\chi; N_i) = \sum_i N_i I_i(\chi)$$

where $i = 1; 2; 3; \ldots; i$ is the ordinal number of a component of a polyfractional mixture of particles.

In this case entropy is written as

$$d_e H = \frac{dI}{\chi} + \frac{fdV}{\chi}.$$

The internal entropy is written as

$$d_{i1} H = -\sum_i \frac{\tau_i d_i N}{\chi}.$$

It is accepted that its change is always positive. If we sum up these two expressions, the total entropy proves to be positive:

$$dH = d_e H + d_i H = \frac{dI}{\chi} + \frac{fdV}{\chi} - \sum_i \frac{\tau_i dN}{\chi} > 0.$$

In certain processes such as separation, phenomena making additional contributions to entropy arise. As already noted, in the process of separation, the effect of solid particles stratification according to their velocities arises. This effect decreases the composition uncertainty in the flow and in separation products in comparison with the initial composition.

We denote by $d\varepsilon$ the number of particles of a certain narrow class N that have stratified according to their steady velocities by a certain moment of time dt. It is clear that the ratio $\frac{d\varepsilon}{dt}$ is the stratification rate. At the initial moment of time at $t = 0, d\varepsilon = 0$. If we take an integral,

$$\int_t \frac{d\varepsilon}{dt} = \varepsilon.$$

The relation between ε and N can be expressed through a stratification coefficient v_k,

$$\varepsilon_k = v_k N_k.$$

Clearly, v_k is taken with a minus sign for the mixture placed into the flow and with a plus sign for separation products leaving the apparatus. In this case, the potential extraction can be considered as a function

$$I(\chi; V; \varepsilon).$$

In these variables, the total differential of I acquires the form

$$dI = \left(\frac{\partial I}{\partial \chi}\right)_{V;\varepsilon} d\chi + \left(\frac{\partial I}{\partial V}\right)_{\chi;\varepsilon} dV + \sum_i \left(\frac{\partial I}{\partial \varepsilon}\right)_{\chi,V,\varepsilon(i\neq k)} d\varepsilon$$

and here the internal entropy increment amounts to

$$d_{i2}H = -\sum_i \frac{\tau_i d\varepsilon_i}{\chi},$$

and the total entropy is written as

$$dH = \frac{dI}{\chi} + \frac{fdV}{\chi} - \sum_i \frac{\tau_i d_e N}{\chi} - \sum_i \frac{\tau_i d\varepsilon_i}{\chi}.$$

This can be explained visually enough by entropy production in the process of diffusion. Diffusion leads to an opposite effect when particles N_1 in some concentration are concentrated in one part of a system, and particles N_2 in a different concentration in another part of it. For the sake of simplicity, we assume that the flow velocity in both parts is the same and equals w. In this case, diffusion of particles from one part to another takes place. Entropy change in this case is

$$d_i H = -\left(\frac{\tau_2 - \tau_1}{\chi}\right) d\varepsilon > 0,$$

since the uncertainty of the mixture composition grows.

In the course of separation, the change in granulometric composition leads to a decrease of the composition uncertainty in the flow and in separation products in comparison with the initial composition, because in each direction of the solid phase motion, a certain composition ordering occurs. Light fine particles are mainly lifted upwards, while heavy coarse ones mostly precipitate downwards.

Here the following is valid:

$$d_{i2}H < 0.$$

This decrease occurs within the system, which contradicts classical ideas, but nevertheless is evident.

It is proved that the system entropy increases until it reaches the maximal possible value for the specific conditions of the process. It is accepted that the attained state of the system is the equilibrium state. What is implied when speaking about equilibrium in a flow? It turns out that in the course of separation, entropy grows up to its extreme value only for one boundary narrow size class. We revert to an entropy expression obtained for particles of one class:

$$H(N; z) = H(N; 0) - \frac{2z^2}{N}.$$

If the regime is chosen so that $z = 0$, entropy acquires its maximal possible value

$$H_{\max}(N; z) \approx H(N; 0) \approx \ln \frac{N!}{\frac{1}{2}N!\frac{1}{2}N!}.$$

The condition $z = 0$, by definition, gives

$$F_f(x) = F_c(x) = 0.5,$$

that is a regular optimality condition. Thus, a kind of equilibrium is attained.

Within the range of velocity change ensuring a critical regime, it is always possible to find a narrow size class that is divided in half between the separation products. This is due to the impossibility of ideal separation. Figure 1.5 illustrates this visually enough. The expressions presented in this section reflect entropy value for one narrow size class. At the transition to polyfractional mixtures, the situation becomes more complicated. Let us examine the arising problems.

9.2 Evaluation of Heterogeneity of Powder Composition

To assess changes in the grain size composition of powders in the process of separation, many attempts to find universal formulas have been made.

Instead of seeking universal formulas, we introduce an objective estimate of the composition heterogeneity, which will allow us to evaluate changes in the granulometry of pourable materials in compliance with dependence (5.20).

We analyze major transformations occurring at the separation of pourable materials. If a material is classified into components so that each component comprises particles of the desired class only without any impurities, such separation is ideal. It means that the more homogeneous the obtained components, the closer to ideal the separation. However, ideal separation is impossible, and therefore, an objective criterion should reflect an increase in the homogeneity of products obtained after separation in comparison with the initial composition.

We perform our analysis from this standpoint. Assume that a material consists of n fractions (we call the fraction size the average size of particles constituting a given fraction) and quantitatively evaluate its composition from the following conditions. We assume that we arrange all the particles of a material in a row and determine the number of permutations with returns available for these particles. This gives us an objective idea of the inhomogeneity degree of the system. (If we regard each particle as a letter and receive messages made of the same letters in different order, the number of permutations with returns is the number of messages that can be composed using these letters).

We denote the total number of particles in the starting material by G, and the number of particles in each fraction by $N_1, N_2, \ldots, N_n$. Then the number of

permutations with returns for this material is $m = \frac{G!}{\prod_{i=1}^{n} N_i!}$. It means that m is the number of possible states of the system. As known from the theory of information, a logarithm of the number of states of a system reflects the amount of information about it.

We write $M = \ln m$.

According to Stirling's formula, for sufficiently high A values

$$\lg A! \approx A(\ln A - 1).$$

Then $M = \ln m = G(\ln G - 1) - \sum_{i=1}^{n} N_i(\ln N_i - 1) = G \times \ln G - G - \sum_{i=1}^{n} N_i \ln N_i = G \times \ln G - \sum_{i=1}^{n} N_i \ln N_i$. The probability of taking at random a particle of size class j from the starting material is $P_j = \frac{N_j}{G}$, hence, $M = -G \sum_{i=1}^{n} P_i \ln P_i$. It is known that the amount of information per one element of a system equals

$$H = \frac{M}{G},$$

hence,

$$H = -\sum_{i=1}^{n} P_i \ln P_i.$$

This function objectively reflecting the heterogeneity (uncertainty) degree of a system is its entropy.

Separation quality criterion should satisfy two boundary conditions:

1. In the case of ideal separation, this criterion should be maximal.
2. In the case of separation with unchanged fractional composition, it should be zero.

Let H_s be the entropy of starting material, and $H_1, H_2, \ldots, H_n -$ entropies of each component after the separation, respectively. Let us check whether the dependence $E = H_s - \sum_{i=1}^{n} \mu_i H_i$ can serve as a criterion of separation quality. Here μ_i is the relative quantity of each component after separation, that is $\sum_{i=1}^{n} \mu_i = 1$.

Let us check whether the initial conditions are satisfied.

1. We consider a component i in the case of ideal separation. Then $H_i = -\frac{N_i}{N_i} \ln \frac{N_i}{N_i} - 1 \ln 1 = 0$. Hence, $E = H_s$, and it is clear that this is the maximal efficiency that can be reached for a specific composition of the starting material.
2. If the separation is absolutely random and involves no changes in the fractional composition of the material, we obtain:

$$H_i = -\sum_{i=1}^{n} \frac{\mu_i N_k}{\mu_i G} \quad \ln \frac{\mu_i N_k}{\mu_i G} = H_s. \tag{9.1}$$

Hence, $E = H_s - \sum_{i=1}^{n} \mu_i H_s = 0$.

It means that the function E is a suitable criterion of the separation quality evaluation. However, a question can arise how to compare separation efficiencies of various materials (maximal separation efficiency of each material is its initial entropy). We define a new function

$$E_1 = \frac{E}{H_s}$$

and clarify whether it is suitable for evaluating separation quality (efficiency).

E_1 is defined when $H_s \neq 0$ ($H_s = 0$ when either the starting material is uniform, or it is completely absent; in both cases separation does not make sense). Under the initial condition 1 (ideal separation) $E_1 = 1$. Under the condition 2 (with composition remaining unchanged at the separation), $E_1 = 0$. We change the notation as follows: $E = E_1$. Then

$$E = 1 - \frac{\sum_{i=1}^{n} \mu_i H_i}{H_s};\ H_s \neq 0 \tag{9.2}$$

is a suitable criterion of the separation quality (efficiency) evaluation.

9.3 Binary Separation

Let us process experimental results using the criterion (9.2). Initial composition of the material is given in Table 9.1.

We primarily estimate the starting material entropy. This material can be considered as two size classes with respect to each boundary:

$$H_s = -(P_1 \ln P_1 + P_2 \ln P_2), \quad \text{where } P_1 = \frac{Q_s}{G}; P_2 = 1 - \frac{Q_s}{G}; G = 1.$$

The table below shows the results of H_s calculation for the starting material. (Entropy was not determined for the boundary of 0.05 mm; we do not take it into account since it is the finest of size classes, and there is no class finer than that one. Thus, is does not fall into the range of product distribution between the classification outputs.)

d (mm)	H_s
1.35	0.114701
0.8	0.526401
0.45	0.608903
0.25	0.267138
0.165	0.177364
0.125	0.056919

Table 9.1 Initial composition of the material

Total residues Q (%)	Partial residues r (%)	Particle dimensions d (mm)
2.44	2.44	1.35
21.96	19.52	0.8
70.23	48.27	0.45
92.47	22.24	0.25
95.7	3.23	0.165
98.88	3.28	0.125
100	1.02	0.05

We determine total residues in the material coming out into the fine product for all experimental velocities. Entropy (H_f) of the material coming out into the fine product is calculated for all separation boundaries and velocities using the equation $H = -\sum_{i=1}^{n} P_i \ln P_i$, where P_i is the probability of taking a particle of a narrow size class i from the material (ratio of the amount of this size class to the initial amount of the material). Entropy for the coarse product is determined in exactly the same way. Further we determine the separation efficiency for all velocities and separation boundaries using the equation $E = 1 - \frac{\mu_f H_f + \mu_c H_c}{H_s}$.

d (mm)	3.5 m/s	3 m/s	2.5 m/s	2 m/s	1.5 m/s	1 m/s	0.75 m/s
1.35	0.191442	0.105605	0.04881	0.16174	0.003574	0.000575	
0.8	0.326884	0.219574	0.108129	0.035322	0.007825	0.001258	
0.45	0.234157	0.358226	0.345936	0.149731	0.033287	0.005322	0.000193
0.25	0.144578	0.251544	0.37099	0.399582	0.164007	0.02599	0.00094
0.165	0.125977	0.222833	0.352829	0.4536	0.282685	0.047778	0.001723
0.125	0.094895	0.170709	0.286395	0.469373	0.888363	0.220642	0.00783

This table shows which velocity ensures the highest efficiency for each boundary

9.4 Multi-product Separation

Let us examine a material consisting of seven size classes and evaluate the efficiency of its separation into seven components by six boundaries. Table 9.2 summarizes the material composition in percents.

Entropy of the starting material composition is

$$H_s = -\sum_{i=1}^{7} \left(\frac{r_{s,f}}{100}\right) \ln\left(\frac{r_{s,f}}{100}\right) = 1.66476$$

Below we present a table of the results of separation into 7 components by 6 boundaries by successive separation by all the boundaries.

d (mm)	7	6	5	4	3	2	1
0.55	1.1	0	0	0	0	0	0
0.356	25.757	2.08	1.72	0.42	0.47	0.34	0.14
0.181	8.47	2.47	3.34	1.08	1.395	1.83	0.39
0.128	2.5	2.04	3.7	3.85	3.13	3.1	0.735
0.09	0.16	0.42	1.39	1.63	3.8	3.94	1.4
0.064	0	0.05	0.17	0.5	1.1	6.74	1.09
0.0265	0	0.01	0.023	0.11	0.47	2.5	4.44
$\mu_{ri}\%$	37.987	7.07	10.343	7.59	10.365	18.45	8.19

$\mu_{ri}\%$ is the percentage of material in each component.

Entropies of each component are calculated below:

7	6	5	4	3	2	1
0.800173	1.298014	1.381915	1.352805	1.517987	1.570894	1.332966

Table 9.2 Multi-component mixture composition

Boundary d (mm)	Component contents $r_{s,f}\%$
0.55	1.1
0.356	31.36
0.181	20.375
0.128	23.015
0.09	12.74
0.064	5.65
0.0265	5.76

Then the separation efficiency is

$$E = 1 - \frac{\sum_{i=1}^{7} \mu_i H_i}{H_s} = 0.463115$$

9.5 Algorithms of Optimization of Separation into n Components

Let us analyze algorithms of material separation into n components in order to reach the highest possible efficiency.

Assume a starting material consisting of particles with sizes from a_0 to a_n that should be separated into n components by specified boundaries. The applied separation method is as follows. The material is separated into two components by one of the boundaries; then each component is separated into two components by one of the internal boundaries, etc., until all the material is separated by all the

boundaries. A problem is to find the order of separation boundaries leading to a maximal separation efficiency. The efficiency is estimated using the formula

$$E = 1 - \frac{\sum_{i=1}^{n} \mu_i H_i}{H_s}.$$

9.5.1 Algorithm 1: Complete Sorting-Out

First the results of separation into two components are determined for each boundary at all the parameters of the apparatus and the process (place of material feed into the apparatus i^*, number of apparatus stages z, air flow velocity w). Then for each of the calculated separation products, the results of separation into two components by all internal boundaries are calculated at all the parameters of the apparatus and the process. The procedure is continued until all possible ways of separating a specific material into n components are calculated for all possible parameters of the apparatus and the process. Then the separation efficiency is determined for all evaluated ways, the highest one is chosen, and thus the most efficient way of separating the material into n components is found.

The described algorithm provides the global maximum of separation efficiency, but its operation takes a very long time, $O(n!)$. A schematic diagram of such separation is shown in the form of a graph (a tree) (Fig. 9.1) in the case of starting material separation by four boundaries (for other numbers of boundaries, the approach remains the same). In this graph, each letter denotes a separation boundary. After the separation by each boundary, fine and coarse products are obtained. If they have internal separation boundaries, the fine product is considered in the graph along the edge 1, and the coarse product along the edge 2.

Another algorithm for finding the way of maximal separation efficiency is examined below.

9.5.2 Algorithm 2: Greedy Algorithm

At the first step, the results of separation into two components are calculated for all the boundaries and apparatus parameters. Each time the efficiency is estimated, the maximal efficiency is chosen, and thus the first boundary in the sequence of separation boundaries and the necessary parameters of the process and apparatus are established. Then the procedure is repeated for each of the two obtained components with respect to the found boundary until the material becomes separated into n components. Assume, for example, that the maximal efficiency of the

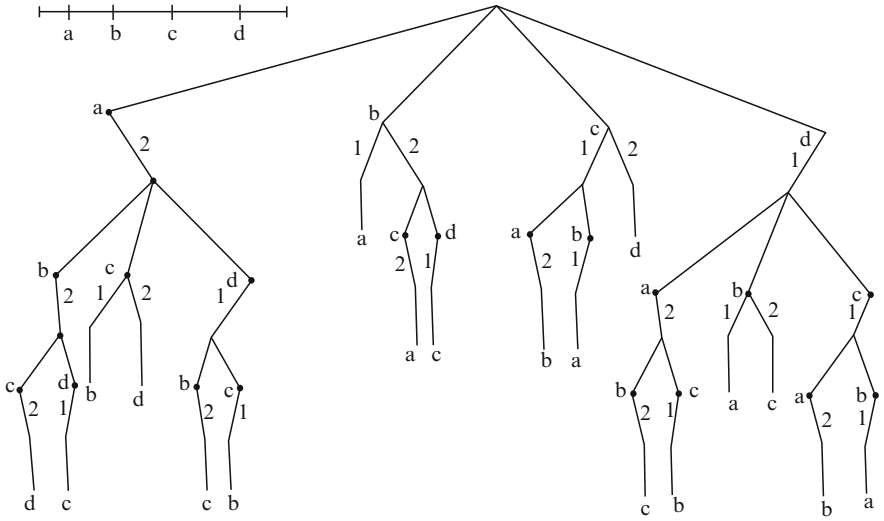

Fig. 9.1 Complete sorting graph

starting material separation into two components is achieved for the boundary a_j, at the air flow velocity w_i, quantity of apparatus stages z_i and number of the stage of material feed into the apparatus i_1^*. Each of the obtained components contains particles from all narrow size classes of the starting material; however, a part of them constitute "impurity" meant for other components. In the first of the obtained components, the separation boundary should be sought (for the efficiency maximization) between the boundaries a_0 and a_{j-1}, and in the second component – between the boundaries a_{j+1} and a_n. The procedure should be continued until the starting material becomes separated by all required boundaries.

This algorithm provides a local maximum of separation efficiency, but its operation time is $O(n \ln n)$, which is considerably less than the operation time of the first algorithm.

When the calculation of the order of separation boundaries for finding the maximal efficiency using the first algorithm proves to be too lengthy, then, starting from a certain calculation step, one can pass to the search for a local maximum using the second algorithm.

Figure 9.2 gives an example of material separation into four components. Here the first algorithm (complete sorting-out) is used at the first step only. Starting from the second step, the search for a local maximum of separation efficiency is performed using the second algorithm. The graph in Fig. 9.2 is a subgraph of the graph in Fig. 9.1.

A concrete example of the calculation of the order of separation boundaries for obtaining a maximal efficiency demonstrates that the greedy algorithm is not so poor, i.e. its results are close to those of a complete sorting-out. We also demonstrate that it is possible to start the search for the order of separation boundaries for

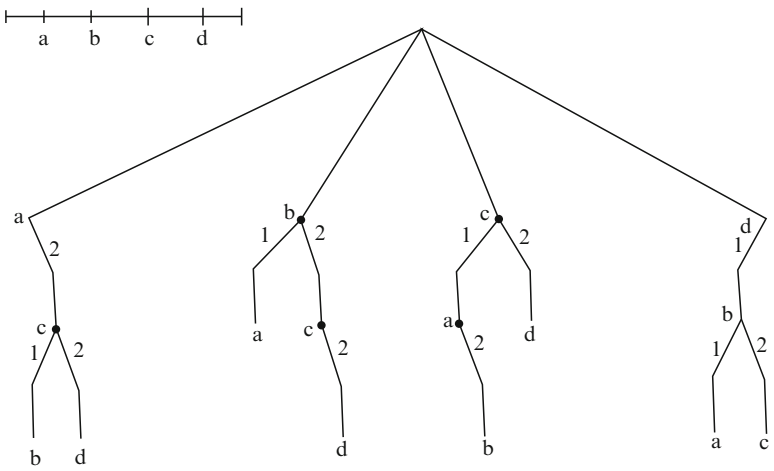

Fig. 9.2 Mixed algorithm of the search for maximal efficiency of separation into components

obtaining maximal separation efficiency with a complete sorting-out and then pass to the search for a local maximum.

9.5.3 Optimization of Separation into Four Components

We examine phosphates in the capacity of the starting material. Their density is $\rho_m = 2,800\,\text{kg/m}^3$. Air density is $\rho_a = 1.2\,\text{kg/m}^3$. Let the velocity of air flow entering the apparatus from below be $w = 1.8$ m/s, the quantity of separation stages in the apparatus $z = 9$, the number of the stage of material feeding into the apparatus $i^* = 5$. (Without any loss of generality, we have assumed that the air flow velocity, quantity of separation stages and place of material feed into the apparatus are constant. In general, these parameters should be varied in the course of optimization.)

We analyze separation by three boundaries at constant parameters of the apparatus. Grain size composition of the starting material is specified in Table 9.3.

We determine the starting material entropy representing the former as two narrow size classes for each of three separation boundaries in turn. First we calculate total material residues for each separation boundary in %.

Narrow class number	$Q_s\%$	$r_s\%$
1	52.2	52.2
2	75.5	23
3	88.6	13.4
4	100	11.4

Initial entropy $H_s = -(P_1 \ln P_1 + P_2 \ln P_2)$, where $P_1 = \frac{Q_s\%}{100\%}$, $P_2 = 1 - P_1$.

Table 9.3 Grain size composition of starting material

Sieve size (mm)	0–0.0265	0.053–0.0635	0.074–0.0875	0.105–0.1275
Partial residues of narrow classes on sieves (%)	11.4	13.4	23	52.2
Narrow class number	4	3	2	1

We denote separation boundaries with letters as follows (narrow class numbers being written above):

4	3	2	1
a		b	c

Initial entropy for each of three separation boundaries equals

	H_s
c	0.692
b	0.56
a	0.355

The separation coefficients for all narrow size classes (k) according to equation $k = 1 - \sqrt{0.4B}$ are:

1	2	3	4
0.40018	0.497452	0.576695	0.40018

We determine the fractional extraction degree for each narrow class (F_f) using Eq. (7.3)

1	2	3	4
0.116769	0.487262	0.824351	0.992503

The amount of the material output into fine and coarse products after the separation into two components for each of three separation boundaries is: $r_f\% = \mathrm{F_f r_s}\%$; $r_c\% = \mathrm{r_s}\% - \mathrm{r_f}\%$.

Table of fine product yield (μ_f):

Amount of material in a component (%)	1	2	3	4
39.67	6.1	11.21	11.05	11.31

Table of coarse product yield (μ_c):

Amount of material in a component (%)	1	2	3	4
60.33	46.1	11.79	2.35	0.09

Let us determine on which of the three separation boundaries the efficiency of separation into two components is the highest.

Tables of complete residues for coarse and fine products are given below.

Table for fine product:

Amount of material in a component (%)	1	2	3	4
39.67	6.1	17.31	28.36	39.67

Table for coarse product:

Amount of material in a component (%)	1	2	3	4
60.33	46.1	57.89	60.24	60.33

Let us determine the entropy of coarse and fine products by all separation boundaries.

For fine product (H_f):

a	b	c
0.598	0.69	0.429

For coarse product (H_c):

a	b	c
0.011	0.0776	0.389

The efficiencies of separation into two components by all the boundaries are:

$$E = 1 - \frac{\mu_f H_f + \mu_c H_c}{H_s}; \quad \mu_f = 0.3967; \quad \mu_c = 0.6033.$$

Calculated efficiencies (E) are given below:

a	b	c
0.313	0.428	0.415

Apparently, maximal efficiency of separation into two components is reached on the boundary b. Meanwhile, each of the remaining components has one internal boundary, and to complete the search, it remains to separate each of the obtained components by it. (If, however, we obtained the maximum efficiency of separation into two components on the boundary a or c, we would have to continue the search for separation boundary in the component with two remaining internal separation boundaries until we find the maximal local efficiency).

In the present case, it remains to separate the two obtained components by the boundaries a and c, respectively.

The result of the first component separation by the boundary a is as follows.

Fine product $(r_f\%)$:

Amount of material in the component (%)	1	2	3	4
26.514	0.712	5.462	9.11	11.23

Coarse product $(r_c\%)$:

Amount of material in the component (%)	1	2	3	4
12.85	5.39	5.75	1.94	0.08

The result of the second component separation by the boundary c is as follows.

Fine product $(r_f\%)$:

Amount of material in the component (%)	1	2	3	4
13.156	5.382	5.745	1.94	0.089

Coarse product $(R_c\%)$:

Amount of material in the component (%)	1	2	3	4
47.174	40.718	6.045	0.41	0.001

We calculate the final efficiency of separation into four components. The entropy of the starting material consisting of four narrow classes is $H_s = 1.2$. Entropies of each component after separation are $H_1 = 1.151; H_2 = 1.041;$

$H_3 = 1.04; H_4 = 0.432$. Then the separation efficiency is $E = 1 - \frac{\sum_{i=1}^{4} \mu_i H_i}{H_s} = 0.437$. It should be emphasized that the material is separated using the algorithm meant for obtaining a local maximum of separation efficiency in the following order of separation boundaries: (b; a; c).

We seek the separation efficiency maximum using a complete sorting-out at the first step and a search for a local maximum starting from the second step.

The fractional extraction degree for each narrow class remains unchanged, since the process parameters remain the same.

We analyze starting material separation as separation by the boundary a.

Fine product $(r_f\%)$:

Amount of material in the component (%)	1	2	3	4
39.67	6.1	11.21	11.05	11.31

Coarse product $(r_c\%)$:

Amount of material in the component (%)	1	2	3	4
60.33	46.1	11.79	2.35	0.09

In the obtained coarse product, we seek a boundary providing maximal efficiency of separation into two components. It can be easily verified that maximal separation efficiency is reached on the boundary b.

We obtain the result of coarse product separation into two components using equations $r_f\% = F_f r_s\%$ and $r_c\% = r_s\% - r_f\%$. They give the following two components (separation by the boundary b).

Fine product $(r_f\%)$:

Amount of material in a component (%)	1	2	3	4
13.156	5.382	5.745	1.94	0.089

Coarse product $(r_c\%)$:

Amount of material in a component (%)	1	2	3	4
41.174	40.718	6.045	0.41	0.001

Let us calculate the separation of the obtained coarse product by the boundary c.

Fine product $(r_f\%)$:

Amount of material in a component (%)	1	2	3	4
8.04	4.754	2.945	0.33798	0.000993

Coarse product $(r_c\%)$:

Amount of material in a component (%)	1	2	3	4
39.13	35.96	3.1	0.07202	0.000007

We study starting material separation in the case of the following order of boundaries: (a; c; b). We use the available results of coarse product separation first by the boundary c. Then we separate the obtained fine product by the boundary b. The result of separation by boundary c is:

Fine product $(r_f\%)$:

Amount of material in a component (%)	1	2	3	4
13.156	5.382	5.745	1.94	0.089

Coarse product $(r_c\%)$:

Amount of material in a component (%)	1	2	3	4
47.174	40.718	6.045	0.41	0.001

Determine the separation of the last fine product by boundary b.

Fine product $(r_f\%)$:

Amount of material in a component (%)	1	2	3	4
5.1176	0.628	2.8	1.6	0.0883

Coarse product $(r_c\%)$:

Amount of material in a component (%)	1	2	3	4
8.04	4.754	2.945	0.34	0.0006

Let us calculate the efficiency for the order of boundaries (a; c; b) under study:

$$H_1 = 1.36; H_2 = 0.433; H_3 = 1.022; H_4 = 0.812; E = 1 - \frac{\sum_{i=1}^{4} \mu_i H_i}{H_s} = 0.282.$$

We study starting material separation into two components as separation by the boundary c.

Fine product $(r_f\%)$:

Amount of material in a component (%)	1	2	3	4
39.67	6.1	11.21	11.05	11.31

Coarse product $(r_c\%)$:

Amount of material in a component (%)	2	3	4	
60.33	46.1	11.79	2.35	0.09

We consider the separation of the obtained fine product by the boundary b and obtain the following two components:

Fine product $(r_f\%)$:

Amount of material in a component (%)	1	2	3	4
26.514	0.712	5.46	9.11	11.23

Coarse product $(r_c\%)$:

Amount of material in a component (%)	1	2	3	4
13.16	5.39	5.75	1.94	0.08

We consider the separation of the obtained fine product by the boundary a:

Fine product $(r_f\%)$:

Amount of material in a component (%)	1	2	3	4
21.4	0.083	2.66	7.51	11.14

Coarse product $(r_c\%)$:

Amount of material in a component (%)	1	2	3	4
5.113	0.629	2.8	1.6	0.084

We calculate separation efficiency for the obtained order of boundaries (a; b; c).

$$H_1 = 0.66; H_2 = 1.04; H_3 = 1.1; H_4 = 0.984; E = 1 - \frac{\sum_{i=1}^{4} \mu_i H_i}{H_s} = 0.333.$$

Let us calculate the results of starting material separation for the order of boundaries (a; b; c). We use the obtained results of separation by the boundary c and consider the fine product separation by the boundary a. Then we separate the obtained fine product by the boundary b.

The result of separation by the boundary a is:

Fine product $(r_f\%)$:

Amount of material in a component (%)	1	2	3	4
26.514	0.712	5.46	9.11	11.23

Coarse product $(r_c\%)$:

Amount of material in a component (%)	1	2	3	4
13.16	5.39	5.75	1.94	0.08

Finally, the efficiency for the order of boundaries (c; a; b) under study is:

$$H_1 = 0.66; H_2 = 1.55; H_3 = 1.015; H_4 = 0.812; E = 1 - \frac{\sum_{i=1}^{4} \mu_i H_i}{H_s} = 0.315.$$

One can see that if the algorithm of the search for a local maximum was used in the complete sorting-out algorithm after separating the starting material by the boundary c, the local maximum would give the order of separation boundaries (a, b, c).

The table below shows separation efficiencies for all possible orders of separation boundaries.

Order of boundaries	b.c.a (obtained in the search for maximal efficiency maximum)	a.b.c (local maximum starting from the second step)	a.c.b.	c.b.a (local maximum starting from the second step)	c.a.b
Efficiency	0.347	0.285	0.282	0.333	0.315

This and other examples show that the algorithm of the search for local separation efficiency maximum is good enough in comparison with the algorithm of complete sorting-out.

9.6 Mathematical Model of Separation into *n* Components

Let a starting material be specified with particle sizes within the range from a_0 to a_n, which should be separated by $(n-1)$-th boundary. We assume, without any loss of generality, that we have obtained using algorithms the following order of separation boundaries for achieving maximal separation efficiency:

$$a_{i_1}, a_{i_2}, a_{i_3}, \ldots, a_i, \ldots, a_{i+1}, \ldots, a_{i_{n-2}}, a_{i_{n-1}}$$

(i.e. separation by a_i boundary occurs before the separation by a_{i+1} boundary, and if it were otherwise, the approach would be exactly the same). The apparatus parameters are also obtained for separation by each boundary (these parameters $z-$ the quantity of stages, i^*- the number of stage of the material feed into the apparatus, $w-$ the velocity of air flow entering the apparatus from below, are different for all boundaries). Assume that it is needed to calculate separation results in the $(i+1)$ component. According to the obtained sequence of separation boundaries, the results of separation in $i+1$ component will be available after separation by a_{i+1} boundary. Let us mark the C-path connecting a_{i_1} and a_{i+1} vertices in the graph presented in Fig. 9.3. Let $r_{s,j}$ be the quantity of j size class material in the starting

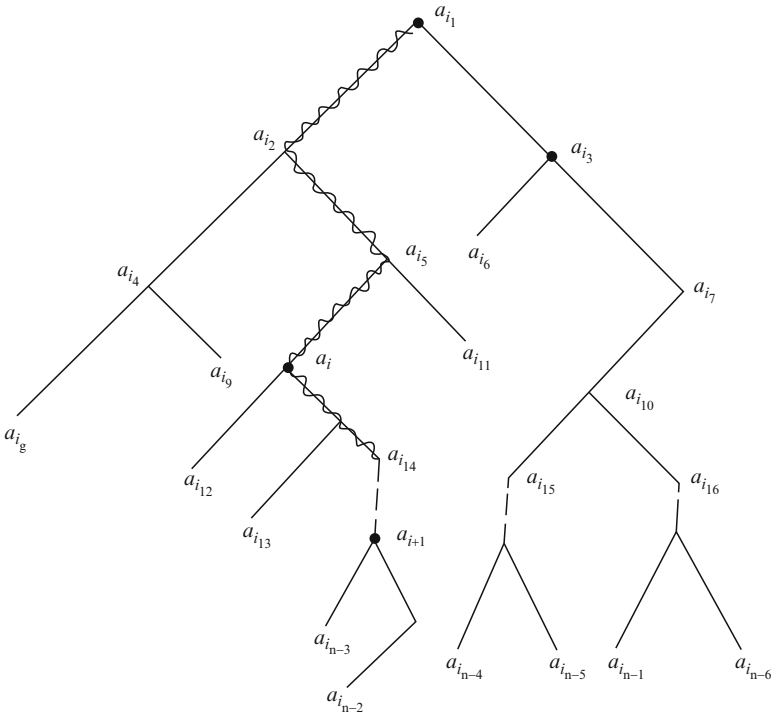

Fig. 9.3 Sequence of separation boundaries

material. Then after the starting material separation by the boundary a_{i_1}, the quantity $r_{s,j}F_{1,f,j}$ of j size class material falls into fine product, and $r_{s,j}(1 - F_{1,f,j})$ into coarse product. Here $F_{1,f,j}$ is the fractional extraction degree of the size class j for the first apparatus performing separation. Further, the material extracted into fine and into coarse products should be separated by the respective internal separation boundaries. The quantity of j size class material falling into coarse and fine product after the separation by each boundary is determined analogously to the first separation stage. Then

$$r_{i+1,f,j} = r_{s,j}F_{i+1,f,j} \prod_{a_k \in C^R} (1 - F_{k,f,j}) \cdot \prod_{a_k \in C^l} F_{k,f,j} \tag{9.3}$$

where $r_{i+1,f,j}$ is the quantity of the material of size class j that came out into the $(i + 1)$ component;

$F_{k,f,j}$ – fractional extraction degree of the class j material into k-th component;

C – path between a_{i_1} and $a_{i+1}, a_k \in C^R$ or $a_k \in C'$, if the edge in the path C after the vertex a_k goes to the right or to the left, respectively (Fig. 9.3).

9.7 Optimum Conditions for Binary Separation

We assume that the original composition of a certain pourable material is described by the grain size characteristic in partial residues shown by curve ABC (Fig. 1.4). We also assume that due to technological needs, this material should be separated with respect to x_0 size. The graph area confined by curve ABC and coordinate axes corresponds, in a certain scale, to the total quantity of starting material. We conditionally take this quantity as a unity and denote the curve for the original composition by $Q(x)$.

In an ideal process, the material should be separated by a straight line Bx_0. With respect to this line, the starting material consists of two parts – fine (D_s) and coarse (R_s).

In a real process, the separation does not proceed ideally, since a number of the fine fractions fall into the coarse product, and a number of coarse ones fall into the fine product.

In this case, the fine product is described by a certain curve $g(x)$, and the coarse product by $n(x)$.

The graph area in Fig. 1.4 is separated by curves of ideal and real processes into four parts:

D_f – fine material in the fine product yield;

R_f – coarse material in the fine product yield;

R_c – coarse material in the coarse product yield;

D_c – fine material in the coarse product yield.

Separation can be optimized by minimizing the absolute value of the contamination of both products. According to Fig. 1.4, for this purpose it is sufficient to minimize the expression

$$A = R_f + D_c. \tag{9.4}$$

As known, an optimum condition can be written using the relation (9.4) as

$$\frac{dA}{dx} = \frac{dR_f}{dx} + \frac{dD_c}{dx} = \frac{d\int_0^x g(x)dx}{dx} + \frac{d\int_x^{x_{\max}} n(x)dx}{dx} = 0. \tag{9.5}$$

A derivative of a definite integral with a variable upper limit and a constant lower limit is known to be equal to the integrand in the upper limit point. Hence, we derive from (9.5):

$$g(x) - n(x) = 0,$$

$$g(x) = n(x). \tag{9.6}$$

It is clear from the curves $g(x)$ and $n(x)$ plotted with respect to curve $Q(x)$ that in the point of optimum, a narrow size class is divided in half.

In Fig. 1.4 only one point satisfies this condition – the intersection point of curves $g(x)$ and $n(x)$ with a respective ordinate x_0.

This can be clearly shown in a purely geometric way. For this purpose, the line should be plotted either to the left or to the right of Bx_0. In both cases, the area of joint contamination graph grows, and it is minimal only at Bx_0.

We determine the second optimum condition from the entropy value as a function of the original composition. For a binary product, we can write:

$$H_s = -[P_1 \log P_1 + P_2 \cdot \ln P_2]$$

or

$$H_s = -[P_1 \log P_1 + (1 - P_1) \cdot \ln(1 - P_1)]. \tag{9.7}$$

Let us differentiate Eq. (9.7):

$$\frac{dH_s}{dP_1} = [1 + \log P_1 - 1 - \log(1 - P_1)] = 0,$$

hence,

$$\log P_1 = \log(1 - P_1)$$

and

$$P_1 = P_2 = \frac{1}{2}. \tag{9.8}$$

Thus, a binary mixture is maximally indefinite when both components of the original composition are equal. It means that separation in this region can give a maximal effect.

9.8 Optimum Conditions for Multi-Product Separation

Figure 9.4 offers a schematic diagram of multi-product separation. In case of m boundaries $(m + 1)$ products are obtained.

According to Fig. 9.4, total contamination due to adjacent products only in case of multi-product separation can be defined as

$$A = (D_1 + R_1) + (D_2 + R_2) + (D_3 + R_3) + \cdots + (D_m + R_m). \tag{9.9}$$

Similarly to the case of binary separation, here we can also obtain the optimization condition by minimizing the absolute value of the contamination of all products.

$$\frac{dA}{dx} = \frac{d(D_1 + R_1)}{dx} + \frac{d(D_2 + R_2)}{dx} + \cdots + \frac{d(D_m + R_m)}{dx} = 0.$$

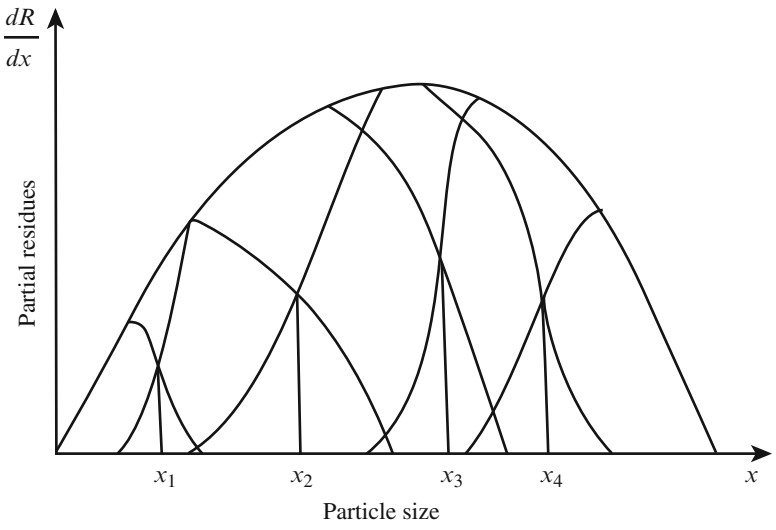

Fig. 9.4 Basic circuit of multi-product separation

This equality can be solved correctly only by setting each brackets to zero, i.e. on each separation boundary the following should be valid.

$$\begin{gathered} g(x_1) = n(x_1) \\ g(x_2) = n(x_2) \\ g(x_3) = n(x_3) \\ \ldots\ldots\ldots\ldots\ldots\ldots \\ \ldots\ldots\ldots\ldots\ldots\ldots \\ g(x_m) = n(x_m) \end{gathered} \tag{9.10}$$

The same result can be obtained in case of each product contamination not only by the material of adjacent fractions. In this case, $R_1; R_2; \ldots; R_n$ imply total contamination of the respective material.

It means that on each separation boundary, a narrow class should be divided in half.

A common zero in Eq. (9.9) can be also obtained due to the boundary displacement to the left of the conditions (9.10) in one case and to the right in another. However, as shown for binary mixtures, it leads to an increase in total contamination. Therefore, the conditions (9.10) are the only correct ones for a multi-product process.

For our studies, we have chosen a shelf classifier. It consists of seven stages with the initial feed to the second one counting from above. In our experiments, we studied crushed quartzite with particles in a broad size range. Main characteristics of this material are given in Table 9.4. The size of a narrow size class was

Table 9.4 Starting material characteristic

Mesh size of sieve, x μm	Narrow class mean size $\overline{x}$ μm	Partial residues on the sieve r%	Products boundaries μm	Product notation	Each product content in the initial one (%)
1	2	3	4	5	6
2,800	3,000	0.78		G	3.02
2,500	2,650	2.24	+2,150		
1,800	2,150	6.73	−2,150	F	6.73
			+1,400		
1,000	1,400	12.07	−1,400	E	23.28
750	825	11.21	+690		
630	690	10.7	−690	D	26.9
400	515	16.2	+357.5		
315	357.5	13.73	−357.5	C	23.93
200	257.5	10.2	+180		
160	180	6.1	−180		
100	130	3.31	+71.5	B	11.84
80	90	2.43			
63	71.5	2.03			
50	56.5	1.28	−71.5	A	4.3
40	45	0.7			
0	20	0.29			

determined as an arithmetic mean of mesh sizes of two adjacent sieves. The entire size range is separated into seven products by six boundaries. Table 9.4 shows the amount of each product in the starting material and which narrow class should be separated in an optimum manner in order to achieve the minimal mutual contamination of the products at each separation act.

$$H_F = +0.6052; H_E = +0.6313; H_D = +0.6361; H_C = +0.5756; H_B = +0.549; H_A = +0.388.$$

Based on this table and using normal logarithms, we obtain from Eq. (9.1) the initial composition entropy:

$$H_s = +1.71.$$

Preliminary experiments made it possible to determine optimum air flow velocities referred to the total classifier cross-section, which ensure optimum separation of narrow classes indicated in column three. It is established that in this apparatus this velocity is 0.95 m/s for 71.5 μm class, 1.34 m/s for 180 μm class, 1.89 m/s for 357.5 μm, 2.62 m/s for 690 μm, 3.74 m/s for 1,400 μm, and 4.63 m/s for 2,150 μm.

Three sets of experiments of successive separation of the starting product into the indicated seven products were carried out.

In the first set of experiments, first the finest product A was separated in an optimum way, then the product B was separated from the residue in an optimum way, as well, then the product C, etc., up to the product G.

The results of this study are summarized in Table 9.5. This Table shows the yield of each product. For example, as for the product D, its yield with respect to the initial composition is $\gamma_D = 26.705\%$. In this product, target fractions, that is particles within the size range from 357.5 to 690 μm, amount to 17.81% of the mentioned quantity ($\gamma_z = 17.81\%$). Besides, this product contains particles exceeding 690 μm and those below 357.5 μm. Their total amount constitutes the contamination of this product. For D product, their amount is 8.895% and is denoted as ($\gamma_p = 8.895\%$).

Entropy of each product is determined based on the contents of target fractions (γ_z) and contamination (γ_p) in it. Here the product is considered independently, that is the sum of these two components is taken as a unity or 100%. In this case,

$$z = \frac{17.81}{26.705} = 66.69\%,$$

$$p = \frac{8.895}{26.705} = 33.31\%.$$

In this case we write the composition entropy for each specific product D as

$$H_D = -(0.6669 \ln 0.6669 + 0.3331 \ln 0.3331) = +0.6362.$$

Similarly, calculated composition entropies for all other products are

$$H_A = +0.6795; H_B = +0.696; H_C = +0.5958; H_E = +0.606; H_F = +0.6096; H_G = +0.6796$$

Then we determine the total efficiency of this multi-product separation using Eq. (9.2):

$$E_I = 0.632.$$

In the second set of experiments, separation of each product from the starting material was performed in a reverse order – from coarse to fine, product G first, then F, etc., up to product A. The results of this set of experiments are given in Table 9.6.

Based on the data of Table 9.6, we have determined for this case the following: $H_G = +0.6718$;

Table 9.5 Results of multi-product separation of the initial material from fine to coarse one

Separation stage and flow velocity	Starting material – 100%	
	Fine product	Coarse product
1 $w = 0.95$ m/s	Product A $\gamma_A = 3.545\%$ $\gamma_z = 2.065\%$ $\gamma_p = 1.48\%$	Residue $\gamma = 96.455\%$
2 $\gamma_B = 12.285\%$ $w = 1.34$ m/s $\gamma_z = 6.115\%$ $\gamma_p = 6.17\%$	Product B $\gamma = 84.17\%$	Residue
3 $w = 1.89$ m/s	Product C $\gamma_C = 20.96\%$ $\gamma_Z = 15.05\%$ $\gamma_P = 5.945\%$	Residue $\gamma = 63.21\%$
4 $w = 2.62$ m/s	Product D $\gamma_D = 26.705\%$ $\gamma_z = 17.81\%$ $\gamma_p = 8.895\%$	Residue $\gamma = 36.5\%$
5 $w = 3.74$ m/s	Product E $\gamma_E = 21.14\%$ $\gamma_z = 14.903\%$ $\gamma_p = 6.237\%$	Residue $\gamma = 15.365\%$
6 $w = 4.63$ m/s	Product F $\gamma_F = 10.01\%$ $\gamma_z = 3.0\%$ $\gamma_p = 7.01\%$	Product G $\gamma_F = 5.362\%$ $\gamma_z = 2.242\%$ $\gamma_p = 3.12\%$

Table 9.6 Results of multi-product separation of the initial material from coarse to fine one

Separation stage and flow velocity	Starting material – 100%	
	Fine product	Coarse product
1 $w = 4.63$ m/s	Residue $\gamma = 94.02\%$	Product G $\gamma_G = 5.98\%$ $\gamma_z = 2.375\%$ $\gamma_p = 3.605\%$
2 $w = 3.74$ m/s	Residue $\gamma = 83.795\%$	Product F $\gamma_F = 10.225\%$ $\gamma_z = 3.0\%$ $\gamma_p = 7.225\%$
3 Residue $w = 2.62$ m/s	Product E $\gamma = 61.74\%$	 $\gamma_E = 22.056\%$ $\gamma_z = 14.868\%$ $\gamma_p = 7.188\%$
4 $w = 1.89$ m/s	Residue $\gamma = 35.04\%$	Product D $\gamma_D = 26.7\%$ $\gamma_z = 17.826\%$ $\gamma_p = 8.874\%$
5 $w = 1.34$ m/s	Residue $\gamma = 14.495\%$	Product C $\gamma_C = 20.545\%$ $\gamma_z = 15.015\%$ $\gamma_p = 5.53\%$
6 $w = 0.95$ m/s	Product A $\gamma_A = 3.453\%$ $\gamma_z = 3.0\%$ $\gamma_p = 0.453\%$	Product B $\gamma_B = 11.049\%$ $\gamma_z = 8.42\%$ $\gamma_p = 2.629\%$

It is determined using Eq. (9.2) that the total efficiency of such multi-product separation was

$$E_{II} = 64.66\%.$$

In the third set of experiments, the idea of efficiency maximization at each separation stage was realized.

First, a narrow size class was established in the starting material with approximately the same ratio of fine and coarse products contents. It is a narrow class with the mean particle size $\overline{x} = 690$ μm. With respect to this class, total residues are $R_s = 43.73\%$, and total passages are $D_s = 56.27\%$. Therefore, the first separation stage was carried out at the air flow velocity $w = 2.62$ m/s. In this case, 62.04% of the total starting material came out into fine product, and 37.96% into coarse product. In the fine product yield, the class with the mean particle size $\overline{x} = 357.5$ μm proved to be the closest to 50% composition. With respect to this class, $R_s = 57.5\%$; $\mathrm{D_s} = 42.5\%$.

In the coarse product yield, an analogous size class was the class with $\overline{x} = 1400$ μm. With respect to this class, $R = 31\%$; $\mathrm{D_s} = 69\%$.

Table 9.7 Results of multi-product separation of starting material according to the principle of maximal efficiency at each stage

Separation stage, air flow velocity	Starting material – 100%	
	Fine product	Coarse product
1 $w = 2.62$ m/s	I Fine product $\gamma = 62.04\%$	I Coarse product $\gamma = 37.96\%$
2 $w = 1.89\%$ of I fine product	II Fine product $\gamma = 35.05\%$	Product D $\gamma_D = 27\%$ $\gamma_z = 17.83\%$ $\gamma_p = 9.13\%$
3 $w = 3.74$ m/s of I coarse product	Product E $\gamma_E = 22.6\%$ $\gamma_z = 14.97\%$ $\gamma_p = 7.63\%$	III Coarse product $\gamma = 15.34\%$
4 $w = 1.34$ m/s of II fine product	IV Fine product $\gamma = 14.97\%$	Product C $\gamma_C = 20.079\%$ $\gamma_z = 15.025\%$ $\gamma_p = 5.054\%$
5 $w = 4.63$ m/s of III coarse product	Product F $\gamma_F = 10.13\%$ $\gamma_z = 3\%$ $\gamma_p = 7.13\%$	Product G $\gamma_G = 5.8\%$ $\gamma_z = 2.11\%$ $\gamma_p = 3.69\%$
6 $w = 0.95$ m/s of IV fine product	Product A $\gamma_A = 3.6\%$ $\gamma_z = 3.08\%$ $\gamma_p = 0.52\%$	Product B $\gamma_B = 11.37\%$ $\gamma_z = 10.153\%$ $\gamma_p = 1.217\%$

The second separation was carried out with the fine product yield at the velocity of $w = 1.89$ m/s, which corresponds to optimum separation by the class of 357.5 μm.

Product D containing 27% of the starting material is the coarse yield material of this separation stage.

The third separation in this set of experiments was carried out on coarse material remaining from the first experiment at the air flow velocity of $w = 3.74$ m/s, which is optimum for a narrow class with the mean particle size $\overline{x} = 1,400$ μm.

Fine yield material at this separation stage is product E. The separation was carried through in a similar way.

A schematic diagram of this separation is presented in Table 9.7.

Based on this Table, entropies of each product composition were calculated:

$$H_D = +0.641; H_E = +0.6396; H_C = +0.6183; H_F = +0.607;$$

$$H_G = +0.6555; H_A = +0.412; H_B = +0.3368.$$

We have determined using Eq. (9.2) that in this case, the total efficiency of separation into seven products is

$$E_{III} = 0.6526,$$

which exceeds the total separation efficiency value in the two previous cases.

The following conclusions can be made from the analysis above:

1. Entropy criterion is applicable for the evaluation and optimization of multi-product separation. It can be also used for unambiguous evaluation of complicated schemes of concentrating plants and other multi-stage processing lines for separating both multi-component and binary mixtures.
2. The value of multi-product separation efficiency is determined by the starting material composition.
3. Maximal possible efficiency is also determined by the chosen sequence of separation boundaries.
4. As the obtained results have shown, maximal effect is reached when two conditions are observed:
   (a) At each separation by any boundary, the optimum condition should be realized at the expense of mutual contamination minimization
   (b) The sequence of separation boundaries should be chosen so that the separation is performed by the boundary for which the ratio of products is the closest to the equality $R_s = D_s = 50\%$.

Chapter 10
Stability and Kinetic Aspects of Mass Distribution in Critical Regimes

Abstract Despite the observed total chaos, a practically deterministic universal separation curve is formed in critical regimes of two-phase flows. We have managed to understand it only by means of an analysis of changes in the entropy of two-phase flows and in other parameters forming a statistical identity. Parameters ensuring the stability of this curve are determined, and the mechanism of their action is shown. A specific equilibrium in the critical regime is substantiated.

Keywords Entropy · Stability · Universal curve · Fluctuation · Parameters · Mass process · Chaos · Order · Regularity

10.1 Entropy Stability

Rapid filming and visual observations of the separation process reveal a completely chaotic motion of particles, especially in cascade facilities with numerous internal components. Particles of a poly-fractional mixture move upwards and downwards, to the left and to the right, take part in vertical motion, form agglomerates that can decay and appear again, collide with each other, as well as with the walls and internal facilities of the channel. All this makes it impossible to predict the motion direction and velocity for at least one particle, not to speak about the behavior of a class of particles. Meanwhile, separation curves obtained as a result of such process have a markedly deterministic stable character. This fact is covered in detail in Chapter 1. It gives the impression that each particle size class behaves autonomously in this chaotic motion, irrespective of the behavior of all other size classes, although, beyond any doubt, the particles interact.

There is nothing unexpected about it. It is an exact analogy of Dalton's law for a mixture of gases. Molecules of all the components interact, and the pressure on the chamber walls is made up from the pressures of all the components, which they would exert if each of them occupied the entire volume.

E. Barsky, *Critical Regimes of Two-Phase Flows with a Polydisperse Solid Phase*, Fluid Mechanics and Its Applications 93,
DOI 10.1007/978-90-481-8838-3_10,

It is experimentally proved that the stability of the universal separation curve obtained on a particular apparatus is practically absolute. It remains constant at varying granulometric composition of the solid phase, air flow velocity within the limits of a turbulent regime, boundary size of separation and even (within certain limits) material concentration in the flow. Naturally, a question arises – what ensures such deterministic stability of separation results in a practically totally chaotic process with the participation of an immense number of particles $(10^{10} - 10^{11})$ of various sizes and densities having irregular shapes? Here the principal parameters of the process are subject to constant fluctuations. Local concentrations and flow velocities, composition of particles of different classes, flow pressure, etc. are non-uniform.

To gain an understanding of all this, we revert to the crucial relation for a system of critical flow with a polyfractional solid phase:

$$dI = \chi dH - fdV + \sum_k \tau_k dN_k. \tag{10.1}$$

In this expression, entropy H and potential extraction I are functions of the state, while χ, τ, f, N are active parameters of the system.

As shown, using Euler's theorem we can obtain from this equation the following:

$$I = \chi H - f V + \sum_k \tau_k N_k.$$

Now we write this expression in a complete differential form:

$$dI = \chi dH + Hd\chi - fdV - Vdf + \sum_k (\tau_k dN_k + N_k d\tau_k).$$

This expression agrees with Eq. (10.1) under the condition that

$$Hd\chi - Vdf + \sum_k N_k d\tau_k = 0.$$

This shows that all active variables of the system under study cannot be independent. For instance, if χ and f are constant, the following is necessary:

$$\sum_k N_k d\tau_k = 0.$$

It is important for the understanding of the effect of fluctuations of various parameters on the process stability. According to the ideas formulated by Clausius, the entropy of a closed system permanently grows. Boltzmann has shown in his

kinetic theory of gases that a closed system evolves to the state with the maximal internal entropy for given conditions and acquires an equilibrium state. The equilibrium state according to Boltzmann is a state in which the interaction of gas molecules cannot affect the magnitude of the attained value of the internal entropy.

Further studies of this problem performed by such scientists as Einstein, Gauss, Prigozhin, have shown that this law is also characteristic of other systems where a spontaneous change proceeds in such a way that the total internal entropy value (H_i) permanently grows until it reaches, under specific conditions, its extreme value

As shown in the previous chapter, this regularity is not characteristic of the process under study. During separation, the total internal entropy decreases as a result of ordering of separation products compositions in comparison with the source feeding composition. In this respect, the critical flow entropy is basically different from the thermodynamic entropy. If the total internal entropy is considered as a sum of entropies of all narrow size classes

$$H_i = \sum_n H_{in},$$

on the whole, it decreases. However, there is one component among the terms of this sum, whose value grows up to the extreme one. We imply the entropy of the boundary size class.

In literature, there is no unanimous concept regarding this value. The known methods of Rubinchik, Povarov and Mayer give different magnitudes of the optimal boundary class value.

Let us determine this value proceeding from the entropy parameter. For this purpose, we revert to relation (3.8):

$$\phi(N,z) = \frac{N!}{\left(\frac{N}{2}+z\right)!\left(\frac{N}{2}-z\right)!},$$

hence we can obtain using Stirling's approximation

$$\begin{aligned} H = \ln\phi &= N\ln N - \left(\frac{N}{2}+z\right)\ln\left(\frac{N}{2}+z\right) - \left(\frac{N}{2}-z\right)\ln\left(\frac{N}{2}-z\right) \\ &= \left(\frac{1}{2}+\frac{z}{N}\right)\ln\left(\frac{1}{2}+\frac{z}{N}\right) - \left(\frac{1}{2}-\frac{z}{N}\right)\ln\left(\frac{1}{2}-\frac{z}{N}\right). \end{aligned}$$

To determine the conditions of entropy maximization, we derive

$$\frac{\partial H}{\partial z} = -\frac{1}{N}\ln\left(\frac{1}{2}+\frac{z}{N}\right) + \frac{1}{N}\ln\left(\frac{1}{2}-\frac{z}{N}\right) = \ln\frac{\frac{1}{2}-\frac{z}{N}}{\frac{1}{2}+\frac{z}{N}} = \ln\frac{N-2z}{N+2z} = 0.$$

For the logarithm to be equal to zero, the expression under the logarithm must equal unity, that is,

$$\frac{N-2z}{N+2z}=1.$$

Hence,

$$z=0 \text{ and } H=H_{opt},$$

that is in the specified conditions, the entropy of this class acquires the maximal possible value. Here a specific kind of equilibrium arises, since this class is separated into both products in equal shares, that is, $F_f(x)=F_c(x)=50\%$.

Obviously, it is the boundary class entropy that must be taken as the basis of the process stability analysis. Clearly, the equilibrium state in a real process is continuously violated by fluctuations of various separation parameters such as χ,τ,f,N fluctuating around their average values. Fluctuations of each parameter cause changes in the equilibrium entropy. Naturally, these changes can be directed to its decrease only, that is,

$$\Delta H_0<0.$$

Non-equilibrium processes in a system level these fluctuations and restore the entropy to its initial value, which is extreme in these conditions. Otherwise, the system can lose its stability, which does not actually occur. Thus, a system is stable against fluctuations if entropy changes are directed to its decrease. The problem is to determine the probability of fluctuations of a specific parameter and the conditions in which they become essential.

L. Boltzmann introduced his famous relationship between the entropy and probability of thermodynamic systems:

$$H=-\sum_n p\ln p.$$

A. Einstein suggested a formula for the probability of thermodynamic quantities fluctuations applying conversely to Boltzmann's idea. He took the entropy as a basis and derived the probability:

$$P(\Delta H)=Ze^{\frac{\Delta H}{k}},$$

where ΔH is the entropy change connected with a fluctuation around the equilibrium state;

Z is a statistical sum;

k is Boltzmann's constant.

Apparently, these two relations are mathematically interconnected, but their meaning is opposite. For Boltzmann, the probability of the system state is a determining parameter, and the fluctuation probability is derived from it.

To obtain the fluctuations probability, entropy change connected with the latter is needed. Thus, the basic problem is reduced to the derivation of ΔH relation with fluctuations of such process parameters as $\delta\chi, \delta\tau, \delta f, \delta N$.

In a general case, entropy can be expanded into a series:

$$H = H_0 + \delta H + \frac{1}{2}\delta^2 H + \cdots, \tag{10.2}$$

where δH is a term of the first infinitesimal order comprising $\delta I, \delta\chi, \delta N$ etc. of the first infinitesimal order; $\delta^2 H$ is a term of the second infinitesimal order comprising $\delta^2 I, \delta^2\chi, \delta^2 N$ etc. of the second infinitesimal order; H_0 is the stable state entropy.

First, we examine the simplest case. Let the fluctuation occur in a small part of a limited system or in a zone. The consequence of this situation is N, χ, f flux from one part of the system to another.

The entropy of the system under study can be expressed by a sum

$$H = H_1 + H_2, \tag{10.3}$$

where 1 is a part of the system where the fluctuation occurred, 2 is the remaining part of the system.

$$H_1 = f(N_1;\ \chi_1;\ \tau_1; f_1;\ \text{etc.}),$$

$$H_2 = \phi(N_2;\ \chi_2;\ \tau_2; f_2;\ \text{etc.}).$$

We examine the process stability against flow velocity fluctuations (w, χ). Using (10.2), we express entropy deviation from the equilibrium state by expanding in a Taylor's series:

$$H - H_0 = \Delta H = \frac{\partial H_1}{\partial I_1}\delta I_1 + \frac{\partial H_2}{\partial I_2}\delta I_2 + \frac{\partial^2 H_1}{\partial I_1^2}\frac{\delta^2 I_1}{2} + \frac{\partial^2 H_2}{\partial I_2^2}\frac{\delta^2 I_2}{2} + \cdots \tag{10.4}$$

Terms of a higher infinitesimal order in this expansion can be neglected. Note that all derivatives in (10.4) refer to an equilibrium state. Since the potential extraction (or extraction from a zone) in a stable state remains constant,

$$\delta I_1 = -\delta I_2 = \delta I.$$

On the other hand, it has been established that

$$\left(\frac{\partial H}{\partial I}\right)_{V,N} = \frac{1}{\chi}.$$

Taking this into account, the dependence (10.4) can be rewritten as

$$\Delta H = \left(\frac{1}{\chi_1} - \frac{1}{\chi_2}\right)\delta I + \left(\frac{\partial}{\partial I_1}\frac{1}{\chi_1} + \frac{\partial}{\partial I_2}\frac{1}{\chi_2}\right)\frac{\delta^2 I}{2}. \tag{10.5}$$

Now we can establish the first and second infinitesimal deviation in the entropy δH and $\frac{\delta^2 H}{2}$:

$$\delta H = \left(\frac{1}{\chi_1} - \frac{1}{\chi_2}\right)\delta I,$$

$$\delta^2 H = \left(\frac{\partial}{\partial I_1}\frac{1}{\chi_1} + \frac{\partial}{\partial I_2}\frac{1}{\chi_2}\right)\frac{\delta^2 I}{2}.$$

In the equilibrium state, $\chi_1 = \chi_2$, hence, $\delta H = 0$. Consequently, changes are introduced into entropy only by fluctuations of the second infinitesimal order. It has been shown that

$$\frac{\partial}{\partial I}\frac{1}{\chi} = -\frac{1}{\chi^2}\frac{\partial \chi}{\partial I} = -\frac{1}{\chi^2}\frac{1}{i}$$

where $i = \frac{\partial I}{\partial \chi}$ is the specific potential extraction.

It can be represented as

$$\delta I = i\delta\chi.$$

Taking this into account,

$$\delta^2 H = -\frac{i(\delta\chi)^2}{\chi^2} < 0.$$

This condition requires a positive potential extraction, that is, $i > 0$. Otherwise, the system loses stability. Hence, in separation processes $i > 0$ is always valid.

We examine the case of fluctuations of the number of particles in a certain part of the system cross-section. As in the first case, we can write for such kind of fluctuations:

$$H - H_0 = \Delta H = \frac{\partial H_1}{\partial N_1}\delta N_1 + \frac{\partial H_2}{\partial N_2}\delta N_2 + \frac{\partial^2 H_1}{\partial N_1^2}\frac{\delta^2 N_1}{2} + \frac{\partial^2 H_2}{\partial N_2^2}\frac{\delta^2 N_2}{2}. \tag{10.6}$$

Note that particles diffusion from one part of the system into another $\delta N_1 = -\delta N_2 = \delta N$, and

$$\frac{\partial H}{\partial N} = -\frac{\tau}{\chi}.$$

Taking these remarks into account, Eq. (10.6) can be rewritten as

$$\Delta H = \delta H + \frac{\delta^2 H}{2} = \left(\frac{\tau_2}{\chi} - \frac{\tau_1}{\chi}\right)\delta N - \left(\frac{\partial}{\partial N_1}\frac{\tau_1}{\chi} + \frac{\partial}{\partial N_2}\frac{\tau_2}{\chi}\right)\frac{\delta^2 N}{2}.$$

Since the derivatives are taken for the equilibrium state, $\tau_1 = \tau_2$, and therefore, here also the first term vanishes, and the dependence for the entropy change amounts, on the whole, to

$$\frac{\delta^2 H}{2} = +\left(\frac{\partial}{\partial N}\frac{\tau}{\chi}\right)\frac{\delta^2 N}{2}.$$

If this condition is satisfied, the system is stable against diffusive particles exchange. Thus, we can determine the influence of other parameters on the entropy stability.

Actually, the effect of fluctuations in a real process is more complicated. Let us examine the chaotizing factor χ. Its changes cause a change not only in the carrying medium flow velocity, but also in other factors, for instance, the number of solid particles N, change in concentration μ and pressure in the flow f. Meanwhile, a change in any of these parameters, for instance, in concentration, can, in turn, affect χ, I, N, f. It results in a crossed impact. The most vivid example is cross diffusion with concentration gradient of particles of a certain size causing a diffusion flow of particles of another size.

One can easily conceive that diffusion is a permanent process in the course of separation, since there is no doubt that particles of different classes do not possess a uniform distribution within the apparatus volume. At the same time, permanent disturbances have other parameters, as well, and it seems extremely difficult to determine their effect on the entropy value. Therefore, to estimate the effect of all aggregate disturbances, the dependence suggested by Prigozhin for thermodynamic entropy fluctuations can be applied, which can be written, by analogy with critical flow, as follows:

$$\Delta H_i = -\frac{mc}{2},$$

where ΔH_i is the mean entropy deviation; m is the number of independent variables; c is a certain constant.

The simplicity of this dependence is both unique and understandable. The point is that fluctuations of the second infinitesimal smallness exert a realistic effect on entropy deviation from its extreme value. Apparently, it is of no importance which parameter fluctuates; their impact is minor and can be summed up in a simple way. Each independent parameter brings in the quantity equal to $-\frac{c}{2}$ into ΔH_i.

Note once more that all conclusions in this Section refer to the boundary size class of separation containing N_0 particles. Entropy stability refers only to this class

of particles. It is especially remarkable that all remaining classes are stable with respect to this class, as well, because the separation curve is constant. The study of stability in a critical flow could we restricted by this point. However, the question – how other classes of particles whose entropy does not reach extreme values acquire stability – remains unsolved. It calls for the continuation of these studies. Probably, a kinetic analysis of the process could clarify the situation.

10.2 Particles Distribution over the Channel Height

All theoretical developments and their results stated above were obtained from primary ideas. It was accepted that the process of separation is based on vertical direction of particle motion velocities only. The value of the velocity (or its projection) was not taken into account. However, even such simplified one-dimensional analysis of the process from the standpoint of statistical analysis in the kinetic theory of gases has provided numerous significant results. It has made it possible to explain many experimental facts and empirical regularities of the process that were unclear previously. Now we are making another step in the development of the theory of the process.

We still examine the one-dimensional situation, that is the projections of particles velocities on the vertical axis, and not their actual directions.

It is rather important to clarify the character of the material concentration distribution over the apparatus height in the process of separation.

For this purpose, special investigations were performed on a facility schematically represented in Fig. 10.1. The main component of this facility is a vertical pipe 150 mm in diameter and 7 m high. The pipe consists of eight separate sections 1, each of them 0.8 m high. The sections are connected by flanges 2 with built-in gates 3. Each gate can be shifted in order to block rapidly the channel by means of a compressed spring and counterweight 4. At the rotation of a lever, control-rod 5 loosens latches 6 of the gates, and they simultaneously and rapidly block the pipe cross-section under the action of springs and counterweights. The entire facility operates under depression created by fan 8. Air consumption is measured by a normal diaphragm and adjusted by gate 9. An even material feeding is realized by feeder 7 with a constant calibrated efficiency of 660 kg/h.

In our experiments we used crushed quartz with the specific density of $\rho = 2.9$ t/m^3. Its fractional composition is given in Table 10.1.

The experiments were performed as follows. A gate establishes a specified air flow rate while a fan is operating; and then the feeder starts working. After a certain period of time sufficient for stabilizing the separation regime, all the gates are simultaneously switched on. They block the channel cross-section, and a certain amount of material remains in each section. Naturally, after that the separation process stops, and the fan is switched off. Then each gate is opened manually, starting with the lowest one, and the amount of material and its grain size composition are determined in each cut-off volume.

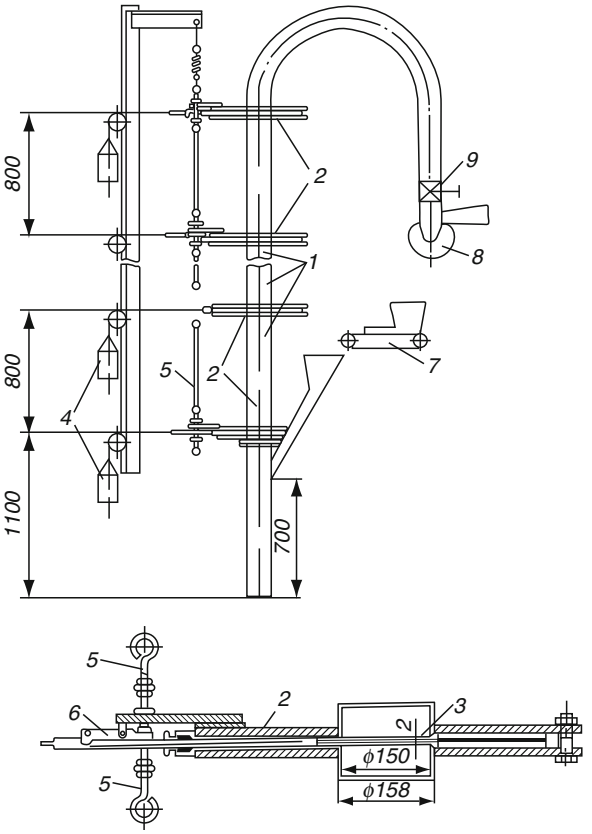

Fig. 10.1 Schematic diagram of the facility for the study of the distribution of various fractions in critical flow regimes

Table 10.1 Fractional composition of crushed quartz

Size class d (mm)	>2.5	1.6–2.5	1.0–1.6	0.85–1.00	0.63–0.85	0.4–0.63	0.315–0.4	<0.315
Partial residues r (mm)	0.26	35.49	45.65	8.77	4.36	1.18	0.19	4.1

First, weight distribution of the material over the pipe height was determined using equation

$$g_i = \frac{G_i}{\sum\limits_i G_i} \cdot 100\%,$$

where g_i is the percentage of the material weight at the i-th gate, %; i is the gate number counting from the lowest one; G_i is the material weight at the i-th gate, kg.

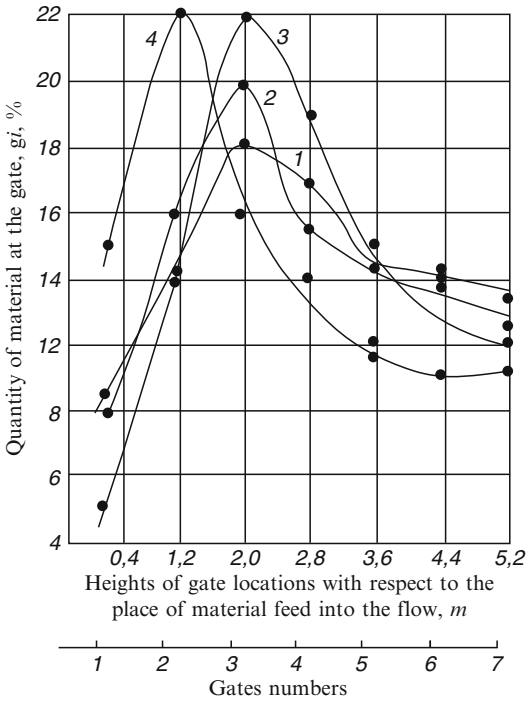

Fig. 10.2 Material distribution in height at various air flow rates: 1 – 10.8 m/s; 2 – 8.85 m/s; 3 – 8.05 m/s; 4 – 6.2 m/s

The dependence of g_i on the pipe height for different air flow rates is shown in Fig. 10.2. It follows that in all cases without any exceptions, material distribution in an ascending flow is characterized by a certain general dependence. While moving away from the site of material input into the flow, its amount grows and reaches a maximum at a certain level. Then this amount starts monotonically decreasing. The decrease is fast at first, and then stabilizes.

At high velocities (from 10.8 to 8.05 m/s), the maximum of material content in a flow corresponds to the position of the third gate. Velocity decrease leads to a decrease in the height at which the maximum is achieved. For instance, at a velocity equal to 6.2 m/s this maximum is shifted towards the second gate.

Hence, an indisputable conclusion follows that the material concentration during separation varies over the flow height. It is of interest to analyze the height distribution of particles of each fraction, as well.

The results of fractional analysis of the material at each gate are given in Table 10.2.

It follows from this table that at first, the separation process is intense and reaches a certain effect at a moderate height (6–8 gauges); then its intensity rapidly attenuates. This testifies that the process of height distribution is of explicitly exponential character.

Based on these experiments, we can make important conclusions on the mechanism of the process.

Table 10.2 Fractional distribution of the material at each gate in percents

Air flow rate (m/s)	Gate number *i*	Fraction size						
		1.6–2.5	1.0–2.6	0.85–1.0	0.63–0.85	0.4–0.63	0.4–0.135	<0.315
1	2	3	4	5	6	7	8	9
	1	25.9	47.45	11.0	5.62	1.9	0.5	7.39
	2	38.6	50.4	10.2	5.2	1.6	0.4	0.75
	3	31.3	50.9	9.3	4.4	1.5	0.4	1.31
10.8	4	29.7	52.1	10.8	4.5	1.6	0.3	0.82
	5	28.6	52.7	11.1	4.9	1.4	0.4	0.88
	6	27.9	50.7	11.8	5.4	1.8	0.3	1.2
	7	26.0	52	12	6.0	2.0	0.5	1.14
	1	20.3	49.8	15.0	7.54	2.71	0.54	3.98
	2	27.9	51.75	11.5	5.6	1.91	0.5	0.85
	3	23.9	55	12.55	5.5	1.6	0.4	1.0
8.85	4	21.7	54.8	13.1	7.1	1.9	0.5	0.97
	5	21.0	56.0	13.0	6.7	1.9	0.41	1.15
	6	19.6	54.9	15.3	6.9	2.0	0.44	1.1
	7	19.0	55.3	16.0	8.2	2.5	0.43	1.05
	1	14.85	51.5	16.95	9.6	3.5	1.2	2.62
	2	30.0	47.2	12.8	6.8	2.24	0.4	0.76
	3	24.9	51.5	14.2	6.4	2.2	0.41	0.8
8.05	4	19.1	56.5	13.3	7.32	2.24	0.59	1.08
	5	13.8	57.4	15.72	8.65	2.74	0.7	1.41
	6	13.0	57.2	17.15	8.15	2.9	0.61	1.05
	7	11.15	55.0	17.1	10.5	4.23	0.82	1.41
	1	1.41	45.5	20.4	13.9	6.6	1.7	10
	2	0.8	43.96	24.8	17	6.97	1.73	5.4
	3	0.8	32.2	27.25	21.45	10.0	2.6	5.68
6.2	4	0.8	32.8	27.2	21.4	9.85	2.33	5.32
	5	0.9	29.95	28.15	22.8	9.73	2.9	5.94
	6	0	26.4	26.5	22.6	11.4	2.7	9.73
	7	1.0	30.2	28.4	23.8	10.9	2.9	3.77

First, the separation process is practically completed at a limited height of a hollow apparatus.

Secondly, this zone corresponds to an unstable mode of the process.

Thirdly, material concentration varies from the site of material supply to the site of fine product discharge from the apparatus.

10.3 Velocity Distribution of Particles of a Narrow Size Class

We have previously shown that on average, one cell of 500 is occupied in the apparatus. Since the material concentration varies with height, cell occupancy is also variable, because the concentration changes depending on the site of material supply into the apparatus in the direction to the zone. Hence, the probability of cell occupancy depends on its position in the apparatus. The distance from the site of

material introduction into the apparatus to a certain cell can be measured by the number of cells, and not in centimeters. Since the system under consideration is three-dimensional, the distance from the lowest point of the apparatus axis to the cell (or its radius-vector) can be defined as

$$k^2 = k_x^2 + k_y^2 + k_z^2,$$

where k_i is the distance measured by the number of cells along different axes. Clearly, k_x, k_y, k_z are positive integers.

The occupancy of cells with the lifting factor E is:

$$f(E) = \lambda e^{-\frac{E}{\gamma}}.$$

Evidently, if there exists a certain level of cells' remoteness from the introduction site k, then the occupancy of cells with a definite lifting factor within the interval dk is the same, since the material concentration in a flow within the interval dk can be assumed constant.

The flow rate of particles of a certain narrow size class in the apparatus can be expressed by the dependence

$$G_i = Fv\mu_i \tag{10.7}$$

where F is the apparatus cross-section, m^2; v is particles velocity, m/s; μ_i is mass concentration of particles in a flow, kg/m^3.

If the mass of one particle is m, then the number of particles per unit volume is:

$$n_i = \frac{\mu_i}{m}.$$

Then Eq. (10.7) can be written as

$$G_i = Fvmn_i. \tag{10.8}$$

The probability for a certain particle of a narrow size class to be located among cells located within the range of k to $k + dk$ is equal to the product of the average number of these cells by the probability of the cell occupancy, that is,

$$ck^2 f(E)dk = ck^2 \lambda e^{-\frac{E}{\gamma}} dk. \tag{10.9}$$

Let $P(v)dv$ be the probability for the particle velocity to be within the interval from v to $v + dv$. This value can be found by substituting dk in (10.9) with $\left(\frac{dk}{dv}\right) \cdot dv$, that is,

$$P(v) \cdot dv = ck^2 \cdot \frac{dk}{dv} \lambda e^{-\frac{E}{\gamma}} \cdot dv.$$

According to (10.8), the magnitude $k^2 \cdot \frac{dk}{dv}$ is proportional to the velocity squared, which complies with classical notions. Therefore, we can write:

$$P(v)dv = Av^2 \lambda e^{-\frac{E}{\chi}} dv, \tag{10.10}$$

where A is a constant determined from normalization conditions.

$$\int_0^\infty P(v) \cdot dv = 1 = A \int_0^\infty \lambda v^2 e^{-\frac{E}{\chi}} dv.$$

Knowing the values of separation factors, the latter can be written as

$$\int_0^\infty P(v)dv = A \cdot \int_0^\infty e^{-\frac{w_{50}^2}{w^2}} v^2 e^{\frac{v^2}{w^2}} dv.$$

We take this integral

$$1 = A \cdot e^{\frac{w_{50}^2}{w^2}} \int_0^\infty e^{-\frac{v^2}{w^2}} v^2 dv$$

and introduce new variables:

$y^2 = \frac{v^2}{w^2}$; hence, $v^2 = y^2 w^2$.

We differentiate both parts of the latter expression:

$$2vdv = 2w^2 ydy,$$

hence,

$$dv = wdy.$$

Taking all this into account, the integral can be written as

$$1 = A \cdot we^{\frac{w_{50}^2}{w^2}} \int_{-\infty}^\infty e^{-y^2} y^2 dy = A \cdot we^{\frac{w_{50}^2}{w^2}} \cdot \frac{\sqrt{\pi}}{2}.$$

Hence

$$A = \frac{2}{w \cdot e^{\frac{w_{50}^2}{w^2}} \sqrt{\pi}},$$

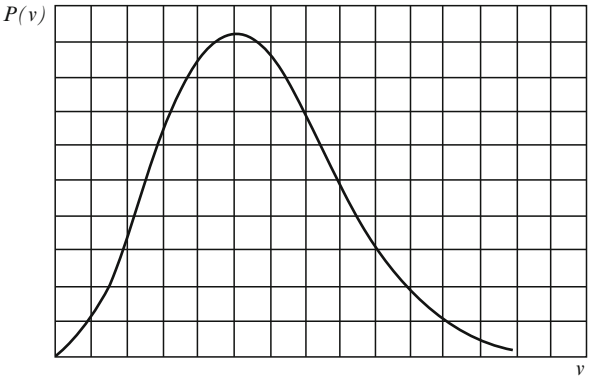

Fig. 10.3 Velocity distribution of particles

and then we obtain from (10.10):

$$P(v) = \frac{2}{\sqrt{\pi}} v^2 e^{-\frac{v^2}{w^2}}. \tag{10.11}$$

The dependence (10.11) is the probability of the velocity distribution of a narrow particle class under the conditions of separation. This function is plotted in Fig. 10.3. It follows from this figure that particles in a flow have a certain maximal velocity, and the velocities of other particles are asymmetrically distributed on both sides of the former.

10.4 Kinetic Aspect of the Material Distribution

Let us revert to the general law obtained experimentally for various designs of air and hydraulic classifiers:

$$F_f(x) = A \cdot e^{-kB} = A \cdot e^{-k\frac{gd}{w^2}\left(\frac{\rho-\rho_0}{\rho_0}\right)}, \tag{10.12}$$

This dependence, confirmed for all cases without any exception, reflects in-depth intrinsic relations characteristic of the entire class of gravitational separation processes in moving media. Apart from simplified models analyzed in the present work, gravitational separation is a mass process with the simultaneous participation of an immense number of particles of various sizes. A broad range of random factors are imposed on their opposite displacements.

In a real process, the displacement of each particle under the action of the flow and its disturbances is purely random; it is impossible to name its instantaneous

velocity magnitude or direction, which makes the general pattern of the process chaotic. However, the presence of chaos in the motion of particles does not imply the absence of general regularities in the behavior of a dispersed continuum. On the contrary, rigid intrinsic regularities can manifest themselves only through a general randomization, as it was established, for example, at the development of the kinetic theory of gases. It seems appropriate to quote a basic statement of M. Katz, "Chaos does not imply the absence of order. On the contrary, it is a rather specific property of the initial distribution that leads, in fact, to general regularities".

Therefore, when developing the kinetic theory of gases, Boltzmann obtained principal regularities confirmed by practical experience in the study of gaseous systems based on the simplest model of the process.

Apparently, this is also the reason why we obtained results allowing us to understand and explain a large number of experimental facts and regularities based on simplest models. Experimentally obtained dependence (10.12) also confirms the validity of M. Katz's statement. This dependence presented in such a form is, to some extent, analogous to the well-known equation of the distribution of uniform randomly moving particles in a force field, which is called the Laplace hypsometric distribution law. For superfine particles, this phenomenon was experimentally confirmed by Perrain (1908), and its kinetic theory was developed by Einstein and Smolukhovsky (1905–1906).

While developing the kinetic theory of gases, Boltzmann demonstrated that the distribution of ideal gas particles depending on the height or level of the potential energy also obeys the hypsometric law.

He established that the distribution of ideal gas particles in the gravity field complies with the equation

$$n = n_0 e^{-\frac{mg(n-n_0)}{kT}} = n_0 e^{-\frac{\Delta u}{kT}} \tag{10.13}$$

where $n; n_0$ are concentrations of ideal gas particles at the levels n and n_0; m is the mass of ideal gas particles; g is gravitational acceleration; k is Boltzmann's constant; T is absolute temperature; Δu is the potential energy increment at the particle transition from level n_0 to level n.

We can establish a certain physical analogy between the phenomena described by expressions (10.12) and (10.13).

First, respective parameters in these expressions have analogous meaning.

The dimensionless criterion B is a measure of the ratio of potential to kinetic energy in a flow. The exponent in Boltzmann's equation has a similar physical meaning. Its numerator is equal to the potential energy of a particle located at a certain distance from the reference level. The denominator is proportional to the temperature characterizing the kinetic energy of the system. Temperature T is a randomizing factor of the process; its value predetermines a certain specific height distribution of these particles.

In the denominator of the exponent in the expression (10.12), the respective place is occupied by $w^2\rho_0$. As established, it is a randomizing factor for the process

under study. Obviously, in both processes the effect of random parameters will grow with increasing randomizing factor.

The kinetic theory of gases is based on the idea that their molecules are solid particles. Their velocity and mean kinetic energy are determined by the energy impact – temperature, while the distribution character – by the mechanical interaction of particles. According to Boltzmann's law, at a constant temperature, particle concentration increases with decreasing potential energy of their position.

It is known that the potential energy minimum corresponds to the steadiest position of a mechanical system. Therefore, gas particles concentration is maximal in the steadiest position. It is a potential position for all particles in the absence of factors disturbing, or randomizing, the distribution. It follows from (10.13) that at $T = 0$ all the particles are located at the level n_0. At high magnitudes of the randomizing factor ($T \to \infty$), particle concentration is equalized in height. As shown by Boltzmann, this law remains valid not only for uniform fields, but also for gas particles distribution in any nonuniform force field. Many physical phenomena occurring in disperse materials correspond to this distribution.

We can find some analogies in the distributions of the processes compared. In the case of gravitational separation, solid particles move at the expense of external energy carried by the flow. A permanent effect of the gravity force field and various disturbing factors are superimposed on this process. Flow velocity change from zero to high values affects separation results similarly to the effect of temperature change on the distribution of gas particles.

In the theory of gases, special attention is usually attracted by the fact that any distribution of particles is formed with respect to a certain mechanically steady position.

In the case of separation, steady position of particles of a narrow size class corresponds to a certain velocity of their motion in a flow ensuring their steady position. As demonstrated above, each size class in a flow is characterized by a certain velocity distribution with a characteristic mathematical expectation of this distribution. The magnitude of mathematical expectation of the velocity corresponds to steady motion of particles of a specific class.

The behavior of a totality of identical particles in a flow is determined by the tendency of each of them to acquire a steady velocity.

However, the difference between a real process and an ideal one leads to a certain probabilistic distribution of particles velocities with respect to its relatively steady value. It means that the more particles velocities differ from the equilibrium one, the lesser is the number of particles having such velocities, and vice versa. In contrast to the Boltzmann law, this distribution has a positive probability density on both sides of the steady velocity.

For a multi-fraction mixture, the velocity distribution of particles has the same character as that of each separate fraction. Particles of each fraction have their steady velocity. The velocities of all the particles of this class are distributed with respect to this steady velocity due to the presence of some random factors. Distributions of different classes are superimposed, which predetermines a final result different from the ideal one.

This analysis clearly leads to the idea of a dominant tendency of polyfractional mixture behavior in a moving flow. Since particles tend to acquire a steady velocity, the tendency of this process consists in a probabilistic stratification of particles with respect to their steady velocities or sizes.

If steady velocities of particles of different size classes in a flow acquire different directions, such a flow ensures a separation process.

If, however, all steady velocities acquire the same direction, such flows ensure transport regimes.

If a set of particles with different aerodynamic characteristics is placed into an ascending flow, at the initial moment the number of particles with a tendency to an opposite motion is maximal in the volume they occupy. After a certain time period, the volume occupied by the particles in a flow starts increasing due to a directed motion to both sides from the input point. In the course of this motion, they tend to acquire their steady velocity, being hindered by random factors leading to a probabilistic distribution of particles velocities with respect to this velocity.

The idea of stratification is not purely abstract. The parameters of this phenomenon determine principal results of separation.

The conclusion that the gravitational separation process is based on statistical stratification of material mixture by steady velocity values or by sizes obtained from theoretical analysis is remarkable because it is confirmed by experimental data.

As for gravitational separation in an ascending flow, it makes sense to consider only stratification by steady motion velocity values or by sizes. The character of the obtained experimental curves can be explained completely enough from the standpoint of stratification as the basis of the gravitational separation process.

In the absence of ventilation, all the material entering the classifier falls into coarse product. There is no stratification in this case, and the efficiency of such process is zero.

With growing flow velocity, the velocity of steady downward motion for particles of different sizes decreases, although it acquires an individual value for each class.

This leads to an increased time of their stay in the apparatus, which may explain the increase in the separation effect in a given range of flow velocity growth.

The maximal time of the stay of particles of a certain size in the apparatus, apparently, corresponds to the velocity of the medium at which the steady motion velocity is zero. Such flow velocity is called hovering velocity; it corresponds to the optimal efficiency value in a hollow channel.

With further increase in the flow velocity, particles of boundary size start moving upwards. It leads to a decreasing time of their stay in the apparatus, and the effect starts decreasing. Clearly, the separation optimum for fine particles corresponds to low flow rates. With increasing boundary size of the separation, the optimums are shifted towards the region of elevated velocities.

An increase in the optimal efficiency in a cascade apparatus at multiple flow disturbances can be attributed to the exponential character of stratification. Although the separation effect in one stage of a cascade can be moderate, a

summation of several exponents over all the stages gives a greater effect than one exponent in a hollow apparatus.

Thus, the idea of stratification as the basis of gravitational separation mechanism makes it possible to cover with a unified idea both generally accepted theoretical notions and ideas arising on the basis of the realization of novel principles of the process organization, and to eliminate contradictions between them.

Chapter 11
Critical Regimes of Two-Phase Flows in Complicated Systems

Abstract Constantly growing industrial requirements to the quality of powdered materials lead to the development of complicated separation systems. Models of duplex cascade, cascades with material feed to different separation stages are developed and solved, which makes it possible to control the quality of powdered materials. A system of combined cascades is developed, and their internal bonds are analyzed. A quality criterion for separation processes estimation and optimization in combined cascades is developed. Fractal principle of constructing schemes of combined cascades is developed, and their potential is analyzed. The adequacy of mathematical models of duplex and combined cascades is experimentally confirmed.

Keywords Cascade · Duplex · Combined cascade · Cascade efficiency · Mathematical model · Markov's chains · Matrix · Section · Apparatus · Working diagram · Connection function · Adequacy · Direct schemes · Reversed schemes

11.1 Problem Setting

The development of the theory of critical regimes of two-phase flows involves the development of theoretical models aimed, in general, at:

1. Physical understanding and mathematical description of the process
2. Revealing quantitative relations between various factors of the process, which ensures the prediction of its results

The latter is of great practical importance, especially for fractionating processes.

For many years, classification of pourable materials had been carried out in hollow channels. However, the efficiency of the process remained rather low. Even a considerable extension of the channels did not essentially improve the quality of

E. Barsky, *Critical Regimes of Two-Phase Flows with a Polydisperse Solid Phase*, Fluid Mechanics and Its Applications 93,
DOI 10.1007/978-90-481-8838-3_11,

the obtained products. Great progress was achieved in the separation technique due to the development and substantiation of the cascade principle of the separation process in critical regimes of two-phase flows. Such apparatuses allowed considerable improvement in the quality of final products due to the change in the number of stages and variation of the place of material feed into the apparatus.

In the model of a regular cascade consisting of identical stages, it is assumed that the distribution coefficient for a narrow class k is the same in all stages. This assumption is based on experimentally established facts:

1. Fractional separation invariance with respect to initial material composition
2. Existence of a self-similarity region with respect to concentration

The developed mathematical model of a regular cascade establishes the dependence of fractional separation in the apparatus on the number of its stages z, place of material feed i and distribution coefficient of a narrow size class k in the form of (7.3).

This model is of great practical importance. It allows the choice of the necessary number of stages and place of the initial material feed into the cascade when solving a specific production problem. Besides, this model allows grounding the choice of the stage design. Numerous experimental checks of the model have demonstrated its adequacy.

The study of regular separation cascades has shown that the effect of increased number of stages is markedly exponential.

Separation efficiency growth practically reaches its limit at eight to nine stages, and further addition of stages does not increase appreciably the separation effect.

Therefore, further improvement of separation apparatuses consists in the development of complex stages and creation of combined systems of $n(z_i)$ type. In the general case, a combined cascade consists of n separation cascades, each of them comprising z_i separating elements working in different regimes.

11.2 Mathematical Model of a Duplex Cascade

A complicated regular cascade built by successive connection of pairwise-similar sections can be called a duplex cascade. Its paired sections have distribution coefficients k_1 and k_2. A schematic diagram of such a cascade is shown in Fig. 11.1. A duplex cascade is considered complete if the number of elements with k_1 equals the number of elements with k_2, since z is an even number. We consider a narrow size class, whose initial quantity is normalized to a unity. We denote a flow of particles of this class through a certain stage by R_i, where i is the stage number counting top-down.

Thus, the amount of material coming out upwards from each odd section is $k_i R_i$, and downwards $-(1-k_1)R_i$. For an even section, the respective amounts are $R_i k_2$ (upwards) and $(1-k_2)R_i$ (downwards).

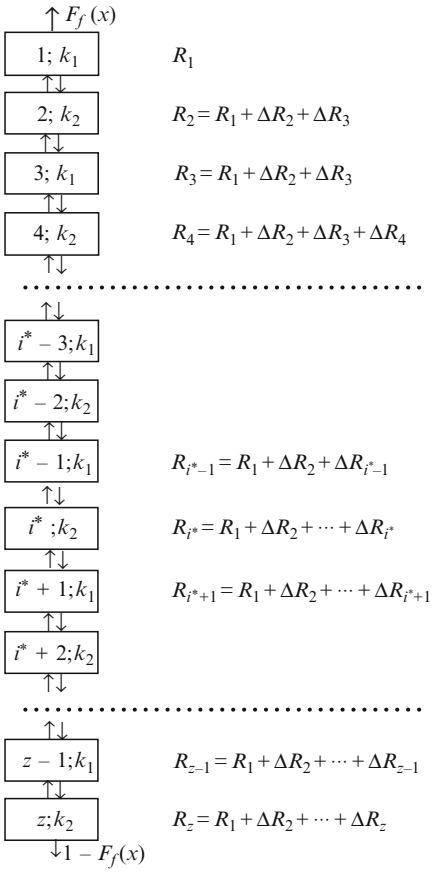

Fig. 11.1 Basic circuit of a duplex cascade

In a stationary process, material balance should be conserved in each section and in the entire apparatus. Taking into account the fact that the amount

$$R_{i-1}(1 - k_1) + R_{i+1}k_1,$$

arrives at the ith stage, and the amount

$$R_i k_2 + R_i(1 - k_2),$$

leaves it, the balance for the section can be written as

$$R_{i-1}(1 - k_1) + R_{i+1}k_1 = R_i k_2 + R_i(1 - k_2)$$

The total balance for the apparatus can be written as

$$R_1 k_1 + R_z(1 - k_2) = 1$$

Proceeding from the relationships

$$\sigma_1 = \frac{1 - k_1}{k_1};\ \sigma_2 = \frac{1 - k_2}{k_2},$$

we can write:

$$R_1 \cdot \frac{1}{1 + \sigma_1} + \frac{\sigma_2}{1 + \sigma_2} \cdot R_z = 1$$

Extreme values acquire the form:

$$R_1 = \frac{1}{\sigma_2} \Delta R_2$$

$$R_z = -\Delta R_z \sigma_1$$

Mathematical balance by sections gives the following:

$$R_1 = \frac{1}{\sigma_2} \Delta R_2$$

$$\Delta R_2 = \frac{1}{\sigma_1} \Delta R_3$$

$$\Delta R_3 = \frac{1}{\sigma_2} \Delta R_4$$

. . . . . .

. . . . . .

$$\Delta R_{i-1} = \frac{1}{\sigma_2} (\Delta R_i + 1)$$

$$\Delta R_i = \frac{1}{\sigma_1} (\Delta R_{i+1})$$

$$\Delta R_{i+1} = \frac{1}{\sigma_2} (\Delta R_{i+2} + 1)$$

. . . . . .

. . . . . .

$$\Delta R_{z-1} = \frac{1}{\sigma_2} \Delta R_z$$

and we can consecutively derive the following:

$$R_1 = \frac{1}{\sigma_2}\Delta R_2$$

$$R_1 = \frac{1}{\sigma_1\sigma_2}\Delta R_3$$

$$R_1 = \frac{1}{\sigma_1\sigma_2^2}\Delta R_4$$

$$R_1 = \frac{1}{\sigma_1^2\sigma_2^2}\Delta R_5$$

. . . . . .

. . . . . .

$$R_1 = \frac{1}{\sigma_1^{i/2-1}\sigma_2^{i/2}}(\Delta R_{i^*} + 1)$$

$$R_1 = \frac{1}{\sigma_1^{i/2}\sigma_2^{i/2}}\Delta R_{i^*+1} + \frac{1}{\sigma_1^{i/2-1}\sigma_2^{i/2}}$$

$$R_1 = \frac{1}{\sigma_1^{i/2}\sigma_2^{i/2+1}}\Delta R_{i^*+2} + \frac{1+\sigma_1}{\sigma_1^{i/2}\sigma_2^{i/2}}$$

. . . . . .

. . . . . .

$$R_1 = \frac{1}{\sigma_1^{z/2} - 1\sigma_2^{z/2}}\Delta R_{z-1} + \frac{1+\sigma_1}{\sigma_1{}^{i/2}\sigma_2^{i/2}}$$

Hence, we obtain a system:

$$\begin{cases} R_1 = -\frac{1}{(\sigma_1\sigma_2)^{z/2}}R_z + \frac{1+\sigma_1}{(\sigma_1\sigma_2)^{z/2}} \\ R_1\frac{1}{1-\sigma_1} + \frac{\sigma_2}{1+\sigma_2}R_z = 1 \end{cases}$$

Solving this system with respect to

$$F_f(x) = R_1 \frac{1}{1-\sigma_1},$$

we obtain

$$F_f(x) = \frac{1 - \frac{1-\sigma_2}{\sigma_1}(\sigma_1\sigma_2)^{\frac{z-i^*}{2}}}{1 - \frac{1-\sigma_2}{\sigma_1}(\sigma_1\sigma_2)^{z/2}} \tag{11.1}$$

We finally obtain

$$F_f(x) = \frac{1 - \frac{1-k}{k_1}(\sigma_1\sigma_2)^{\frac{z-i^*}{2}}}{1 - \frac{1-k_2}{k_1}(\sigma_1\sigma_2)^{z/2}} \tag{11.2}$$

At $k_1 = k_2$ this formula becomes a dependence for a regular cascade. Eq. (11.2) is valid at even z and i. At an odd i, the formula acquires the form:

$$F_f(x) = \frac{1 - (\sigma_1\sigma_2)^{\frac{z-i^*+1}{2}}}{1 - (\sigma_1\sigma_2)^{z/2}\frac{1-k_1}{k_2}}$$

11.3 Mathematical Model of a Cascade Process Allowing Control of the Effect of the Material Feed Site on Separation Results

Figure 7.1 shows a way of redistribution of a narrow size class with the distribution coefficient k in a cascade apparatus. The process under study is similar to a random up and down wandering, with a transition upwards with the probability k and downwards with the probability $1 - k$, and two absorbing states. Hence, the redistribution of particles of a fixed class in an apparatus consisting of z stages can be represented by a Markov absorbing circuit with a transfer matrix of the following form:

$$\begin{vmatrix}
1 & 0 & 0 & 0 & 0 & 0 & \dots & 0 \\
k & 0 & 1-k & 0 & 0 & 0 & \dots & 0 \\
0 & k & 0 & 1-k & 0 & 0 & \dots & 0 \\
\cdot & \cdot & \cdot & \cdot & \cdot & \cdot & \cdot & \cdot \\
\cdot & \cdot & \cdot & \cdot & \cdot & \cdot & \cdot & \cdot \\
0 & 0 & \dots & 0 & k & 0 & 1-k & 0 \\
0 & 0 & \dots & 0 & 0 & 0 & 0 & 1-k \\
0 & 0 & 0 & 0 & 0 & 0 & 0 & 1
\end{vmatrix}$$

This matrix has $z+2$ lines and columns, with the first and last states being outputs into the coarse and fine products, and the rest of the states refer to the probabilities of particles transitions between the apparatus stages.

Let us transform this matrix into an easier-to-use canonic form by combining all ergodic (absorbing) states into one group, and all non-recurrent states into another. There are z non-recurrent states corresponding to the number of the apparatus stages, and two ergodic states corresponding to the coarse and fine products. Then the canonic form is as follows:

$$
\begin{array}{c|cc|cccccc|c}
 & \downarrow I & & & & & & \downarrow O & & \\
 & 1 & 0 & 0 & 0 & . & . & \ldots & 0 & 0 & \\
 & 0 & 1 & 0 & 0 & . & . & \ldots & 0 & 0 & \\
 & k & 0 & 0 & 1-k & 0 & . & . & \ldots & 0 & \\
 & 0 & 0 & k & 0 & 1-k & 0 & . & \ldots & 0 & \\
 & 0 & 0 & 0 & k & 0 & 1-k & 0 & \ldots & 0 & \\
\underset{\rightarrow}{R} & . \quad . & . & . \quad . & . & . & . & . & . & . & \underset{\leftarrow}{Q} \\
 & 0 & 0 & 0 & \ldots & 0 & k & 0 & 1-k & 0 & \\
 & 0 & 0 & 0 & 0 & \ldots & 0 & k & 0 & 1-k & \\
 & 0 & 1-k & 0 & 0 & 0 & \ldots & 0 & k & 0 &
\end{array}
$$

Here the region O totally consists of zeros; the submatrix Q (with the dimension $z \times 2$) describes the particle behavior before leaving the apparatus (from the set of non-recurrent states); the submatrix R with the dimension $z \times 2$ corresponds to the transitions from the apparatus into coarse and fine products (from non-recurrent into ergodic state); and the submatrix S (with the dimension $z \times 2$) refers to the process following the particle discharge from the apparatus (after the particle has reached the ergodic state). The probability of reaching one of such states in an absorbing circuit tends to 1. It means that sooner or later, a particle reaches a certain absorbing state, i.e. comes out into one of two separation products, with the probability of 1.

For any absorbing circuit, Q^n tends to zero, and $I-Q$ is reversible, wherein $(I-Q)^{-1} = \sum_{k=0}^{\infty} Q^k$.

For a Markov absorbing circuit, the matrix $N = (I-Q)^{-1}$ is called fundamental.

We denote by n_j a function equal to the total number of redistribution acts with the particle staying in the stage j, i.e. in a non-recurrent state j. Then we can assert that the mathematical expectation of the fact that a particle located at the initial moment of time at stage i will be located at stage j after n_j redistribution acts represents the ij coordinate of the matrix N, i.e.

$$\{E_i(n_j)\} = N \tag{11.3}$$

Hence, the average time of a particle stay at a specified stage is always finite, and these average times constitute the matrix N.

Each particle gets into the apparatus through the stage i^*, and using Eq. (11.3), we can calculate the time spent by the particle at each stage.

We introduce the following notations:

$$N_2 = N(2N_{dg} - I) - N_{sq}$$

is a matrix of $z \times z$ dimensions, where N_{dg} corresponds to a matrix whose diagonal equals that of the matrix N, and the rest of the elements are zero; N_{sq} corresponds to a matrix whose elements are squared elements of the matrix N. Evidently, in the general case $A^2 \neq A_{sq}$ for any matrix A, and an equality is valid for diagonal matrices only.

$B = NR$ is a matrix with the dimensions $z \times 2$.

$$\tau = N\xi$$

where ξ is a vector column with all the elements equal to 1;

$$\tau_2 = (2N - I)\tau - \tau_{sq}$$

We can assert that, in absorbing Markov chains, the dispersion of the fact that a particle located at the initial moment of time at stage i will get to stage j after n_j redistribution acts, is ij coordinate of the matrix N_2, i.e.,

$$\{D_i(n_j)\} = N_2 \tag{11.4}$$

Let the function T be equal to the total time (number of redistribution acts including the initial position) that a particle spends in the apparatus before leaving it. The magnitude T shows how many steps are necessary for a Markov process to get into an ergodic set.

If at the initial moment of time a particle is at stage i, the mathematical expectation of the number of redistribution acts until the particle goes out into the coarse or fine product is the ith coordinate of the vector τ, and the dispersion of the former is the ith coordinate of the vector τ_2, i.e.,

$$\{E_i(\mathrm{T})\} = \tau$$

$$\{D_i(\mathrm{T})\} = \tau_2$$

In the process of separation, a particle is introduced into the apparatus through the stage i^*, and, consequently, we can determine the average time (the number of redistribution acts) of the particle stay in the apparatus and deviations from this time.

Let b_{ij} be the probability for the particle located in stage i to get into a coarse or a fine product ($j = 1$ for fine product and $j = 2$ for coarse product). Then

$$\{b_{ij}\} = B = NR$$

b_{ij} is the fractional separation at the introduction of the size class under study to the stage i. Hence, it is possible to control the probability of a particle output into the required product by changing the place of its input into the apparatus.

11.4 Cascade Model with Two or More Material Inputs into the Apparatus

As follows from the previous section, the position of the material input into the apparatus can affect the quality of the obtained products. Therefore, it is of interest to analyze the results of cascade separation in case of two or more inputs of the initial material. Let us examine a regular cascade consisting of z identical sections. Let the material be fed into two sections. The amount of the material fed into section i^* is equal to a, and that of the material fed to section j^* – to b. We assume that $a + b = 1$ (Fig. 11.2). Then, by analogy with previous cases, under the condition $\sigma_1 = \sigma_2$, we obtain:

$$R_1 + \sigma R_z = 1 + \sigma$$

$$R_1 = \frac{1}{\sigma}\Delta R_2$$

$$R_z = -\sigma \Delta R_z$$

For the vicinity of the material input:

$$R_{i^*-1} = \frac{1}{\sigma}(\Delta R_i + a)$$

$$R_{i^*} = \frac{1}{\sigma}\Delta R_{i^*+1}$$

$$R_{i^*+1} = \frac{1}{\sigma}\Delta R_{i^*+2} + a$$

. . . . . .

. . . . . .

$$R_{j^*-1} = \frac{1}{\sigma}(\Delta R_{j^*} + b)$$

$$R_{j^*} = \frac{1}{\sigma}\Delta R_{j^*+1}$$

$$R_{j^*+1} = \frac{1}{\sigma}\Delta R_{j^*+1} + b$$

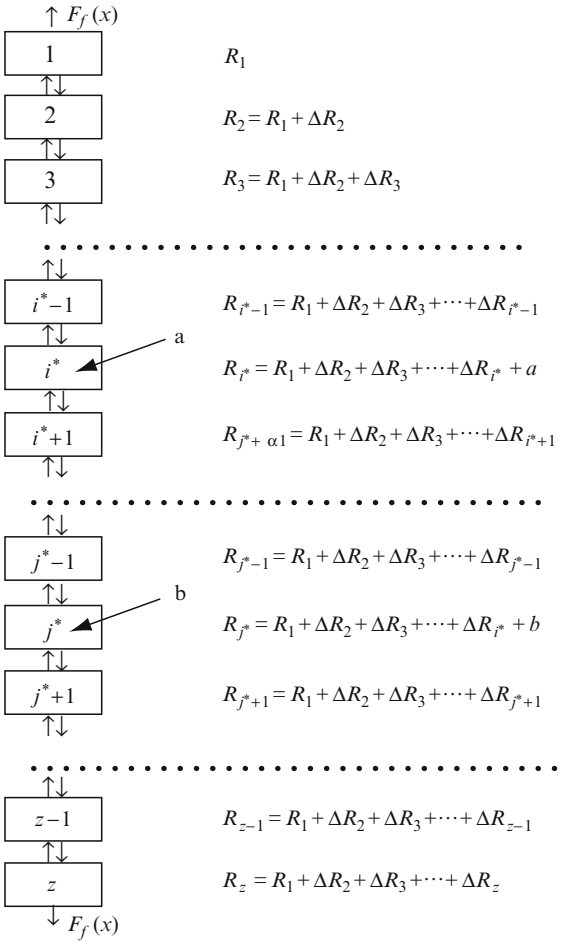

Fig. 11.2 Basic circuit of a cascade with two material inputs

Hence, we obtain

$$R_1 = \frac{1}{\sigma^{i^*+1}} \Delta R_{i^*+2} + \frac{a(1+\sigma)}{\sigma^{i^*}}$$

$$R_1 = \frac{1}{\sigma^{j^*+1}} \Delta R_{j^*+2} + \frac{b(1+\sigma)}{\sigma^{j^*}}$$

Further we obtain

$$R_1 = \frac{1}{\sigma^{z-1}} \Delta R_z + \frac{(1+\sigma)(b + a\sigma^{j^*-i^*})}{\sigma^{j^*}}$$

Taking into account all stated above, we can write:

$$\begin{cases} R_1 = -\frac{1}{\sigma^z} R_z + \frac{(1+\sigma)(b+a\sigma^{j^*-i^*})}{\sigma^{j^*}} \\ R_1 + \sigma R_z = 1 + \sigma \end{cases}$$

It follows from the latter system:

$$F_f(x) = \frac{1 - a\sigma^{z+1-i^*} - b\sigma^{z+1-j^*}}{1 - \sigma^{z+1}}$$

If we assume that either a or b in this equation are zero, we obtain a dependence for one input of the material. Similarly, for three and more inputs, this equation acquires the form

$$F_f(x) = \frac{1 - a\sigma^{z+1-i^*} - b\sigma^{z+1-j^*} - c\sigma^{z+1-e^*}}{1 - \sigma^{z+1}} \tag{11.5}$$

under the condition that $a + b + c = 1$.

11.5 Combined Cascade Classifiers

11.5.1 Combined Cascades of $n(z)$ Type

The simplest embodiment of a combined cascade of $n(z)$ type comprises n identical separating cascades of the first order consisting of the same number of stages z with a fixed site of the initial material feed into one of the apparatuses, with all the apparatuses working in the same regime. Examples of various combined apparatuses are shown in Fig. 11.3.

Even in this extremely simplified case, such a combined separator can have many structural schemes of connection between its elements. As experiments have demonstrated, some of these schemes realize a higher order of the process organization in comparison with the separating cascade of the first order. They are not equivalent to a simple increase in the number of elements in a cascade apparatus.

To avoid further misunderstandings, it is expedient to define the following notions:

- Free output – a free local flow coming out into a combined fine or coarse product from an individual column
- Connection – a constrained local output from one column to another
- Structural scheme – a scheme of outputs, inputs and connections between individual separating elements in a combined cascade

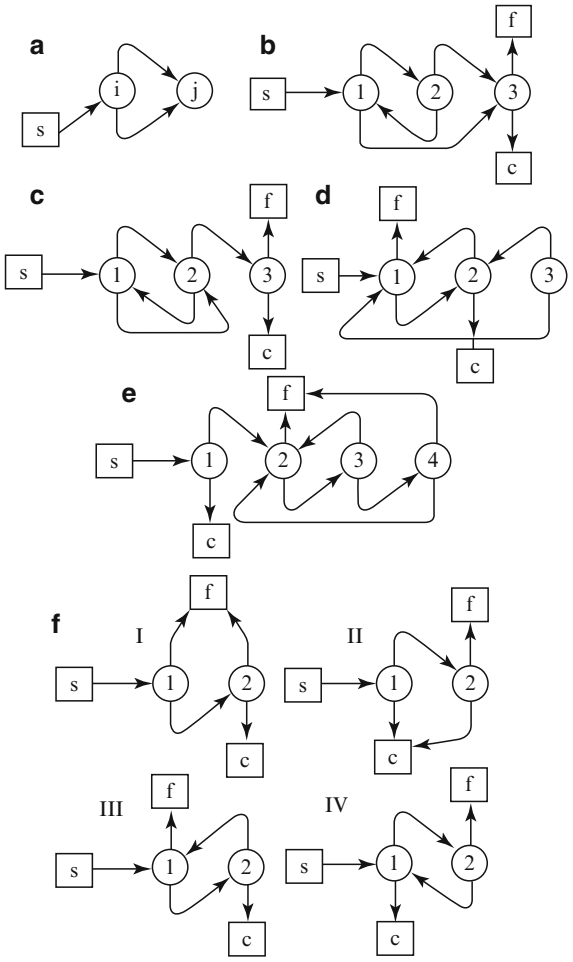

Fig. 11.3 Examples of various structural schemes of combined cascades: (**a**–**d**) defective schemes; (**e**) transporting scheme; (**f**) four working versions of a two-element combined cascade; s – initial material; f – fine product; c – coarse product

– Isomorphic schemes – schemes having the same connection functions
– Inverted schemes – schemes made up from given ones by rearranging some of the columns with unchanged former outputs and connections; apparently, inverted schemes are isomorphic

F_0 is fractional extraction of fine product in an individual column.

F is fractional extraction into the fine product for the entire combined cascade.

$F(F_0)$ is the connection function corresponding to each specific structural scheme.

– Reversed scheme – a scheme where all outputs and connections related to the fine product become identical to outputs and connections related to the coarse

product, and vice versa. The connection function for a reversed scheme is $F^{-1}(F_0)$. Apparently, for a reversed scheme, the connection function related to the coarse product is identical to the function $F(F_0)$ with the argument F_0 substituted with $(1 - F_0)$, i.e.

$$F_c^{-1}(F_0) = F(F_0 \Rightarrow 1 - F_0),$$

where F_c is defined;

- Working schemes – operable schemes for a combined cascade (Fig. 11.3f).
- Defective schemes – schemes with some elements excluded from the process (Fig. 11.3a–c), or with some elements having no active connections with other elements (Fig. 11.3d), or else with some elements functioning as conveyers (Fig. 11.3e). There can be schemes with several defects listed above at the same time.

11.5.2 Working Schemes for Combined Cascades of $n(z)$ Type

We examine all possible options of working schemes, since only their complete analysis makes it possible to find the most advanced ones.

In the case of n elements in a combined cascade, the total number of free outputs and connections is $2n$. The minimal number of free outputs is

$$P_{\min} = 2$$

Hence, the maximal possible number of connections between n elements is

$$S_{\max} = 2n - 2$$

The minimal number of connections is

$$S_{\min} = n - 1$$

Taking this into account, the maximal number of outputs is

$$P_{\max} = n + 1$$

If the number of free outputs in a combined scheme is P, then the number of connections among n elements is

$$S = 2n - P \tag{11.6}$$

In a general case, the number of schemes equals the number of possible ways of organizing S connections. For any column, any connection can be organized with any of the remaining $(n-1)$ columns. Since there are S connections with $(n-1)$ directions each, the number of different schemes amounts to

$$N_P = (n-1)^S \tag{11.7}$$

Taking (11.6) into account, we can write:

$$N_P = (n-1)^{2n-P} \tag{11.8}$$

In a general case, we can obtain the total number of all kinds of non-isomorphic schemes including direct, inverted, reversed ones and all kinds of defective schemes.

$$N_{\sum} = \sum_{P=2}^{n+1} \left[(n-1)^{2n-P} \sum_{m=1}^{P-1} \left(c_n^m c_n^{P-m} \right) \right] \tag{11.9}$$

where $c_n^m = \frac{n!}{m!(n-m)!}$ is the number of combinations of n elements m at a time (the meaning of m being the number of free outputs into the fine product).

It is noteworthy that the number of schemes determined by Eq. (11.9) greatly exceeds the number of operating schemes. For example, at $n = 2$, according to (11.9)

$$N_{\sum} = 8,$$

while the number of operating schemes is only

$$N_d = 4.$$

For $n = 3$, respectively,

$$N_{\sum} = 348;\ N_d = 47$$

and for $n = 4$

$$N_{\sum} = 30348;\ N_d = 904$$

Structural schemes of all operating options for $n = 2$ are presented in Fig. 11.3f.

11.5.3 Connection Functions for Combined Cascades

The connection function for a combined separator constitutes an equation of the type

$$F = F(F_0)$$

where F is the fine product extraction in the entire apparatus, and F_0 is the fine product extraction in one element of a combined cascade.

First, we examine the simplest case of the apparatus $z \times 2$ under the condition that both elements are identical regular cascades of the first order.

Figure 11.3f shows all the four possible schemes of this apparatus. It is noteworthy that the schemes I and II are reversed with respect to each other, and so are the schemes III and IV. For scheme I,

$$F_1 = F_0,\ F_2 = (1 - F_0)F_0$$

In this case, the connection function is

$$F(F_0) = F_1 + F_2 = F_0 + (1 - F_0)F_0 = 1 - (1 - F_0)^2$$

For the reversed scheme II, the connection function can be written as

$$F(F_0) = F_0^2$$

For the scheme III, the total output of fine material can be written in the form of an infinite series

$$F(F_0) = F_0 + F_0^2(1 - F_0)^2 + F_0^3(1 - F_0)^2 + \cdots + F_0^n(1 - F_0)^{n-1}$$

Here we obtain a geometrical progression with the sum

$$F(F_0) = \frac{F_0^n(1 - F_0)^{n-1}F_0(1 - F_0) - F_0}{F_0(1 - F_0) - 1}$$

The first term in the nominator of this expression tends to zero, since $F_0(1 - F_0) \leqslant 0.25$.

Hence,

$$F(F_0) = \frac{F_0}{1 - F_0 + F_0^2}$$

On the basis of similar considerations, we can obtain the following for the reversed scheme IV:

$$F(F_0) = \frac{F_0^2}{1 - F_0 + F_0^2}$$

Here we have found expressions for the simplest case. However, it is difficult to obtain a general expression for more complicated schemes using this method.

Therefore, we revert to another method of formalization of combined cascades. It has turned out that a combined cascade of any complexity consisting of n independent elements can be represented by a square matrix $n \times n$.

Figure 11.4 shows a combined cascade separator consisting of three elements. Its connection function determined by lengthy calculations using the previously used method is:

$$F(F_0) = \frac{F_0^3 - F_0^2 + F_0}{F_0^3 - F_0 + 1}$$

We represent this scheme in the form of a connection matrix:

$\frac{j}{i}$	1	2	3
1	F_0	$1 - F_0$	0
2	0	$1 - F_0$	F_0
3	F_0	$1 - F_0$	0

Matrix element a_{ij} at $i \neq j$ denotes the ingress from the ith apparatus to the input of the jth apparatus. Diagonal elements a_{ii} denote outputs from the entire facility.

The jth column represents inputs from all the apparatuses.

The ith line represents the output from the ith apparatus to all the rest.

Such presentation of a combined cascade makes it possible not only to describe any combined facility, but also to map out a large number of inoperable schemes, because such a matrix should possess the following properties:

1. Matrix element a_{ij} can acquire one of the following four values: 0; F_0; $1 - F_0$; 1
2. $\sum_{i-1}^{n} (a_{ij} - a_{ii}) \neq 0 \quad j \geqslant 2$

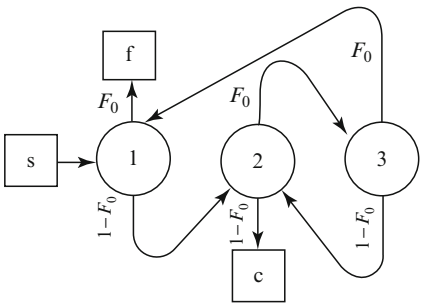

Fig. 11.4 Schematic diagram of connections of a three-element combined cascade

It means that something should be necessarily fed into each apparatus excluding the first one (into which the initial material taken as a unity is fed).

3. $\sum_{j=1}^{n} a_{ij} = 1$

Each apparatus has an output of both fine (F_0), and coarse $(1 - F_0)$ products.

4. $\sum_{i=1}^{n} a_{ii} \neq 0$

A combined facility should necessarily have an output. Among the elements $a_{ii}(i = 1, 2, 3, \ldots, n)$, there should be simultaneously F_0 and $(1 - F_0)$ or 1, since the material is not accumulated in the apparatus.

It is noteworthy that such a matrix is functional because F_0 is a function of the sizes and velocities of particles, place of material feeding into the apparatus, etc. For instance, if all the three elements of a combined cascade are different or operate in different regimes (Fig. 11.3b), such a non-uniform cascade is also described by a similar matrix. Here all ith elements acquire a respective index:

$$\begin{pmatrix} F_1 & 1 - F_1 & 0 \\ 0 & 1 - F_2 & F_2 \\ F_3 & 1 - F_3 & 0 \end{pmatrix} = A \tag{11.10}$$

Such a form of presentation allows us to derive the connection function $F(F_i)$ and find simple algorithms for the enumeration and analysis of n-unit cascades in a general case. Thus, if we denote a matrix representing a specific combined cascade with A, its connection function can be written as

$$A^{T^*} \times \begin{pmatrix} r_1 \\ r_2 \\ r_3 \\ \vdots \\ r_n \end{pmatrix} = \begin{pmatrix} -1 \\ 0 \\ 0 \\ \vdots \\ 0 \end{pmatrix} \tag{11.11}$$

where A^{T^*} is a matrix obtained from A by transposition and substitution of all elements a_{ii} with (-1);

$r_1, r_2, r_3, \ldots, r_n$ is the flow of material through a corresponding element (initial content of each element). Thus, for the matrix (11.10) we can write:

$$A^{T^*} = \begin{pmatrix} -1 & 0 & F_0 \\ 1 - F_0 & -1 & 1 - F_0 \\ 0 & F_0 & -1 \end{pmatrix} \tag{11.12}$$

It follows from (11.11) that the connection function is based on the balance of material flows. It is known that

$$F_{f_i} = \frac{r_{f_i}}{r_i}$$

where F_{fi} is the narrow class extraction into the fine product in the ith element of a combined cascade.

r_{fi} is the amount of the narrow class extracted into the fine product.

r_i is the initial amount of this class in the ith element.

Taking this into account, we can write

$$\begin{aligned} r_{f_1} &= F_1 r_1 \\ r_{f_2} &= F_2 r_2 \\ &\vdots \\ r_{f_n} &= F_n r_n \end{aligned}$$

It follows from balance conditions that

$$\begin{aligned} r_1 &= 1 + a_{r1} r_2 + a_{31} r_3 + \cdots + a_{n1} r_n \\ r_2 &= a_{12} r_1 + a_{32} r_3 + \cdots + a_{n2} r_n \\ &\cdots\cdots\cdots\cdots\cdots\cdots\cdots\cdots\cdots\cdots \\ r_n &= a_{1n} r_1 + a_{2n} r_2 + \cdots + a_{n-1} r_{n-1} \end{aligned} \tag{11.13}$$

In the general case, the connection equation is written as

$$\begin{pmatrix} -1 & a_{21} & a_{31} \ldots a_{n1} \\ a_{12} & -1 & a_{32} \ldots a_{n2} \\ \ldots & \ldots \quad \ldots & \ldots \quad \cdots \\ a_{1n} & a_{2n} & a_{3n} \ldots -1 \end{pmatrix} \begin{pmatrix} r_1 \\ r_2 \\ \vdots \\ r_n \end{pmatrix} = \begin{pmatrix} -1 \\ 0 \\ \vdots \\ 0 \end{pmatrix} \tag{11.14}$$

In a particular case, we can write for an arbitrary three-element cascade:

$$\begin{aligned} -r_1 + a_{21} r_2 + a_{31} r_3 &= -1 \\ a_{12} r_1 - r_2 + a_{32} r_3 &= 0 \\ a_{13} r_1 + a_{23} r_2 - 1 &= 0 \end{aligned}$$

Taking this into account, the matrix form of the coupling equation is:

$$\begin{pmatrix} -1 & a_{21} & a_{31} \\ a_{12} & -1 & a_{32} \\ a_{13} & a_{23} & -1 \end{pmatrix} \begin{pmatrix} r_1 \\ r_2 \\ r_3 \end{pmatrix} = \begin{pmatrix} -1 \\ 0 \\ 0 \end{pmatrix} \tag{11.15}$$

The left-hand side of Eq. (11.15) is a product of a matrix reflecting a concrete scheme of a combined cascade by the vector of material flow through individual elements of the apparatus. The right-hand side of Eq. (11.15) is the vector of material feed into the apparatus. If the material is fed into each element of a combined cascade by portions a, b, c, then, assuming that their sum equals unity, we rewrite the right-hand side of Eq. (11.15) as follows:

$$\begin{pmatrix} -a \\ -b \\ -c \end{pmatrix}$$

The connection equation allows us to compute material flows $r_1, r_2, r_3, \ldots, r_n$ through all the elements of the combined cascade, as well as to determine the connection function $F(F_0)$.

Material flows are obtained by solving the connection equation, and the connection function is determined using the equation

$$F(F_0) = \sum_{i=1}^{n} r_i \Delta_i \tag{11.16}$$

$$\Delta_i = \begin{cases} F_0 & a_{ii} = F_0 \quad a_{ii} = 1; \\ 0 & a_{ii} = 1 - F_0 \quad a_{ii} = 0. \end{cases}$$

Thus, for the scheme shown in Fig. 11.3 we can write

$$F(F_0) = F_0 r_1$$

Solving the matrix equation, we obtain

$$r_1 = \frac{1 - F_0 + F_0^2}{1 - F_0 + F_0^3}$$

Hence,

$$F(F_0) = \frac{F - F_0^2 + F_0^3}{1 - F_0 + F_0^3},$$

which corresponds to the connection function for this scheme of the combined cascade obtained using a more complicated method.

For the general case of n-element combined cascade, the matrix equation acquires the form

$$\begin{pmatrix} -1 & & a_{21} & & a_{31} \ldots a_{n1} \\ a_{12} & & -1 & & a_{32 \ldots a_{n2}} \\ \ldots & \ldots & \cdots & \ldots & \ldots \\ \ldots & \ldots & \ldots & \ldots & \ldots \\ a_{n1} & & a_{2n} & & a_{3n} \ldots - 1 \end{pmatrix} \begin{pmatrix} r_1 \\ r_2 \\ r_3 \\ \vdots \\ r_n \end{pmatrix} = \begin{pmatrix} -a \\ -b \\ -c \\ \vdots \\ 0 \end{pmatrix} \tag{11.17}$$

Thus this method, based only on balance equations for the amounts of the material in each element of the combined cascade, makes it possible to estimate

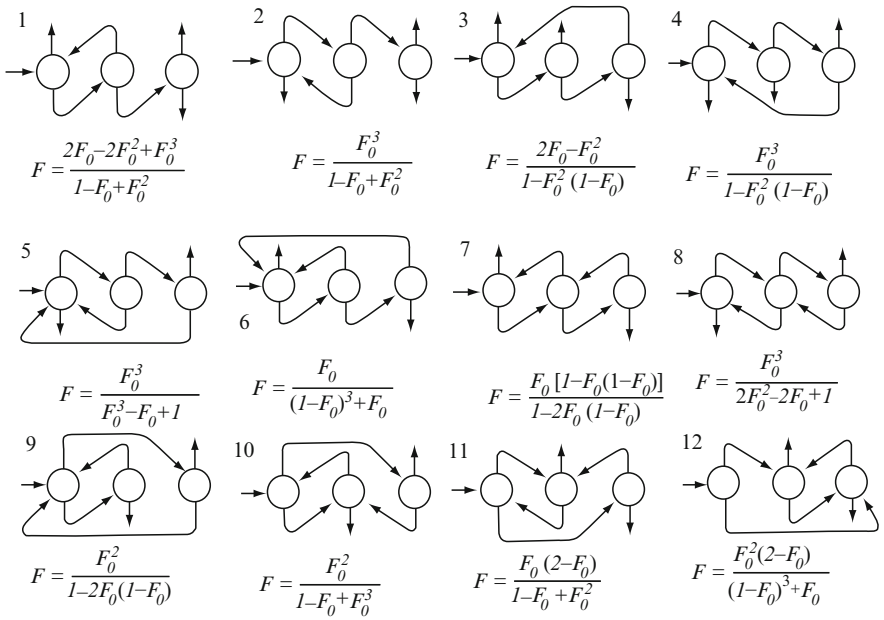

Fig. 11.5 Schematic diagrams and connection functions for 12 three-element combined cascades

an apparatus of any complexity with arbitrary connections, regimes and material feed into its individual elements.

Figure 11.5 shows some schemes of practical interest of three-element combined cascades and connection functions for each of them determined using the described method.

11.5.4 Experimental Verification of the Adequacy of Mathematical Models of Combined Cascades

To verify the calculated dependences, several sets of experiments were performed under laboratory and industrial conditions. Under laboratory conditions, apparatuses of $z \times 2$ type (Fig. 11.3f – I, II) with consecutive repurification of coarse and fine products were studied.

Industrial tests were performed on a combined cascade of $z \times 8$ type with consecutive repurification of the coarse product.

These apparatuses comprised the following elements constituting a cascade:

1. A polycascade classifier (Fig. 11.6c) with the number of stages $z = 9$ and initial material feeding to the stage $i^* = 3$
2. A classifier with radial grates
3. A shelf classifier (Fig. 11.6a) with $z = 6; i^* = 6; n = 8$

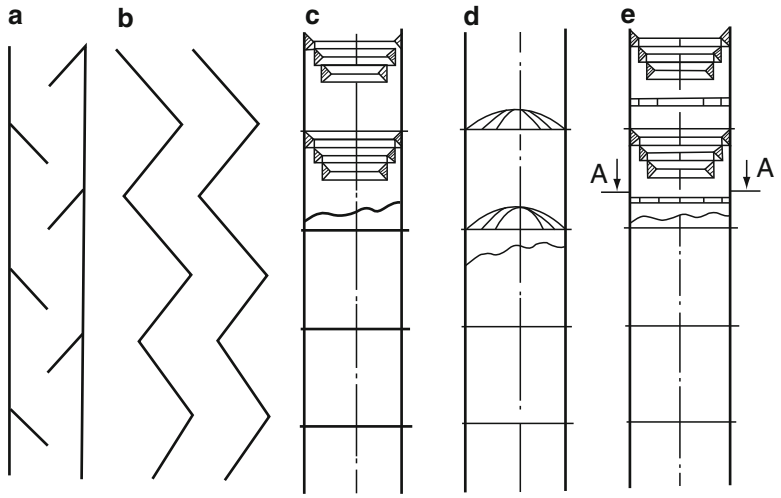

Fig. 11.6 Examples of various constructions of cascade stages: (**a**) inclined shelves; (**b**) zigzag channel; (**c**) poly-cascade; (**d**) radial grates; (**e**) combined stage

Under laboratory conditions, the experiments were carried out on ground quartzite and foundry sand. Under industrial conditions, the experiments were carried out on a potassium salt. Elements of the apparatuses in each set of experiments were identical, and air flow rates in them were equal, too. Material concentration in the flow was maintained constant or varied within the limits of the self-similarity region from 1.1 to 2.5 kg/m^3. In each set of experiments, five different air flow rates were specified equal to 2.8, 3.07, 4.13, 4.98, 6.14 m/s.

$F_0(l)$ – fractional extraction of a narrow class for one element of the apparatus, and $F(l)$ – fractional extraction for the entire apparatus, were determined experimentally. The same design parameters were determined through connection functions:

$F = 1 - (1 - F_0)$ – for coarse product repurification

$F = F_0^2$ – for fine product repurification

$F = 1 - (1 - F_0)^8$ – for eightfold fine product repurification

It is established on the basis of experimental data that for each element of the apparatus the value $F_0(l)$ is constant.

By way of example, Fig. 11.7 shows $F_0(l)$ values obtained at the fractionating of fine-grain potassium chloride for each element of an eight-row apparatus with the capacity of 40 t/h at the air flow rate $w = 6.14$ m/s.

The ratio of calculated (F) and experimental $F_0(l)$ values for the given apparatus at different flow rates is presented in Fig. 11.8.

It follows from the graph that the discrepancy between calculated values and experimental data does not exceed 5.0%, which is within the accuracy of measurements under industrial conditions. A similar coincidence takes place for all laboratory studies.

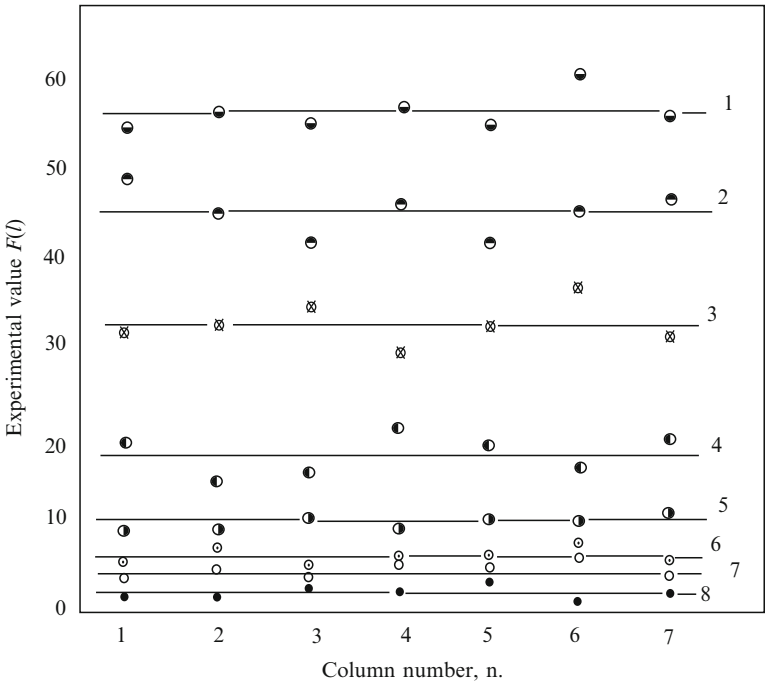

Fig. 11.7 Dependence $F_0(l)$ on the number of columns in an eight-row apparatus. Notations for average particle sizes in micrometers: 1 – 82; 2 – 130; 3 – 180; 4 – 258; 5 – 358; 6 – 450; 7 – 565; 8 – 715

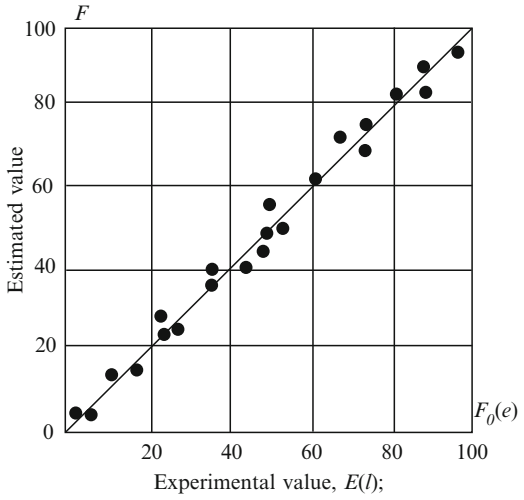

Fig. 11.8 Correlation between estimated (F) and experimental $F_0(l)$ values for an eight-row separator

11.6 Quality Criterion for Combined Cascades

When evaluating a combined cascade, one has to single out the perfection of connections between its elements, i.e. the perfection of the connection function.

For an unbiased evaluation of a combined cascade by its connection functions, we have to formulate a quality criterion that must satisfy several requirements:

1. It should be independent of the characteristic of an isolated element of a combined classifier, i.e. of F_0, since it evaluates connections between elements, and not elements themselves.
2. The criterion should be the same for direct and reversed schemes, since in both cases the connection scheme is the same.

The connection function for the reversed scheme is derived by a formal substitution $F_0 \Rightarrow 1 - F_0$. Although as a result, the connection function for the reversed scheme is different, their quality criterion should give the same numerical value.

3. The criterion should equal unity for schemes consisting of one or several elements when

$$F(F_0) = F_0 \tag{11.18}$$

4. The criterion should be infinite when it realizes an ideal cascade, i.e. for the connection function

$$F(F_0) = \begin{cases} 1.0 & F_0 > 0.5 \\ 0.5 & F_0 = 0.5 \\ 0 & F_0 < 0.5 \end{cases} \tag{11.19}$$

where $\overline{F_0}$ is the value of the parameter F_0, at which $F(F_0) = \frac{1}{2}$.

5. This parameter should be monotonic.
6. The quality criterion should take into account the displacement of the optimal separation boundary for a combined cascade with respect to an analogous boundary in an isolated element.

To clarify the generalized quality criterion, Fig. 11.9 shows some structural schemes of a three-element combined cascade, connection function for these schemes and their plots.

A quality criterion for the evaluation of a combined scheme perfection, which satisfies all above requirements, has the form

$$J(F_0) = \frac{4}{3}\overline{F_0}(1 - \overline{F_0}) \cdot E(F), \tag{11.20}$$

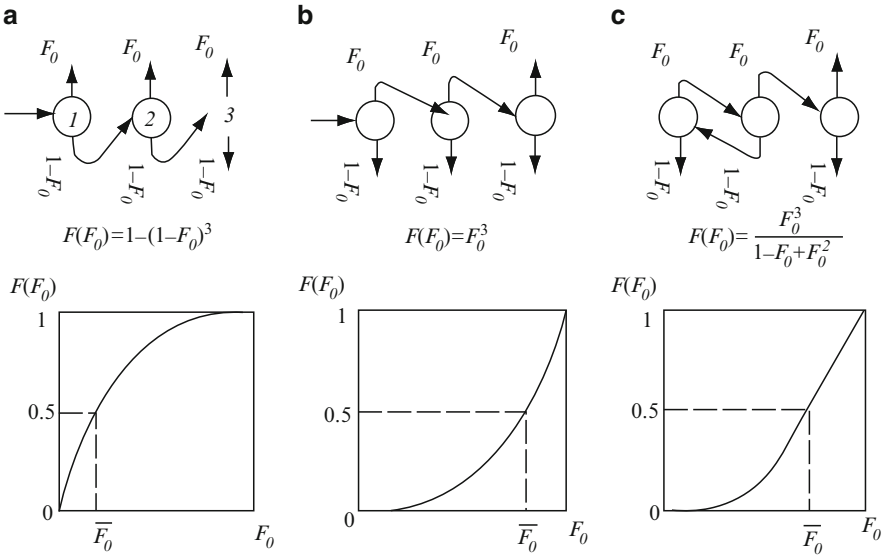

Fig. 11.9 Certain types of three-element combined cascades, their plots and connection functions

where $J(F_0)$ is the quality criterion.

$\frac{4}{3}$ is a normalizing coefficient.

$F(F_0)$ is the connection function (fractional extraction into the fine product for a combined cascade).

Obviously, by definition

$$F(\overline{F_0}) = \frac{1}{2}$$

The parameter $E(F)$

$$E(F) = \left(\frac{1}{1 - E^*(F_0)} - 1\right), \tag{11.21}$$

where

$$E^*(F_0) = \int_0^{\overline{F_0}} [1 - F(F_0)]dF + \int_{\overline{F_0}}^{1} F(F_0)dF_0 \tag{11.22}$$

If we apply the graphs shown in Fig. 11.9 for these calculations, it becomes clear that

$$E^*(F_0) = 1 - S_t^*,$$

where S_t^* is Trompf's area modified for these conditions.

Let us examine in detail the conditions formulated above.

The first condition is due to the purpose of the index to evaluate the perfection of the separation scheme from the standpoint of the approach to an ideal process independent of the characteristics of a separate element.

The second condition is analogous to the requirement of unambiguity. From the standpoint of the problem under study, the direct and reversed schemes are symmetrical and, therefore, should be equivalent as to the degree of perfection. The formulated criterion satisfies this requirement, which can be checked using formula (11.20) with a formal substitution $F_0 \Rightarrow 1 - F_0$.

Normalization conditions 3, 4 are chosen for clearness and convenience, as well as for reasons of the sensitivity of the index.

If $J(F_0) \leqslant 1,$, such combined cascade has no advantages over an isolated column and is of no interest.

The graph obtained for the connection function $F(F_0) = F_0$ is symmetrical (Fig. 11.10).

$$\begin{aligned} S_t^* &= 1 \times 0.5 - 0.5 \times 0.5 \times 0.5 - 0.5 \times 0.5 + 0.5 \times 1 - 0.5 \times 0.5 - 0.5 \\ &\quad \times 0.5 \times 0.5 \\ &= 1 - 3 \times 0.25 = 0.25 \end{aligned}$$

Taking this into account,

$$E^*(F_0) = 1 - S_t^* = 1 - 0.25 = \frac{3}{4}$$

Hence, a normalizing factor arises equal to $\frac{4}{3}$.

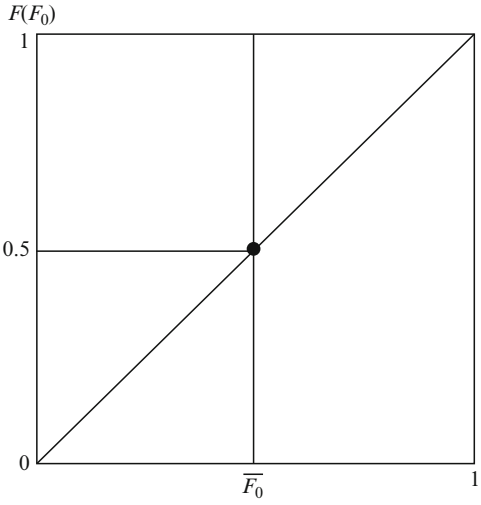

Fig. 11.10 Plot of connection function $F(F_0) = F_0$

In this case, the general index is

$$J(F_0) = \frac{4}{3} \cdot 0.5 \times 0.5\left(\frac{1}{1-0.75} - 1\right) = \frac{1}{3} \times 3 = 1$$

For an ideal modified cascade, modified Trompf's area tends to zero, i.e., $S_t^* \to 0$, and it means that $E^*(F_0) \to 1, E(F) \to \infty$.

Thus,

$$J(E) \to \infty$$

under the condition that

$$F(F_0) = \begin{cases} 1 & F_0 > \overline{F_0} \\ 0,5 & F_0 = \overline{F_0} \\ 0 & F_0 < \overline{F_0} \end{cases}$$

If $F(F_0) = \text{const}$, we obtain $J(E_0) = 0$.

For a two-element cascade, there are only four working schemes (Fig. 11.3f). Their principal parameters are presented in Table 11.1.

Table 11.1 shows that:

1. Direct and inverse schemes have the same magnitude of the quality index, although they realize separation by different boundaries.
2. Combined classifiers with fine or coarse product recycling are more efficient than simple schemes.

There are 47 working schemes for a three-element cascade. They have been analyzed from the standpoint of the stated method. Fourteen of them have the parameter $J(F_0) \leqslant 1$. These schemes are of no interest. The most efficient schemes are shown in Fig. 11.5, and their principal parameters are summarized in Table 11.2.

It follows from this table that the direct and reversed schemes have different connection functions and magnitudes of the parameters $\overline{F_0}$, but the same quality criterion obtained using the proposed method. On the basis of this table, we can arrange all combined three-element cascades according to their perfection degree. In this case, the apparatus presented in Fig. 11.5(9) occupies the first place.

Table 11.1 Principal parameters of two-element combined cascades

No. in Fig. 11.2f	Connection function	$\overline{F_0}$	$E(F_0)$	$J(F_0)$
I	$F(F_0) = 1 - (1 - F_0)^2$	0.2929	4.1213	1.2211
II	$F(F_0) = F_0^2$	0.7071	4.1213	1.221
III	$F(F_0) = \frac{F_0}{1-F_0+F_0^2}$	0.38197	4.1990	1.3384
IV	$F(F_0) = \frac{F_0^2}{1-F_0+F_0^2}$	0.6180	4.1190	1.338

Table 11.2 Principal parameters of three-element combined cascades

No. in Fig. 11.5	Connection function	$\overline{F_0}$	$E(F_0)$	$J(E_0)$
1	$F=\frac{2F_0-2F_0^2+F_0^3}{1-F_0+F^2}$	0.261	5.1249	1.5912
2	$F=\frac{F_0^3}{1-F_0+F_0^2}$	0.739	5.1249	1.5912
3	$F=\frac{2F_0-F_0^2}{1-F_0^2(1-F_0)}$	0.7549	5.4204	1.4474
4	$F=\frac{F_0^3}{1-F_0^2(1-F_0)}$	0.2541	5.4204	1.4474
5	$F=\frac{F_0^3}{F_0^3-F_0+1}$	0.6823	5.3799	1.5905
6	$F=\frac{F_0}{(1-F_0)^3+F_0}$	0.3177	5.3799	1.5905
7	$F=\frac{F_0[1-F_0(1-F_0)]}{1-2F_0(1-F_0)}$	0.3522	5.1061	1.5634
8	$F=\frac{F_0^3}{2F_0^2-2F_0+1}$	0.6478	5.1061	1.5634
9	$F=\frac{F_0^2}{1-2F_0(1-F_0)}$	0.5	5.5178	1.8393
10	$F=\frac{F_0^2}{1-F_0+F_0^3}$	0.5549	5.1803	1.7127
11	$F=\frac{F_0(2-F_0)}{1-F_0+F_0^2}$	0.5	4.7262	1.5754
12	$F=\frac{F_0^2(2-F_0)}{(1-F_0)^3+F_0}$	0.4450	5.1803	1.7127

Using this method, we can analyze combined apparatuses consisting of any number of elements and determine the most effective ones.

11.7 Fractal Principle of the Construction of Schemes of Combined Classifiers

11.7.1 Fractal Principle of Combination

Examples of various combined apparatuses consisting of two elements are shown in Fig. 11.3f.

Experimental testing of certain types of such apparatuses has demonstrated their progressive character. In these apparatuses separation efficiency is greatly increased in comparison with cascade classifiers.

We use these two-element classifiers as a basis for explaining a new method of constructing combined schemes.

We take the amount of the narrow class entering the first element as unity; r_2F_0 passes into it from the second element. Thus, we can write:

$$r_1 = 1 + r_2F_0,$$

similarly, for the second element:

$$r_2 = r_1(1 - F_0).$$

Thus, we obtain two equations with two unknown quantities. Hence,

$$r_1 = \frac{1}{1 - F_0 + F_0^2},$$

and the connection function is:

$$F(F_0) = \frac{F_0}{1 - F_0 + F_0}$$

Similarly, we obtain for scheme IV:

$$F(F_0) = \frac{F_0^2}{1 - F_0 + F_0}.$$

Multiple choice of connections even in case of three or four elements leads to an uncertainty in the choice of efficient combined cascades. To regulate this choice, we apply principles of a relatively new concept in mathematics – fractal geometry.

Fractals are constructed according to the following principle. The entire scheme is inserted instead of each element in the existing scheme at the first step, retaining external and internal connections. At the second stage, the entire initial scheme with all connections is inserted again into each element of the newly obtained scheme, etc.

Figure 11.11 shows fractal combined classifiers, where schemes (a) and (d) correspond to schemes I and II shown in Fig. 11.3, whereas (b), (c) and (e), (f) represent the results of the fractal method application in order to obtain schemes in one and two transformation steps.

Let us examine connection functions for newly obtained apparatuses.

Initial apparatus I:

(a) For the initial combination:

$$F_1(F_0) = 1 - (1 - F_0)^2;$$

(b) For a four-element apparatus, we can write:

$$F_2(F_0) = 1 - [1 - F_1(F_0)]^2 = 1 - (1 - F_0)^4$$

c) For an eight-element apparatus, we can write:

$$F_3(F_0) = \left\{1 - [1 - F_2(F_0)]^2\right\}^2 = 1 - (1 - F_0)^8;$$

(d) For any scheme obtained at the nth step, we can write:

$$F_N(F_0) = 1 - (1 - F_0)^N \tag{11.23}$$

where N is the number of elements in the scheme.

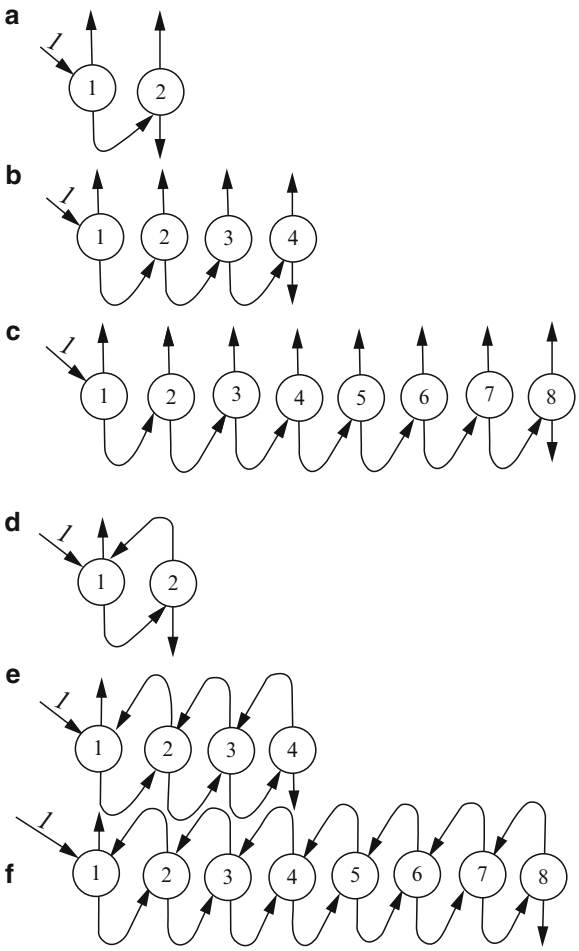

Fig. 11.11 Constructing combined schemes using fractal methods

Similarly, for the initial apparatus II (Fig. 11.3) we obtain

$$F_N(F_0) = F_0^N \tag{11.24}$$

Consider option III (Fig. 11.3) as the initial apparatus. The connection function for an apparatus comprising two elements is

$$F_1(F_0) = \frac{F_0}{1 - F_0 + F_0^2} \tag{11.25}$$

According to the rule of fractals, the connection equation for a four-element apparatus is:

$$F_2(F_0) = \frac{F_1(F_0)}{1 - F_1(F_0) + F_1(F_0)^2} = \frac{\frac{F_0}{1-F_0+F_0^2}}{1 - \frac{F_0}{1-F_0+F_0^2} + \frac{F_0^2}{(1-F_0+F_0)}}$$

$$= \frac{F_0^3 - F_0^2 + F_0}{F_0^4 - 3F_0^3 + 4F_0^2 - 3F_0 + 1}$$

Similarly, we can find the connection equation for apparatuses comprising 8, 16, 32, etc. elements. One can easily check that for the newly obtained connection functions, the efficiency of respective schemes exceeds unity. However, here the solving method can be somewhat different.

11.7.2 Progressive Nature of Multi-element Apparatuses

We have to prove that each subsequent fractal scheme is more efficient than the previous one, if the initial scheme efficiency exceeds unity.

As follows from Table 11.1, primary schemes of two-element apparatuses are characterized by the ratio

$$J[F(F_0)] > 1$$

for any of the available connection functions $F(F_0)$. Schemes with $J[F(F_0)] \leqslant 1$ are not considered.

On the basis of these initial data, we demonstrate an increase in the effect in combined apparatuses with their growing complexity. We will prove that if $J[F(F_0)] > 1$ for the connection function, we should write for a series of fractals:

$$J[F_N(F_0)] > J[F_{N-1}(F_0)] > \cdots > J[F_2(F_0)] > J[F_1(F_0)] > 1 \tag{11.26}$$

This means that the efficiency of each subsequent fractal is higher than that of the previous one. Let us prove it by using the method of mathematical induction.

Clearly, the connection function for an apparatus consisting of one column is:

$$F(F_0) = F_0 \text{ and } J(F_0) = 1.$$

For a scheme consisting of an apparatus of this type,

$$J[F_1(F_0)] > 1,$$

i.e., under this condition, it is more efficient than one element.

Now we assume that this statement is valid for $(N - 1)$ fractal, i.e.,

$$J[F_{N-1}(F_0)] > \cdots > J[F_2(F_0)] > J[F_1(F_0)] > 1.$$

For a fractal of the Nth order we assume that a fractal of $(N-1)$th order constitutes a scheme with a certain $F(F_0)$. We insert a fractal of the first order as an element into a scheme of $(N-1)$th order. It has been proved that a second-order apparatus is better than a first-order one (independent of its design), and then we can assert that

$$J[F_N(F_0)]>J[F_{N-1}(F_0)],$$

which proves the validity of the statement.

Another problem is how economically efficient it is to complicate the apparatus and where to stop. This is determined by various factors: cost of the material to be separated, requirements for the product purity and cost of one element of the apparatus.

The function $F(F_0)$, which gives the value $J[F(F_0)] = \infty$, has the following form (Fig. 11.10, lines $0F_0; AB$ and the 0 point):

$$F_\infty(F_0) = \begin{cases} 1 & 1 \geqslant F_0 > 0,5 \\ 0,5 & F_0 = 0,5 \\ 0 & 0 \leqslant F_0 < 0,5 \end{cases}$$

It would be reasonable to ask whether there exists a function $F(F_0)$ for which $J[F_n(F_0)]_{n\to\infty} \to \infty$.

Shannon and Muret have demonstrated that such functions are continuous in the segment [0,1]. Hence, they belong to C [0,1] (the space of continuous functions in the segment [0,1]). This space is complete, i.e. any Cauchy sequence in it converges, and hence, the limit of any sequence of the form $F_n(F_0)$ is a continuous function. It means that one can never reach $F_\infty(F_0)$.

Therefore, the fractal method of constructing combined cascades does not ensure ideal separation. Besides the fractal method, other methods of replacing elements of the initial scheme with a certain scheme in order to increase its efficiency are possible. Similarly, it can be shown that in this case it is also impossible to ensure the combined cascade efficiency tending to infinity even by constructing an infinite sequence of functions. It is shown in the mentioned paper of Shannon and Muret that the connection function can intersect the line $y = x$ not more than once.

We examine the general form of some schemes with $J[F(F_0)]>1$. Among them, there are schemes improving the fine product extraction and worsening that of the coarse product, i.e. concave ones (see, e.g., Fig. 11.9c). There are also schemes giving the opposite result, i.e. convex ones (Fig. 11.9a). There are schemes with S-like character of the connection function as in Fig. 11.15(3). If the intersection point of the function with the straight line $y = x$ equals 0.5, for such a scheme optimal separation conditions are realized. Evidently, it is preferable to use such a scheme as a basis for placing other schemes into it instead of its elements.

In this case, at the application of the fractal method, the scheme efficiency grows at every step. However, as demonstrated, it cannot tend to infinity, because even this method does not ensure, in principle, an ideal separation.

11.7.3 Combined Scheme with Successive Recirculation of Both Products

This scheme is similar to a simple cascade with unit stages used instead of the elements of the apparatus. Therefore, for the case corresponding to Fig. 11.3f we can write:

$$F(F_0) = \frac{1 - \left(\frac{1-F_0}{F_0}\right)^N}{1 - \left(\frac{1-F_0}{F_0}\right)^{N+1}} \tag{11.27}$$

This dependence is valid at the feeding of the initial material to the first element of the apparatus. In case of feeding to any i^*th element, Eq. (11.27) acquires the form:

$$F(F_0) = \frac{1 - \left(\frac{1-F_0}{F_0}\right)^{N+1-i^*}}{1 - \left(\frac{1-F_0}{F_0}\right)^{N+1}} \tag{11.28}$$

Respectively, for $F_0 = 0.5$ we obtain

$$F(F_0) = \frac{N+1-i^*}{N+1} \tag{11.29}$$

It follows from (11.29) that for the combined scheme under study, there is no displacement of the boundary size of separation only at

$$i^* = \frac{N+1}{2}$$

In this case we obtain the connection function from (11.28):

$$F(F_0) = \frac{1}{1 + \left(\frac{1-F_0}{F_0}\right)^{\frac{N+1}{2}}}$$

As in this case there is no boundary displacement, we can estimate the curve steepness and the separation efficiency of the combined scheme by the derivative in the point $F_0 = 0.5$:

$$\left[\frac{dF(F_0)}{dF_0}\right]_{F_0=0,5} = \left\{\frac{\frac{N+1}{2}\left(\frac{1-F_0}{F_0}\right)^{\frac{N-1}{2}}\left(\frac{1}{F_0}\right)^2}{\left[1 + \left(\frac{1-F_0}{F_0}\right)^{\frac{N+1}{2}}\right]^2}\right\}_{F_0=0,5} = \frac{N+1}{2}$$

Hence, with increasing N, separation efficiency of the combined scheme continuously grows and exceeds the separation efficiency of a single column starting from $N = 3$.

Thus, the separation efficiency of a combined scheme with successive recirculation considerably exceeds that of a cascade classifier constituting its element.

11.7.4 Combined Cascade with an Alternating Bypass of Both Products

The described method of obtaining combined schemes opens broad opportunities for creating highly-efficient separation systems. We examine another case where the limiting effect is achieved using a restricted number of elements (Fig. 11.12). This figure clarifies the principle of bypass construction, where in the general scheme, each element is connected with the next nearest one. On the basis of this figure we can write a system of equations for a narrow size class in different elements of the schemes:

$$\left.\begin{array}{c} F_1 = 1 \\ F_1^* = F_1(1 - F_0) \\ F_2 = (F_1 + F_1^*)F_0 \\ F_2^* = (F_2 + F_1^*)(1 - F_0) \\ \cdots\cdots\cdots\cdots\cdots\cdots\cdots \\ F_i = (F_{i-1} + F_{i-1}^*)F_0 \\ F_i^* = (F_i + F_{i-1}^*)(1 - F_0) \\ \cdots\cdots\cdots\cdots\cdots\cdots\cdots \\ F_n = (F_{n-1} + F_{n-1}^*)F_0 \\ F_n^* = (F_n + F_{n-1}^*)(1 - F_0) \end{array}\right\} \qquad (11.30)$$

where F_i is the total fractional flow in the ith element.

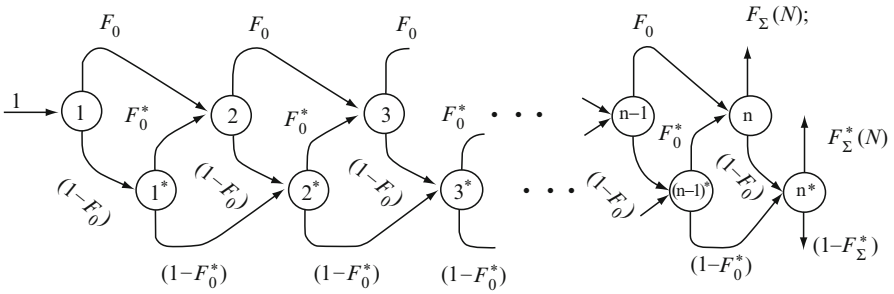

Fig. 11.12 Schematic diagram of a combined classifier with a bypass of both products at each stage

F_i^* is a flow of particles of the same fixed narrow size class through the element i^*.

Fractional extraction into the fine product for the entire apparatus is

$$F_{\sum}(N) = F_N \cdot F_0, \tag{11.31}$$

if the number of elements is odd and equals $N = 2m - 1$. If the number of elements is even and equals $N = 2m$, we obtain:

$$F^*_{\sum}(N) = (F_N + F_N^*) \cdot F_0 \tag{11.32}$$

It follows from (11.30) that

$$F_N = (F_{N-1} + F^*_{N-1}) \cdot F_0^2$$

Taking (11.32) into account, we can write:

$$F_{\sum}(N) = F_0 \cdot F^*_{\sum}(N-1) \tag{11.33}$$

Thus, the problem of determining fractional extraction into the fine product for the entire apparatus is reduced to determining the flows F_N and F_N^*.

The system of equations (11.30) can be transformed as follows:

$$\begin{gathered} F_1 = 1 \\ F_1^* = 1 - F_1 \cdot F_0 \end{gathered}$$

From this, we express $F_1 \cdot F_0$ and substitute into the third equation of the system (11.30) obtaining

$$F_2 = 1 - F_1^* + F_1^* \cdot F_0 = 1 - F_1^*(1 - F_0)$$

The value $F_1^*(1 - F)$ is substituted into the fourth equation of the system (11.30):

$$F_2^* = F_2(1 - F_0) + (1 - F_2) = 1 - F_2 F_0$$

Proceeding further in a similar way, we obtain:

$$F_3 = 1 - F_2^*(1 - F_0)$$

$$F_3^* = 1 - F_3 \cdot F_0$$

It can be easily proved using the method of complete mathematical induction that in the general case the following is valid:

$$F_i = 1 - F^*_{i-1}(1 - F_0) \tag{11.34}$$

$$F_i^* = 1 - F_i \cdot F_0 \tag{11.35}$$

Expressions (11.34) and (11.35) allow us to write two independent recurrent equations:

$$F_i = 1 - (1 - F_{i-1} \cdot F_0)(1 - F_0)$$

After simplification, we obtain

$$F_i - F_{i-1} \cdot F_0(1 - F_0) = F_0 \tag{11.36}$$

Similarly, taking into account (11.34), we can derive from (11.35) the following:

$$F_i^* - F_{i-1}^* \cdot F_0(1 - F_0) = (1 - F_0) \tag{11.37}$$

Equations (11.36) and (11.37) are non-uniform linear finite-difference equations of the first order with boundary conditions.

$$F_1 = 1 \text{ and } F_1^* = 1 - F_0$$

They can be solved both by standard and by elementary methods. Thus, applying consecutively (11.36), we obtain:

$$F(1) = 1$$
$$F(2) = F_0 + F_0(1 - F_0)$$
$$F(3) = F_0 + F_0^2(1 - F_0) + F_0^2(1 - F_0)^2$$
$$F(4) = F_0 + F_0^2(1 - F_0) + F_0^3(1 - F_0)^2 + F_0^3(1 - F_0)^3$$
$$\cdots\cdots\cdots\cdots\cdots\cdots\cdots\cdots\cdots\cdots$$

$$F(i) = F_0 + F_0^2(1 - F_0) + F_0^3(1 - F_0)^2 + \cdots + F_0^{i-1}(1 - F_0)^{i-2} + F_0^{i-1}(1 - F_0)^{i-1}$$
$$F(N) = F_0 + F_0^2(1 - F_0) + F_0^3(1 - F_0)^2 + \cdots + F_0^{N-1}(1 - F_0)^{N-2} + F_0^{N-1}(1 - F_0)^{N-1}$$

It is clear that we are dealing with a geometrical progression. We denote the progression ratio by

$$g = F_0(1 - F_0)$$

Then

$$F(N) = F_0 + F_0 g + F_0 g^2 + \cdots + F_0 g^{n-2} + g^{n-1}$$

or

$$F_0 g^{n-1} - g^{n-1} + F(N) = F_0 + F_0 g + F_0 g^2 + \cdots + F_0 g^{n-1}$$

Multiplying both parts of the equality by $g(g \neq 0)$:

$$F_0 g^n - g^n + g \cdot F(N) = F_0(g + g^2 + \cdots + g^n)$$

We convolute the right-hand part

$$F_0 g^n - g^n + gF(N) = F_0 \frac{g + g^{n+1}}{1 - g}$$

Hence,

$$F(N) = g^{n-1} + \frac{1 - g^{n-1}}{1 - g} \cdot F_0$$

Passing from the flow to the extraction on the *N*th element, we obtain

$$F(N) = F_0 g^{n-1} + F_0^2 \frac{1 - g^{n-1}}{1 - g} \tag{11.38}$$

A similar examination of the second recurrent equation gives

$$F^*(N) = g \frac{1 - g^n}{1 - g} \tag{11.39}$$

which well agrees with (11.33).

In case of a combined cascade of this type, we can restrict ourselves with its incomplete scheme, since its complete scheme would comprise a great number of stages. We assume that this incomplete scheme contains an odd number of elements. In this case, fractional extraction of the entire combined cascade acquires the simplest form:

$$F_{\sum}(N) = F_0 g^{n-1} + F_0^2 \frac{1 - g^{n-1}}{1 - g} \tag{11.40}$$

Hence, we obtain

$$F_{\sum}(N) = \frac{1 - F_0}{1 - g} g^n + \frac{F_0^2}{1 - g} \tag{11.41}$$

Note that fractional extraction of a single element and of the entire apparatus are connected by a relationship

$$F_{\sum}(N) \leqslant F_0$$

For example, it follows from (11.40) that

$$F_0 - F_{\sum}(N) = \left(1 - g^{n-1}\right)\left(1 - \frac{F_0}{1-g}\right),$$

but $\frac{F_0}{1-g} = \frac{F_0}{1-F_0+F_0^2} < 1$ is always valid at $F_0 \neq 1$.

Equation (11.41) allows us to plot the dependence $F_{\sum}(N) = f(F_0)$ for different numbers of elements (Fig. 11.13). It follows from this plot that at $N > 4$ all the curves practically merge, and the optimal separation boundary is determined by the regime in an individual element $\overline{F}_0 = 0.618$.

Here the steepness of separation curves for the entire apparatus considerably exceeds the steepness of the curves for an individual column, which points to its higher efficiency.

It also follows from this plot that it is inexpedient to use this apparatus with more than four elements $(N \leqslant 6)$.Under such restriction, this scheme of a combined apparatus is progressive.

Thus, combined apparatuses offer immense potential for increasing the efficiency of bulk materials separation and creating various schemes both for multiproduct separation and for separation with the production of powders with specified compositions.

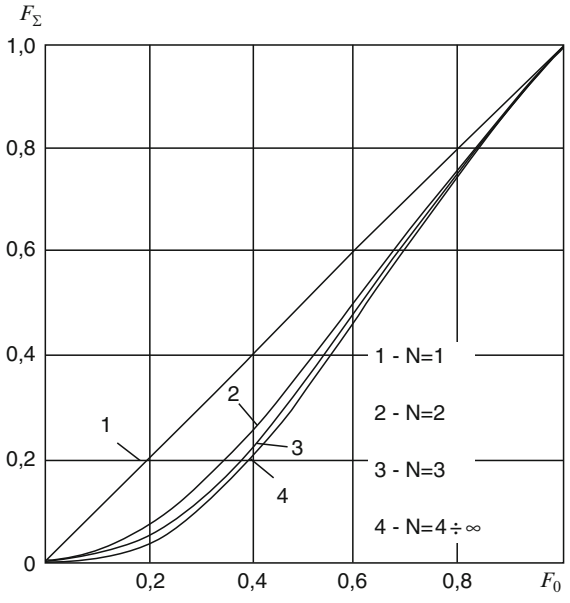

Fig. 11.13 Dependence $F_\Sigma(N) = F(F_0)$ for combined apparatuses with a bypass of both products at a varying number of elements N

11.7.5 On the Potential of Fractal Combined Schemes

Examination of the above examples can give rise to doubts as to the ability of fractal combined schemes to ensure a high separation effect at moderate costs, but that would be a wrong conclusion. If we choose an initial scheme according to the above method, we can achieve highly efficient separation after several steps. Let us examine a concrete example with only one condition $F(\overline{F_0}) = 0.5$ satisfied. There are many such variants, but we choose one of them (Fig. 11.14a).

The connection equation for this scheme can be derived from the flow balance. According to this scheme, we can write a system of equations:

$$\begin{cases} r_1 = 1 + r_2 F_0 + r_3(1 - F_0) \\ r_2 = r_1(1 - F_0) \\ r_3 = r_1 F_0 \end{cases}$$

We substitute the second and third equations of this system into the first one and solve it with respect to r_1. As a result, we obtain:

$$r_1 = \frac{1}{1 - 2F_0 + 2F_0^2}$$

Then according to the scheme, the connection equation for this combined cascade is:

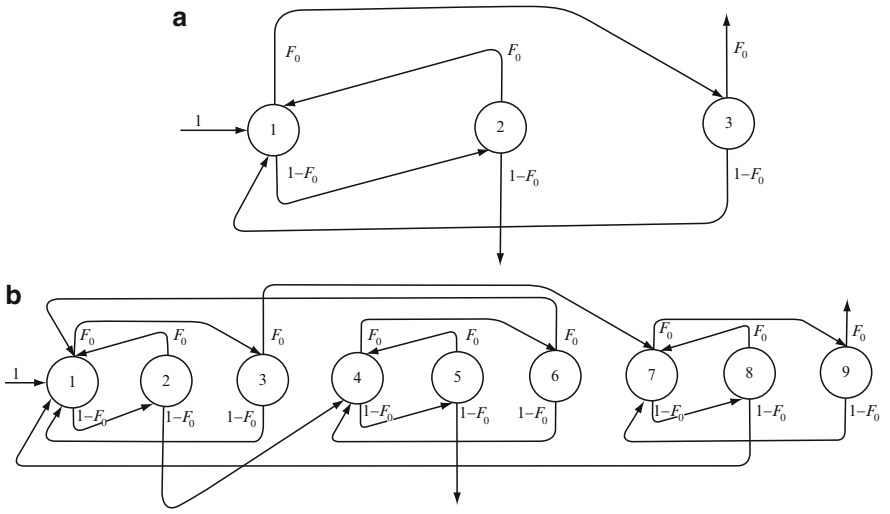

Fig. 11.14 (**a**) Three-element combined schematic diagram with $F\ (F_0) = 0.5$. (**b**) Fractally transformed schematic diagram with nine elements

$$F(F_0) = \frac{F_0^2}{1 - 2F_0 + 2F_0^2} \tag{11.42}$$

Apparently, at $\overline{F_0} = 0.5$, the magnitude $F(\overline{F_0}) = 0.5$.

Note that the efficiency of this scheme is high; for this scheme, $J(E_0) = 1.8393$ at $E(F_0) = 5.5178$.

The plot of the function (11.42) is shown in Fig. 11.15. By the definition of efficiency, the smaller Trompf's area, the higher the effect. Its value is inversely proportional to the separation quality. At the passage from a single element to a three-element apparatus, this area gets considerably reduced. Even at the first step of fractal transformation, it significantly decreases. This scheme leads to a significant growth of separation results.

For the scheme shown in Fig. 11.15b, we can obtain the connection function proceeding from the fact that in Fig. 11.16, scheme B has been obtained from scheme A by placing it into itself as the initial element. The connection function for scheme B shown in Fig. 11.17 is

$$F[F(F_0)] = \frac{F(F_0)^2}{1 - 2F(F_0) + 2[F(F_0)]^2} = \frac{F_0^4}{2F_0^4 - 4F_0^3 + 6F_0^2 - 4F_0 + 1} \tag{11.43}$$

Here also the relationship

$$F[F(0,5)] = 0,5 \tag{11.44}$$

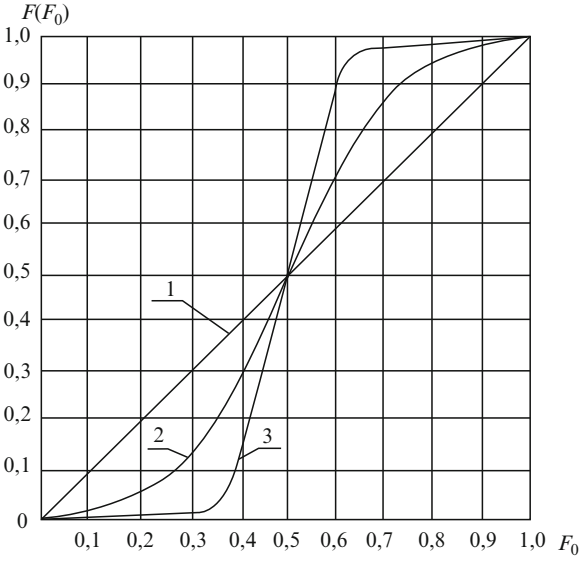

Fig. 11.15 Connection functions: $1 - F(F_0) = F_0$; $2 - F(F_0) = \frac{F_0^2}{1-2F_0+2F_0^2}$; $3 - F(F_0) = \frac{F_0^4}{1-2F_0+4F_0^3-2F_0^4}$

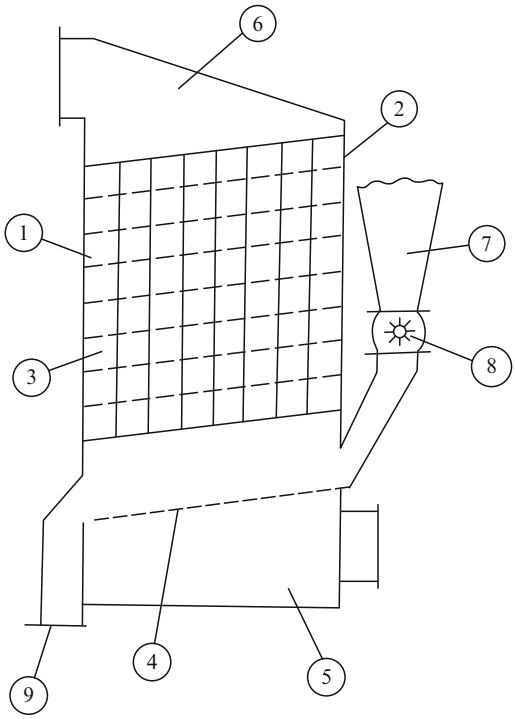

Fig. 11.16 Schematic diagram of an industrial multi-row classifier: 1 – element of the apparatus; 2 – body; 3 – element of the cascade; 4 – distributing grate; 5 – air supply; 6 – fine fraction collector; 7 – initial material; 8 – feeder; 9 – coarse material output

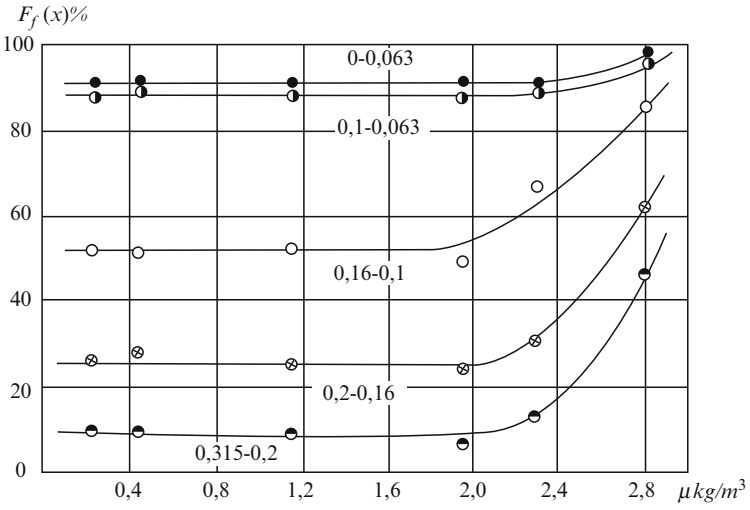

Fig. 11.17 Fractional separation dependence on consumed solid phase concentration for an industrial apparatus

is valid.

Thus, fractal transformation of combined separators has a great potential allowing the design of highly-efficient separation apparatuses. However, it is not the only possible way of improving the operation of these separators. Combined schemes obtained by the fractal method, where recycling is additionally realized, possess a great potential for improving the final product quality.

11.8 Some Methods of Combined Schemes Optimization

11.8.1 Multi-row Classifier

To develop large-tonnage separators, where the influence of a scaling factor is leveled out, multi-row combined separators were developed (Fig. 11.16).

An industrial separator for dedusting fine-grained potassium chloride was constructed according to the scheme shown in Fig. 11.16. Inclined shelves were used as cascade-forming elements. The end product obtained on it is dedusted potassium chloride powder. Grain-size composition of the initial material is given in Table 11.3.

The method of studies of an industrial apparatus includes the following operations:

1. A constant air flow through the apparatus is established.
2. Initial material feeding into the apparatus is stabilized.
3. Sampling of the initial material flow and both classification products is performed according to a standard method in order to analyze chemical and grain-size composition.
4. Material flows of the output of classification products are measured using the cutoff method after certain time intervals.
5. During the entire experiment, a continuous control of the total air flow in the apparatus and in individual sections is performed.

To expand the experimental range, optimal fractionating regimes by four size classes – 63, 100, 160, 200 μm were worked through.

Table 11.3 Initial material composition

Mesh size x (mm)	+0.63	+0.5	+0.4	+0.315	+0.2	+0.16	+0.1	+0.063	−0.063
Partial residues on the sieve, r_s%	8.8	9.2	9.8	10.4	20.4	8.6	11.6	8.0	13.2
Total residues on the sieve, R_s%	8.8	18	27.8	38.2	58.6	67.2	78.8	86.6	100

First of all, we have determined the range of solid substance concentration in the air flow that does not affect the degree of fractional separation of particles of different narrow size classes.

Figure 11.17 shows the results of these studies at a constant air flow rate $Q = 15{,}100\ \text{m}^3/\text{h}$ through the apparatus. It follows that both in the industrial scale and under laboratory conditions, the limiting consumed concentration of the solid phase in the flow is within the range of $\mu = (2.0 \div 2.2)\ \text{kg/m}^3$.

In our further studies, air flow through the apparatus was smoothly varied within the range of 15,000–22,000 m^3/h, and in each section of the apparatus the same flow rate was established.

Experimental curves for this apparatus were determined at different numbers of elements. They are presented in the same plot for comparison (Fig. 11.18). When passing from one to two elements, from two to four and from four to eight, the curves become steeper, and $\overline{F_0}$ value is shifted towards a larger size.

The characteristic of dedusted product depending on the total air flow rate is shown in Table 11.4.

It follows from this table that the apparatus ensures an efficient enough separation in the range of separation boundary sizes under study. For the class of 63 μm, dedusting is practically complete in all regimes of the apparatus operation. For the separation by 100 μm class, the end product amounts up to 75% with the fine product content at least 2%. In this case, the product yield is close to the theoretical one, equal to 78.85.

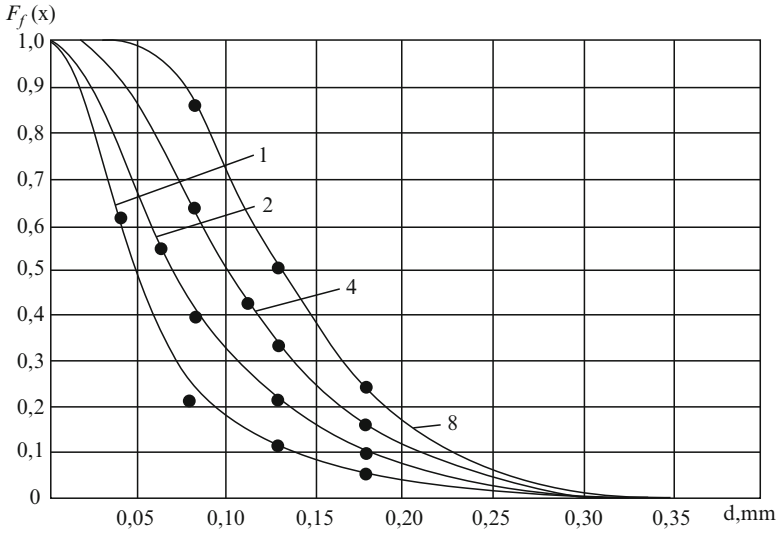

Fig. 11.18 Separation curves for an industrial apparatus in case of 1, 2, 4 and 8 elements

Table 11.4 Coarse product characteristic as to fine classes content depending on the classifier regime parameters

Classifier efficiency (t/h)	Air flow rate m^3/h	Fine classes contents in complete passages (%) D_s				Coarse product yield, γ_c%	Material concentration kg/m^3
		−0.63	−0.1	−0.16	−0.2		
16.3	21,600	0	0	0.2	1.0	25.5	0.75
16.9	22,430	0	0	0.4	1.4	26.8	0.75
17.1	15,200	0	0.4	1.2	5.2	37.8	1.14
35.9	15,330	0.2	1.6	2.8	7.2	34.4	2.34
20.4	13,500	1.2	1.4	3.6	8.2	73.8	1.51
35.7	17,280	1.0	1.6	6.6	13.0	73.4	2.04
21.8	15,850	0.0	1.0	7.0	15.4	61.4	1.38
34.1	16,700	0.4	2.8	8.4	16.0	72.4	2.04
33.2	15,100	1.4	2.6	10.6	19.4	74.5	2.20
18.3	15,480	1.4	2.4	10.4	19.6	64.1	1.19
42.4	17,800	0.4	0.8	4.6	10.8	49.9	2.38
16.6	11,250	0	8.2	23.2	35.0	73.7	1.48
48.2	19,800	1.6	8.6	8.6	17.2	60.7	2.43
25.9	16,800	0.4	0.8	4.0	10.0	56.9	1.54
19.2	15,680	0.6	1.0	3.6	9.2	50.6	1.22
39.8	17,550	0.4	1.0	4.0	9.4	43.2	2.27

With growing boundary size of the separation, these characteristics decrease, but remain within the limits acceptable for industrial conditions. Thus, at separation by the class of 160 μm, coarse product yield amounts up to 56.9% (at the theoretically possible one equal to 67.2%), and its contamination with fine product is about 4%.

Hence, it is expedient to use these apparatuses for dedusting large masses of pourable materials within the range of boundary sizes from 60 to 160 μm. Unfortunately, because of concrete production conditions, we have failed to increase the apparatus productivity above 48.2 t/h. Such a load ensures the coarse product yield $\gamma_c = 60.7\%$, and the product quality is high, since the contamination at the separation by the boundary of 63 μm is only 1.6%. For this separation boundary, the specific productivity of the apparatus amounts to 40 t/h per lm^2 of the apparatus grate area.

It is noteworthy that in contrast to a single-row cascade, in this scheme a higher order of the process organization is realized due to successive-parallel coarse product recleaning.

This scheme is not equivalent to a simple increase in the number of stages of a cascade apparatus, which is confirmed by experimental results. In a multi-row cascade, the process is organized according to the principle of a self-regulated recycle. Such organization of the process takes place in well-known methods of bypassing and dephlegmation. This allows a considerable improvement of the separation quality at increased productivities.

11.8.2 Method of Estimating a Multi-row Classifier

Fractional separation dependence on the Froude criterion for one column (1) and for the entire apparatus (2) is shown in Fig. 11.19. Here

$$Fr = \frac{gx}{w^2}$$

where x is the average size of particles of a narrow class
w is the air flow rate recalculated per the apparatus cross-section.

It has been established earlier that in the range of solid phase concentration in the flow within the limits up to $\mu = 2 \div 3$ kg/m^3, the behavior of particles of each narrow size class is invariant with respect to other classes.

A combined cascade consists of n separating columns operating in parallel, each of them comprising elements of the same type. Air flow rate in all the columns is the same.

Under such conditions, the degree of fractional extraction F_0 in all the columns is also the same and can be determined taking into account the fact that for the given assembly of the apparatus $z = i^*$.

If we take the amount of any narrow fraction fed into the apparatus as unity, the extraction of the first column into the fine product is

$$m_1 = \lambda F_0 \tag{11.45}$$

where λ is a coefficient of transfer of the narrow fraction under study from the grate into the column.

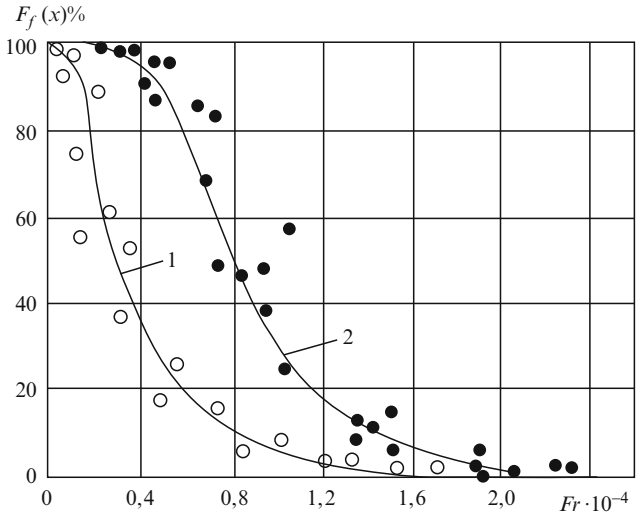

Fig. 11.19 Fractional separation dependence on the Froude criterion for an industrial apparatus: 1 – curve for one vertical element; 2 – curve for eight parallel vertical elements

For the second column

$$m_2 = F_0(1 - F_0)$$

For the third column

$$m_3 = F_0(1 - F_0)(1 - F_0) = F_0(1 - F_0)^2$$

For the nth column

$$m_n = F_0(1 - F_0)^n$$

The total extraction for the size class under study is a sum of terms formed by the geometrical progression with the first term F_0 and the step equal to $(1 - F_0)$.

Finally, we obtain the fine product extraction in the entire apparatus in the form

$$F(F_0) = 1 - (1 - F_0)^n \tag{11.46}$$

The amount of the narrow class extracted into the fine product is determined as

$$r_f = F(F_0)r_s \tag{11.47}$$

where r_s is the content of this class in the initial feed.

The content of this class in the coarse product amounts to

$$r_s - r_f = r_c \tag{11.48}$$

The developed model has made it possible to create a method of predicting fractional composition of both separation products in a multi-row cascade classifier, which is reduced to a successive determination of parameters.

1. The Froude criterion is determined for a specific narrow size class:

$$Fr_j = \frac{gx_j}{w^2};$$

2. Fractional separation of a single column is determined using the formulas given in the beginning of this chapter. Proceeding from the structural model of the process and experimental data, the authors have reliably determined in their previous studies that for a cascade consisting of shelves, the distribution coefficient is determined from the expression

$$k = 0.8678(1 - \sqrt{0.4B}),$$

where $B = \frac{gx}{w^2}\frac{(\rho - \rho_0)}{\rho_0}$,

Table 11.5 Ratio of experimental and estimated values of fractional extraction of different classes in an industrial apparatus

Average size class, x (mm)	0.13	0.18	0.258	0.358	0.45	0.565
Experimental values of $F\%$	91.5	52.6	27.0	10.2	5.7	3.8
Estimated values of $F\%$	91.2	52.4	27.0	10.2	5.7	3.8

ρ, ρ_0 are densities of the material and moving medium, respectively.

3. From the determined value of F_0, the parameter $F(F_0)$ is determined for each narrow class according to dependence (11.46).
4. The output of each fraction into coarse and fine products is determined using the dependencies (11.47) and (11.48).
5. Then the grain size composition and other characteristics of both separation products are determined.

By way of example, Table 11.5 shows the results of the comparison of estimated and experimentally determined fractional extractions of the fine product in an apparatus consisting of eight rows at the air flow rate $Q = 16{,}200$ m^3/h.

As the table shows, the degree of coincidence is high enough.

11.8.3 Optimal Scheme of a Multi-row Industrial Classifier

The analysis of obtained results has shown that fine product is most intensely contaminated with coarse product in outermost columns of a multi-row apparatus located closer to the coarse product discharge. Contamination occurs in all the rows of the classifier, but it increases monotonically starting from the feeding place.

To decrease losses of the target component, it is expedient to recirculate the material of the outermost columns of the apparatus by returning them to initial feed. This technique is especially important when it is desirable to increase the output of one plant.

We have developed a classifier with the output of 100 t/h comprising 12 rows of cascade repurification combined into three separate groups of four rows each. Each group is connected with a separate cyclone for trapping fine product, and after passing the cyclones, the flows are united in one manifold for sanitary purification from dust.

The apparatus is meant for fractionating potassium chloride containing 79.7% of material with the size above 100 μm. In compliance with technological conditions, dust fractions (–100 μm) contents in the dedusted product should not exceed 2%. To estimate fractionating schemes, relationship (11.46) was applied.

Grain size composition of the initial raw material is given in Table 11.6.

The estimation is performed using the described method for the optimal air flow velocity, which amounts to $w = 2.05$ m/s according to industrial tests.

Table 11.6 Initial composition of the material

Particles size, $\overline{x}$ (mm)	2.5	12.5	25	45	65	90	180	357.5	450	565	715
Partial residues, $r_s\%$	0.79	1.58	2.37	3.16	4.3	8.1	20.4	33.0	12.0	6.8	5.8
Complete passages, $D_s\%$	100	99.21	97.63	95.26	92.1	87.8	79.7	59.3	26.3	14.3	7.5

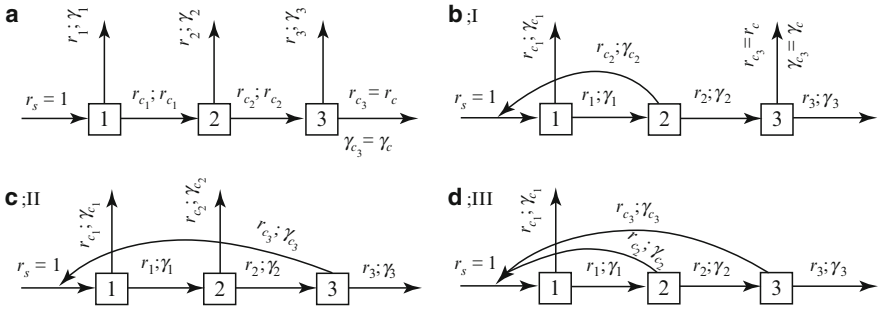

Fig. 11.20 Schematic diagrams for multi-row separation optimization: (**a**) open cycle; (**b**) recycle of the second section; (**c**) recycle of the third section; (**d**) recycle of the second and third sections

To determine the construction optimality, we examine several options.

Scheme of apparatus operation without recirculation (Fig. 11.20a).

Product yield from each group of cascades is determined by the following dependencies:

first group

$$\gamma_1 = \sum r_s F_4;$$

second group

$$\gamma_2 = \sum r_s (F_8 - F_4)$$

third group

$$\gamma_3 = \sum r_s (F_{12} - F_8),$$

where $F_4; F_8; F_{12}$ are fractional extractions of narrow size classes in the first, second and third groups (each group consisting of four columns).

Products compositions in each group are determined by the following dependencies:

first group

$$r_1 = \frac{r_s F_4}{\gamma_1};$$

second group

$$r_2 = \frac{r_s(F_8 - F_4)}{\gamma_2};$$

third group

$$r_3 = \frac{r_s(F_{12} - F_8)}{\gamma_3}$$

In the case under study, coarse product estimated by this method contains 0.4% of contamination.

For the open scheme of the process organization, when the three fine products are combined into a dust fraction, we obtain the following process characteristics:

For the entire apparatus

$$\gamma_f = 64.3\%,\ R_{-0,1} = 0.4\%;$$

For the first group

$$\gamma_1 = 24.34\%,\quad R_{+0.1} = 28.4\%,\quad R_{s(+0.1)} = 6.91\%;$$

For the second group

$$\gamma_2 = 7.08\%,\ R_{+0.1} = 70\%,\ R_{s(+0.1)} = 4.96\%;$$

For the third group

$$\gamma_3 = 4.28\%,\ R_{+0.1} = 87.49\%,\ R_{s(+0.1)} = 3.75\%,$$

where $R_{+0.1}$ is the content of coarse fractions with respect to the product yield, %;

$R_{s(+0.1)}$ is the content of coarse fractions recalculated per the initial product.

This scheme ensures a sufficiently low yield (64.3%) of dedusted product; besides, a considerable part (15.62%) of coarse fractions is lost in the fine product. As to the second and third groups with their low yields (7.08% and 4.28%), losses of +0.1 mm class amount to 8.71% of the initial product, i.e. half of the total losses. Therefore, it is expedient to classify additionally fine products of the second and third groups in the same apparatus, and not to mix them with the dust product of the first group.

Option with recycling of the fine product of the second group of cascades (Fig. 11.20b).

We introduce the following notations:

$r_{f_1}; r_{f_2}; r_{f_3}$ – contents of a fixed size class in the fine product of the first, second and third groups

$r_{c_1}; r_{c_2}; r_{c_3}$ – contents of the same class in the coarse product of respective groups of cascades

In a general case, we can obtain the following design formulas for this scheme of the process organization.

$$F = \frac{r_f}{r_s}\gamma_f = \frac{r_{f_1}}{r_s}\gamma_{f_1} + \frac{r_{f_2}}{r_s}\gamma_{f_2} \tag{11.49}$$

$$F_{0_1} = \frac{r_{f_1}}{r_s}\gamma_{f_1} + \frac{r_{f_3}}{r_s}\gamma_{f_3} \tag{11.50}$$

$$F_{0_2} = \frac{r_{f_2}\gamma_{f_2}}{r_{c_1}\gamma_{c_1}} \tag{11.51}$$

$$F_{0_3} = \frac{r_{f_3}\gamma_{f_3}}{r_{c_2}\gamma_{c_2}} \tag{11.52}$$

$$\left.\begin{array}{c} r_s = r_{f_2}\gamma_{f_2} = r_{f_1}\gamma_{f_1} + r_{c_1}\gamma_{c_1} \\ r_{c_1}\gamma_{c_1} = r_{f_2}\gamma_{f_2} = r_{c_2}\gamma_{c_2} \\ r_{c_2}\gamma_{c_2} = r_{f_3}\gamma_{f_3} + r_{c_3}\gamma_{c_3} \\ r_s = r_{f_1}\gamma_{f_1} + r_{f_2}\gamma_{f_2} + r_{c_3}\gamma_{c_3} \end{array}\right\} \tag{11.53}$$

where $F; F_{0_1}; F_{0_2}; F_{0_3}$ are fractional extractions of a narrow size class for the apparatus, first, second and third groups, respectively.

For the option under study, we have to apply corresponding expressions (11.50–11.53) in dependence (11.49). We obtain

$$F = \frac{F_1 + F_3 - F_1F_2 - F_2F_3 + F_1F_2}{1 - F_1 + F_1F_2} \tag{11.54}$$

According to our condition, when each group consists of four parallel cascades, we can write:

$$F_1 = F_2 = F_3 = 1 - (1 - F_1)^4$$

Taking this into account, relationship (11.54) is transformed to

$$F = \frac{1 - F_{c_1}^4 + F_{c_1}^8 - F_{c_1}^{12}}{1 - F_{c_1}^4 + F_{c_1}^8}$$

where $F_{c_1} = 1 - F_0$ is the extraction of a narrow size class into coarse product in one separation column.

Hence, for the option (Fig. 11.20) we obtain

$$F_c = \frac{F_{c_1}^{12}}{1 - F_{c_1}^4 + F_{c_1}^8} \tag{11.55}$$

Table 11.7 Parameters of multi-row apparatus with recycle

Option	$\gamma_c\%$	$D_{-0,1}\%$	$\gamma_f\%$	Losses R% of initial composition
b	66.61	0.434	33.39	13.38
c	66.0	0.379	34	13.94
d	69.682	0.449	30.318	10.33

For the option (Fig. 11.20c) we obtain:

$$F_c = \frac{F_c^{12}}{1 - F_{c_1}^{8} + F_{c_1}^{12}} \tag{11.56}$$

For the option (Fig. 11.20d) the coarse product extraction amounts to

$$F_c = \frac{F_{c_1}^{12}}{1 - F_{c_1}^{4} - F_{c_1}^{12}} \tag{11.57}$$

All principal results for all three options were calculated according to the exposed method and summarized in Table 11.7 for comparison.

Thus, option d (a scheme with recirculation of the product of the second and third sections) is the most efficient for dedusting potassium chloride with grain size composition given in Table 11.6. This option increases the end product yield by 5% and decreases the loss of target product into dust fraction down to 10.33% (compare with 15.62% in the open cycle). The increase in the apparatus productivity by 11% does not change the regime of the classifier operation.

Thus, a large-tonnage classifier for efficient dedusting of fine-grain products has been developed. It ensures a high quality of both coarse and fine products. Recycling application in this apparatus provides both a flexible control of separation effect and a decrease in qualified product losses.

Chapter 12
Stochastic Model of Critical Regimes of Two-Phase Flows

Abstract An attempt of developing and solving a mathematical model of a process is made taking into account a probabilistic distribution of determining parameters. It is based on correlation methods, namely, on the study of the relations between principal characteristics of a random process, – correlation, moment, structural or related functions. Statistical modeling of critical regimes in turbulent flows is carried out. Systems of non-closed equations are derived and carried to solution using certain simplifications. Systems of particles motion equations are composed taking into account their rotation around the center of mass in the flow. Stationary and non-stationary processes are mathematically described. All these models are reduced to numerical estimations. In conclusion, an example calculation is given, and an approximate estimation method based on its analysis is developed.

Keywords Stochastic equations · Correlation · Moment functions · Ergodicity · Stochastic differential equations · Innovative systems of equations · Nonlinear process · Order of the moment function · Mathematical expectation · Statistical linearity

12.1 Principal Definitions

Statistical methods of the study of mass processes share a border with the analysis of stochastic models of processes, which has been extensively developed in recent years. The analysis presented in this book would be incomplete without an attempt at solving such problems.

Methods of the study of stochastic equations characteristic of the separation processes under study, as well, can be subdivided into two classes: correlation and kinetic ones.

E. Barsky, *Critical Regimes of Two-Phase Flows with a Polydisperse Solid Phase,*
Fluid Mechanics and Its Applications 93,
DOI 10.1007/978-90-481-8838-3_12,

Correlation methods are based on the study of relationships between principal characteristics of random processes – correlation, moment, structural or related functions. For a comprehensive description of a phenomenon, it is necessary to define a complete system of moment functions of the first two orders – mathematical expectations (average values) and moment functions of the second order, which are called correlation functions.

Critical flow regimes can be examined in two aspects – stationary and non-stationary. It is generally assumed that a process is stationary, if all of its probabilistic characteristics are time independent. This mathematical tool has been developed reliably enough for stationary random processes. As for non-stationary processes, it has not been developed with the same degree of reliability even for linear systems.

Obviously, the behavior of an ensemble of particles under the conditions of classification possesses an ergodicity property. It means that sufficiently long realizations of these processes contain practically all information about their statistical properties. For ergodic random processes, averaging over an ensemble of realizations can be replaced with averaging in time.

The main task of correlation methods is to find characteristics of the output parameters of a process through correlation functions of its primary parameters.

Having derived stochastic differential equations connecting input and output parameters, one can easily obtain differential equations for moment functions of different orders. The construction of involution (Jacobian) systems of differential equations in the moment functions is performed by termwise multiplication of stochastic equations by sought functions and their products taken at various moments of time, using averaging over the ensemble of realizations. In a general case, we obtain a sequence of coupled simultaneous differential equations. Equations for moment functions of a given order contain moment functions of a higher order and, hence, do not constitute a closed system of equations. This method of constructing equations in moment functions was applied in turbulence theory by Keller, Friedman, Karman, Kolmogorov, Millionschikov and others for deriving differential equations connecting moment functions of the velocity field of different orders from the Navier–Stokes equations.

We distinguish linear and nonlinear processes. A process is considered statistically nonlinear, if equations of the process comprise products of random values or functions. The process of gravitational classification is an example of a nonlinear process.

The system of equations describing this process can be solved by integrating the equations in moment functions. The arising difficulties can be overcome by linearizing statistically nonlinear relationships.

Methods of describing stochastic processes based on differential equations that express the distribution function evolution in time are usually called kinetic.

Kinetic equations were first introduced by Boltzmann. Later, kinetic equations were widely used in the theory of Brownian motion by Fokker, Planck, Langevin, Smolukhovsky and Einstein.

Application of the mentioned methods makes it possible to determine velocity moments of the particles or velocity distribution densities for particles of each narrow class, which serves as a basis for plotting separation curves.

Note that the meaning of some notations in this chapter differs from those accepted in previous chapters. In such cases, they are clarified in detail in the text.

12.2 Statistical Description of Gravitational Separation in Turbulent Flows

It is most convenient to derive equations of motion of the center of mass of disperse particles in a moving medium or a stochastic model of the process from symbolic equations of the system dynamics

$$\frac{d\overline{\chi}}{dt} = \overline{\Phi} \tag{12.1}$$

where $\overline{\chi}$ is a momentum vector of particles of a narrow size class at the moment of time t under study (a random function of time); $\overline{\Phi}$ is the principal vector of external forces acting on the system (a random function of time).

Equations for moment functions of the first order are obtained by applying a mathematical expectation operator to Eq. (12.1). Due to statistical linearity of Eq. (12.1), we obtain:

$$\frac{d\overline{K}}{dt} = \overline{F} \tag{12.2}$$

where $\overline{K} = <\overrightarrow{\chi}>$ is the mathematical expectation of the momentum of particles of a certain size class at a given moment of time t; $\overline{F} = <\overrightarrow{\Phi}>$ is the mathematical expectation of the principal vector of external forces acting on the system.

To pass from Eq. (12.1) to equations in moment functions of the second order, we first write these equations in fluctuations with respect to two arbitrary moments of time:

$$\frac{d\delta\chi_i^{(1)}}{dt_1} = \delta\Phi_i^{(1)}; \frac{d\delta\chi_j^{(2)}}{dt_2} = \delta\Phi_j^{(2)}, \tag{12.3}$$

where $\delta\chi_i^{(1)} = \chi_i^{(1)} - K_i^{(1)}, \delta\Phi_i^{(1)} = \Phi_i^{(1)} - F_i^{(1)}$ are fluctuations of momentum and of the principal vector of external forces referred to the moment of time t_1; $\delta\chi_j^{(2)} = \chi_j^{(2)} - K_j^{(2)}; \delta\Phi_j^{(2)} = \Phi_j^{(2)} - F_j^{(2)}$ are fluctuations of momentum and of the principal vector of external forces referred to the moment of time t_2.

We multiply the first equation of the system (12.3) by the momentum fluctuation $\delta\chi_j^{(2)}$, and the second one by $\delta\chi_i^{(1)}$, and apply the mathematical expectation operator after each multiplication. As a result, we obtain a system of two partial differential equations of the first order for determining the moment function of the second order $K_{ij} = <\delta\chi_i^{(1)}\delta\chi_j^{(2)}>$ of the system momentum:

$$\frac{\partial K_{ij}}{\partial t_1} = K_j^i; \frac{\partial K_{ij}}{\partial t_2} = K_i^j, \tag{12.4}$$

where

$$K_j^i = <\delta\Phi_i^{(1)}\delta\chi_j^{(2)}>; K_i^j = <\delta\chi_i^{(1)}\delta\Phi_j^{(2)}>$$

denote the moments of the connection function of the second order between the system momentum and external forces acting on the system.

The system of equations (12.4) is not closed, since it contains moment connection functions of the second order. To determine these unknown moment functions, we multiply the first equation of the system (12.3) by fluctuations of external forces vector $\delta\Phi_j^{(2)}$, and the second equation of this system by fluctuations $\delta\Phi_j^{(1)}$. Applying the mathematical expectation operator, we obtain

$$\frac{\partial K_i^j}{\partial t_1} = F_{ij}; \frac{\partial K_j^i}{\partial t_2} = F_{ij}, \tag{12.5}$$

where $F_{ij} = <\delta\chi_i^{(1)}\delta\chi_j^{(2)}>$ are moment functions of the second order of the principal vector of external forces acting on the system defined by the problem specification.

Equations (12.4) and (12.5) taken together form a closed system. Methods of solving linear partial differential equations of the first order for one unknown function are well-known. Thus, integrating Eq. (12.5) under respective initial conditions, we determine the unknown moment functions K_j^i and K_i^j.

A system of two linear partial differential equations of the first order for one unknown function of two independent variables is an involutory (Jacobian) system of differential equations, because the system of equations (12.5) satisfies integrability conditions

$$\frac{\partial K_i^j}{\partial t_1} = \frac{\partial K_j^i}{\partial t_2}. \tag{12.6}$$

Relationships (12.6) are identically true for systems of equations with continuous functions, which can be easily proved on the basis of relationships (12.5). Therefore, methods known from the general theory of partial differential equations

for complete involutory (Jacobian) systems are applicable to the solution of the present linear system of differential equations. When solving specific problems of gravitational classification, it is expedient to proceed as follows. First, we determine the entire set of functions satisfying the first equation of the system (12.4); then we determine a subset of functions satisfying the second equation of the same system. By solving jointly Eqs. (12.4) and (12.5), we determine moment functions of the second order. Hence, at the superposition of two arbitrarily chosen points in four-dimensional space, we obtain the momentum dispersion of the system.

To obtain a system of differential equations determining moment functions of the third and higher orders, an analogous approach should be used with a corresponding number of arbitrarily chosen points. For example, to determine moment functions of the third order, we should write expressions for fluctuations of Eq. (12.1) in three arbitrary points of a four-dimensional space:

$$\frac{d\delta\chi_i^{(1)}}{dt_1} = \delta\Phi_i^{(1)}; \frac{d\delta\chi_j^{(2)}}{dt_2} = \delta\Phi_j^{(2)}; \frac{d\delta\chi_m^{(3)}}{dt_3} = \delta\Phi_m^{(3)}. \tag{12.7}$$

We multiply the first equation of the system (12.7) by the product of fluctuations $\delta\chi_j^{(2)}\delta\chi_m^{(3)}$, the second equation – by $\delta\chi_i^{(1)}\delta\chi_m^{(3)}$, and the third – by $\delta\chi_i^{(1)}\delta\chi_j^{(2)}$.

After each multiplication, we apply the operator of mathematical expectation. As a result, we obtain a system of three linear partial differential equations of the first order for one unknown moment function of the third order $K_{ijm} = <\delta\chi_i^{(1)}\delta\chi_j^{(2)}\delta\chi_m^{(3)}>$ of three independent variables:

$$\frac{\partial K_{ijm}}{\partial t_1} = K_{jm}^i; \frac{\partial K_{ijm}}{\partial t_2} = K_{im}^j; \frac{\partial K_{ijm}}{\partial t_3} = K_{ij}^m \tag{12.8}$$

where the following notations are offered for mutual moment functions of the third order between the momentum vector of the system and the resultant vector of external forces acting on the system:

$$K_{ij}^m = <\delta\chi_i^{(1)}\delta\chi_j^{(2)}\delta\Phi_m^{(3)}>; K_{jm}^i = <\delta\Phi_i^{(1)}\delta\chi_j^{(2)}\delta\chi_m^{(3)}>; K_{im}^j = <\delta\chi_i^{(1)}\delta\Phi_j^{(2)}\delta\chi_m^{(3)}>.$$

This system of equations involves unknown moment functions of the third order K_{jm}^i, K_{im}^j and K_{ij}^m. To determine the moment function K_{jm}^i, we multiply the second equation of the system (12.7) by the product of fluctuations $\delta\Phi_i^{(1)}\delta\chi_m^{(3)}$ in two other points, and apply the mathematical expectation operator. As a result, we obtain a partial differential equation of the first order with an unknown moment function of the third order $K_m^{ij} = <\delta\Phi_i^{(1)}\delta\Phi_j^{(2)}\delta\chi_m^{(3)}>$ in its right-hand part. Then we multiply the third equation of the system (12.7) by the product of fluctuations $\delta\Phi_i^{(1)}\delta\Phi_j^{(2)}$ and apply the operator of mathematical expectation. As a result of the second operation, we find the second equation for determining the moment function K_m^{ij}. Thus, to

determine the moment function of the third order K^i_{jm}, we have a system of partial differential equations of the first order:

$$\frac{\partial K^i_{jm}}{\partial t_2} = K^{ij}_m; \frac{\partial K^{ij}_m}{\partial t_3} = F_{ijm}. \tag{12.9}$$

In the same way, we derive a system of partial differential equations for determining the moment function of the third order K^j_{im}

$$\frac{\partial K^j_{im}}{\partial t_1} = K^{ij}_m; \frac{\partial K^{ij}_m}{\partial t_3} = F_{ijm}. \tag{12.10}$$

To determine the moment function of the third order K^m_{ij}, we can write

$$\frac{\partial K^m_{ij}}{\partial t_1} = K^{im}_j; \frac{\partial K^{im}_j}{\partial t_3} = F_{ijm}. \tag{12.11}$$

From the solution of systems (12.8)–(12.11) with specified initial conditions, we determine unknown moment functions appearing in the right-hand parts of the system of differential equations (12.8). A system of three linear partial differential equations of the first order for determining one unknown third-order moment function of three independent variables is an involutory system of differential equations, since the integrability conditions are satisfied.

$$\frac{\partial K^i_{jm}}{\partial t_2} = \frac{\partial K^j_{im}}{\partial t_1}; \frac{\partial K^i_{jm}}{\partial t_3} = \frac{\partial K^m_{ij}}{\partial t_1}; \frac{\partial K^j_{im}}{\partial t_3} = \frac{\partial K^m_{ij}}{\partial t_2}. \tag{12.12}$$

In fact, the first integrability condition in the system (12.12) holds true on the basis of Eqs. (12.9) and (12.10). The second integrability condition also holds true, since the moment functions of the third order satisfy the following equations:

$$\frac{\partial K^m_{ij}}{\partial t_1} = K^{im}_j; \frac{\partial K^{im}_j}{\partial t_3} = K^{im}_j. \tag{12.13}$$

The validity of the third condition follows from the existence of the following relationships between moment functions of the third order:

$$\frac{\partial K^j_{im}}{\partial t_3} = K^{jm}_i; \frac{\partial K^m_{ij}}{\partial t_2} = K^{jm}_i. \tag{12.14}$$

Hence, the system of differential equations (12.8) is involutory. One can easily make sure that it is complete. Based on known properties of complete involutory systems of partial differential equations of the first order, a general solution to this system exists and is unique. In particular, the solution can be obtained by Mayer's method, method of successive solutions, etc.

Thus, we can readily obtain a system of partial differential equations for moment functions of an arbitrary order and formulate the conditions of their integrability. In the general case, it is a complete Jacobian system of partial differential equations of the first order for determining moment functions of an arbitrary order for the momentum and mutual moment functions between the system momentum and external forces, whose solution exists and is unique.

12.3 Equations of Particles Motion Taking into Account Their Rotation Around the Center of Mass in a Turbulent Flow

An equation of rotary motion of particles around the center of mass for a stochastic model of the process of gravitational classification can be obtained from the following equation of the system motion:

$$\frac{d\overline{\lambda}}{dt} = \overline{\pi}, \tag{12.15}$$

where $\overline{\lambda}$ is the momentum of particles of a certain size class at the moment of time under consideration (a random function of time); $\overline{\pi}$ is the total moment (principal moment) of external forces with respect to the gravity center of the system (a random function of time).

Equations for moment functions of the first order are obtained by applying the operator of mathematical expectation to Eq. (12.15)

$$\frac{d\overline{L}}{dt} = \overrightarrow{\mu}, \tag{12.16}$$

where $L = <\lambda>$ is the mathematical expectation of the momentum of particles of a certain size class (one particle or all initial material) at a given moment of time; $\mu = <\pi>$ is the mathematical expectation of the principal moment of external forces acting on the system.

Due to statistical linearity of the system of equations (12.15), the form of the system of equations (12.16) for moment functions of the first order coincides with corresponding classical equations of motion around the center of masses or system dynamics.

Let us write down fluctuations of Eq. (12.16) with respect to two arbitrary moments of time. Subtracting Eq. (12.16) from Eq. (12.15), we obtain

$$\frac{d\delta\lambda_i^{(1)}}{dt_1} = \delta\pi_i^{(1)}; \frac{d\delta\lambda_i^{(2)}}{dt_2} = \delta\pi_i^{(2)}, \tag{12.17}$$

where $\delta\lambda_i^{(1)} = \lambda_i^{(1)} - L_i^{(1)}; \delta\pi_i^{(1)} = \pi_i^{(1)} - \mu_i^{(1)}$ are fluctuations of the particles momentum and principal vector of external forces at the moment of time t_1;

$\delta\lambda_j^{(2)} = \lambda_j^{(2)} - L_j^{(2)}; \delta\pi_j^{(2)} = \pi_j^{(2)} - \mu_j^{(2)}$ are fluctuations of the particles momentum and principal vector of external forces at the moment of time t_2.

We multiply the first equation of the system (12.17) by the momentum fluctuation $\delta\lambda_j^{(2)}$, and the second equation by the momentum fluctuation $\delta\lambda_i^{(1)}$, and apply the mathematical expectation operator after each multiplication. As a result, we obtain a system of two partial differential equations of the first order for determining the moment function of the second order for the system momentum $L_{ij} = <\delta\lambda_i^{(1)}\delta\lambda_j^{(2)}>$:

$$\frac{\partial L_{ij}}{\partial t_1} = L_j^i; \frac{\partial L_{ij}}{\partial t_2} = L_i^j \tag{12.18}$$

where

$$L_j^i = <\delta\pi_i^{(1)}\delta\lambda_j^{(2)}>; L_i^j = <\delta\lambda_i^{(1)}\delta\pi_j^{(2)}>$$

denote moment connection functions of the second order between the system momentum and total moment of external forces with respect to the gravity center of the system.

The system of equations (12.18) is not closed, since it contains unknown moment connection functions of the second order L_j^i and L_i^j. To determine these moment functions, we multiply the first equation of the system (12.17) by the fluctuation of the principal moment of external forces $\delta\pi_j^{(2)}$, and the second equation of the system by the fluctuation $\delta\pi_i^{(1)}$. Applying the mathematical expectation operator, we obtain

$$\frac{\partial L_i^j}{\partial t_1} = \mu_{ij}; \frac{\partial L_j^i}{\partial t_2} = \mu_{ij}, \tag{12.19}$$

where

$$\mu_{ij} = <\delta\pi_i^{(1)}\delta\pi_j^{(2)}>$$

can be considered as known moment functions of the second order of the principal moment of external forces.

Equations (12.18) and (12.19) form a closed system. For its solution, well-known methods developed for systems of partial differential equations of the first order are used.

A system of two partial differential equations (12.18) of the first order for one unknown moment function of the second order of two independent variables satisfies the integrability condition

$$\frac{\partial L_i^j}{\partial t_1} = \frac{\partial L_j^i}{\partial t_2}$$

and, hence, is an involutory system of differential equations. As demonstrated above, a general solution of such a system exists and is unique. In this case, systems of differential equations for determining moment functions of an arbitrary order are obtained by methods similar to those described.

Systems obtained as a result of these derivations should be completed by equations of mutual moment functions between the momentums of the system under study. We write

$$\begin{aligned} B_i^j &= <\delta\chi_i^{(1)}\delta\lambda_j^{(2)}>; & B_j^i &= <\delta\lambda_i^{(1)}\delta\chi_j^{(2)}>; \\ P_i^j &= <\delta\Phi_i^{(1)}\delta\lambda_j^{(2)}>; & P_j^i &= <\delta\lambda_i^{(1)}\delta\Phi_j^{(2)}>; \\ Q_i^j &= <\delta\chi_i^{(1)}\delta\pi_j^{(2)}>; & Q_j^i &= <\delta\pi_i^{(1)}\delta\chi_j^{(2)}>; \\ R_i^j &= <\delta\Phi_i^{(1)}\delta\pi_j^{(2)}>; & R_j^i &= <\delta\pi_i^{(1)}\delta\Phi_j^{(2)}>. \end{aligned} \tag{12.20}$$

Then a system of two linear differential equations for determining one moment function B_i^j of two independent variables acquires the following form:

$$\frac{\partial B_i^j}{\partial t_1} = P_i^i; \frac{\partial B_i^j}{\partial t_2} = Q_i^j, \tag{12.21}$$

where unknown moment functions on the right-hand sides of the equations are determined by integrating systems with partial derivatives of the first order:

$$\frac{\partial P_i^j}{\partial t_2} = R_i^j; \frac{\partial Q_i^j}{\partial t_1} = R_j^i, \tag{12.22}$$

moment functions R_i^j being defined by the problem specification.

The system of partial differential equations (12.21) is an involutory system, since on the basis of relationships (12.22), integrability conditions are satisfied:

$$\frac{\partial P_i^j}{\partial t_2} = \frac{\partial Q_i^j}{\partial t_1}.$$

Moment functions B_j^i are determined by integrating a system of two partial differential equations of the first order:

$$\frac{\partial B_j^i}{\partial t_2} = P_{ji}^i; \frac{\partial B_j^i}{\partial t_1} = Q_j^i, \tag{12.23}$$

where the moment functions in the right-hand sides of the equation satisfy the relationships

$$\frac{\partial P_j^i}{\partial t_1} = R_{ji}^i; \frac{\partial Q_j^i}{\partial t_2} = R_{ji}^i. \tag{12.24}$$

The conditions of simultaneous equations

$$\frac{\partial P_j^i}{\partial t_1} = \frac{\partial Q_j^i}{\partial t_2}$$

are satisfied, as evident from Eq. (12.24). Therefore, the system of differential equations (12.23) is involutory. Hence, its solution exists and is unique.

In a general case, a system of partial differential equations of the first order for mutual moment functions of an arbitrary order between the system momentum and the moment of momentum is also an involutory system of differential equations whose solution exists and is unique.

12.4 Description of One-Dimensional Stationary Process of Gravitation Separation in a Turbulent Flow

We apply the developed computation method to the construction of a one-dimensional, somewhat simplified model of a stochastic process of gravitation separation in a turbulent flow. In this case, the momentum of particles of a narrow size class equals

$$\chi = \mu v. \tag{12.25}$$

The principal vector of external forces acting on a system is a random function of time

$$\Phi = -\mu g + \frac{1}{2}\alpha\rho_0\omega(v - \overline{\omega})^2, \tag{12.26}$$

where α is aerodynamic drag coefficient of particles of a narrow size class (a random magnitude); $\overline{\omega}$ is a random flow rate.

Substituting expressions of the momentum and principal vector of external forces (12.26) into Eq. (12.25), we obtain an equation of motion of particles of a narrow size class:

$$\mu\frac{dv}{dt} = -\mu g + \frac{1}{2}\alpha\rho_0\omega(v - \overline{\omega})^2. \tag{12.27}$$

Equation (12.27) is analogous to the Langevin-type equation of Brownian motion of particles. It is also symbolic, since it contains random magnitudes and functions. Speaking about operations with random magnitudes and functions, we imply operations with respective moment functions. Equations (12.27) are statistically nonlinear (they contain products of random magnitudes). For each narrow size class and small, in the generalized sense, variations of ascending flow

rates (i.e. in the sense of smallness of the ascending flow rate dispersion), Eq. (12.27) can be linearized by a known method. We denote

$$m = <\mu>;\ \lambda = <\alpha>;\ F = <\omega>.$$

Using the direct linearization method and applying the mathematical expectation operator to Eq. (12.27), we obtain

$$m\frac{d<\upsilon>}{dt} = -mg + \frac{1}{2}\lambda\rho_0 F(<\upsilon> - <\overline{\omega}>)^2. \tag{12.28}$$

This equation has the following solution:

$$<\upsilon> = <\overline{\omega}> - \sqrt{\frac{2mg}{\lambda\rho_0 F}}th\left(t\sqrt{\frac{\lambda\rho_0 Fg}{2m}}\right). \tag{12.29}$$

The problem of choosing an analytical formula of mean velocity of a turbulent flow fitting experimental data has been extensively discussed. Equation (12.29) describes mean velocity of particles of a narrow size class for a non-stationary process. In a steady (stationary) regime of particles motion in a turbulent counter-flow, this formula is simplified:

$$<\upsilon> = <\overline{\omega}> - \sqrt{\frac{2mg}{\lambda\rho_0 F}}, \tag{12.30}$$

where the average time of a transient process t_0 is determined from the relationship

$$t_0 \geqslant \sqrt{\frac{8m}{\lambda\rho_0 Fg}}.$$

The expression (12.30) differs from the formula of mean velocity of particles in a motionless medium by its first term only, which describes, in the present case, the velocity of an ascending medium flow averaged over an ensemble of realizations.

Let us determine central moments of random velocity of particles of a narrow size class for the case of a steady regime, i.e. when the momentum of these particles is a random value. It follows from this condition that the time derivative of the mean velocity of particles of a narrow size class and of correlational connection moments of various orders is identically equal to zero. Correlational connection moments of higher orders of random values appearing in Eq. (12.27) for a stationary process possess similar properties. We derive from Eqs. (12.27)–(12.29) the following linearized variational equations with respect to random values for a stationary process:

$$\delta\upsilon = \delta\overline{\omega} + \left(-\frac{\delta\mu}{m} + \frac{\delta\omega}{F} + \frac{\delta\alpha}{\lambda}\right)\sqrt{\frac{mg}{2\lambda\rho_0 F}}. \tag{12.31}$$

When deriving equations for determining central moments of the velocity of particles of a narrow class in a turbulent counterflow, it is assumed that the values $\overline{\omega}, \mu, \omega$ and α are uncorrelated random values. Successively multiplying Eq. (12.31) by variations $\delta\upsilon, \delta\overline{\omega}, \ \delta\mu, \delta\omega, \delta\alpha$ and applying the mathematical expectation operator after each multiplication, we obtain the following system of algebraic equations:

$$\begin{gathered}
<(\delta\upsilon)^2> = <\delta\overline{\omega}\delta\upsilon> + \left(\frac{<\delta\mu\delta\upsilon>}{m} + \frac{<\delta\omega\delta\upsilon>}{F} + \frac{<\delta\alpha\delta\upsilon>}{\lambda}\right)\sqrt{\frac{mg}{2\lambda\rho_0 F}}; \\
<\delta\upsilon\delta\overline{\omega}> = <(\delta\overline{\omega})^2>; \\
<\delta\upsilon\delta\omega> = -\frac{<(\delta\omega)^2>}{F}\sqrt{\frac{mg}{2\lambda\rho_0 F}}; \\
<\delta\upsilon\delta\mu> = \frac{<(\delta\mu)^2>}{m}\sqrt{\frac{mg}{2\lambda\rho_0 F}}; \\
<\delta\upsilon\delta\alpha> = \frac{<(\delta\alpha)^2>}{\lambda}\sqrt{\frac{mg}{2\lambda\rho_0 F}}.
\end{gathered} \tag{12.32}$$

From Eq. (12.23) we determine the velocity dispersion:

$$<(\delta\upsilon)^2> = <(\delta\overline{\omega})^2> + \left[\frac{<(\delta\mu)^2>}{m^2} + \frac{<(\delta\omega)>^2}{F^2} + \frac{<(\delta\alpha)^2>}{\lambda^2}\right]\sqrt{\frac{mg}{2\lambda\rho_0 F}}. \tag{12.33}$$

As follows from the equations, the output velocity of particles of a narrow size class correlates negatively with the mass of particles and positively – with their midlength section value and aerodynamic drag coefficient. It means that the output (extraction) velocity of particles of a narrow size class decreases with an increase in their mass and increases with increasing midlength section and aerodynamic drag coefficient, which corresponds to experimental data.

To write equations for the third-order moments of the velocity of particles of a narrow size class, we successively multiply Eq. (12.31) by variations of the following values:

$(\delta\upsilon)^2;\delta\upsilon\delta\overline{\omega};\delta\upsilon\delta\mu;\delta\upsilon\delta\alpha;(\delta\overline{\omega})^2;\delta\overline{\omega}\delta\mu;\delta\omega\delta\overline{\omega};\delta\overline{\omega}\delta\alpha;(\delta\mu)^2;\delta\mu\delta\omega;\delta\mu\delta\alpha;(\delta\omega)^2;\delta\omega$ $\delta\alpha;\delta(\alpha)^2$. Applying the mathematical expectation operator after every multiplication and rejecting terms identically equal to zero, we obtain:

$$\begin{gathered}
<(\delta\upsilon)^3> = <\delta\overline{\omega}(\delta\upsilon)^2> + \left(-\frac{<\delta\mu(\delta\upsilon)^2>}{m} + \frac{<\delta\omega(\delta\upsilon)^2}{F^2} + \frac{<\delta\alpha(\delta\upsilon)^2>}{\lambda^2}\right)\sqrt{\frac{mg}{2\lambda\rho_0 F}}; \\
<\delta\omega(\delta\upsilon)^2> = \frac{<(\delta\overline{\omega})^3>}{F}\sqrt{\frac{mg}{2\lambda\rho_0 F}}; \\
<\delta\omega(\delta\upsilon)^2> = <(\delta\overline{\omega})^3>; \\
<\delta\mu(\delta\upsilon)^2> = -\frac{<(\delta\mu)^3>}{\lambda}\sqrt{\frac{mg}{2\lambda\rho_0 F}}; \\
<\delta\alpha(\delta\upsilon)^2> = \frac{<(\delta\alpha)^3>}{\lambda}\sqrt{\frac{mg}{2\lambda\rho_0 F}}.
\end{gathered} \tag{12.34}$$

From the derived equations, we determine the central moment of the third order of the velocity of particles of a fixed size class:

$$<(\delta v)^3> = <(\delta\overline{\omega})^3> + \left(-\frac{<(\delta\mu)^3>}{m^3} + \frac{<(\delta\omega)^3>}{F^3} + \frac{<(\delta\alpha)^3}{\lambda^3}\right) \times \sqrt{\frac{mg}{2\lambda\rho_0 F}} \cdot \frac{mg}{2\lambda\rho_0 F}. \tag{12.35}$$

The central moment of the velocity of particles of a narrow size class of the fourth order is determined in a similar way. Multiplying successively Eq. (12.31) by products of variations of random values $(\delta v)^3; (\delta\overline{\omega})^3; (\delta\mu)^3;\ (\delta\omega)^3; (\delta\alpha)^3; (\delta v)^2 \times \times\delta\omega; (\delta v)^2\delta\alpha; (\delta v)^2\delta\mu$, etc., and applying the mathematical expectation operator after every multiplication, we obtain a system of algebraic equations for determining the fourth-order moment of the velocity of particles of a narrow size class and all remaining correlation moments. The final formula obtained by solving this system for the fourth-order central moment of the velocity of particles of a narrow size class in a turbulent flow is determined by the dependence

$$<(\delta v)^4> = <(\delta\overline{\omega})^4> + \left(\frac{<(\delta\mu)^4>}{m^4} + \frac{<(\delta\omega)^4>}{F^4} + \frac{<(\delta\alpha)^4>}{\lambda^4}\right)\frac{m^2 g^2}{4\lambda^2\rho_0^2 F^2}. \tag{12.36}$$

Thus, we have obtained a sequence of moments $<v>; <(\delta v)^3>;\ <(\delta v)^4>$, etc. for a random velocity of particles of a narrow size class. Now the initially stated problem can be formulated as follows: To reconstruct the distribution density of the velocity of particles of a narrow size class by its weighed moments (12.30), (12.33), (12.35), (12.36). This problem is known in mathematics as the classical Hausdorff moment problem**.**

One of the possible ways of reconstructing an arbitrary distribution density is based on an expansion in series by the normal law (Gram–Charlier series). Expanding the density function $f(x)$ in series using the normal distribution function and restricting ourselves with five terms of the series, we obtain

$$f(x) = \frac{1}{\sqrt{<(\alpha v)^2>}} \times \left[\phi(z) - \frac{1}{6}\cdot\frac{<(\delta v)^3>}{<(\delta v)^2>^{3/2}}\phi^{III}(z) + \frac{1}{24}\left(\frac{<(\delta v)^4>}{<(\delta v)^2>^2} - 3\right)\phi^{IV}(z)\right], \tag{12.37}$$

where $\phi(z) = \phi\left(\frac{x-<v>}{<(\delta v)^2>}\right) = \frac{1}{2\pi}\phi^{-\frac{1}{2}z^2}$ is the normal distribution density, $\phi^{III}(z)$ and $\phi^{IV}(z)$ are, respectively, the third and fourth derivatives of the normal density with respect to z.

The approximation precision of the mentioned method in each specific case can be evaluated by higher-order (fifth, sixth, etc.) moments using subsequent terms of the expansion series.

12.5 One-Dimensional Model of a Non-stationary Process

We examine the process of gravitational separation of materials on one-dimensional model of the process in a non-stationary case. We can write moment functions equations for each narrow size class and small (in a generalized sense) velocity fluctuations of a statistically homogeneous turbulent flow using the method of direct linearization of Eq. (12.27). Later on, as usual, when we mention operations with random functions, we imply operations with corresponding moment functions.

Now we pass from a system of ordinary differential equations to partial equations in moment functions of the first order. We assume initial conditions for moment functions of the velocity of particles of a narrow size class equal to the respective moments of the flow velocity, and zero initial conditions for the remaining moment functions. Then moment functions of the velocity of particles of a narrow size class of an arbitrary order for the process under consideration can be expressed as follows:

$$\begin{gathered} <\upsilon> = <\overline{\omega}> - \sqrt{\frac{2g<\mu>}{\rho_0<\alpha><\omega>}} th\left(t\sqrt{\frac{\rho_0 g<\alpha><\omega>}{2<\mu>}}\right); \\ K(t_1 \ldots t_k) = <(\delta\overline{\omega})^k> + \left[\frac{<(\delta\mu)^k>}{<\mu>^k}(-1)^k + \frac{<(\delta\omega)^k>}{<\omega>^k} + \frac{<(\delta\alpha)^k>}{<\alpha>^k}\right] \prod_{i=1}^{k} f(t_k) \\ \text{where } f(t) = \sqrt{\frac{<\mu>g}{2<\alpha><\omega>\rho_0}} th\left(t\sqrt{\frac{\rho_0 g<\alpha><\omega>}{2<\mu>}}\right) + t\,\mathrm{csc}\,h^2\left(t\sqrt{\frac{\rho_0 g<\alpha><\omega>}{2<\mu>}}\right). \end{gathered} \tag{12.38}$$

At $t_i \to \infty (i = 1, 2, \ldots, k)$, moment functions of the velocity of particles of a narrow size class of an arbitrary order tend to a constant value coinciding, in the limit, with the moments of particles velocities for a stationary process.

12.6 Statistical Equations of a Random Process of Gravitational Separation

For a deterministic flow, we restrict ourselves to an account of only two random values – particles distributions by mass and by their midlength cross-section area.

First we assume that the particles distributions by mass and by their midlength section area are close to a normal law, although it is not always the case in real conditions.

$$\phi_1(\mu) = \frac{1}{\sqrt{2\pi}\sigma_\mu} e^{-\frac{(\mu - <\mu>)^2}{2\sigma_\mu^2}};$$

$$\phi_2(\omega) = \frac{1}{\sqrt{2\pi}\sigma_\omega} e^{-\frac{(\omega - <\omega>)^2}{2\sigma_\omega^2}},$$

where ϕ_1 and (μ) are, respectively, densities of the normal law of particles distributions by mass and by their midlength section area; σ_μ and σ_ω are root-mean-square deviations of the values μ and ω; $<\mu>$ and $<\omega>$ are mathematical expectations of the mass and characteristic area of a particle.

The particle velocity at the initial section of motion up to the moment of time $t \leqslant \sqrt{\frac{4}{\gamma g}}$ is a random function of time

$$\upsilon = \omega - \sqrt{\frac{g}{\gamma}} th \sqrt{\gamma g} t,$$

where $\gamma = \frac{1}{2} C_\rho \frac{\omega}{\mu}$ is a random value; C_ρ is a product of all constants.

At the further motion $t \geqslant \sqrt{\frac{4}{\gamma g}}$ the particle velocity is time-independent:

$$\upsilon = \omega - \sqrt{\frac{g}{\gamma}} \tag{12.39}$$

Let us find the regularity of the velocity distribution for a steady-state motion. For this purpose, we transform formula (12.33) as follows:

$$\upsilon = \omega - \sqrt{b\eta}, \tag{12.40}$$

where $b = \frac{2g}{C_\rho}, \eta = \frac{\mu}{\omega}$.

As evident from Eq. (12.40), to find this regularity, two problems should be solved:

1. To find the distribution density for the magnitude $\eta = \frac{\mu}{\omega}$, where μ and ω are random values distributed according to the normal law
2. To find the distribution density of a continuous random magnitude $[\upsilon - f(\upsilon)]$, if another magnitude η is connected by a stochastic dependence with it:

$$\upsilon = \omega - \sqrt{b\eta}$$

We find the solution of the first problem in the assumption that the magnitudes μ and ω are independent. It means that their combined distribution density is a product of density functions μ and ω.

The probability of the relationship $\frac{\mu}{\omega} \leqslant x$ is expressed by an integral of the combined density function over the region determined by inequalities $\omega > 0$ and $\mu < x\omega$,

$$P(x) = -\frac{1}{2\pi\sigma_\mu\sigma_\omega} \iint\limits_{\substack{\omega > 0 \\ \mu < x\omega}} e^{-\frac{(\mu-<\mu>)^2}{2\sigma_\mu^2}} e^{-\frac{(\omega-<\omega>)^2}{2\sigma_\omega^2}} d\mu d\omega. \tag{12.41}$$

We perform the following change of variables in Eq. (12.41):

$$\mu = uv, \omega = v.$$

Then we obtain

$$P(x) = \frac{1}{2\pi\sigma_\mu\sigma_\omega} \int\limits_{-\infty}^{x} du \int\limits_{0}^{\infty} ve^{-\frac{(uv-<\mu>)^2}{2\sigma_\mu^2}} e^{-\frac{(v-<\omega>)^2}{2\sigma_\omega^2}} dv. \tag{12.42}$$

We transform the internal integral:

$$\int\limits_{0}^{\infty} ve^{-\frac{(uv-<\mu>)^2}{2\sigma_\mu^2}} e^{-\frac{(v-<\omega>)^2}{2\sigma_\omega^2}} dv = \int\limits_{0}^{\infty} ve^{P(u)v^2+2q(u)v-r} dv = -e^{-r} \int\limits_{0}^{\infty} ve^{-Pv^2+2qv} dv,$$

where

$$\left.\begin{array}{c} P(u) = \frac{1}{2\sigma_\mu^2} + \frac{u^2}{2\sigma_\mu^2} \\ q(u) = \frac{<\omega>}{2\sigma_\mu^2} + \frac{u<\mu>}{2\sigma_\mu^2} \\ r = \frac{<u>^2}{2\sigma_\mu^2} + \frac{<\omega>}{2\sigma_\mu^2} \end{array}\right\}. \tag{12.43}$$

Taking into account Eq. (12.43), Eq. (12.42) acquires the following form after integration:

$$P(x) = \frac{1}{2\pi\sigma_\omega\sigma_\mu} e^{-r} \int\limits_{-\infty}^{x} \left\{\frac{1}{2P(u)} + e^{\frac{q^2}{P}} \frac{q}{2P} \sqrt{\frac{\pi}{P}} \left[1 + \Phi\left(\frac{q}{\sqrt{P}}\right)\right]\right\} du. \tag{12.44}$$

Differentiating Eq. (12.44) with respect to x, we get the distribution density of the magnitude

$$f(u) = \frac{1}{2\pi\sigma_\mu\sigma_\omega} e^{-r} \left\{\frac{1}{2P} + e^{\frac{q^2}{P}} \frac{q}{2P} \sqrt{\frac{\pi}{P}} \left[1 + \Phi\left(\frac{q}{\sqrt{P}}\right)\right]\right\} \tag{12.45}$$

Thus, the first problem is solved.

Now we solve the second problem, i.e. find the distribution density of the magnitude

$$\upsilon = \omega - \sqrt{b\eta},$$

where the magnitude η is distributed according to Eq. (12.45).

As shown in probability theory, the differential distribution function of the magnitude η is determined by the dependence

$$\phi(\upsilon) = f[\psi(\upsilon)]|\psi'|,$$

where $\eta = \psi(\upsilon) = \frac{(\omega-\upsilon)^2}{b}$; $\psi' = \frac{2(\omega-\upsilon)}{b}$.

Thus, we obtain

$$\phi(\upsilon) = \frac{2}{b} f\left[\frac{(\omega-\upsilon)^2}{b}\right]|\upsilon - \omega|, \tag{12.46}$$

where the function $f(x)$ is specified by Eq. (12.45).

An integral function of the velocity distribution is estimated, as known, through the differential function using the equation

$$F(x) = \int_{-\infty}^{x} \phi(\upsilon)d\upsilon.$$

12.7 Computation of Fractional Separation of a Narrow Class

Numerical computations of the distribution density of particles velocities are performed using Eqs. (12.45) and (12.46) with the following initial data:

1. Boundary size of separation $d = 0.003$ m
2. Mathematical expectation of the particles midlength section area $<\omega> = 7 \times 10^{-6}\text{m}^2$
3. Root-mean-square deviation of the midlength section area $\sigma_\omega = 2 \times 10^{-6}$ m^2
4. Mathematical expectation of the particle mass $<\mu> = 3 \times 10^{-6}$ kg s^2/m
5. Root-mean-square deviation of the particle mass $\sigma_\mu = 1 \times 10^{-6}$ kg s^2/m
6. Air flow rate $\omega = 14$ m/s
7. Aerodynamic drag coefficient of the particles $C = 0.42$ (that of a sphere)

The computation is performed for the range of velocities of particles of the examined class from -8 to $+10$ m/s. To clarify the sequence of computations, we give below a computation for one point corresponding to $\upsilon = 2$ m/s :

$$b = \frac{2g}{C_\rho} = \frac{2 \times 9.8}{0.42 \times 0.125} = 373.333;$$

$$\lambda = \frac{(\omega - \upsilon)^2}{b} = \frac{(14-2)^2}{373.333} = 0.3857;$$

$$r = \frac{1}{2}\left(\frac{<\mu>^2}{\sigma_\omega^2} + \frac{<\omega>^2}{\sigma_\omega^2}\right) = \frac{1}{2}\left(\frac{9\times 10^{-12}}{1\times 10^{-12}} + \frac{49\times 10^{-12}}{4\times 10^{-12}}\right) = 10.625;$$

$$p(\lambda) = \frac{1}{2}\left(\frac{1}{\sigma_\omega^2} + \frac{\lambda^2}{\sigma_\omega^2}\right) = \frac{1}{2}\left(\frac{1}{4}\times 10^{12} + 10^{12}\times 0.1488\right) = 0.1994\times 10^{12};$$

$$q(\lambda) = \frac{1}{2}\left(\frac{<\omega>}{\sigma_\omega^2} + \frac{\lambda<\mu>}{\sigma_\omega^2}\right) = \frac{1}{2}\left(\frac{7\times 10^{-6}}{4\times 10^{-12}} + \frac{0.3857\times 3\times 10^{-6}}{10^{-12}}\right)$$
$$= 1.4536\times 10^6;$$

$$f(\lambda) = \frac{e^{-r}}{4\pi\sigma_\omega\sigma_\mu p}\left\{1 + \sqrt{\pi}\frac{q}{\sqrt{p}}e^{\frac{q^2}{p}}\left[1 + \Phi\left(\frac{q}{\sqrt{p}}\right)\right]\right\}$$
$$= \frac{0.0000243}{4\times 3.14\times 2\times 10^{-6}\times 1\times 10^{-6}\times 0.1994\times 10^{12}}$$
$$[1 + 1.7724\times 3.256\times 40070(1+1)] = 2.24039;$$

$$\phi(\upsilon) = \frac{2}{b}\psi(\lambda)|\upsilon - \omega| = \frac{2\times 2.24039}{373.333}\times 12 = 0.144026.$$

Distribution density at other particle velocity values is determined in the same way.

Figure 12.1a shows a differential function of particles velocity distribution, and Fig. 12.1b an integral function of particles velocities distribution. It follows from Fig. 12.1b that 32% of particles of the class under study get into the coarse product and 68% into the fine product. In other words, this computation allows us to establish the degree of fractional extraction of a narrow size class and, hence, principal parameters of the process.

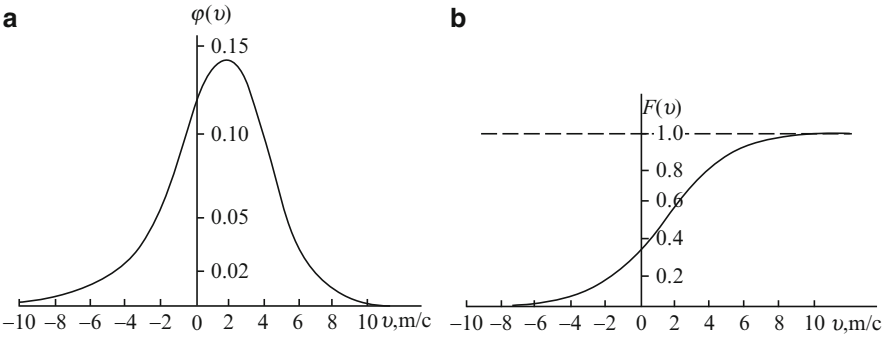

Fig. 12.1 (**a**) Differential function of particles distribution in velocities. (**b**) Integral function of particles distribution in velocities

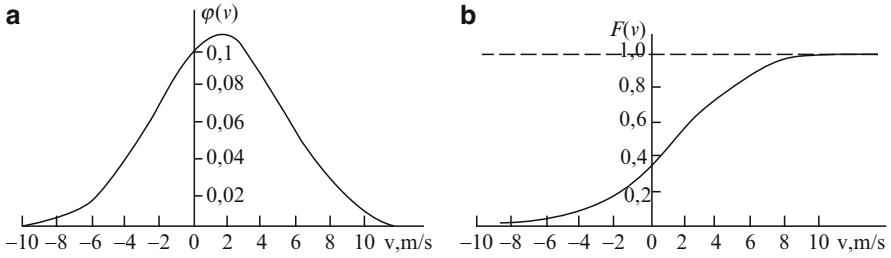

Fig. 12.2 (**a**) Differential distribution function of particles velocity estimated by approximate method. (**b**) Integral distribution function of particles velocity estimated by approximate method

12.8 Approximate Computation Method

An exact method of computing the differential distribution function can be essentially simplified by assuming the normal law of the particles velocity distribution in the form

$$f(\upsilon) = \frac{1}{\sqrt{2\pi}\sigma_\upsilon} e^{-\frac{(\upsilon - <\upsilon>)^2}{2\sigma_\upsilon^2}}. \tag{12.47}$$

Now it remains to find the parameters of this law – mathematical expectation and particles velocity dispersion.

To find mathematical expectation and particles velocity dispersion, we use equation

$$\upsilon = \omega - \sqrt{b\frac{\mu}{\omega}}. \tag{12.48}$$

It follows from Eq. (12.48) that particle velocity is a certain statistically nonlinear function of two independent variables (containing products of random magnitudes). We perform direct linearization of this equation with respect to mathematical expectation by a known method that is the most widely used in the theory of random functions. As a result, we obtain:

$$\upsilon = \omega - \left[\sqrt{b\frac{<\mu>}{<\omega>}} + \frac{1}{2}\sqrt{\frac{b}{<\omega><\mu>}}(\mu - <\mu>) - \frac{1}{2<\omega>^2}\sqrt{b<\mu><\omega>}(\omega - <\omega>)\right] \tag{12.49}$$

Applying the mathematical expectation operator to Eq. (12.49), we derive an expression for the mathematical expectation of particles velocity:

$$<\upsilon> = \omega - \sqrt{b\frac{<\mu>}{<\omega>}}. \tag{12.50}$$

To determine particles velocity dispersion, we rewrite Eq. (12.49) in variations:

$$\delta\upsilon = \frac{1}{2}\sqrt{\frac{b}{<\omega><\mu>}}\delta\mu - \frac{1}{2<\omega>^2}\sqrt{b<\mu><\omega>}\delta\omega, \tag{12.51}$$

where, by definition of the variation of a random value, the following notations are used:

$$\delta\upsilon = \upsilon - <\upsilon>;\ \delta\mu = \mu - <\mu>;\ \delta\omega = \omega = <\omega>.$$

By definition, random value dispersion is the mathematical expectation of squared variation of this random value. Therefore, to compute the particles velocity dispersion, it is sufficient to multiply Eq. (12.51) by itself and apply the mathematical expectation operator. Using the condition of independence of random values ω and μ (whence it follows that the correlation moment $<\delta\mu\delta\omega> = 0$), we obtain the following equation for the dispersion of a random value:

$$\sigma_\upsilon^2 = \frac{1}{4}\left(\frac{b}{<\omega><\mu>}\sigma_\mu^2 + \frac{b<\mu>}{<\omega>}\sigma_\omega^2\right). \tag{12.52}$$

Thus, the parameters of the particles distribution function are determined through the mathematical expectation and dispersion of mass and midlength section of particles. To construct differential and integral distribution functions, it is expedient to reduce them to tabulated functions – a normalized and centralized distribution density function and the Laplace integral. Tables of these functions can be found in textbooks and manuals on probability theory and mathematical statistics. For this purpose, we perform the following change of variables

$$\frac{\upsilon - <\upsilon>}{\sigma_\upsilon} = t$$

in equation

$$f(\upsilon) = \frac{1}{\sqrt{2\pi}\sigma_\upsilon}e^{-\frac{(\upsilon-<\upsilon>)^2}{2\sigma_\upsilon^2}}. \tag{12.53}$$

Then Eq. (12.46) is transformed into

$$f(\upsilon) = \frac{1}{\sigma_\upsilon}T,$$

where $T = \frac{1}{\sqrt{2\pi}}e^{-\frac{t^2}{2}}$ is a tabulated function.

We express the distribution function of random velocity υ through the Laplace function:

$$F(x) = P(\upsilon < x) = \frac{1}{2}\left[\Phi\left(\frac{<\upsilon> - x}{\sigma_\upsilon\sqrt{2}}\right) + 1\right], \tag{12.54}$$

where $\Phi(x)$ is a tabulated function.

Since the functions $T(x)$ and $\Phi(x)$ are tabulated, it considerably simplifies the construction of differential and integral distribution functions using an approximation method. It is sufficient to compute mathematical expectation and dispersion of particles velocities using Eqs. (12.50) and (12.51), find the tabular values of $T(x)$ and $\Phi(x)$ functions corresponding to the computed values and perform the remaining operations according to Eq. (12.54).

To evaluate the accuracy of the approximate method, numerical calculations were performed on the basis of initial data given above.

The calculations were performed according to the following scheme:

$$b = \frac{2g}{C_\rho} = \frac{2 \times 9.8}{0.42 \times 0.125} = 373.333;$$

$$\Delta = \sqrt{b\frac{<\mu>}{<\omega>}} = \sqrt{373.333 \times \frac{3 \times 10^{-6}}{7 \times 10^{-6}}} = 12.65;$$

$$<\upsilon> = \omega - \Delta = 14 - 12.65 = 1.35;$$

$$\sigma_\upsilon^2 = \frac{b}{4}\left(\frac{1}{<\omega><\mu>}\sigma_\mu^2 + \frac{<\mu>}{<\omega>^3}\sigma_\omega^2\right)$$

$$= \frac{373.333}{4}\left(\frac{1 \times 10^{-12}}{7 \times 10^{-6} \times 3 \times 10^{-6}} + \frac{3 \times 10^{-6} \times 4 \times 10^{-12}}{7^3 \times 10^{-18}}\right) = 7.72.$$

The parameter t and the Laplace function argument are determined from mathematical expectation and root-mean-square deviation. Tabular values of T and Φ functions corresponding to the computed values are taken, and the differential and integral functions are found using the respective formulas.

Figure 12.2 presents the differential and integral distribution functions of the particles velocities computed using the approximate method. It is obvious from the comparison of curves given in Figs. 12.1 and 12.2 that the approximate method of determining the velocity distribution function gives a sufficiently reliable approximation. The systematic error in the determined integral distribution function does not exceed 5%.

Thus, the obtained dependencies make it possible to determine the probability of the output of particles of a narrow size class into classified products, i.e. to determine the extent of fractional separation of various classes. This creates the

necessary prerequisites for computed prediction of the anticipated effect and other parameters of the gravitational classification process.

It is noteworthy that other distribution laws of random values are equally applicable, for example, a more general normal-logarithmic law, which best meets the parameters of particles of milled materials.

Chapter 13
Mass Transfer in Critical Regimes of Two-Phase Flows

Abstract A mathematical model of separating cascade is developed using chain fractions. For its solution, a system of $2z$ coupled equations (z being the number of stages in the cascade) was examined. On the basis of their solution, final expressions for fractional extraction in the cascade are derived. The analysis of these expressions has revealed the best stage for material feed into the apparatus. A stationary model of the process is developed and discretely solved. This solution allowed us to obtain an instant distribution of the material mass over the cascade stages. Optimization conditions for principal parameters of multistage separation are analyzed. Their empirical adequacy to the obtained results is shown.

Keywords Cascade · Stage · Extraction · Chain fractions · System of equations · Optimization · Efficiency · Adequacy · Distribution · Discontinuity · Stability

13.1 Mathematical Model of a Separating Cascade

Separation of solid bulk materials is a complicated process because their initial composition is, as a rule, a fractional mixture, and all fractions simultaneously participate in the separation process distributing the material among final products in certain ratios. Cascade separation can be clearly described using chain fractions.

Cascade separation is characterized by a combination of several separation stages within one apparatus. Figure 7.1a shows several types of cascade pneumatic classifiers for bulk materials. Air flow is fed to a particular cascade apparatus from below, while the material to be separated can be fed to any stage. Light fine particles are carried upwards by the flow and trapped in special facilities, and heavy coarse ones settle against the flow. Changing the number of stages in the apparatus and the

E. Barsky, *Critical Regimes of Two-Phase Flows with a Polydisperse Solid Phase*, Fluid Mechanics and Its Applications 93,
DOI 10.1007/978-90-481-8838-3_13,

site of material feed, we can affect both the separation efficiency and the quality of the obtained products, depending on technological requirements. The total polyfractional initial composition of the material can be conventionally represented as consisting of particles of narrow size classes. It is generally accepted in engineering calculations that in a narrow class the maximal size of particles exceeds twice the minimal one, for example, (1–0.5), (0.5–0.25), (0.25–0.125), etc.

A schematic diagram of a narrow fraction distribution in a cascade separator is presented in Fig. 7.1a. Figure 7.1b shows a separation mechanism in one stage. In these figures, stages are numbered top-down. We denote by i^* the stage into which the initial material to be separated is fed. The number of stages in a specific apparatus is denoted by z. Any stage between 1 and z except i^* is denoted by i.

The value characterizing a narrow class extraction upwards in one stage can be represented as

$$k = \frac{r_{i-1}}{r_i},$$

where r_i is the initial content of particles of the class under study at the ith stage; r_{i-1} is the number of particles of the same class passing to the stage above.

It is noteworthy that this factor can vary for different classes within the limits of $0 \leq k \leq 1$.

Since in a steady regime the material is not accumulated in stages, a portion of the initial fraction equal to $(1 - k)$ passes to a stage located below.

To simplify the conclusions, we take the total content of a narrow class in the initial mixture as a unity. Here the following relations are always valid:

$$\left.\begin{array}{c} F_f(x) + F_c(x) = 1 \\ F_f(x) = r_1 \cdot k \\ F_c(x) = r_z(1-k) \\ r_f(x) = F_f(x) \cdot r_s(x) \\ r_f(x) + r_c(x) = r_s(x) \end{array}\right\} \tag{13.1}$$

where $F_f(x)$ is a portion of a narrow class with the mean size x that has passed out of the entire apparatus upwards.

$F_c(x)$ is a portion of the same narrow class that has passed out of the apparatus downwards.

r_1 is a portion of the narrow class content in the first upper stage.

r_z is a portion of the same class content in the last lower stage.

$r_f(x); r_c(x)$ is a particular narrow class content in the output of the upper and lower products.

$r_s(x)$ is the narrow class content in the initial product.

Special studies have been carried out in order to find the dependence of the coefficient k on the number of the apparatus stages. The experiments were performed on a shelf apparatus (Fig. 13.1a). In the first group of experiments, the initial material was fed to the upper stage $(i^* = 1)$, and the number of stages amounted to $z = 2; 6; 10; 14$.

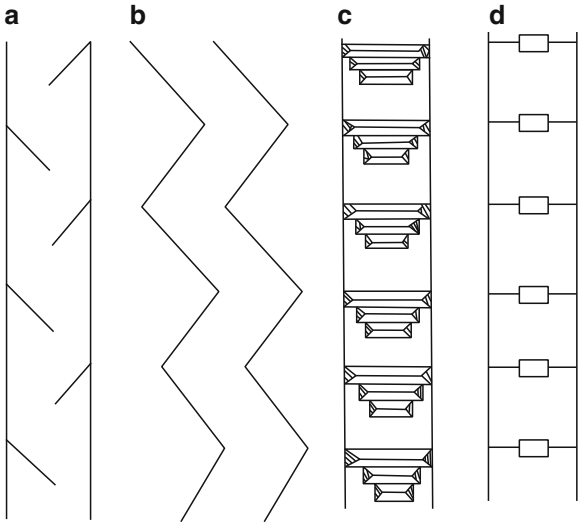

Fig. 13.1 Certain types of cascade classifiers: (**a**) with inclined shelves; (**b**) "zigzag"; (**c**) poly-cascade; (**d**) with radial grates

In the second group of experiments, the material was fed to the middle part of the apparatuses.

$$(z = 3; i^* = 2)$$
$$(z = 7; i^* = 4)$$
$$(z = 11; i^* = 6)$$
$$(z = 15; i^* = 8)$$

Ground quartzite with the average size of narrow classes equal to 0.094, 0.1875, 0.375, 0.75 mm was used in the experiments. The experiments were carried out at exactly the same air flow velocity ensuring the distribution of all classes into both products at different values of k and solid phase concentration in the flow. Experimental results are shown in Fig. 13.2. It follows that the value of the coefficient k in these conditions remains stable. Apparently, it is due to the structural similarity of the stages and similarity of aerodynamic conditions therein.

In the stationary regime of the process, the quantity of particles in each stage remains unchanged in time. It means that the number of particles entering a certain stage i equals the number of particles leaving this stage, since the material is not accumulated within a stage. Hence, for any stage i the following relation is valid (Fig. 7.1a):

$$r_i(1-k) + r_i \cdot k = r_{i-1}(1-k) + r_{i=1} \cdot k. \tag{13.2}$$

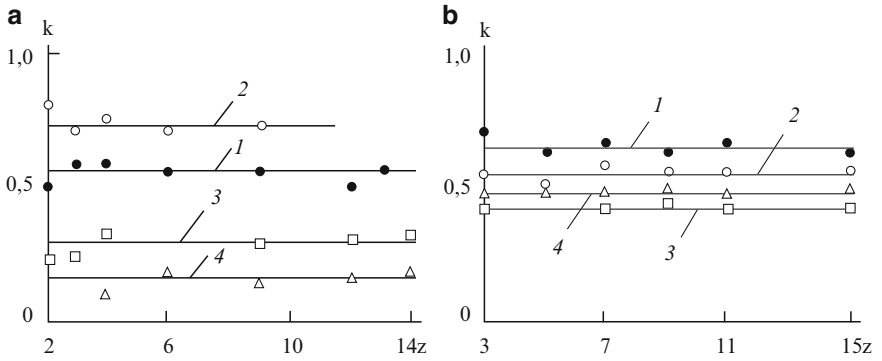

Fig. 13.2 Dependence of the distribution coefficient k on the number of stages in a cascade classifier with upper (a) and mid-point (b) feeding of the material: (**a**) 1 – $k = 0.57$; 2 – $k = 0.73$; 3 – $k = 0.3$; 4 – $k = 0.18$; (**b**) 1 – $k = 0.65$; 2 – $k = 0.57$; 3 – $k = 0.43$; 4 – $k = 0.49$

For the material fed from above $(i^* = 1)$ into an apparatus consisting of z stages, the relative material content at each stage can be described by a system of z equations:

$$\left.\begin{array}{c} r_1 = r_2 \cdot k + 1 \\ r_2 = r_1(1-k) + r_3 \cdot k \\ r_3 = r_2(1-k) + r_4 \cdot k \\ \cdots\cdots\cdots\cdots\cdots\cdots \\ r_i = r_{i-1}(1-k) + r_{i+1} \cdot k \\ \cdots\cdots\cdots\cdots\cdots\cdots \\ r_{z-1} = r_{z-2}(1-k) + r_z \cdot k \\ r_z = r_{z-1}(1-k) \end{array}\right\}. \tag{13.3}$$

Proceeding from (13.3), the narrow fraction quantity in the next-to-last stage can be expressed by excluding their content at the last stage:

$$r_{z-1} = r_{z-2}(1-k) + r_{z-1}(1-k)k,$$

hence,

$$r_{z-1} = \frac{r_{z-2}(1-k)}{1-k(1-k)}.$$

Similarly, the following can be written for $z-2$ stage:

$$r_{z-2} = r_{z-3}(1-k) + \frac{r_{z-2}(1-k)k}{1-k(1-k)}$$

and

$$r_{z-2} = \frac{r_{z-3}(1-k)}{1-\frac{k(1-k)}{1-k(1-k)}}.$$

Analogous reasoning shows that a recurrent relation expressed by a chain fraction

$$r_i = r_{i-1}\frac{(1-k)}{z-1\left\{\begin{array}{l} 1-\frac{k(1-k)}{1-\frac{k(1-k)}{1-\frac{k(1-k)}{1-\frac{k(1-k)}{\ddots}}}} \\ \qquad\qquad \ddots \\ 1-\frac{k(1-k)}{1} \end{array}\right.} \tag{13.4}$$

corresponds to the system of equations (13.3).

The chain fraction (13.4) makes it possible to find the share of the narrow class content at any stage of a cascade and visually demonstrates the contribution of all other stages to this content. It follows from (13.3) for the first stage that

$$r_1 = r_2 \cdot k + 1$$

It follows from (13.4) that for the second stage we can write

$$r_2 = \frac{r_1(1-k)}{z-2\left\{\begin{array}{l} 1-\frac{k(1-k)}{1-\frac{k(1-k)}{1-\frac{k(1-k)}{\ddots}}} \\ \qquad\qquad \ddots \\ 1-k(1-k) \end{array}\right.} \tag{13.5}$$

We substitute (13.5) into the expression for the first stage denoting the denominator of the chain fraction by A_{z-2} :

$$r_1 = \frac{r_1(1-k)}{A_{z-2}} \cdot k + 1.$$

Hence,

$$r_1\left(1-\frac{k(1-k)}{A_{z-2}}\right) = 1$$

$$r_1 = \frac{1}{z-1\left\{\begin{array}{l} 1-\frac{k(1-k)}{1-\frac{k(1-k)}{1-\frac{k(1-k)}{1-\frac{k(1-k)}{\ddots}}}} \\ \qquad\qquad \ddots \\ 1-k(1-k) \end{array}\right.} \tag{13.6}$$

Proceeding from the fact that

$$F_f(x)_{(z-1)} = r_1 \cdot k,$$

we obtain for $F_f(x)_{(z-1)}$, implying that the apparatus height is limited by the $(z-1)$ stage,

$$F_f(x)_{(z-1)} = \frac{k}{z-1\left\{\begin{array}{c} 1-\frac{k(1-k)}{1-\frac{k(1-k)}{1-\frac{k(1-k)}{\ddots}}} \\ \ddots \\ 1-k(1-k) \end{array}\right.} \tag{13.7}$$

We can write for the entire apparatus:

$$F_f(x)_{(z)} = \frac{k}{z\left\{\begin{array}{c} 1-\frac{k(1-k)}{1-\frac{k(1-k)}{1-\frac{k(1-k)}{\ddots}}} \\ \ddots \\ 1-k(1-k) \end{array}\right.} \tag{13.8}$$

At the distribution coefficient $k \neq 0.5$, we can find a general expression for the chain fraction.

We denote the denominator of the chain fraction by A_n, where n corresponds to the number of units in the continuous fraction.

Let us find the form of A_n dependence keeping in mind that

$$A_n = 1 - \frac{k(1-k)}{A_{n-1}}.$$

We can write:

$$A_1 = 1 = k + (1-k) = \frac{k^2 - (1-k)^2}{k-(1-k)};$$

$$A_2 = 1 - \frac{k(1-k)}{A_1} = k + (1-k)^2 = \frac{\left[k + (1-k)^2\right]k - (1-k)}{k^2 - (1-k)^2} = \frac{k^3 - (1-k)^3}{k^2 - (1-k)^2};$$

$$A_3 = 1 - \frac{k(1-k)}{A_2} = 1 - (1-k)\frac{k^2 - (1-k)^2}{k^3 - (1-k)^3} = \frac{k^4 - (1-k)^4}{k^3 - (1-k)^3}.$$

Using the mathematical induction method, we will prove that

$$A_n = \frac{k^{n+1} - (1-k)^{n+1}}{k^n - (1-k)^n}. \tag{13.9}$$

Clearly, this dependence is valid at $n = 0; 1; 2; 3$. We assume that it is valid at any $z - 1$,

$$A_{z-1} = \frac{k^z - (1-k)^z}{k^{z-1} - (1-k)^{z-1}} \tag{13.10}$$

and prove that for z

$$A_z = \frac{k^{z+1} - (1-k)^{z+1}}{k^z - (1-k)^z}. \tag{13.11}$$

It is clear that

$$A_z = 1 - \frac{k(1-k)}{A_{z-1}}.$$

We substitute A_{z-1} from the expression (13.10):

$$A_z = 1 - \frac{k(1-k)\left[k^{z-1} - (1-k)^{z-1}\right]}{k^z - (1-k)^z} = \frac{k^z - (1-k)^z - k^z(1-k) + k(1-k)^z}{k^z - (1-k)^z}$$

$$= \frac{k^{z+1} - (1-k)^{z+1}}{k^z - (1-k)^z}. \tag{13.12}$$

Substituting (13.12) into the dependence (13.8), we obtain

$$F_f(x)_{(z)} = k\frac{k^z - (1-k)^z}{k^{z+1} - (1-k)^{z+1}}. \tag{13.13}$$

It is clear from (13.12) that at $k = 0,5$ we arrive at an uncertainty. At $k = 0.5$, the dependence is simplified and reduced to the expression

$$F_f(x) = \frac{z}{z+1}.$$

All this is valid for a cascade separator with any number of stages at the material feed from above $(i^* = 1)$.

A system of equations

$$\left.\begin{array}{c} r_1 = r_2 k \\ r_2 = r_1(1-k) + r_3 k \\ \vdots \\ r_{i^*} = r_{i^*-1}(1-k) + r_{i^*+1}k + 1 \\ \vdots \\ r_{z-1} = r_{z+2}(1-k) + r_z k \\ r_z = r_{z-1}(1-k) \end{array}\right\} \tag{13.14}$$

corresponds to a general case, where the initial material is fed for separation into any stage i^*.

Since the material distribution proceeds according to the previous scheme until the i^* stage, taking into account the expression (13.4), we can write

$$r_{i^*} = r_{i^*-1}(1-k) + \frac{r_{i^*}(1-k)k}{z-i^* \left\{\begin{array}{c} 1 - \frac{k(1-k)}{1-\frac{k(1-k)}{1-\frac{k(1-k)}{\ddots}}} \\ \ddots \\ 1 - k(1-k) \end{array}\right.} + 1 \tag{13.15}$$

It follows that

$$r_{i^*}\left[1 - \frac{k(1-k)}{A_{z-i^*}}\right] = r_{i^*-1}(1-k) + 1.$$

Taking into account the dependencies (13.7) and (13.8), we can write

$$r_{i^*}\left[1 - F_f(x)_{z-i^*}(1-k)\right] = r_{i^*-1}(1-k) + 1.$$

Hence,

$$r_{i^*} = \frac{r_{i^*-1}(1-k)+1}{1-F_f(x)_{z-i^*}(1-k)} = \frac{r_{i^*-1}(1-k)}{1-F_f(x)_{z-i^*}(1-k)} \cdot \frac{k}{k} + \frac{1}{1-F_f(x)_{z-i^*}(1-k)} \cdot \frac{k}{k}$$

$$= \frac{1-k}{k} r_{i^*-1} F_f(x)_{z-i^*+1} + \frac{1}{k} F_f(x)_{z-i^*}. \tag{13.16}$$

Similar calculations for the previous stages give

$$r_{i^*-1} = \frac{1-k}{k} r_{i^*-2} \cdot F_f(x)_{z-i^*+2} + \frac{1}{k} F_f(x)_{z-i^*+1} \cdot F_f(x)_{z-i^*+2},$$

$$r_{i^*-2} = \frac{1-k}{k} r_{i^*-3} \cdot F_f(x)_{z-i^*+3} + \frac{1}{k} F_f(x)_{z-i^*+1} \cdot F_f(x)_{z-i^*+2} \cdot F_f(x)_{z-i^*+3}$$

where $F_f(x)_{z-i^*}$ and $F_f(x)_{z-i}$ are fractional extractions in case the apparatus height were limited by the corresponding stage. The content in the first stage from above is

$$r_1 = r_2 \cdot k = (1` - k) \cdot r_1 \cdot F_f(x)_{z-1} + F_f(x)_{z-i^*+1} \cdot F_f(x)_{z-i^*+2} \times \cdots \times F_f(x)_{z-1}.$$

Hence,

$$\begin{aligned} r_1 &= \frac{F_f(x)_{z-i^*+1} \cdot F_f(x)_{z-i^*+2} \cdot F_f(x)_{z-i^*+3} \times \cdots \times F_f(x)_{z-1}}{1 - (1-k)F_f(x)_{z-1}} \\ &= \frac{1}{k} F_f(x)_{z-i^*+1} \cdot F_f(x)_{z-i^*+2} \times \cdots \times F_f(x)_z. \end{aligned}$$

Here the total fractional extraction amounts to

$$F_f(x)_z^{i^*} = F_f(x)_{z-i^*+1} \cdot F_f(x)_{z-i^*+2} \times \cdots \times F_f(x)_z. \tag{13.17}$$

Here we have i^* multipliers, which correspond to fractional extractions of apparatuses limited in height by the indices above.

We substitute the relation (13.13) into (13.17):

$$\begin{aligned} F_f(x)_z^{i^*} = k \frac{k^z - (1-k)^z}{k^{z+1} - (1-k)^{z+1}} \cdot k \frac{k^{z-1} - (1-k)^{z-1}}{k^z - (1-k)^z} \cdot \\ k \frac{k^{z-i^*+1} - (1-k)^{z-i^*+1}}{k^{z-i^*+2} - (1-k)^{z-i^*+2}}. \end{aligned} \tag{13.18}$$

Reducing identical terms in (13.18), we obtain:

$$F_f(x)_z^{i^*} = k^{i^*} \frac{k^{z-i^*+1} - (1-k)^{z-i^*+1}}{k^{z+1} - (1-k)^{z+1}}. \tag{13.19}$$

This is the most general expression for determining fractional extraction of a cascade consisting of z stages at the material feed to i^* stage counting from above under the condition $k \neq 0.5$.

We determine the value of the parameter k from a somewhat different standpoint. For this purpose, we digress from the chain fractions model and consider mass transfer in a cascade as a system of equations characteristic of each stage.

According to Fig. 13.3a, we denote fractional extraction of the considered (or fixed) class of particles upwards at each stage by f_i, and fractional extraction of the same particles at the same stage downwards by c_i. As already shown, irrespective of the amount of material arriving at a stage, its certain fraction is extracted upwards from this stage (k), while the remaining amount $(1 - k)$ is extracted downwards.

In the general case of a cascade with identical stages according to Fig. 13.3a, we can make up a system of $2z$ simultaneous equations: z equations of fractional extraction and z equations of material balance for z stages:

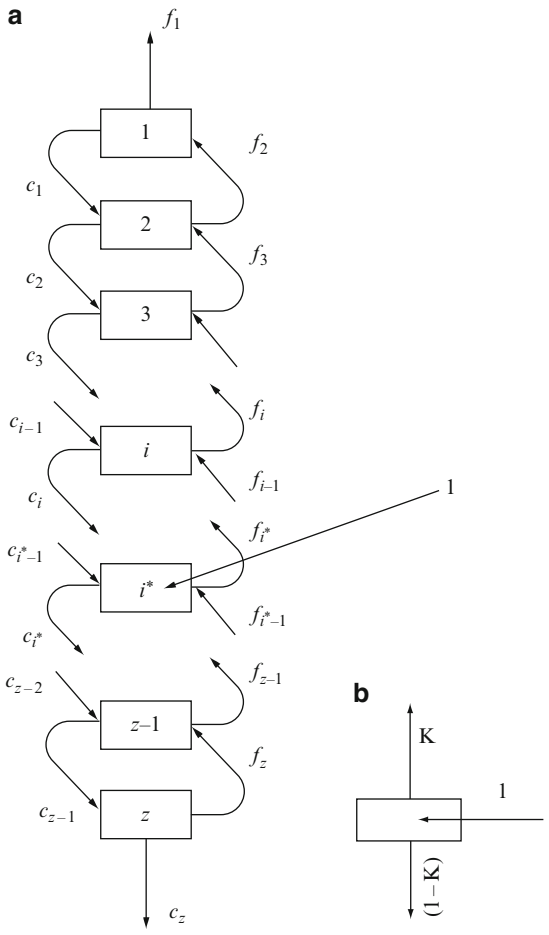

Fig. 13.3 (**a**) Schematic diagram of mass transfer in a cascade; (**b**) schematic diagram of distribution within one stage

$$
\begin{cases}
f_1 = f_2 k \\
f_2 = (c_1 + f_3)k \\
f_3 = (c_2 + f_4)k \\
\cdots\cdots\cdots\cdots\cdots\cdots \\
\cdots\cdots\cdots\cdots\cdots\cdots \\
f_{i^*} = (c_{i^*-1} + f_{i^*+1})k + k \\
\cdots\cdots\cdots\cdots\cdots\cdots \\
\cdots\cdots\cdots\cdots\cdots\cdots \\
f_i = (c_{i-1} + f_{i+1})k \\
\cdots\cdots\cdots\cdots\cdots\cdots \\
\cdots\cdots\cdots\cdots\cdots\cdots \\
f_{z-1} = (c_{z-2} + f_z)k \\
f_z = c_{z-1} \cdot k
\end{cases}
\tag{13.20}
$$

$$\begin{cases} f_1 + c_1 = f_2 \\ f_2 + c_2 = c_1 + f_3 \\ f_3 + c_3 = c_2 + f_4 \\ \cdots\cdots\cdots\cdots\cdots\cdots \\ \cdots\cdots\cdots\cdots\cdots\cdots \\ f_{i^*} + c_{i^*} = c_{i^*-1} + f_{i^*+1} + 1 \\ \cdots\cdots\cdots\cdots\cdots\cdots\cdots \\ \cdots\cdots\cdots\cdots\cdots\cdots\cdots \\ f_i + c_i = c_{i-1} + f_{i+1} \\ \cdots\cdots\cdots\cdots\cdots\cdots \\ \cdots\cdots\cdots\cdots\cdots\cdots \\ f_{z-1} + c_{z-1} = c_{z-2} + f_z \\ f_z + c_z = c_{z-1} \end{cases} \tag{13.21}$$

In these expressions, k is the material distribution coefficient in one stage. At each stage, the total input of particles equals their output from the stage. Therefore, the following relation can be written for each of them:

$$c_i = f_i \frac{(1-k)}{k}. \tag{13.22}$$

Taking an equation for stage i from the system (13.21) and substituting, instead of c_i and c_{i-1}, their respective values from (13.22), we obtain a recurrent equation corresponding to the systems (13.20) and (13.21):

$$f_i = f_{i-1}(1-k) + f_{i+1} \cdot k. \tag{13.23}$$

Equation (13.23) is a uniform finite-difference equation of the second order with constant coefficients. It can be written somewhat differently:

$$f_{i+2} - f_{i+1} \cdot \frac{1}{k} + f_i \cdot \frac{1-k}{k} = 0. \tag{13.24}$$

Using the dependence (13.22), we determine three boundary conditions for the recurrent equation (13.24):

$$\begin{cases} f_1 = f_2 \cdot k \\ f_{i^*} = f_{i^*-1} \cdot (1-k) + f_{i^*+1} \cdot k + k \\ f_z = f_{z-1} \cdot (1-k) \end{cases} \tag{13.25}$$

The characteristic equation corresponding to Eq. (13.24) can be written as

$$\lambda^2 - \frac{1}{k}\lambda + \frac{1-k}{k} = 0.$$

Solving this equation, we obtain the following roots:

$$\lambda_1 = \frac{1-k}{k};\ \lambda_2 = 1.$$

Under the condition $k = 0.5$ we obtain

$$\lambda_1 = \lambda_2 = 1.$$

The general solution of (13.24) in case $\lambda_1 \neq \lambda_2$ has the form:

$$f_i = b_1\lambda_1^i + b_2\lambda_2^i.$$

Using boundary conditions (13.25), we find for $1 \leq i \leq i^*$,

$$f_i = \frac{\left[1-\left(\frac{1-k}{k}\right)\right]^{z+1-i^*}\left[1-\left(\frac{1-k}{k}\right)^i\right]k}{\left[1-\left(\frac{1-k}{k}\right)^{z+1}\right](2k-1)}. \tag{13.26}$$

For stages within the limits of $i^* \leq i \leq z$,

$$f_i = \frac{\left[1-\left(\frac{k}{1-k}\right)^{i^*}\right]\left[\left(\frac{1-k}{k}\right)^{z+1}-\left(\frac{1-k}{k}\right)^i\right]k}{\left[1-\left(\frac{1-k}{k}\right)^{z+1}\right](2k-1)}. \tag{13.27}$$

In case of $k = 0.5,$ i.e. at $\lambda_1 = \lambda_2 = 1$, the general solution is:

$$f_i = b_1 i\lambda^i + b_2\lambda^i = b_1 i + c_2.$$

Using boundary conditions (13.25), we obtain

$$f_i = i\frac{(z+1-i^*)}{(z+1)}\ (1 \leqslant i \leqslant i^*), \tag{13.28}$$

$$f_i = i^*\frac{(z+1-i)}{(z+1)}\ (i^* \leqslant i \leqslant z). \tag{13.29}$$

Let us revert to Fig. 13.3a. It is clear from this figure that the total extraction of the considered narrow size class into the fine product corresponds to the value of its extraction from the first stage, i.e., f_1. Respectively, this class is extracted into the coarse product from the last stage, and the value of this extraction is c_z.

Clearly,

$$F_f = f_1;\quad F_c = c_z;\quad F_f + F_c = 1. \tag{13.30}$$

According to (13.27), at $i = 1$ we obtain

$$F_f = \frac{1 - \left(\frac{1-k}{k}\right)^{z+1-i^*}}{1 - \left(\frac{1-k}{k}\right)^{z+1}} \text{ at } k \neq 0,5. \tag{13.31}$$

At $k = 0.5$, it follows from (13.29) that

$$F_f = \frac{z + 1 - i^*}{z + 1}. \tag{13.32}$$

It follows from the analysis of the separation process mechanism in cascade apparatuses that a symmetric medium feed of the material into the apparatus does not shift the separation boundary. This corresponds to the condition

$$i^* = \frac{z + 1}{2}.$$

In this case, the expression (13.31) acquires the form

$$F_f = \frac{1}{1 + \left(\frac{1-k}{k}\right)^{\frac{z+1}{2}}}. \tag{13.33}$$

The steepness of the fractional separation curve shows the process perfection. It can be defined as the slope ratio of the tangent in the middling point, i.e. at $F_f(x) = 0.5$,

$$\left(\frac{dF_f}{dk}\right)_{k=0,5} = \left\{ \frac{\frac{n+1}{2}\left(\frac{1-k}{k}\right)^{\frac{z-1}{2}}\frac{1}{k^2}}{\left[1 + \left(\frac{1-k}{k}\right)^{\frac{z+1}{2}}\right]^2} \right\}_{k=0,5} = \frac{z + 1}{2}. \tag{13.34}$$

Hence, with increasing z, separation efficiency continuously grows. It is noteworthy that the effect of an increasing number of cascade stages subsides with increasing z. It means that an excessive growth of the number of stages in a cascade does not make sense. The parameter k reflects structural and dynamic foundations of the process. Since all cascade stages are identical and hydrodynamic conditions in them are the same, we must assume that the value of this parameter in such conditions is constant.

The value of the parameter k can be determined for practical use by a somewhat simplified structure of a two-phase flow. It is established that the velocity profile in the cross-section of a vertical two-phase turbulent flow stretches in the mid part in comparison with an analogous one-phase flow. To the first approximation, such a profile can be considered as parabolic (Fig. 13.4):

$$u_r = 2w\left[1 - \left(\frac{r}{R}\right)^2\right] \tag{13.35}$$

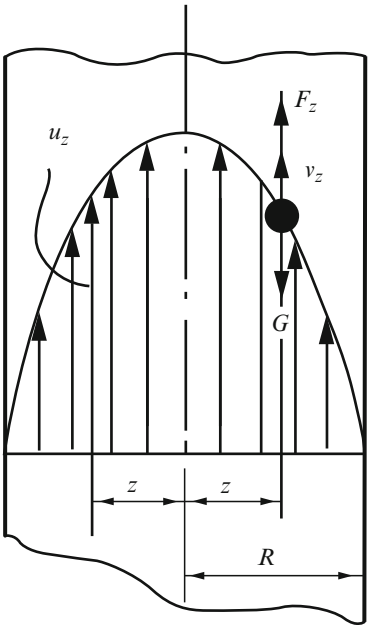

Fig. 13.4 Schematic presentation of flow structure

where u_r is the local velocity at the distance r from the channel axis, m/s; w is the mean flow velocity, m/s; R is the geometrical radius of the channel, m; r is the distance from the channel axis to the point under study, m.

We assume that a narrow size class x is separated in this flow between two outlets. At a uniform distribution of these particles over the cross-section according to the profile, in the central part they rise upwards and go down near the walls. Between these zones we can single out a radius r_0 where they hover, i.e. are in a dynamic equilibrium. An equation of such equilibrium is written as

$$\frac{\pi x^3}{6}(\rho - \rho_0) = \lambda \frac{\pi x^2}{4} \rho^* \frac{u_{r_0}^2}{2g} \tag{13.36}$$

where x is the size of particles of a narrow class, m; r_0 is the distance from the channel axis to the point where the absolute velocity of a particle of the size x is zero, m; ρ is the material density, kg/m^3; ρ_0 is the medium density, kg/m^3; ρ^* is the apparent specific weight of the flow, kg/m^3.

The effect of a two-phase flow on a particle owing to collisions with other particles is somewhat stronger than that of a single-phase flow. To a certain precision, we can assume at the concentration $\mu = 2$ kg/m^3 that $\rho^* = 2$ kg/m^3. It follows from the flow structure (Fig. 13.4) that

$$k = \frac{Sr_0}{S_R} = \frac{\pi r_0^2}{\pi R^2} = \left(\frac{r_0}{R}\right)^2. \tag{13.37}$$

Taking this observation into account, we substitute (13.35) into (13.36):

$$\frac{4}{3}gx(\rho-\rho_0)=\lambda\rho^*\left\{2w\left[1-\left(\frac{r_0}{R}\right)\right]^2\right\}^2 \tag{13.38}$$

and then (13.37) into (13.38)

$$\frac{1}{3\lambda}\frac{gd}{w}\cdot\frac{(\rho-\rho_0)}{\rho^*}=(1-k^2). \tag{13.39}$$

Hence,

$$k=1-\sqrt{\frac{1}{3\lambda}\frac{\rho-\rho_0}{\rho^*}\frac{gx}{w^2}}=1-\sqrt{\frac{1}{3\lambda\cdot 1,67}\frac{\rho-\rho_0}{\rho_0}\frac{gx}{w^2}}.$$

At $\lambda=0.5$, this expression acquires the form

$$k=1-\sqrt{0.4\cdot B},$$

where $B=\frac{gx}{w^2}\frac{(\rho-\rho_0)}{\rho_0}$. Refined dependencies for estimating a cascade apparatus can be obtained from an equilibrium balance model of the process.

The material going out upwards, or into the fine product, arrives from the first stage only and amounts to

$$R_1k=F_f \tag{13.40}$$

(Fig. 13.5), where F_f is fractional extraction of the size class under study into the fine product; R_1 is the content of this class in the first stage. The material going out downwards, or into the coarse product, arrives from the last stage only and amounts to

$$R_z(1-k)=F_c \tag{13.41}$$

where F_c is fractional extraction of the narrow size class into the coarse product; R_z is the content of the class under study at the stage z.

Clearly,

$$F_f+F_c=1,$$

i.e.,

$$R_1\cdot k+R_z(1-k)=1. \tag{13.42}$$

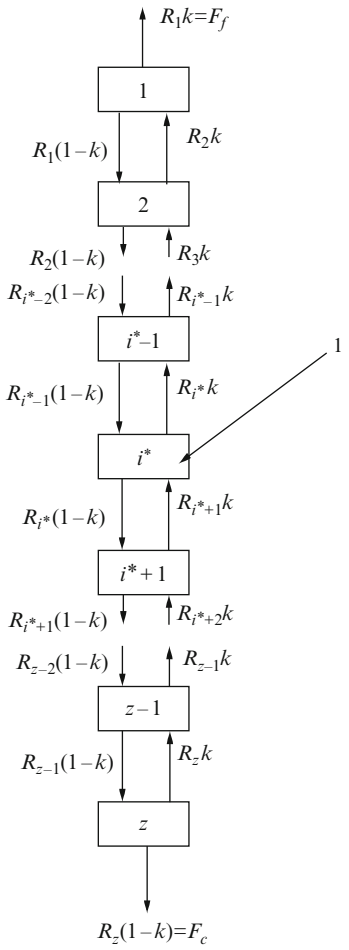

Fig. 13.5 Schematic diagram of a cascade separator and pourable material distribution in stages

By the upper part we imply cascade stages from the first one to the feeding stage, i.e., $1 \leqslant i \leqslant i^\bullet$ (i is the current stage).

Let us examine the material balance condition from the first to the $i*$ th stage,

$$R_1k + R_i(1-k) = R_{i+1}k \quad (i \leqslant i^\bullet - 1).$$

Taking (13.40) into account, we can write

$$R_{i+1}k - R_i(1-k) = F_f. \tag{13.43}$$

Consider an analogous equation for the lower part of the cascade:

$$R_z(1-k) + R_ik = R_{i-1}k \ (i \geqslant i^\bullet + 1).$$

Taking (13.41) into account, we obtain:

$$R_{i-1}k - R_i(1-k) = F_c. \tag{13.44}$$

The dependencies (13.43) and (13.44) lead to an important conclusion. The cascade distributes material in such a way that:

1. The difference in the material quantities in two adjacent stages in the upper part equals fractional extraction of the entire cascade into the fine product.
2. The same difference in the lower part equals fractional extraction of the entire cascade into the coarse product.

Changing the indexation in recurrent equations (13.43) and (13.44), we can write for the feeding stage

$$\begin{aligned} R_{i^\bullet}k - R_{i^\bullet-1}(1-k) &= F_f \quad (i \leqslant i^\bullet) \\ R_{i^\bullet}(1-k) - R_{i^\bullet-1}k &= 1 - F_f \quad (i \geqslant i^\bullet) \end{aligned} \tag{13.45}$$

Equation (13.45) at $i = i^\bullet$ expresses the material balance condition for the stage $i^\bullet$.

To illustrate the validity of the latter, it is enough to sum up left- and right-hand parts of Eq. (13.45). In the left-hand part we obtain all inputs and outputs for $i^\bullet$th stage, and in the right-hand part unity, which fits the facts. We apply a parameter

$$\sigma = \frac{1-k}{k}.$$

Proceeding from (13.43), we can write for the upper part of the cascade:

$$\left.\begin{array}{c} R_1k = F_f \\ R_2k = R_1(1-k) + F_f \\ R_3k = R_2(1-k) + F_f \\ \ldots\ldots\ldots\ldots\ldots\ldots \\ R_ik = R_{i-1}(1-k) + F_f \\ \ldots\ldots\ldots\ldots\ldots\ldots \\ R_{i^\bullet}k = R_{i^\bullet-1}(1-k) + F_f \end{array}\right\}. \tag{13.46}$$

Using the method of successive substitutions, we can obtain from (13.46) for $i \leqslant i^\bullet$ stages:

$$\left.\begin{array}{c} R_1k = F_f \\ R_2k = \frac{F_f}{k}(1-k) + F_f = F_f\sigma + F_f \\ R_3k = \sigma^2F_f + \sigma F_f + F_f \\ R_4k = \sigma^3F_f + \sigma^2F_f + \sigma F + F_f \\ \ldots\ldots\ldots\ldots\ldots\ldots\ldots\ldots\ldots\ldots \\ R_ik = F_f(\sigma^{i-1} + \sigma^{i-2} + \cdots + \sigma^2 + \sigma + 1) \end{array}\right\}. \tag{13.47}$$

The latter expression can be written as

$$R_i k = \frac{F_f}{\sigma}(\sigma^{i^*} + \sigma^{i^*-1} + \cdots + \sigma^3 + \sigma^2 + \sigma). \tag{13.48}$$

For $i^\bullet$ stage we obtain

$$R_{i^\bullet} k = \frac{F_f}{\sigma}(\sigma^{i^\bullet} + \sigma^{i^\bullet-1} + \cdots + \sigma^i + \sigma^{i-1} + \cdots + \sigma^2 + \sigma) = \frac{F_f A}{\sigma} \tag{13.49}$$

where $A = (\sigma^{i^\bullet} + \sigma^{i^\bullet-1} + \cdots + \sigma^3 + \sigma^2 + \sigma)$.

According to the recurrent equation (13.44), we can write a system of equations for the lower part $(i \geqslant i^*)$:

$$\left.\begin{array}{c} R_{i^\bullet+1} k = R_{i^*}(1-k) - F_c \\ R_{i^\bullet+2} k = R_{i^\bullet-1}(1-k) - F_c \\ \cdots\cdots\cdots\cdots\cdots\cdots \\ \cdots\cdots\cdots\cdots\cdots\cdots \\ R_z k = R_{z-1}(1-k) - F_c \end{array}\right\}. \tag{13.50}$$

Taking (13.49) into account, this system is transformed into

$$\left.\begin{array}{c} R_{i^\bullet+1} k = R_{i^\bullet}\sigma - F_c = F_f A - (1-F_f) \\ R_{i^\bullet+2} k = \sigma F_f A - \sigma(1-F_f) - (1-F_f) \\ R_{i^\bullet+3} k = \sigma^2 F_f A - \sigma^2(1-F_f) - \sigma(1-F_f) - (1-F_f) \\ \cdots\cdots\cdots\cdots\cdots\cdots\cdots\cdots\cdots\cdots\cdots\cdots\cdots\cdots\cdots\cdots \\ R_z k = \sigma^{z-i^\bullet-1} F_f A - (1-F_f)(\sigma^{z-i-1} + \sigma^{z-i-2} + \sigma^2 + \sigma + 1 \end{array}\right\}. \tag{13.51}$$

It follows from the latter that

$$R_z k = \frac{F_f}{\sigma}(\sigma^z + \sigma^{z-1} + \cdots + \sigma^2 + \sigma) - \frac{1}{\sigma}(\sigma^{z-i^\bullet} + \sigma^{z-i^\bullet-1} + \cdots + \sigma^2 + \sigma). \tag{13.52}$$

It follows from the last line of (13.50) that

$$R_z(1-k) = 1 - F_f.$$

We multiply and divide the left-hand part by k :

$$R_z \sigma k = 1 - F_f. \tag{13.53}$$

Taking into account (13.43), it follows from equation (13.42) that:

$$F_f = \frac{1 + \sigma^{z-i^\bullet} + \sigma^{z-i^\bullet-1} + \cdots + \sigma^2 + \sigma}{1 + \sigma^z + \sigma^{z-1} + \cdots + \sigma^2 + \sigma}. \tag{13.54}$$

In the numerator and denominator of the expression (13.54) we obtain sums of geometric series terms. Calculating these sums, we obtain

$$F_f = \frac{1 - \sigma^{z-i^\bullet+1}}{1 - \sigma^{z+1}}. \tag{13.55}$$

Thus, we get a dependence of the value of fractional extraction of a narrow size class on the principal structural parameters of a cascade apparatus.

A detailed sound justification of separation mechanism in a cascade process can be obtained by examining a discrete stationary model of the process.

13.2 Discrete Stationary Model of Critical Regimes of Vertical Two-Phase Flows

A characteristic property of such flows is a non-stationary multi-directional motion of particles and their ability to change the motion direction many times during their stay in the channel. The direction can be altered at any point along the channel height. All this considerably complicates the analysis of the flow mechanism and of the solid phase distribution between two outputs of the process – upper and lower. Such processes are widely used in industrial practice, for instance, in fractionation of bulk materials according to particles sizes or densities.

We assume that a poly-fractional bulk material is fed into a vertical channel. Under the action of air flow, a part of this material goes out upwards, and another part settles downwards. The finest particles are completely carried out upwards, and the coarsest particles settle downwards. Particles of intermediate classes are shared by two outputs – those of fine and coarse products.

If the initial granulometric composition of the material is known, determining the composition of one of the outputs allows automatic determination of the product composition in another output. We assume that the fine product is the determining one.

To develop a model of the process of a critical two-phase flow, we define its boundary conditions.

1. The process model is discrete both in space and time.

Spatial discreteness is determined by the following reasons. If we take a differential of the amount of material at a certain level of the channel height and then

integrate over the entire height, it leads to nothing, since changes in the direction of the particles motion can start at any level.

Therefore, we mentally divide the vertical channel along its height into a finite number of identical elements and call each element a stage. The idea of channel subdivision into stages consists in the assumption that changes in the direction of the particles occur only within a stage, and the latter exchanges particles with adjacent stages only. Material can be fed into such a flow from above, from below or into any stage.

Assume that the channel under study consists of z stages (z being a natural number). We count the stages top-down and denote any stage by $i(1 \leqslant i \leqslant z)$. If we consider a certain stage i, the material located therein partially goes out into the overlying stage $(i-1)$ under the action of an ascending flow, while another part gets into the stage $(i+1)$ located below. At the same time, a part of the same material arrives from these stages at the stage i. We denote the stage of the initial material feed by i^*. Clearly, in a general case, $1 \leq i^* \leq z$. Time discreteness is stipulated by the fact that, putting aside a continuous temporal transformation of the vector of polyfractional mixture composition, the latter is considered only at certain fixed moments of time with the interval $\Delta\tau$. It means that this model examines instantaneous and simultaneous particles redistribution in all stages of the channel occurring at discrete moments of time with the same interval $\Delta\tau$. We call such distribution of polydisperse material a solitary separation act.

2. The model is related to the field of self-similar processes with respect to the average consumed material concentration μ in the flow. In the concentration range up to 2.5 kg/m^3, separation in the flow is independent of the solid phase content in it. This result is independent of concentration, the method of the material feed, mean flow velocity value or the number of stages.

3. Each narrow size class of particles is separated in such flows independently, irrespective of the presence of other classes of particles. Statements 2 and 3 are closely interconnected and experimentally established. Statement 3 allows us to pass from a polydisperse material to the examination of independent behavior of each monofraction separately r_{ij}^n. Further we omit the index n, and all our conclusions are related to one monofraction only.

If we successively determine distributions of all narrow classes, we obtain complete information on the result of the process. Usually, this is an objective of any prediction. Each redistribution of a monofraction at discrete moments of time in all channel sections represents an isolated separation act (ISA).

Here we denote by ρ_{ij} the amount of monofraction in the ith stage at the jth ISA at a single initial feed of this fraction into the flow.

Respectively, r_{ij} is the total flow of this monofraction in the ith stage during j ISAs. In the general case, at an arbitrary feed:

$$r_{ij} = \sum_{0}^{j} \rho_{ij}.$$

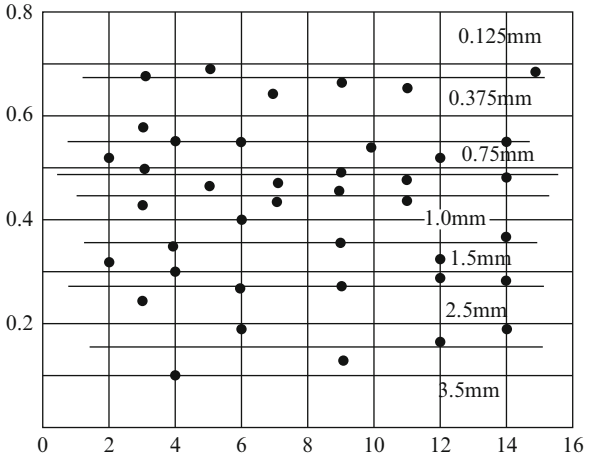

Fig. 13.6 Dependence of the distribution coefficient k for various size classes on the number of identical stages z at a constant air flow velocity w

4. We examine an equilibrium model implying the conservation of material balance between the amounts of particles contained in and leaving any section during an arbitrary ISA.

5. We examine a stationary model only, which assumes that the number of particles entering a certain stage (i) equals the number of particles leaving this stage.

6. We assume that particles separation coefficient in any stage remains unchanged at an unchanged ascending flow velocity. Here the separation coefficient k implies the portion of particles of a narrow size class passing into the overlying cascade section during an ISA, i.e., $k = \frac{r_{i-1}}{r_i}$. For identical stages, the value $k = \text{const}$, which has been confirmed experimentally (Fig. 13.6).

According to items 4 and 6, the distribution of an arbitrary monofraction in any section during the $(j + 1)$th ISA is expressed as follows (Fig. 7.1a):

$$\rho_{ij} = \rho_{ij} \cdot k + \rho_{ij}(1 - k)$$

where ρ_{ij} is the number of particles of a fixed narrow size class staying in the ith stage during the jth ISA at a discrete moment of time; $\rho_{ij} \cdot k$ is the fraction of these particles that passed to the overlying $(i - 1)$th stage at the $(j + 1)$th ISA at a discrete moment of time; $\rho_{ij}(1 - k)$ is the fraction of particles that passed to $(i + 1)$th stage.

Particles content in a fixed fraction in separate stages during an arbitrary number j of ISA can be expressed by a certain matrix of values.

We examine a single feed of the initial number of particles taken as unity (a portion). A general pattern of particles distribution in separate stages during

an arbitrary number j of ISA can be expressed by the following matrix of values:

$$
\begin{array}{cccccccc}
\tau_j & \tau_0 & \tau_1 & \tau_2 & \tau_3 & \tau_4 & \cdots & \tau_j \\
j/_i & 0 & 1 & 2 & 3 & 4 & \cdots & j \\
1 & \rho_{10} & \rho_{11} & \rho_{12} & \rho_{13} & \rho_{14} & \cdots & \rho_{i,j} \\
\vdots & \vdots & \vdots & \vdots & \vdots & \vdots & \cdots & \vdots \\
i^\bullet - 1 & 0 & k & 0 & 3k^2(1-k) & \rho_{i^\bullet-1,4} & \cdots & \rho_{i^\bullet-1,j} \\
i^\bullet - \rightarrow 1 & 0 & 2k(1-k) & 0 & 6k^2(1-k)^2 & & \cdots & \rho_{i^\bullet,j} \\
i^\bullet + 1 & 0 & 1-k & 0 & 3k(1-k)^2 & \rho_{i^\bullet+1,4} & \cdots & \rho_{i^\bullet+1,j} \\
\vdots & \vdots & \vdots & \vdots & \vdots & \vdots & \cdots & \\
z-1 & \rho_{z-1,0} & \rho_{z-1,1} & \rho_{z-1,2} & \rho_{z-1,3} & \rho_{z-1,4} & \cdots & \vdots \\
z & \rho_{z,0} & \rho_{z,1} & \rho_{z,2} & \rho_{z,3} & \rho_{z,4} & \cdots & \rho_{z-1,j} \\
 & & & & & & & \rho_{z,j}
\end{array}
$$

where $\tau_j = j\Delta\tau$ are discrete moments of time.

In case of a single feed, we obtain an infinite matrix in the general form:

$$
\rho_{ij} = \begin{bmatrix}
\rho_{10} & \rho_{11} & \rho_{12} & \cdots & \rho_{ij} & \cdots \\
\rho_{20} & \rho_{21} & \rho_{22} & \cdots & \rho_{ij} & \cdots \\
\cdots & \cdots & \cdots & \cdots & \cdots & \cdots \\
\rho_{i0} & \rho_{i1} & \rho_{i2} & \cdots & \rho_{ij} & \cdots \\
\cdots & \cdots & \cdots & \cdots & \cdots & \cdots \\
\rho_{z0} & \rho_{z1} & \rho_{z2} & \cdots & \rho_{zj} & \cdots
\end{bmatrix}.
$$

It follows from the preceding distribution scheme that

$$
\rho_{ij} = \rho_{i-1,j-1}(1-k) + \rho_{i+1,j-1}k \tag{13.56}
$$

under the initial conditions:

$$
\left.\begin{array}{c} \rho_{i0} i \neq i^\bullet = 0 \\ \rho_{i^\bullet,0} = 1 \end{array}\right\}
$$

and boundary conditions:

$$
\left.\begin{array}{c} \rho_{1,j} = \rho_{2,j-1}k \\ \rho_{z,j} = \rho_{z-1,j-1}(1-k) \end{array}\right\}.
$$

Theoretically, in the most general case, the number of elements in any line of the matrix $[\rho_{ij}]$ is infinite. However, in practice, after a certain period of time $(T_m = m \cdot \Delta\tau)$ all the particles leave the apparatus passing into fine or coarse product, so that

$$\rho_{ij/j \geqslant m+1} = 0.$$

Thus, the initial infinite matrix can be restricted by m ISAs

$$\left[\rho_{i_1 \infty}\right] = \left[\rho_{i,m}\right] = \begin{bmatrix} \rho_{10} & \rho_{11} & \rho_{12} & \cdots & \rho_{1m} \\ \rho_{20} & \rho_{21} & \rho_{22} & \cdots & \rho_{2m} \\ \cdots & \cdots & \cdots & \cdots & \cdots \\ \rho_{z0} & \rho_{z1} & \rho_{z2} & \cdots & \rho_{zm} \end{bmatrix}. \tag{13.57}$$

In the general case, the distribution r_{ij} of a narrow class of particles along the channel height depends on the number of stages, distribution coefficient, initial and boundary conditions, fixed moment of time, site and method of the initial material feed.

A discrete model presupposes the initial product feed in equal portions at equal time intervals $\Delta T = t\Delta\tau (t = 1, 2, 3, \ldots, m)$. Evidently, $t \geq 1$, because otherwise the number of feeds would exceed the number of ISAs, which would lead to unlimited accumulation of particles. Thus, particles content in the general case is expressed as

$$r_{ij} = f(k, z, i^{\bullet}, i, j, t). \tag{13.58}$$

The realization of various methods of the initial material feed leads to the following main regimes of feeding:

(a) A continuous regime (within the bounds of a discrete model) is realized at the step of $t = 1$. The interval between subsequent separate feeds is $\Delta\tau$. Since the moment of time $\tau_j = \tau_m$, the distribution becomes stationary.

The discontinuity of the moments of time with the step $\tau = j\Delta\tau$ corresponds to:

$$j = 0, 1, 2 \ldots$$

Then the amount of a monofraction at a given moment of time j (during j ISAs) is described by a relationship

$$r_{ij} = \sum_{\gamma_0}^{j} (\rho_{i(j-j_0)}. \tag{13.59}$$

The latter can be written as

$$r_{ij} = \rho_{ij} + \rho_{i,j-1} + \cdots + \rho_{i,0} = \sum_{0}^{j} \rho_{ij}.$$

A similar expression is valid in the matrix form of (13.57) type:

$$\left[r_{ij}\right] = \sum_{0}^{j} \left[\rho_{ij}\right]. \tag{13.60}$$

Since $\rho_{ij/j\geqslant m+1} = 0,$ we can write

$$r_{ij/j\geqslant m} = \sum_{0}^{m} \rho_{ij}.$$

Thus, since the moment of time $\tau_j = \tau_m$, a stationary distribution regime ensues, which is characterized by an invariable particles flow over the sections:

$$r_i = r_{ij/\gamma\geqslant m} = \sum_{0}^{m} \rho_{ij} = \text{const}. \tag{13.61}$$

Hence, in this case, the number of dependent variables decreases in comparison with (13.58):

$$r_i = f(r, z, i*, i). \tag{13.62}$$

Using (13.56) we can describe an equilibrium particles flow in any section of the channel. For this purpose, we sum up the expression

$$\rho_{i;j+1} = \rho_{i-1;j}(1-k) + \rho_{i+1;j}k \tag{13.63}$$

over j at its variation from 0 to m:

$$\sum_{0}^{m} \rho_{i;j+1} = (1-k)\sum_{0}^{m} \rho_{i-1;j} + k\sum_{o}^{m} \rho_{i+1;j}. \tag{13.64}$$

Since at $i \neq i^{\bullet}$,

$$\sum_{0}^{m} \rho_{i;j+1} = \sum_{0}^{m} \rho_{i;j},$$

because $\rho_{i0} = \rho_{i;m+1} = 0,$ we obtain

$$\sum_{0}^{m} \rho_{i;j} = (1-k)\sum_{0}^{m} \rho_{i-1;j} + k\sum_{0}^{m} \rho_{i+1;j}. \tag{13.65}$$

In accordance with (13.61), this equation can be written in the form

$$r_i = r_{i-1}(1-k) + r_{i+1}k. \tag{13.66}$$

Since (13.66) is stipulated by the model equilibrium and stationary state, the same dependence can be derived from the equation of material balance of a stage:

$$r_i = r_i(1-k) + r_i(k) = r_{i-1}(1-k) + r_{i+1}k \tag{13.67}$$

at the boundary condition of the material feed into the flow

$$r_{i^\bullet} = 1 + r_{i^\bullet-1}(1-k) + r_{i^\bullet+1}k, \tag{13.68}$$

and the boundary conditions of material outlet of the channel to both sides

$$\left.\begin{array}{c} r_1 = r_2 k \\ r_z = r_{z-1}(1-k) \end{array}\right\}. \tag{13.69}$$

(b) Periodic regime of feeding with the step $t = m + 1$.

It means that each new unit portion of a monofraction enters the flow when all the particles of the previous portion have left the channel.

The corresponding moments of the material feed are

$$j = 0; (m+1), 2(m+1), 3(m+1) \ldots .$$

For this case, the following is valid:

$$r_{ij} = \rho_{ij}, \tag{13.70}$$

since individual feeds do not overlap.

Hence, it is obvious that within any cycle, the respective flows are repeated (the process is stationary within the bounds of a cycle):

$$\rho_{ij} = \rho_{ij+s(m+1)} = r_{i,j+s(m+1)} = r_{i,j+st;}(s = 0, 1, 2, 3 \ldots). \tag{13.71}$$

(c) Periodic regime of feeding with the step $1 < t < m + 1$.

In contrast to a continuous feed, here moments of feed are

$$j = 0; t; 2t; 3t \ldots .$$

Besides, after a time interval $\tau = t \cdot \Delta\tau$, the total flow in any stage is repeated, i.e. starting from the moment of time $\tau_j = \tau_{m+1-t}$, a cyclically stationary regime ensues within the bounds of one feed step.

By analogy with (13.59), in this case we can write:

$$r_{ij} = \sum_{s=0}^{c} \rho_{i;st-j_0} = \sum_{s=0}^{c} \rho_{i;st}. \tag{13.72}$$

Summing up, we can conclude that at any method of feeding a single monofraction into the flow, the process is stationary (the content in stages is repeated after every step).

Thus, starting from the moment of time $\tau_i = \tau_m$, a stationary regime ensues, which is characterized by an unchanged content of particles in stages:

$$r_{ij/j\geqslant m} = r_i = \sum_{j=0}^{m} \rho_{ij} = \text{const.} \tag{13.73}$$

Hence, in this regime $r_i = f(k; z; i^{\bullet}; i)$.

Using Eq. (13.56), we can express the equilibrium content of particles in an arbitrary section through their contents in neighboring sections. For this purpose, we summarize the expression

$\rho_{i,j+1} = \rho_{i-1,j}(1-k) + \rho_{i+1,j}k$; over j at j varying from 0 to m

$$\sum_{j=0}^{m} \rho_{i,j+1} = \sum_{j=0}^{m} \rho_{i-1,j}(1-k) + \sum_{j=0}^{m} \rho_{i+1,\,j}k.$$

However, at $i \neq i^{\bullet}$; $\sum_{j=0}^{m} \rho_{i,j+1} = \sum_{j=0}^{m} \rho_{ij}$; since $\rho_{i0} = \rho_{i,m+1}$, hence,

$$\sum_{j=0}^{m} \rho_{ij} = \sum_{j=0}^{m} \rho_{i-1,j}(1-k) + r_{i+1,j}k.$$

According to (13.73), this equation can be written as

$$r_{i,j} = r_{i-1}(1-k) + r_{i+1}k. \tag{13.74}$$

Since it has been proved that expression (13.74) reflects the process equilibrium and stationarity, we can obtain principal dependencies of material balance without reverting to onefold feeds and irrespective of time (Fig. 7.1a). From the equilibrium conditions, we obtain

$$\underbrace{r_i}_{\text{Content in section } i} = \underbrace{r_i(1-k) + r_i k}_{\text{input to section } i}$$

and from the stationarity conditions:

$$\underbrace{r_i(1-k) + r_i k}_{\text{Removal from section } i} = \underbrace{r_{i-1}(1-k) + r_{i+1}k}_{\text{input to section } i}$$

It follows that

$$r_{i\bullet} = 1 = r_{i\bullet-1}(1-k) + r_{i\bullet+1}k \tag{13.75}$$

with the boundary conditions of the particles' escape from the apparatus

$$\left.\begin{array}{c} r_1 = r_2 k \\ r_z = r_{z-1}(1-k) \end{array}\right\}. \tag{13.76}$$

It can be noted that particles distribution by sections depends on the method of material feed. If we pass to fractional extraction of particles $\left(F_f\right)$, this parameter will be invariable at various feeding regimes. By way of example, it can be demonstrated as follows.

Let us examine a stationary distribution in a continuous regime of feeding the initial material and periodic feed of a monofraction with the step $t = m + 1$. Let n single portions be fed into the channel in both cases with the intervals $1 \cdot \Delta\tau$ and $(m+1)\Delta\tau,$ respectively. During any ISA, $\rho_{1j}k$ particles of a narrow size class are always extracted from the upper part of the channel. In the first case, since particles content in all stages is stationary, the total amount of a fixed monofraction extracted upwards is $P_1 = nr_1k$.

In the second case, at the feed of a single portion of particles, the output is expressed as follows:

$$\rho_2^1 = \rho_{10}k + \rho_{12}k + k \ldots + \rho_{1m}k = k\sum_{j=0}^{m}\rho_{1j}.$$

According to (13.61)

$$\sum_{j=0}^{m}\rho_{1j} = r_1,$$

consequently,

$$P_2^1 = r_1 k.$$

Respectively, at the feed of n unit portions, the extraction is:

$$P_2 = nr_1k.$$

Thus, in both cases we arrive at the same fractional outputs. It can be also demonstrated for the case of a periodic feed regime with an arbitrary step $1 < t < m + 1$. In order to pass to fractional extraction – the most important characteristic of the process, – it is sufficient to examine a stationary regime of the apparatus operation with an interval $\Delta\tau$ between feeds.

In this regime, the extraction of a fixed monofraction into the fine product during an ISA amounts to $F_f(x) = r_1 k$. During n arbitrary ISAs, the value of fractional extraction is exactly the same, since in this case,

$$F_f(x) = \frac{n r_1 k}{n} = r_1 k.$$

To establish a functional dependence $F_f(x) = f(k; z; i; i^\bullet)$, it is necessary to find a general expression of fractional particles content $r_1 = \phi(k; z; i; i^\bullet)$ described by a recurrent equation (13.74). To solve the latter, we apply the method of calculus of finite differences. We write Eq. (13.74) in the following form:

$$r_{i-1} k - r_i + r_{i-1}(1 - k) = 0,$$

i.e. we obtain a uniform linear finite-difference equation of the second order with constant coefficients. Its general solution is

$$r_i = c_i \lambda_1^i + c_2 \lambda_2^i \ (\text{in case of } \lambda_1 \neq \lambda_2),$$

where λ_1 and λ_2 are roots of a corresponding characteristic equation

$$\lambda^2 k - \lambda + 1 - k = 0. \tag{13.77}$$

Solving this equation, we obtain:

$$\lambda_1 = 1; \lambda_2 = \frac{1 - k}{k}$$

at $k \neq 0.5$ $\lambda_1 \neq \lambda_2$. Hence,

$$r_i = c_1 + c_2 \left(\frac{1 - k}{k} \right)^i. \tag{13.78}$$

To determine c_1 and c_2, we use boundary conditions (13.75) and (13.76) for $1 \leqslant i \leqslant i^\bullet$,

$$r_1 = r_2 k = \left[c_1 + c_2 \left(\frac{1 - k}{k} \right)^2 \right] k = c_1 + c_2 \frac{1 - k}{k}.$$

Expanding the left-hand side of the last equality, we obtain

$$c_1 k + c_2 k \left(\frac{1 - k}{k} \right)^2 = c_1 + c_2 \frac{1 - k}{k},$$

whence

$$c_1 = \frac{c_2}{1-k}\left[k\left(\frac{1-k}{k}\right)^2 - \frac{1-k}{k}\right] = \frac{c_2}{1-k}\,\frac{1-k}{k}(1-k-1); c_1 = -c_2. \quad (13.79)$$

To determine c_1, we use boundary condition (13.76).
At $i^\bullet \leqslant i \leqslant z$

$$r_i = c_3 + c_4\left(\frac{1-k}{k}\right)^i. \quad (13.80)$$

Since $r_{i/i=z} = r_z = r_{z-1}(1-k)$, we derive from the expression (13.80):

$$c_3 + c_4\left(\frac{1-k}{k}\right)^z = \left[c_3 + c_4\left(\frac{1-k}{k}\right)^{z-1}\right](1-k).$$

Solving this equation with respect to c_3, we obtain

$$c_3 = -c_4\left(\frac{1-k}{k}\right)^{z+1}. \quad (13.81)$$

We substitute c_3 into Eq. (13.75):

$$r_{i^\bullet} = 1 + \left[-c_2 + c_2\left(\frac{1-k}{k}\right)^{i^\bullet-1}\right](1-k) + \left[-c_4\left(\frac{1-k}{k}\right)^{z+1} + c_4\left(\frac{1-k}{k}\right)^{i^\bullet+1}\right]k. \quad (13.82)$$

According to the unambiguity condition, we also obtain

$$r_{i^\bullet/i\leqslant i^\bullet} = -c_2 + c_2\left(\frac{1-k}{k}\right)^{i^\bullet} = r_{i^\bullet/i\leqslant i^\bullet} = -c_4\left(\frac{1-k}{k}\right)^{z+1} + c_4\left(\frac{1-k}{k}\right)^{i^\bullet}. \quad (13.83)$$

Solving Eq. (13.83) with respect to c_2, we obtain

$$c_2 = c_4\frac{\left(\frac{1-k}{k}\right)^{z+1-i^\bullet} - 1}{\left(\frac{k}{1-k}\right)^{i^\bullet} - 1}.$$

We substitute the result into Eq. (13.82):

$$1 + c_4 \frac{\left(\frac{1-k}{k}\right)^{z+1-i^\bullet} - 1}{\left(\frac{k}{1-k}\right)^{i^\bullet} - 1} \left[-1 + \left(\frac{1-k}{k}\right)^{i^\bullet - 1}\right](1-k)$$
$$+ c_4 \left[-\left(\frac{1-k}{k}\right)^{z+1} + \left(\frac{1-k}{k}\right)^{i^\bullet + 1}\right] k$$
$$= c_4 \left[-\left(\frac{1-k}{k}\right)^{z+1} + \left(\frac{1-k}{k}\right)^{i^\bullet}\right],$$

and hence,

$$c_4 = \frac{\left[1 - \left(\frac{k}{1-k}\right)^{i*}\right]}{(1-2k)\left[1 - \left(\frac{1-k}{k}\right)^{z+1}\right]}.$$

Consequently,

$$c_2 = \frac{\left[1 - \left(\frac{1-k}{k}\right)^{z+1-i^\bullet}\right]}{(1-2k)\left[1 - \left(\frac{1-k}{k}\right)^{z+1}\right]}.$$

Substituting c_2 and c_4 into (13.78) and (13.80) taking into account (13.79) and (13.82), we obtain:

$$r_i = \frac{\left[1 - \left(\frac{1-k}{k}\right)^{z+1-i^\bullet}\right]\left[1 - \left(\frac{1-k}{k}\right)^{i}\right]}{\left[1 - \left(\frac{1-k}{k}\right)^{z+1}\right](2k-1)} \quad (1 \leqslant i \leqslant i^\bullet); \tag{13.84}$$

$$r_i = \frac{\left[1 - \left(\frac{k}{1-k}\right)^{i^\bullet}\right]\left[\left(\frac{1-k}{k}\right)^{z+1} - \left(\frac{1-k}{k}\right)^{i}\right]}{\left[1 - \left(\frac{1-k}{k}\right)^{z+1}\right](2k-1)} \quad (i^\bullet \leqslant i \leqslant z). \tag{13.85}$$

In case of multiple roots of the characteristic equation (13.77) $\lambda_1 = \lambda_2 = 1$, at $k = 0.5$ the general solution is

$$r_i = c_1 i \lambda^i + c_2 \lambda^i = c_1 i + c_2. \tag{13.86}$$

Then at $1 \leqslant i \leqslant i^\bullet$ $r_i = c_1 i + c_2$, and at $i^\bullet \leqslant i \leqslant z$ $r_i = c_3 i + c_4$.
Using the upper boundary condition $r_1 = r_2 k$, we obtain

$$c_1 + c_2 = (c_1 2 + c_2)\frac{1}{2}$$

or

$$2c_1 + 2c_2 = 2c_1 + c_2.$$

Hence, $c_2 = 0,$ and then

$$r_{i/i\leqslant i^\bullet} = c_1 i.$$

Using the lower boundary condition $r_z = r_{z-1}(1-k),$ we obtain

$$c_3 z + c_4 = [c_3(z-1) + c_4]\frac{1}{2},$$

whence

$$c_4 = -c_3(z+1).$$

Consequently,

$$r_{i/i\geqslant i^\bullet} = -c_2(z+1-i). \tag{13.87}$$

Using the single-valuedness condition, we obtain

$$r_{i^\bullet/i\leqslant i^\bullet} = c_1 i^\bullet = r_{i^\bullet/i\geqslant i^\bullet} = -c_3(z+1-i^\bullet),$$

hence,

$$c_3 = -c_1\frac{i^\bullet}{(z+1-i^\bullet)}.$$

Substituting the obtained expression into (13.87), we get

$$r_{i/i\geqslant i^\bullet} = c_1\frac{i^\bullet}{(z+1-i^\bullet)}(z+1-i). \tag{13.88}$$

We use the boundary condition of the feed:

$$r_{i^\bullet} = c_1 i^\bullet = c_1(i^\bullet - 1)\frac{1}{2} + c_1\frac{i^\bullet}{z+1-i^\bullet}(z-i^\bullet)\frac{1}{2} + 1.$$

Solving this equation with respect to $c_1,$ we obtain

$$c_1 = 2\frac{z+1-i^\bullet}{z+1}.$$

Substituting c_1 into (13.86) and (13.88), we finally obtain

$$r_i = \frac{(z+1-i^\bullet)}{z+1}2i, \quad (1 \leqslant i \leqslant i^\bullet); \tag{13.89}$$

$$r_i = \frac{2i^\bullet}{z+1}(z+1-i^\bullet), \ (i^\bullet \leqslant i \leqslant z). \tag{13.90}$$

According to (13.84), fractional extraction into the fine product amounts to

$$F(x)_{k\neq 0,5} = \frac{\left[1-\left(\frac{1-k}{k}\right)^{z+1-i^\bullet}\right]}{\left[1-\left(\frac{1-k}{k}\right)^{z+1}\right]}. \tag{13.91}$$

Using the expression (13.89) for $i = 1,$ we obtain

$$F(x)_{k=0,5} = \frac{z+1-i^\bullet}{z+1}. \tag{13.92}$$

It is noteworthy that the obtained results can be successfully extended to cascade separation processes of various nature, such as adsorption, rectification, extraction, isotope separation, etc. Note that processes of different nature have different mechanisms accounting for the formation of the values of distribution coefficients of monocomponents k.

On the basis of the developed model of the process, it is possible to perform an exhaustive computation of cascade fractionating of bulk materials. Figure 13.7 gives an estimated dependence of F_f on the parameter B for crushed quartzite separation on a zigzag-type apparatus of rectangular cross-section (Fig. 13.1b). The number of stages in the cascade is $z = 6,$ the site of material feed is $i^* = 3,$ the material density is $\rho = 2,650$ kg/m^3. The initial composition comprises narrow classes with the average particle size of 0.125, 0.75, 1.5, 2.5, 4 and 6 mm.

The zigzag apparatus is hollow, with symmetrically alternating stages having a certain slope (at the angle of 45–60°) each. The material is fed to one of the stages. The air is introduced into the apparatus from below, the fine product obtained as a result of separation goes out of the first stage, and the coarse product from the last, the lowest one.

Fractional extraction of a narrow class was experimentally determined from the relation

$$F_f(x_j) = \gamma_f \frac{r_f(x_j)}{r_s(x_i)} \cdot 100\%,$$

where $F_f(x_i)$is fractional extraction of particles of the narrow class x_j from the apparatus into the fine product; $r_s(x_j)$ is the content of size x_j particles in the initial

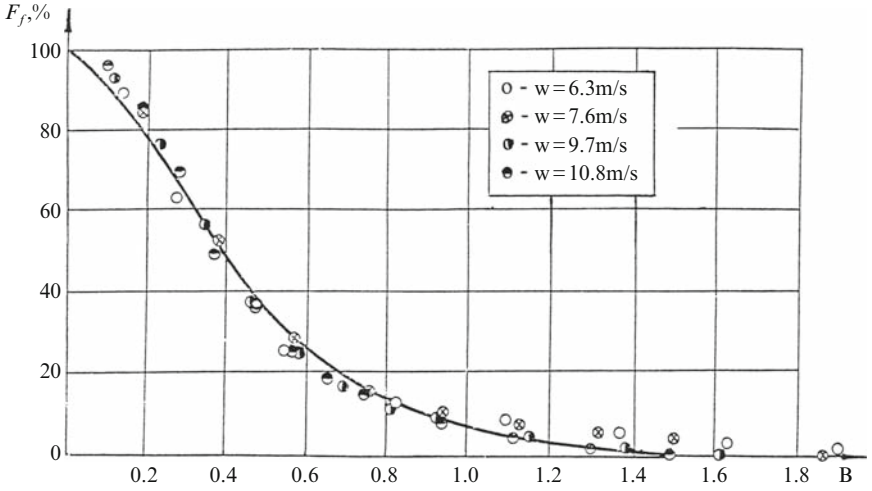

Fig. 13.7 Fractional extraction dependence on the parameter B for zigzag-type cascade. ○ ◓ ◑ ⊗ – experimental points; —— – estimated curve

material; $r_f(x_j)$is the content of size x_j particles in the fine product output; γ_f is the fine product output in percents of the amount of the initial material.

The coefficient k value was determined using the dependence (13.39) with a correction for the rectangular cross-section:

$$k = \frac{\pi}{4}\left[1 - \sqrt{0.4B}\right].$$

The same graph gives experimental points obtained during crushed quartzite separation on this apparatus at air flow velocities equal to 6.3, 7.6, 9.7 and 10.8 m/s.

As follows from the graph, estimated curve deviation from experimental points does not exceed 7%, which points to a sufficiently reliable mathematical model adequacy to a real separation process in the regimes of developed turbulence.

13.3 Optimization of Principal Parameters of Multi-stage Separation

It is assumed that in critical regimes of two-phase flows a part of the solid phase moves along the flow, while another part settles against the flow.

Such a flow is extremely complicated and chaotic due to various random factors. Among them, we can mention mechanical interaction of particles of various sizes with each other and with channel walls, nonuniform concentration and velocity fields, multidirectional solid phase motion, presence of turbulent vortices and local irregularities, poly-fractional solid phase composition, irregular particles shape, etc.

Despite a huge number of papers dealing with the account for all these factors published in recent decades, the problem remains unsolved as yet.

Therefore, it is rather urgent to establish physically grounded similarity criteria for these flows.

Before developing a model of the process, let us examine the relation between the concentration and number of particles in real conditions in a narrow size class, e.g. with the average particle size of 30 μm. If the particles density is $\rho = 2,600$ kg/m^3, then at the consumed concentration of $\mu = 2$ kg/m^3, volumetric concentration of the solid material in the air flow is insignificant and amounts to 7.7×10^{-4} $\left(\beta = \frac{2}{2600}\right)$. The weight of one 30-μm particle is 0.3674×10^{-11}kg. If they account for 10% only in the initial composition, then 1 m^3 contains $n = \frac{0.2}{0.3674 \times 10^{-11}} = 5.4 \times 10^9$ of them. It means that 1 m^3 of air contains 5.4 milliard of these particles, which is comparable with the number of molecules in a rarefied gas.

To develop mathematical models of gaseous or liquid systems, Navier–Stokes equations are applied. It has been shown that after overcoming certain difficulties, these equations can be used for describing heterogeneous systems.

An equation for particles of one narrow class can be written with respect to vertical axis z as follows:

$$\frac{1}{\rho}\frac{\partial p}{\partial z} = P_z - \frac{dv_z}{dt} + c\nabla^2 v_z \tag{13.93}$$

where ρ is the particles density, p denotes internal forces of the flow acting on particles accumulation in a unit mass; P_z denotes external forces acting on a unit particles mass; v_z is the velocity of particles of a narrow class in vertical direction; c is a proportionality coefficient; ∇^2 is a Laplacian (a sum of second partial derivatives of the value under the sign of this operator (v_z) with respect to coordinate axes $(x; y; z)$. This parameter reflects tangential forces acting on a unit mass of particles.

In a general case, the velocity is a function of coordinates and time, and therefore its total differential equals

$$dv_z = \frac{\partial v_z}{\partial t}dt + \frac{\partial v_z}{\partial z}dz + \frac{\partial v_z}{\partial x}dx + \frac{\partial v_z}{\partial y}dy.$$

We divide each summand in this expression by dt; keeping in mind that $\frac{dz}{dt} = v_z$; $\frac{dx}{dt} = v_x$; $\frac{dy}{dt} = v_y$, we can write:

$$\frac{dv_z}{dt} = \frac{\partial v_z}{\partial t} + v_z\frac{\partial v_z}{\partial z} + v_x\frac{\partial v_z}{\partial x} + v_y\frac{\partial v_z}{\partial y}. \tag{13.94}$$

In our further derivation, we omit z for the sake of convenience.

It is impossible to obtain a general solution to Eq. (13.93) due to the lack of physical data. However, we can obtain similarity criteria for the process under study from Eq. (13.93).

Two physical phenomena are assumed to be similar, if the homonymous properties in all similar points of geometrically similar channels differ by constant factors only. Mathematical descriptions of similar systems are identical.

We write (13.93) for two analogous points in similar systems in a stationary process taking into account (13.94):

$$\frac{1}{\rho_1}\frac{\partial p_1}{\partial z_1} = p_1 - \left(v_1\frac{\partial v_1}{\partial z_1} + \cdots\right) + c_1\left(\frac{\partial^2 v_1}{\partial z_1^2} + \cdots\right), \tag{13.95}$$

$$\frac{1}{\rho_2}\frac{\partial p_2}{\partial z_2} = p_2 - \left(v_2\frac{\partial v_2}{\partial z_2} + \cdots\right) + c_2\left(\frac{\partial^2 v_2}{\partial z_2^2} + \cdots\right). \tag{13.96}$$

The expressions in brackets are written in an abbreviated form. However, no information is lost, since the structure of all summands in brackets is the same.

By the definition of physical similarity, we can write:

$$\frac{\rho_1}{\rho_2} = m_\rho;\quad \frac{p_1}{p_2} = m_p;\quad \frac{p_1}{p_2} = m_m;\quad \frac{v_1}{v_2} = m_v;\quad \frac{z_1}{z_2} = m_l;\quad \frac{c_1}{c_2} = m_c.$$

The parameters $m_\rho; m_p; m_m; m_v$ etc. are called similarity factors. Following these considerations, we can write:

$$\rho_1 = m_\rho\rho_2;\quad pm_p p_2;\quad P_1 = m_m P_2;\quad v_1 = m_v v_2;\quad z_1 = m_l z_2;\quad c_1 = m_c c_2.$$

Substitute the obtained expressions into (13.95):

$$\frac{m_\rho}{m_\rho m_l}\frac{1}{\rho_2}\frac{\partial \rho_2}{\partial z_2} = m_m P_2 - \frac{m_v^2}{m_l}\left(v_2\frac{\partial v_2}{\partial z_2} + \cdots\right) + \frac{m_c m_v}{m_l^2}\left(\frac{\partial^2 v_2}{\partial z_2^2} + \cdots\right). \tag{13.97}$$

This expression describes the system (13.95) in notations of the system (13.96).

By the definition of physical similarity, Eqs. (13.96) and (13.97) should be identical. It is possible in one case only – when the expressions composed from similarity factors are identical and can be taken out of brackets. Hence, we can conclude from (13.97) that

$$\frac{m_\rho}{m_\rho m_l} = m_m = \frac{m_v^2}{m_l} = \frac{m_t m_v}{m_{lt}^2}. \tag{13.98}$$

Similarity criteria characterizing the process can be obtained from (13.98). We are interested in a criterion reflecting physical fundamentals of a critical flow. Obviously, such criterion should be a measure of the ratio between gravity and inertia forces. Therefore, we examine only one equality of equation (13.98), namely

$$m_m = \frac{m_v^2}{m_l}.$$

Let us disclose its content for a unit mass. By definition, we can write:

$$\frac{g_1}{g_2} = \frac{v_1^2 l_2}{v_2^2 l_1}.$$

Combining values with the same indices in different sides,

$$\frac{g_1 l_1}{v_1^2} = \frac{g_2 l_2}{v_2^2} = \frac{gl}{v^2} = Fr,$$

we obtain the Froude criterion (Froude number).

Earlier, the role of this criterion in the process under study has been revealed in a purely empirical way. This criterion allows obtaining universal separation curves when separating powders in turbulent regimes of the medium flow. Let us clarify this by some examples.

A set of experiments was carried out on a cascade classifier with inclined shelves ($z = 4; i^* = 1$) at average air flow velocities of $w = 2.25$, 3.12, 3.84, 4.3, 5.35, 6.25, 7.0, 7.68, 8.82, 9.9, 10.65, 11.3 and 12.65 m/s. Granulometric composition of the bulk material was in the range from 0.25 to 10 mm. Figure 13.8 shows the dependence of fractional separation of various narrow size classes on air flow velocity for this set of experiments. Figure 13.9 shows the transformation of these dependencies into a universal curve using the Froude criterion. In this case, the range of air flow velocities lies totally within the turbulent region. For smaller particles, affinization of curves using this criterion does not occur. Figure 13.10 shows a similar dependence obtained at the separation of aluminum powder on a cascade classifier ($z = 10, i^* = 5$)at the air flow velocities $w = 0.27$, 0.36, 0.5, 0.9, 1.32, 1.7 m/s. Granulometric composition of the powder is in the range from 10 to 180 μm.

Here an expression proportional to the Froude criterion is used as abscissa:

$$B = Fr\frac{\rho - \rho_0}{\rho_0}$$

where ρ is the material density, kg/m^3. ρ_0 is the medium density, kg/m^3.

To find the parameters of separation curves affinization in all regimes, we make an attempt to solve Eq. (13.93) in a somewhat simplified form.

After overcoming certain difficulties, we can use equations derived in Chapter 2 for heterogeneous systems, i.e. particles motion in a flow:

$$-\frac{\partial n}{\partial t} = \frac{\partial (nv_x)}{\partial x} + \frac{\partial (nv_y)}{\partial y} + \frac{\partial (nv_z)}{\partial z} \tag{13.99}$$

or

$$\frac{\partial n}{\partial t} + \frac{\partial (nv_x)}{\partial x} + \frac{\partial (nv_y)}{\partial y} + \frac{\partial (nv_z)}{\partial z} = 0. \tag{13.100}$$

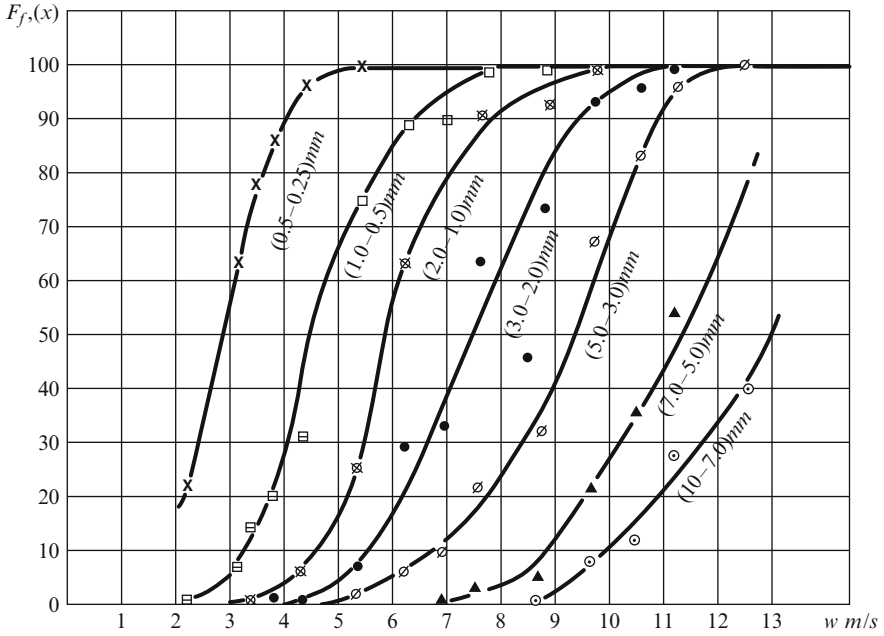

Fig. 13.8 Dependence of fractional separation of various narrow size classes of quartzite on the flow velocity at $z = 4$; $i^* = 1$

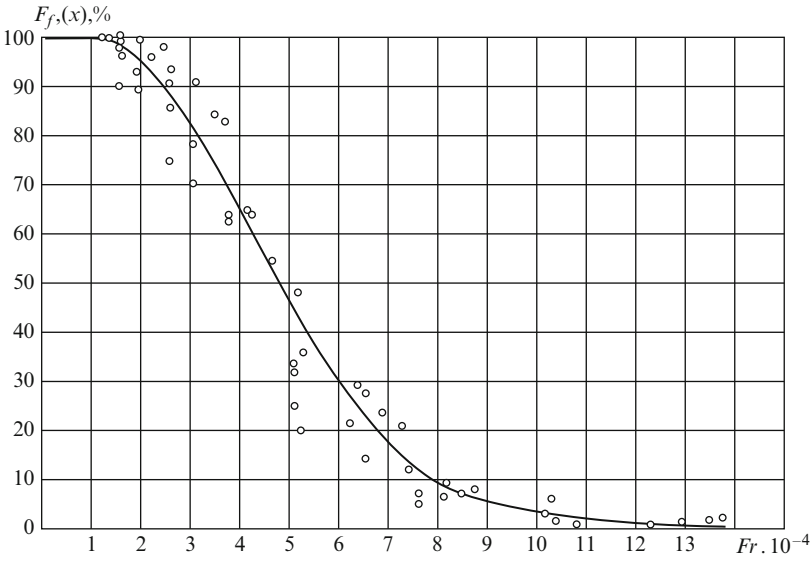

Fig. 13.9 Dependence of fractional separation of various narrow size classes of quartzite on the Froude criterion at $z = 4$; $i^* = 1$

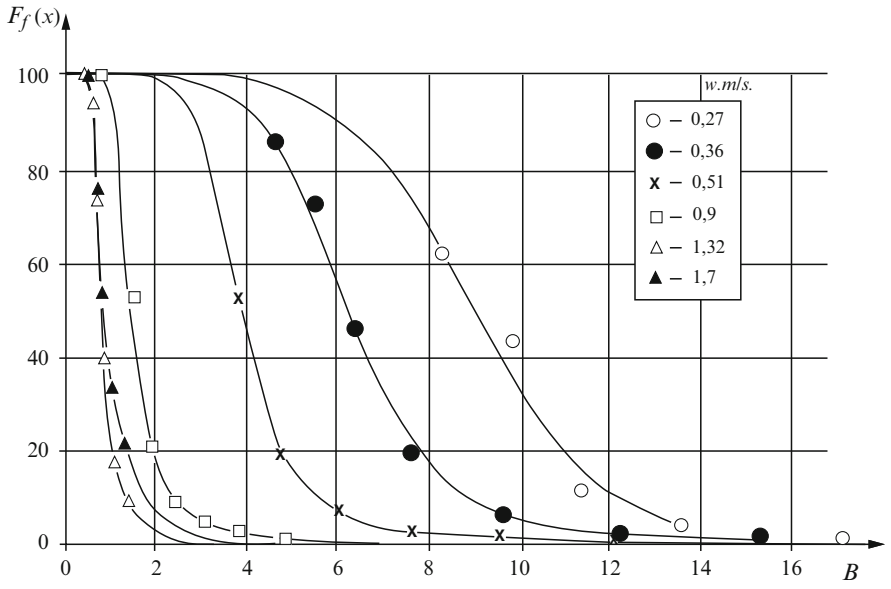

Fig. 13.10 Dependence of fractional separation of various narrow size classes of aluminium powder on B criterion at $z = 10$; $i^* = 5$

Clearly, integration of (13.100) with specified initial conditions (single-valuedness condition) leads to the conservation law.

Under certain conditions, Eq. (13.100) can be considerably simplified. First, a stationary process, in which all characteristics of a two-phase flow are time-independent, is of greatest interest. In such conditions,

$$\frac{\partial n}{\partial t} = 0.$$

Secondly, we can restrict ourselves with a quasi-one-dimensional model of transfer along the z axis, since the separation result depends only on the latter.

Reliable experimental data for determining transfer characteristics along the transverse axes (x, y) are unavailable as yet. Therefore, we assume that particles concentration changes only with height and remains unchanged over the cross-section at any level, the particles being uniformly distributed over this cross-section.

In this case,

$$\frac{\partial (n v_x)}{\partial x} = \frac{\partial (n v_y)}{\partial y} = 0, \tag{13.101}$$

and for Eq. (13.99) this condition is written as

$$\frac{\partial n}{\partial x} = \frac{\partial n}{\partial y} = 0.$$

What remains from Eq. (13.100) is

$$\frac{d(nv_z)}{dz} = 0,$$

and from Eq. (13.101)

$$v_z \frac{dn}{dz} = 0.$$

Mean flow velocity in a channel with a constant cross-section is constant; therefore, these two expressions are identical and can be written as

$$\frac{dn}{dz} = 0. \tag{13.102}$$

This dependence reflects a certain condition of optimum distribution of solid particles in a flow with respect to the channel height.

By solving Eq. (13.102), we can find parameters for optimal organization of the process of gravitational separation of particles in vertical channels.

Multi-directional motion of particles of one narrow size class takes place simultaneously at all levels over the channel height.

It is rather hard to develop a continuous mathematical model in this case. Therefore, we apply a somewhat different approach and develop a discrete model.

We mentally subdivide a vertical hollow channel into a finite number of segments (N), which we call stages. If the channel height is H, and the number of stages is N, the height of one stage is

$$\Delta h = \frac{H}{N}.$$

The coordinate z can be written as $z = H - i\Delta h$. The derivative in (13.102) is

$$\frac{\partial n}{\partial z} = \frac{\partial n}{\partial (H - i\Delta h)} = -\frac{\partial n}{\Delta h \partial i}.$$

We express the number of particles at a certain stage i as

$$n_i = n_s r_i$$

where n_s is the quantity of particles in the initial material; r_i is the percentage of particles in the initial composition. It has been shown that in the site of material feed into the channel $r = 1$.

Since in the stationary regime material is not accumulated in the channel, at any stage a certain part of the material (k) rises, and another part $(1 - k)$ goes down.

It is established that if all the sections are identical, and the flow velocity is constant, then the separation factor (k) is constant for all stages, i.e.,

$$k = \text{const}.$$

The separation factor is a function of the mean flow velocity, particles sizes and the diameter of the channel cross-section:

$$k = f(w; d; D).$$

As it has been agreed that the model under study is stationary and in equilibrium, it can be based on the material balance of a stage.

From the equilibrium condition,

$$r_i = r_i(1-k) + r_i k,$$

i.e. the content of particles in stage i equals their transfer in both directions.

From the stationary state condition,

$$r_i(1-k) + r_i k = r_{i-1}(1-k) + r_{i+1}k,$$

i.e. particles departure from the stage i equals their arrival at this stage.

Hence, we can obtain:

$$r_i = r_{i-1}(1-k) + r_{i+1}k \quad (i \neq i^*). \tag{13.103}$$

Boundary conditions for the initial material feed are

$$r_{i^*} = 1 + r_{i^*-1}(1-k) + r_{i^*}k \tag{13.104}$$

and boundary conditions for particles departure from the channel are

$$\begin{cases} r_1 = r_2 k \\ r_N = r_{N-1}(1-k) \end{cases}. \tag{13.105}$$

To determine the functional dependence

$$r_i = r(k; N; i; i^*),$$

we make use of the recurrent equation (13.103). To solve this equation, we use the calculus of finite differences. We rewrite this equation in the form

$$r_{i+1}k - r_i + r_{i-1}(1-k) = 0. \tag{13.106}$$

We obtain a system analogous to that obtained at the examination of a discrete-stationary system. Its solution comprises the following equations:

$$r_i = \frac{\left[1 - \left(\frac{1-k}{k}\right)^{N+1-i^*}\right]\left[1 - \left(\frac{1-k}{k}\right)^{i}\right]}{\left[1 - \left(\frac{1-k}{k}\right)^{N+1}(2k-1)\right]} \quad (1 \leqslant i \leqslant i^*), \tag{13.107}$$

$$r_i = \frac{\left[1 - \left(\frac{k}{1-k}\right)^{i^*}\right]\left[\left(\frac{1-k}{k}\right)^{N+1}\left(\frac{1-k}{k}\right)^{i}\right]}{\left[1 - \left(\frac{1-k}{k}\right)^{N+1}\right](2k-1)} \quad (i^* \leqslant i \leqslant N). \tag{13.108}$$

Fractional extraction of the size class under study upwards from the channel (into the fine product) at $i = 1$ amounts to

$$F_f(x) = r_1 k = \frac{\left[1 - \left(\frac{1-k}{k}\right)^{N+1-i^*}\right]}{\left[1 - \left(\frac{1-k}{k}\right)^{N+1}\right]}. \tag{13.109}$$

Fractional extraction into the coarse product at $i = N$ amounts to

$$F_c(x) = z_z(1-k) = \frac{\left[\left(\frac{1-k}{k}\right)^{-i^*} - 1\right]\left(\frac{1-k}{k}\right)^{N+1}}{\left[1 - \left(\frac{1-k}{k}\right)^{N+1}\right]}. \tag{13.110}$$

The sum $F_f(x) + F_c(x) = 1,$ which reflects the implication of the process, i.e. each narrow size class is completely distributed into both outlets.

Let us take a derivative of (13.107) with respect to z or i:

$$\frac{\partial r_i}{\partial i} = \frac{\left[1 - \left(\frac{1-k}{k}\right)^{N+1-i^*}\right]\left[\ln\left(\frac{1-k}{k}\right)\left(\frac{1-k}{k}\right)^{i}\right]}{\left[1 - \left(\frac{1-k}{k}\right)^{N+!}\right](2k-1)} = 0.$$

Since $\ln\left(\frac{1-k}{k}\right)\left(\frac{1-k}{k}\right)^{i} \neq 0,$ consequently, $1 - \left(\frac{1-k}{k}\right)^{N+1-i^*} = 0.$

This equality is possible at any N and i^* values in one case only, at $1 - \left(\frac{1-k}{k}\right) = 1,$ i.e. at $k = 0.5$. Another condition

$$N + 1 - i^* = 0$$

does not make sense, since it leads to

$$i^* = N + 1.$$

A derivative of (13.108) gives an analogous result. Thus, $k = 0.5$ value corresponds to optimal separation within one stage. At $k = 0.5$, for the entire channel

$$F_f(x) = 0,5 = \frac{N+1-i^*}{N+1}.$$

Consequently,

$$i^* = \frac{N+1}{2}. \tag{13.111}$$

This means that in order to attain optimal separation, the initial material should be fed into the middle of the vertical channel.

It has been empirically established that to obtain high-quality separation, the initial material must not be fed from above or from below.

Substituting (13.111) into (13.109), we obtain

$$F_f(x) = \frac{1}{1+\left(\frac{1-k}{k}\right)^{\frac{N+1}{2}}}. \tag{13.112}$$

Reverting to (13.102), we proceed with the analysis of the obtained dependencies.

Let us take a derivative of $F_f(x)$ with respect to k:

$$\frac{dF_f(x)}{dk} = \left[\frac{\frac{N+1}{2}\left(\frac{1-k}{k}\right)^{\frac{N-1}{2}}\left(\frac{1}{k}\right)^2}{\left[1+\left(\frac{1-k}{k}\right)^{\frac{N+1}{2}}\right]^2}\right]_{k=0,5} = \frac{N+1}{2}. \tag{13.113}$$

It is important to determine the limit fractional extraction of a narrow size that the class tends to with an increasing number of cascade stages and to find reasonable limits of the apparatus height. To do this, we write the relation (13.109) for a cascade apparatus in the general form:

$$F_f(x) = \frac{\left(\frac{k}{1-k}\right)^{z+1} - \left(\frac{k}{1-k}\right)^{i^\bullet}}{\left(\frac{k}{1-k}\right)^{z+1} - 1}. \tag{13.114}$$

Let us examine possible alternatives:

1. $k>0.5$, $\frac{1-k}{k}<1$, in the limit, the denominator of (13.109) tends to unity.

Let us define the limit for this case:

$$\lim_{z\to\infty} F_f(x) = \lim_{z\to\infty}\left[1-\left(\frac{1-k}{k}\right)^{z+1-i^\bullet}\right] = 1 - \lim_{z\to\infty}\left(\frac{1-k}{k}\right)^{z+1-i^\bullet}.$$

The final result depends on the ratio between z and $i^\bullet$ values:
(a) At the material feed into the apparatus from above, $i^\bullet = 1$,

$$\lim_{z\to\infty} F_f(x) = 1 - \lim_{z\to\infty} \left(\frac{1-k}{k}\right)^z = 1.$$

In this case, all material comes out upwards.
(b) At the material feed from below, $i^\bullet = z$,

$$F_f(x) = 1 - \lim_{z\to\infty} \left(\frac{1-k}{k}\right)^1 = 1 - \frac{1-k}{k} = \frac{2k-1}{k}.$$

This part of the material is extracted upwards.
(c) At the material feed in the middle part of the apparatus, $i^\bullet = \frac{z+1}{2}$,

$$\lim_{z\to\infty} F_f(x) = 1 - \lim_{z\to\infty} \left(\frac{1-k}{k}\right)^{\frac{z+1}{2}} = 1.$$

Finally, in this case, as well, all material is extracted into fine product.
2. If $k<0.5$, then $\frac{1-k}{k}>1$, and $\frac{k}{1-k}<1$.
In this case, we can derive from (13.114) that

$$\lim_{z\to\infty} F_f(x) = \lim_{z\to\infty} \frac{\left(\frac{k}{1-k}\right)^{z+1} - \left(\frac{k}{1-k}\right)^{i^\bullet}}{\left(\frac{k}{1-k}\right)^{z+1} - 1} = \left(\frac{k}{1-k}\right)^{i^\bullet}.$$

Let us examine possible alternatives of material feed into the apparatus for this case, as well:
(a) Feed from above, $i^\bullet = 1$, $\lim\limits_{z\to\infty} F_f(x) = \frac{k}{1-k}$.
(b) Feed from below, $i^\bullet = z$, $\lim\limits_{z\to\infty} F_f(x) = 0$.
In this case, all material goes out downwards.
(c) Feed in the middle of the apparatus, $i^\bullet = \frac{z+1}{2}$, $\lim\limits_{z\to\infty} F_f(x) = 0$
In this case, too, all material goes out downwards.
3. If $k = 0.5$, then $\lim\limits_{z\to\infty} F_f(x) = \lim\limits_{z\to\infty} \left[1 - \frac{i^\bullet}{z+1}\right]$.
In this case, as well, everything depends on z and $i^\bullet$ ratio:
(a) At the feed from above, $i^\bullet = 1$, $F_f(x) = 1$.
All material rises upwards;
(b) at the feed from below, $i^\bullet = z$, $F_f(x) = 0$.
All material goes out downwards.
(c) At the feed in the middle of the apparatus, $i^\bullet = \frac{z+1}{2}$, $\lim\limits_{z\to\infty} F_f(x) = \lim\limits_{z\to\infty} \left[1 - \frac{i^\bullet}{z+1}\right] = \frac{1}{2}$.

Thus, in this case only, irrespective of the number of stages, equal extraction of a narrow size class into both outlets is attained. As shown, this determines the optimality condition for the entire apparatus with respect to this boundary size.

To determine the separation optimality in a cascade in the general case at any $i^\bullet$ value, the value k is determined from the ratio:

$$\frac{1-\left(\frac{1-k}{k}\right)}{1-\left(\frac{1-k}{k}\right)^{z+1}}^{z+1-i^\bullet} = 0.5. \tag{13.115}$$

This clearly leads to the dependence of separation coefficient k on the quantity of stages and the site of material feed into the apparatus:

$$k = f(z; i^\bullet).$$

To attain optimality with respect to the boundary size value $x_{0.5}$, it is necessary to ensure the ascending flow velocity $w_{0.5}$ corresponding to the realization of (13.115) relation, i.e., in the general case,

$$x_{0.5} = f(w_{0.}; z; i^\bullet).$$

The obtained results can be illustrated by a particular example.

The conditions of separation optimality for a cascade separator consisting of 11 identical stages $(z = 11)$ were determined for the entire apparatus and for one stage at a successive change in the material feed site from the upper $(i^\bullet = 1)$ to the lower $(i^\bullet = 11)$ stage. Principal results are summarized in Table 13.1:

Important conclusions follow:

1. Flow velocity equal to hovering velocity of boundary-size particles ensures the separation in one case only – at the material feed into the middle of the apparatus.
2. At any other feed site, hovering conditions do not ensure separation optimality. To attain optimality at the material feed above the middling stage, the flow velocity should be less than the hovering velocity, and at the feed below the middling stage, the flow velocity should exceed the hovering velocity.
3. All this points to the fact that the velocity hypothesis, which is a determining factor in today's theories of gravitational separation, is insufficient.
4. As follows from the table, in the general case, separation optimality is determined not only by hydrodynamic properties of solid particles and the flow, but also, to a considerable extent, by the apparatus design and its boundary conditions.

Table 13.1 Dependence of fractional extraction of one stage and the entire apparatus on the site of the material feed into the apparatus under optimal conditions

Material feed stage $i^\bullet$	1	2	3	4	5	6	7	8	9	10	11
Fractional extraction of the apparatus $F(x)\%$ at $k = 0.5$	91.6	83.3	75	66.7	58.3	50	41.7	33.3	25	16.7	8.3
Fractional extraction in one stage at $F(x) = 50\%$	0.33	0.42	0.45	0.47	0.485	0.5	0.515	0.535	0.55	0.585	0.667

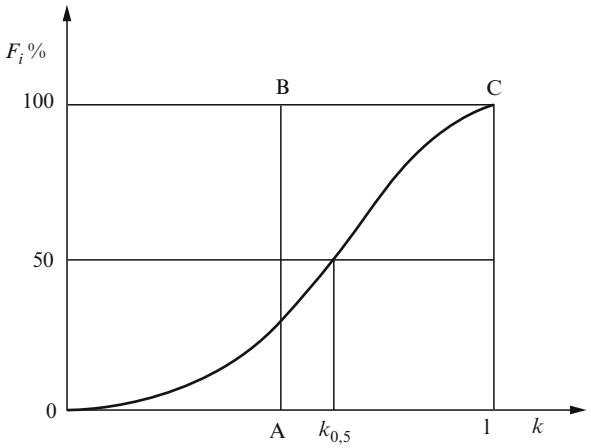

Fig. 13.11 Fractional separation $F_f(x)$ dependence on the distribution parameter (k)

Now let us revert to the relation (13.113). Let us elucidate it using a graph of the function $F_f(x) = f(k)$ in Fig. 13.11. This figure shows an actual separation curve, and the path *OABC* shows ideal separation. The dependence (13.113) shows the slope angle of a tangent at the point $F_f(x) = 0.5$. It is clear from the graph that the closer the curve to the ideal separation line, the higher the process efficiency. It means that the steeper the tangent under consideration, the more efficient the separation. It follows from (13.113) that the greater the number of stages, the higher the efficiency. However, such efficiency growth is limited. Thus, at $z = 3$, the tangent slope angle is $\alpha = 63.5°$; at $z = 7$, $\alpha = 76°$, and at $z = 15$, $\alpha = 83°$. Therefore, the number of stages in one cascade should be limited maximum by $z = 10 \div 11$. Further increase in the number of stages does not result in an appreciable growth of the effect.

Chapter 14
Universal Curves Criteria

Abstract Affinization criterion for turbulent regimes was first obtained empirically. It was validated by analyzing a two-phase flow as a statistical system. The analysis of physical aspects of the process has allowed us to define new criteria for obtaining universal separation curves in transient and laminar flow regimes. It is shown that the entire range of flows can be covered by two parameters for obtaining universal curves. It has turned out that their ratio corresponds to the Reynolds criterion. Examples of practical application of these parameters are presented.

Keywords Universality · Separation cures · Reynolds number · Archimedes number · Distribution coefficient · Generalizing criterion · Turbulent · Laminar and Transient flow regimes

14.1 Substantiation of the Curves Universality

Similarity criteria for such processes as gravitational separation of bulk materials allow us to obtain universal separation curves.

The universality of these curves consists in the fact that at an appropriate transformation of the abscissa axis, all separation curves obtained on a particular classifier for various narrow size classes and various flow velocities are transformed into the same curve. This considerably simplifies the estimation of process results and optimization and makes the comparison of different separators absolutely unbiased. For turbulent separation regimes, such criteria have been found previously in a purely empirical way, as shown in Chapter 10. Parameters suitable for separation curves generalization in case of transient and laminar motion of the medium have not been found yet. It is extremely important to find such parameters for further development of theory and practice of gravitational separation of bulk materials.

E. Barsky, *Critical Regimes of Two-Phase Flows with a Polydisperse Solid Phase,*
Fluid Mechanics and Its Applications 93,
DOI 10.1007/978-90-481-8838-3_14,

Let us illustrate such properties of separation curves by particular examples. A set of experiments with fractionation of a coarse-grained material – chromium oxide – was carried out on an air cascade classifier with inclined shelves at the consumed material concentration $\mu = 2.0 \div 2.2$ kg/m^3. Separation was performed on a five-stage cascade apparatus $(z = 5)$, at the initial feed to the third shelf from above $(i^* = 3)$.

Granulometric composition of the initial material is presented in Table 14.1.

The experiments were carried out at air flow velocities equal to 2.7, 3.0, 3.25, 4.15, 4.75 m/s. As a generalizing criterion for this case, we used an expression:

$$B = \frac{gd}{w^2} \frac{(\rho - \rho_0)}{\rho_0}$$

derived previously. Figure 14.1 shows a graphic dependence

$$F_f(x) = \phi(B),$$

Table 14.1 Chromium oxide granulometric composition ($\rho = 3{,}600$ kg/m^3)

Average particles size, d (mm)	0.025	0.0565	0.0815	0.13	0.18	0.258	0.358	0.515	0.815	1.3	2.05	3.75
Narrow Class content, $r_i(\%)$	10.7	4.3	5.9	6.9	4.1	9.7	7.1	11.4	11.2	11.1	14.3	3.2

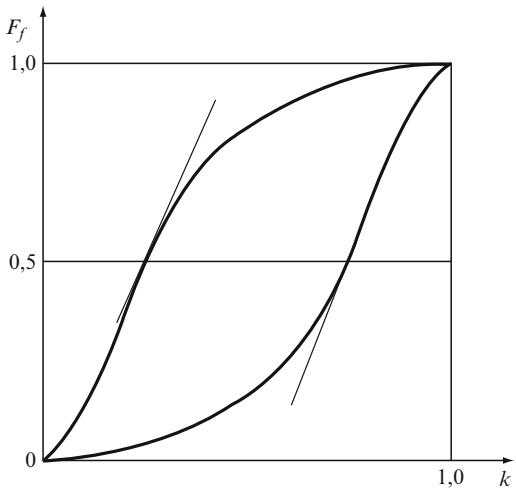

Fig. 14.1 $F_f(x) = f(k)$ dependence

obtained on the basis of experiments carried out for all flow velocities and narrow particle classes under study. This figure brings us to a conclusion that the parameter B in this case allows us to obtain a universal curve.

Another example is fine-grained material – aluminum powder – separation in a cascade shelf apparatus consisting of ten stages $(z = 10; i^* = 5)$ at the consumed material concentration $\mu = 1.5 \div 2.2$ kg/m^3.

Granulometric composition of the aluminum powder is presented in Table 14.2.

Experiments were carried out at air flow velocities equal to 0.27, 0.36, 0.51, 0.9, 1.32, 1.7 m/s. An analogous dependence

$$F_f(x) = \phi(B)$$

for this set of experiments is shown in Fig. 14.2.

It follows that in this case the parameter B does not ensure the possibility of obtaining a universal curve. Apparently, it is due to the fact that in the first case turbulent overflow of particles occurs, while in the second case of finer particles and lower flow velocities, the overflow regime is transient or laminar. Therefore, we make an attempt to find generalizing parameters for these regimes, as well, from the

Table 14.2 Aluminum powder granulometric composition ($\rho = 2{,}700$ kg/m^3)

Average particles size, d (μm)	10	25	40	56.5	71.5	90	112.5	142.5	180	>180
Narrow class content, $r_i(\%)$	3.6	7.2	17.0	8.2	7.8	6.7	6.5	7.5	7.8	27.7

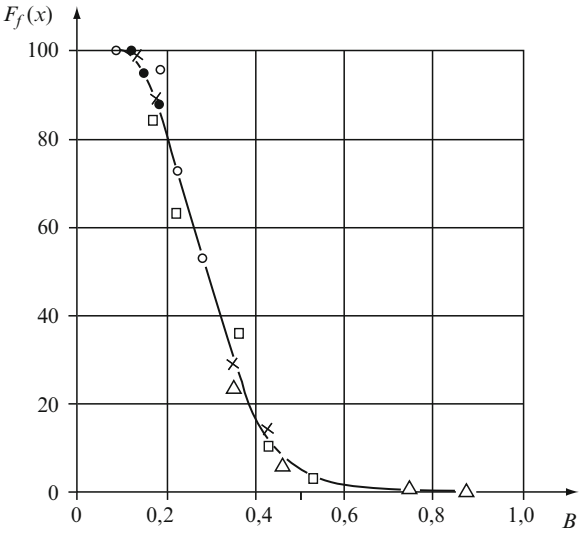

Fig. 14.2 Dependence of fractional separation of different narrow size classes of chromium oxide on the parameter B. Particle size notations: • – 0.13 mm; ○ – 0.258 mm; × – 0.51 mm; □ – 0.815 mm; Δ – 2.05 mm

standpoint of the results obtained by examining structural and cascade models of the process.

We have obtained the following value of the distribution coefficient for a laminar overflow regime:

$$K = 1 - \frac{\sqrt{Ar \cdot B}}{36}. \tag{14.1}$$

In the general case, this parameter is determined by the expression

$$K = \left[1 - \frac{n}{n+2} \frac{\sqrt{Ar \cdot B}}{(18 + 0.61\sqrt{Ar})}\right]^{\frac{2}{n}}.$$

It has been established by numerous researches that in transient and turbulent regimes of two-phase flows, the profile of the flow becomes somewhat elongated in the central region and approaches a parabolic one. Thus, under certain assumptions, we can accept $n = 2$ for all regimes. Then we can write for an arbitrary regime of particles overflow:

$$K = \left(1 - \frac{\sqrt{Ar \cdot B}}{36 + 1.22\sqrt{Ar}}\right). \tag{14.2}$$

In turbulent regimes, Ar acquires large values. Therefore, for such values, 36 in the denominator can be neglected, and

$$K = (1 - \sqrt{0.4B}). \tag{14.3}$$

The expression (14.3) leads to an interesting conclusion. The generalizing parameter in it is unambiguously connected with the distribution coefficient K determined through the flow structure. Based on this expression and, by analogy, on (14.1) and (14.2), we can formulate new criteria for gravitational classification:

– For turbulent overflow regimes:

$$H_1 = 1 - K = \sqrt{0.4B}, \tag{14.4}$$

– For a laminar overflow:

$$H_2 = \frac{\sqrt{Ar \cdot B}}{36}, \tag{14.5}$$

– For an arbitrary regime of particles overflow:

$$H_3 = \frac{\sqrt{Ar \cdot B}}{36 + 1.22\sqrt{Ar}}. \tag{14.6}$$

14.2 Generalizing Criteria

Let us apply the obtained criteria for processing experimental data presented in the first part of the present chapter. Experimental data on aluminum powder separation shown in Fig. 13.10 and recalculated using Eq. (14.5) give the dependence shown in Fig. 14.3, and those recalculated using Eq. (14.7) – the dependence shown in Fig. 14.4. The results of chromium oxide separation presented in Fig. 14.2 and recalculated using Eq. (14.5) are shown in Fig. 14.5. It follows from these examples that all these criteria ensure a generalizing effect.

We revert to the dependence (14.5). Clearly, 36 in the denominator is a scale factor, and the physical meaning of the parameter is in the numerator. Let us analyze it:

$$\sqrt{Ar \cdot B} = \frac{qd^2(\rho - \rho_0)}{\mu \cdot w}.$$

Here we obtain a new dimensionless criterion, which is valid in laminar overflow regimes. These regimes ensure most wet separation processes and dry separation of very fine particles.

Thus, we have formulated generalizing parameters allowing us to obtain universal separation curves:

– At a turbulent overflow of particles:

$$B = \frac{qd}{w^2} \frac{(\rho - \rho_0)}{\rho_0},$$

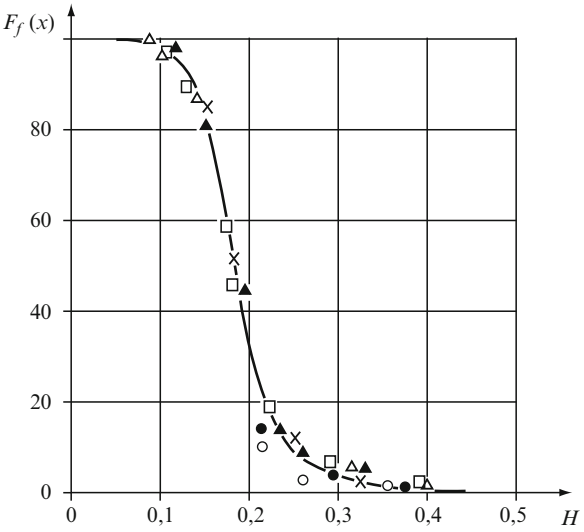

Fig. 14.3 Dependence of fractional separation of aluminum powder on H criterion at $z = 10$; $i^* = 5$

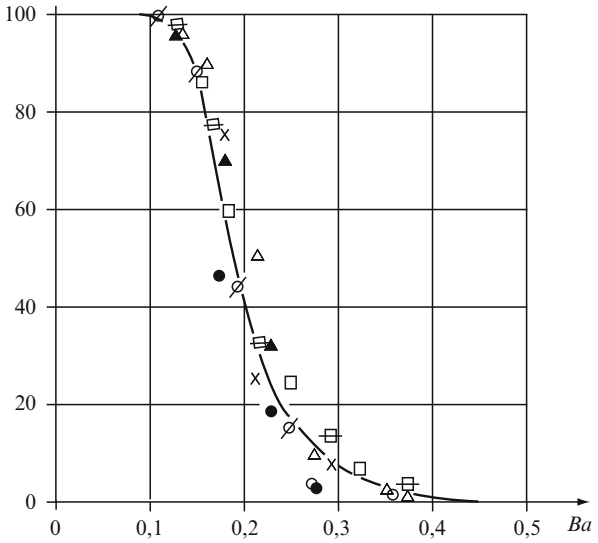

Fig. 14.4 Dependence of fractional separation of aluminum powder on B_α criterion at $z = 10$; $i^* = 5$

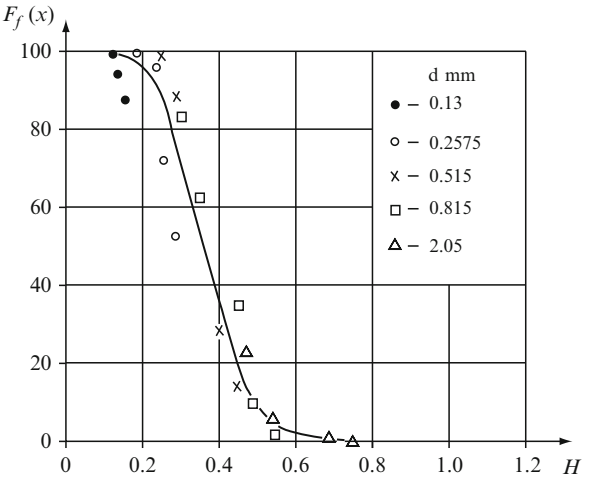

Fig. 14.5 Dependence of $F_f(x) = f(H)$ type for chromium oxide

– At a laminar overflow of particles:

$$B_\alpha = \frac{qd^2(\rho - \rho_0)}{\mu w}, \tag{14.7}$$

– At any overflow regimes:

$$H = \frac{\sqrt{Ar \cdot B}}{36 + 1.22\sqrt{Ar}}. \tag{14.8}$$

Let us analyze the relations between B and B_α criteria by dividing one of them by another:

$$\frac{B_\alpha}{B} = \frac{qd^2(\rho - \rho_0)w^2\rho_0}{\mu \cdot w \cdot qd(\rho - \rho_0)} = \frac{dw\rho_0}{\mu} = \mathrm{Re}. \tag{14.9}$$

This relation gives the Reynolds number defined for a particle. Thus, we can write:

$$B_\alpha = B \cdot \mathrm{Re}. \tag{14.10}$$

This relation has a fundamental physical meaning. In the regimes of turbulent overflow of particles, the Reynolds criterion degenerates, and then the criterion B only is sufficient. In the laminar region, where particles resistance is proportional to Re, the product $B \cdot \mathrm{Re}$ is required for the generalization of separation curves.

Thus, we have established similarity criteria for obtaining universal separation curves in various regimes – laminar, transient and turbulent. However, the bounds of either criterion application under particular separation conditions remain unclear.

Solid particle interaction with moving medium in case of simple settling occurs in the vicinity of the particle surface.

If the steady-state particle velocity acquires the value v, the relative velocity of its overflow with the motionless medium equals the absolute velocity of the particle motion:

$$w = -v.$$

Due to cohesion forces, an elementary layer moving together with the particle is formed directly on the particle surface. The velocity is transferred by viscosity forces from this layer to elementary masses of the medium located close to it. This leads to a monotonic velocity decrease in the boundary layer from v to 0 along the normal to the surface, the transition being smooth. This takes place at moderate settling velocities in the front part of the solid or over its entire surface at a non-interrupted overflow.

A different situation takes place at the motion with boundary layer separation. At high settling velocities, the medium is hindered by counter-pressure arising along the particle surface, which causes medium motion against the overflow direction.

At a certain point, the boundary layer is separated from the particle surface. The counter-flow completely disorganizes the motion. While the boundary layer before

its separation from the surface has been laminar, after the separation it behaves as a free jet in a submerged space and becomes turbulent. In the separation point, the surface layer becomes unstable and curls into one or several vortices.

It is established that all quantitative features of settling process – boundary layer thickness, separation point location, velocity profile in the boundary layer and the character of its change, the total resistance value – depend on the Reynolds number calculated for the particle:

$$\mathrm{Re}_\rho = \frac{vd\rho_0}{\mu},$$

where v is the particle velocity, m/s; d is the particle diameter, m; μ is the dynamic coefficient of the medium viscosity, kg/m $\times$ s; ρ_0 is the medium density, kg/m^3. Using this criterion, we can distinguish laminar, turbulent and intermediate overflow regimes.

A moving flow complicates all phenomena occurring on the particles surface. For example, particle overflow in a laminar flow can be either laminar or turbulent depending on the particle size. Even in case of fine particles, external turbulence can affect the overflow character. As known, the flow regime is also determined by the Reynolds number calculated for the flow:

$$\mathrm{Re}_D = \frac{wD\rho_0}{\mu},$$

where D is the channel diameter, m; w is the flow velocity averaged over the channel cross-section, m/s.

Here a problem of the choice of similarity criteria for separation processes arises – which of the previously determined criteria should be used in particular separation conditions. Let us try to clarify it.

14.2.1 Turbulent Regimes of Particles Overflow

As known, in these conditions, the dynamic effect of the flow on an isolated solid particle is

$$F = \lambda \frac{\pi d^2}{4} \rho_0 \frac{(u_r - v_r)^2}{2},$$

where λ is the resistance coefficient of a particle; r is a characteristic coordinate of an arbitrary point of the apparatus cross-section, m; u_r is the local velocity of the medium motion at a point with coordinate r, m/s; v_r is the local velocity of the particle motion at the same point, m/s. The flow direction is chosen as the positive direction of v_r and u_r velocities.

Equilibrium condition for a particle in a steady-state regime is:

$$\frac{\pi d^3}{6} q(\rho - \rho_0) = \lambda \frac{\pi d^2}{4} \rho_0 \frac{(u_r - v_r)^2}{2},$$

or

$$u_r - v_r = w\sqrt{\frac{4}{3\lambda} B}, \tag{14.11}$$

where $B = \frac{\rho - \rho_0}{\rho_0} \cdot \frac{qd}{w^2}$ is a generalized classification parameter for turbulent regimes. A turbulent regime of a particle overflow is characterized by a constant resistance coefficient. In this case, Reynolds criterion for a particle based on experimental data $\mathrm{Re}_\rho \geq 500$, i.e.,

$$d\rho_0 \frac{(u_r - v_r)}{\mu} \geqslant 500.$$

Hence, taking into account (14.11), we get

$$\frac{w\sqrt{\frac{4}{3\lambda} B} d\rho_0}{\mu} \geqslant 500. \tag{14.12}$$

The condition (14.12) taking into account $\lambda = 0.5$ corresponds to the expression

$$\sqrt{\frac{8}{3} Ar} \geqslant 500,$$

where $Ar = \frac{qd^3(\rho - \rho_0)\rho_0}{\mu^2}$ is Archimedes criterion. It follows from this expression that

$$Ar \geqslant 93750.$$

As applied to air medium under ordinary temperature conditions $\left(\mu = 1.75 \times 10^{-5} \text{ kg/m s}; \rho_0 = 1.2 \text{ kg/m}^3\right)$, particle size characterized by turbulent overflow in case of settling in a motionless medium is

$$d \geqslant 10^{-3} \sqrt[3]{\frac{2550}{\rho}}.$$

Hence, for quartzite $(\rho = 2{,}600 \text{ kg/m}^3)$, particles of $d \geqslant 1$ mm size are in the regime of turbulent overflow. We obtain from the condition (14.12):

$$\frac{\rho_0}{\mu} \geqslant \frac{500}{w\sqrt{\frac{4}{3\lambda} Bd}}. \tag{14.13}$$

Substitute this expression in the Reynolds formula for the flow:

$$\mathrm{Re}_D = \frac{D}{d} \cdot \frac{500}{\sqrt{\frac{4}{3\lambda}B}}. \tag{14.14}$$

The condition (14.14) allows us to estimate the regime of medium motion in a separator at a turbulent overflow of particles.

Obviously, $(\mathrm{Re}_D)_{\min}$ should be evaluated at $d_{\max}$, at which the parameter $B = B_{\max}$. It is experimentally established that at the classification of materials down to the size on the order of $d = 60$ μm, for all mono-fractions $B_{\max} = 2.7 - 3.0$ and slightly depends on the apparatus design. The ratio $\left(\frac{D}{d}\right)$ is on the order of 10^2 for experimental apparatuses and an order of magnitude higher for industrial ones. Taking into account $\lambda = 0.5$, we can obtain from (14.14):

$$(\mathrm{Re}_D)_{\min} \geqslant 1.75 \times 10^4.$$

Even for an apparatus with $D = 100$ mm, at the velocity of 100 μm-particles equal to $w = 1.0$ m/s, $\mathrm{Re} \geq 10^4$.

Thus, in the conditions of turbulent overflow of particles, the entire process (from the fine particles output $\gamma_f = 0$) practically occurs at a turbulent regime of the medium motion in the separator. It is confirmed by a reliable generalization of separation curves using the criterion B.

14.2.2 Laminar Regimes of Particles Overflow

Such regimes can take place at air classification of fine powders or wet separation. We can write the following expression for a particle at a laminar overflow:

$$\mathrm{Re}_\rho = \frac{(u_r - v_r)d\rho_0}{\mu} \leqslant 1. \tag{14.15}$$

Equilibrium conditions at the particle overflow are

$$\frac{\pi d^3}{6} q(\rho - \rho_0) = 3\pi\mu(u_r - v_r)d.$$

Taking into account (14.15), this expression can be transformed into

$$Ar = 18\mathrm{Re} \text{ or } Ar \leqslant 18.$$

In the conditions of air medium, it is valid for particles with the size

$$d \leqslant 10^{-3} \sqrt[3]{\frac{0.4954}{\rho}}.$$

In case of quartzite, these are particles with $d \leqslant 57$ μm. It follows from the equality (14.15) that

$$\frac{\rho_0}{\mu} \leqslant \frac{1}{(u_r - v_r)d}.$$

Substitute the latter into the expression for Re_D

$$\mathrm{Re}_D \leqslant \frac{D}{d} \cdot \frac{w}{(u_r - v_r)}. \tag{14.16}$$

It is known that the resistance coefficient of a particle at its laminar overflow is

$$\lambda = \frac{24}{\mathrm{Re}_\rho} = \frac{24\mu}{(u_r - v_r)d\rho_0}.$$

Taking this into account, it follows from the dependence (14.11) that

$$\frac{u_r - v_r}{w} = \sqrt{\frac{4}{3}B\frac{(u_r - v_r)d\rho_0}{24\mu}},$$

and hence,

$$\frac{u_r - v_r}{w} = \frac{1}{18}\mathrm{Re}_\rho \cdot B.$$

Taking into account the fact that $\mathrm{Re}_\rho^2 B = Ar,$ we obtain

$$\frac{u_r - v_r}{w} = \frac{\sqrt{Ar \cdot B}}{18}.$$

Substitute the obtained result into (14.16),

$$\mathrm{Re}_D \leqslant \frac{D}{d}\frac{18}{\sqrt{Ar \cdot B}}.$$

Since for laminar regime $Ar \leqslant 18,$ we finally obtain

$$\mathrm{Re}_D \leqslant 10^3 \div 10^4.$$

Thus, regions of laminar and turbulent overflow of particles are overlapped by flow regimes. Evidently, a running flow somewhat changes the pattern of particles overflow obtained at their settling in a motionless medium.

14.3 Universal Curves

As a result, the entire range of powders separation can be described by two similarity criteria:

– For coarse-grained materials (turbulent overflow):

$$B = \frac{qd}{w^2} \frac{(\rho - \rho_0)}{\rho_0},$$

– For fine powders:

$$B_\alpha = \frac{qd^2(\rho - \rho_0)}{\mu w}.$$

It can be visually illustrated by particular examples. Consider two materials of different granulometry and density, whose composition is shown in Tables 14.1 and 14.2.

Figure 14.2 shows a method of obtaining a universal curve for lightweight fine powders (aluminum powder) using the relation

$$F_f(x) = \phi(B_\alpha).$$

For a heavier and coarser product (chromium oxide) a universal dependence is obtained using the relation

$$F_f(x) = \phi(B),$$

and in this case, as follows from Fig. 14.1, all experimental values ensure the possibility of obtaining a universal separation curve for all narrow size classes.

Using these universal curves, we can obtain any information on the process parameters and apparatus design: optimal regimes, products outputs and compositions, separating ability of the structure, etc.

The most interesting point is that any of these experimental curves can be obtained from one experiment only. The analysis of the initial material and separation products leads to a conclusion that every experiment contains all information both about the process and about the separator design.

Bibliography

1. Prigogine, I., Stengers, I.: Time, Chaos, Quantum. URSS, Moscow (2005)
2. Borel, E.: Probability and Reliability. Nauka, Moscow (1967)
3. Feynman, R.: Lectures in Physics. Mir, Moscow (1967)
4. Samoilovich, O.G.: Thermodynamics and Statistical Physics. Gosgortekhizdat, Moscow (1954)
5. Morse, P.: Thermal Physics. Nauka, Moscow (1967)
6. Lorentz, H.A.: Lectures in Thermodynamics. Gosgortekhizdat, Moscow (1946)
7. Prigogine, I., Stengers, I.: Order out of Chaos. URSS, Moscow (2005)
8. Landau, L.D., Lifshitz, E.M.: Statistical Physics. Nauka, Moscow (1964)
9. Zeemansky, M.: Very Low and Very High Temperatures. Mir, Moscow (1968)
10. Peitgen, H.-O., Richter, P.H.: Beauty of Fractals. Mir, Moscow (1993)
11. Reist, P.C.: Introduction to Aerosol Science. MacMillan, New York (1987)
12. Fuks, N.A.: Mechanics of Aerosols. Akademizdat, Moscow (1955)
13. Landau, L.D., Lifshitz, E.M.: Mechanics of Continuous Media. Akademizdat, Moscow (1953)
14. Kouzov, P.A.: Fundamentals of the Analysis of Disperse Composition of Industrial Dusts and Grinded Materials. Khimia, Moscow (1974)
15. Barsky, M.D., Revnivtsev, V.I., Sokolkin, Yu.V.: Gravitational Classification of Granular Materials. Nedra, Moscow (1974)
16. Barsky, M.D.: Optimization of Processes of Granular Materials Separation. Nedra, Moscow (1978)
17. Barsky, M.D.: Fractionating of Powders. Nedra, Moscow (1980)
18. Kirchberg, H.: Mineral Dressing. Gosgortekhizdat, Moscow (1960)
19. Handbook on Ore Dressing, vol. I. Nedra, Moscow (1972)
20. Eder, H.: Probleme der Trennscharfe, Aufbereitungs-Technik, No. 3 (1960)
21. Hancock, R.T.: Efficiency of classification. Eng. Min. J. **210** (1920)
22. Mayer, F.M.: Algemeine Grundlagen V-Kurven, Aufbereitungs-Technik, teil I N 8; 1967; teil II N 8, 1967; teil III N 1 (1968)
23. Prigogine, I.: The End of Certainty. The Free Press, New York (1997)
24. Rosen, A.M.: Theory of Isotope Separation in Columns. Atomizdat, Moscow (1960)
25. Soo, S.L.: Fluid Dynamics of Multiphase Systems. Blaisdell Publishing Co., New York (1971)
26. Altshul, A.D., Kiselev, P.A.: Hydrodynamics and Aerodynamics. Stroyizdat, Moscow (1975)
27. Babukha, G.L., Shraiber, A.A.: Interaction of Polydispersed Material Particles in a Two-Phase Flow. Naukova Dumka, Kiev (1972)

28. Gorbis, Z.R.: Heat Exchange and Hydromechanics of Dispersed Flows. Energia, Moscow (1970)
29. Monin, A.S., Yaglom, A.M.: Statistical Hydromechanics. Nauka, Moscow (vol. I, 1965; vol. II, 1967)
30. Urban, N.: Pneumatic Transport. Mashinostroenie, Moscow (1967)
31. Uspensky, V.A.: Pneumatic Transport. Mashinostroenie, Moscow (1963)
32. Mednikov, E.P.: Turbulent Transfer and Aerosols Precipitation. Nauka, Moscow (1984)
33. Happel, I., Brenner, H.: Low Reynolds Number Hydrodynamics. Prentice-Hall, Englewood Cliffs, NJ (1965)
34. Kizevalter, B.V.: Theoretical Foundations of Gravitational Dressing Processes. Nedra, Moscow (1979)
35. Gibbs, J.W.: Elementary Principles in Statistical Mechanics Developed with Especial Reference to the Rational Foundation of Thermodynamics. Yale University Press, New Haven, CT (1902)
36. Tolmon, R.C.: Principles of Statistical Mechanics. Oxford University Press, London (1938)
37. Kittel, C.: Thermal Physics. Wiley, New York (1977)
38. Brilloun, L.: Science and Information Theory. Academic, New York (1977)
39. Chambodall, P.P.: Evolution et applications du concept d'entropie. Dunov, Paris (1963)
40. Muschelknautz, E.: Teoretische und experimentale Untersuchungen uber die Druckverluste pneumatischer Forderleitungen unter besonderer Berucksichtigung des Einflusses von Gutreibung und Gutgewicht, Dusseldorf: Forschung-geschelt, t. 25 (1959)
41. Gantmacher, F.R.: Applications of the Theory of Matrices. Wiley, New York (1959)
42. Kemeny, J., Snell, J.: Finite Markov Chains. Princeton, New York (1967)
43. Kemeny, J., Snell, J., Knapp, A.: Markov Chains. Springer, New York (1976)
44. Shraiber, A.A., Milutin, N.I., Yatsenko, V.P.: Hydrodynamics of Two-Component Flows with Poly-Dispersed Solid. Naukova Dumka, Kiev (1980)
45. Kondepudi, D., Prigogine, I.: Modern Thermodynamics. Wiley, New York (2000)
46. Seader, J.D., Henley, E.J.: Separation Process Principles. Wiley, New York (1998)
47. Khony, F.M.: Predicting the Performance of Multistage Separation Process. CRC Press, Boca Raton, FL (2000)
48. Bond, F.: Theory of Isotope Separation. J. R. Stat. Soc. N.Y. **4** (1951)
49. Einstein, W.G.: General Course of Chemical Technology Processes and Apparatuses, vols. I and II. Lotos, Moscow (2002)
50. Bird, R., Stewart, V., Lightfoot, E.: Transfer Phenomena. Khimia, Moscow (1974)
51. De Groot, S., Mazur, P.: Non-equilibrium Thermodynamics. Mir, Moscow (1964)
52. Abramovich, G.N.: Applied Gas Dynamics. Nauka, Moscow (1976)
53. Gelperin, N.I.: Principal Processes and Apparatuses of Chemical Technology. Khimia, Moscow (1981)
54. Levich, V.G.: Physico-Chemical Hydrodynamics. Fizmatgiz, Moscow (1959)
55. Zakgeim, A.Yu.: Introduction to Modeling Chemico-Technological Processes. Khimia, Moscow (1982)
56. Billing, C.E.: Controlling Airborne Particles. National Academy of Sciences, Washington, DC (1980)
57. Chapman, S., Cowling, T.G.: The Mathematical Theory of Non-Uniform Gases. Cambridge University Press, Cambridge (1961)
58. Einstein, A.: The Theory of Brownian Movement. Dover, New York (1956)
59. Amelin, A.G.: Theory of Fog Condensation. Hebrew University Press, Jerusalem (1967)
60. Deir Mendjian, D.: Electromagnetic Scattering on Spherical Polydispersions. Elsevier, New York (1969)
61. Green, H.L., Lane, W.R.: Particulate Clouds: Dusts, Smokes and Mists. Van Nostrand, New York (1964)
62. McDaniel, E.W.: Collision Theory in Ionized Gases. Wiley, New York (1964)
63. Schlichting, H.: Boundary Layer Theory. Mc-Graw Hill, New York (1968)

64. Shterenlikht, D.V.: Hydraulics. Energoatomizdat, Moscow (1984)
65. Konstantinov, Yu.M.: Hydraulics. Vysshaya Shkola, Moscow (1988)
66. Sedov, L.I.: Planar Problems of Hydrodynamics and Aerodynamics. Nauka, Moscow (1966)
67. Barsky, E.: Mathematical Models of Separation Process and Optimization of these Processes. M.Sc. thesis, Ben-Gurion University of the Negev (1998)
68. Govorov, A.V.: Cascade and Combined Processes of Bulk Materials Fractionating. Thesis, Urals Polytechnic Institute, Sverdlovsk (1986)
69. Shishkin, S.F.: Intensification of the Process of Gravitational Pneumatic Classification. Thesis, Urals Polytechnic Institute, Sverdlovsk (1983)
70. Fermi, E.: Notes on Thermodynamics and Statistics. Chicago University Press, Chicago, IL (1966)
71. Barsky, M., Barsky, E.: Criterion for efficacy of separation of a pourable material into N components. Proceedings of the 29th International Symposium on Computer Applications in the Mineral Industries, 2001
72. Barsky, M., Barsky, E.: Algorithms for optimization of classification of a pourable material into N components. Proceedings of the 29th International Symposium on Computer Applications in the Mineral Industries, 2001
73. Barsky, E.: Theoretical basis for separation of pourable materials in vertical flows. Sci. Isr Technol. Advant. **1** (2003)
74. Lorentz, H.A.: Les Theories Statistiques en Thermodynamique. B. G. Teubner Verlag, Leipzig-Berlin (1916)
75. Barsky, E., Barsky, M.: Optimal air flow velocities in gravity separation processes. Miner. Process. J. Enrichment Ores, St. Petersburg **2** (2002)
76. Fortier, A.: Mechanics of Suspensions. Mir, Moscow (1971)
77. Kay, J.M.: An Introduction to Fluid Mechanics and Heat Transfer. Cambridge University Press, Cambridge (1957)
78. Barsky, E., Buikis, M.: Mathematical Model for Gravitational Cascade Separation of Pourable Materials at Identical Stages of a Classifier. Progress in Industrial Mathematics. Springer, The Netherlands (2004)
79. Moore, E.F., Shannon, C.E.: Reliable circuits using less reliable relays. J. Franklin Inst. **262** (1956)
80. Barsky, E., Barsky, M.: Cascade Separation of Powders. Cambridge International Science Publishing, Cambridge (2006)
81. Barsky, E., Barsky, M., Govorov, A.: Lifting Power and Structure of Two-Phase Flows in Gravity Separation Regimes. Sci. Isr Technol. Advant. **4** (2002)
82. Volkenshtein, M.V.: Configurational Statistics of Polymers. Academy of Sciences of the USSR, Leningrad (1959)
83. Gibbs, J.W.: The Scientific Papers of J. Willard Gibbs. Vol. 1: Thermodynamics. Dover, New York (1961)
84. Barsky, E., Barsky, M.: Master curve of separation processes. Phys. Sep. Sci. Eng. **2** (2004)
85. Barsky, E.: Algorithms for efficacy of separation of pourable material. ECMI Newsl. Math. Ind. **36** (2004)
86. Barsky, E.: Efficacy of separation of pourable material. ECMI Newsl. Math. Ind. **36** (2004)
87. Barsky, E.: Conditions providing optimum separation. Phys. Sep. Sci. Eng. **3** (2004)
88. Barsky, E. Absorbing Markov chain in gravitational cascade separation of pourable materials at different stages of a classifier. ECMI Newsl. Math. Ind. **37** (2005)
89. Barsky, E., Barsky, M., Shishkin, S.: Mathematical model of combined cascade classifiers. Math. Model. Anal. **3** (2005)
90. Barsky, E.: Medium motions regimes and universal curves of gravitational separation. Int. J. Miner. Process. **3** (2007)
91. Barsky, E., Barsky, M.: Correlation Between the Velocities of Particle Settling and the Optimal Stream Velocity in Gravity Separation. XXII International Mineral Processing Congress, Cape Town, 2003

92. Barsky, E.: Chaos and order in turbulent two-phase currents. Proceeding of First International Conference on Discrete Chaotic Dynamics in Nature and Society, 1998
93. Shteinberg, A.: Preparation of Coarse Dust of Brown Coal. Metallurgizdat, Moscow (1970)
94. Taggart, A.: Fundamentals of the Enrichment. Metallurgizdat, Moscow (1958)
95. Hawking, S.: Brief History of Time. Batman Books, New York (1988)
96. Heisenberg, W.: The Physical Principles of the Quantum Theory. Chicago University Press, Chicago, IL (1930)
97. Mandelbrot, B.: The Fractal Geometry of Nature. Freeman, New York (1982)
98. De Leener, M.: Classical Kinetics of Fluids. Wiley, New York (1977)
99. Balescu, R.: Equilibrium and Non-Equilibrium Statistical Mechanics. Wiley, New York (1975)
100. Tabor, M.: Chaos and Integrability in Nonlinear Dynamics. Wiley, New York (1989)
101. Prigogine, I.: From Being to Becoming. Freeman, San Francisco, CA (1980)